UNIVERSITÀ DEGLI STUDI DI TRIESTE

UNIVERSITÀ DEGLI STUDI DI TRIESTE

XXXV CICLO DEL DOTTORATO DI RICERCA IN

SCIENZE DELLA RIPRODUZIONE E DELLO SVILUPPO

INNOVATIVE APPROACHES FOR POLYSACCHARIDE ELECTROSPINNING IN THE PREPARATION OF NANOSTRUCTURED MEMBRANES FOR THE TREATMENT OF NON-HEALING WOUNDS

Settore scientifico-disciplinare: **MED/50**

DOTTORANDA
Martina Gruppuso

COORDINATORE
Prof. Paolo Gasparini

SUPERVISORE DI TESI
Prof. Eleonora Marsich

CO-SUPERVISORE DI TESI
Prof. Gianluca Turco

TUTOR
Dott. Davide Porrelli

ANNO ACCADEMICO 2021/2022

UNIVERSITÀ
DEGLI STUDI
DI TRIESTE

UNIVERSITÀ DEGLI STUDI DI TRIESTE

XXXV CICLO DEL DOTTORATO DI RICERCA IN

SCIENZE DELLA RIPRODUZIONE E DELLO SVILUPPO

INNOVATIVE APPROACHES FOR POLYSACCHARIDE ELECTROSPINNING IN THE PREPARATION OF NANOSTRUCTURED MEMBRANES FOR THE TREATMENT OF NON-HEALING WOUNDS

Settore scientifico-disciplinare: **MED/50**

DOTTORANDA
Martina Gruppuso

COORDINATORE
Prof. Paolo Gasparini

SUPERVISORE DI TESI
Prof. Eleonora Marsich

CO-SUPERVISORE DI TESI
Prof. Gianluca Turco

TUTOR
Dott. Davide Porrelli

ANNO ACCADEMICO 2021/2022

"Nella vita niente deve essere temuto,
ma solo capito.
È tempo di capire di più,
in modo da temere di meno."

Marie Curie

TABLE OF CONTENTS

LIST OF PUBLICATIONS

(1) Gruppuso, M.; Turco, G.; Marsich, E.; Porrelli, D. Polymeric Wound Dressings, an Insight into Polysaccharide-Based Electrospun Membranes. *Applied Materials Today* **2021**, 24, 101148. https://doi.org/10.1016/j.apmt.2021.101148.

(2) Porrelli, D.; Gruppuso, M.; Vecchies, F.; Marsich, E.; Turco, G. Alginate Bone Scaffolds Coated with a Bioactive Lactose Modified Chitosan for Human Dental Pulp Stem Cells Proliferation and Differentiation. *Carbohydrate Polymers* **2021**, 273, 118610. https://doi.org/10.1016/j.carbpol.2021.118610.

(3) Gruppuso, M.; Guagnini, B.; Musciacchio, L.; Bellemo, F.; Turco, G.; Porrelli, D. Tuning the Drug Release from Antibacterial Polycaprolactone/Rifampicin-Based Core–Shell Electrospun Membranes: A Proof of Concept. *ACS Applied Materials & Interfaces* **2022**, 14 (24), 27599–27612. https://doi.org/10.1021/acsami.2c04849.

(4) Gruppuso, M.; Iorio, F.; Turco, G.; Marsich, E.; Porrelli, D. Hyaluronic Acid/Lactose-Modified Chitosan Electrospun Wound Dressings – Crosslinking and Stability Criticalities. *Carbohydrate Polymers* **2022**, 288, 119375. https://doi.org/10.1016/j.carbpol.2022.119375.

(5) Gruppuso, M.; Turco, G.; Marsich, E.; Porrelli, D. Antibacterial Multilayer Matrices Based on Hyaluronic Acid and Lactose Modified Chitosan: The Multimodal Use of Electrospinning in Chronic Wound Care. ***In preparation***.

(6) Mardirossian, M.; Gruppuso, M.; Guagnini, B.; Mihalic, F.; Turco, G.; Porrelli, D. Alginate and Agarose/Hydroxyapatite Based Porous Bone Scaffolds Loaded with an Optimized Proline-Rich Antimicrobial Peptide. ***In preparation***.

LIST OF POSTERS

(1) Gruppuso, M.; Iorio, F.; Turco, G.; Marsich, E.; Porrelli, D. Hyaluronic Acid/Lactose-Modified Chitosan Electrospun Wound Dressings – Crosslinking and Stability Criticalities. PS16.30. Presented at the *Tissue Engineering and Regenerative Medicine International Society, Inc. (TERMIS) - European Chapter 2022*.

ABSTRACT

In this PhD thesis, the advantages of electrospun matrices (such as biomimetic architecture, high porosity, and surface area) have been combined with the bioactivity of polysaccharides, focusing on hyaluronic acid (naturally present in the extracellular matrix, or ECM) and on a lactose-derivative of chitosan (CTL), which has been studied for its bioactive properties, including the anti-inflammatory activity in the wound microenvironment, and which is used here for the first time for the preparation of electrospun nanofibers.

The limitations associated to polysaccharide electrospinning have been overcome by blending them with a synthetic polymer (polyethylene oxide, PEO) and using a surfactant (namely, Tween® 20) to reduce solution surface tension, thereby producing thin and defect-free nanofibers with a diameter in the range of collagen ECM fibers (50-500 nm). Attention then turned to the more critical step of stabilization in water as the rapid dissolution of the electrospun polysaccharides would hamper their use as wound dressings. For this purpose, various crosslinking methods already investigated in the literature have been tested (such as EDC/NHS, glutaraldehyde, genipin, or heat treatment), all of which being unsuccessful given the highly hydrophilic nature of both hyaluronic acid and CTL. Hence, previously untested crosslinkers in the electrospinning field have been explored, with carbonyldiimidazole (CDI) exhibiting the best results in terms of water stability and fibrous morphology maintenance. Moreover, the ability of the electrospun products to retain a surprisingly high quantity of fluids while favoring water-vapor permeation has been demonstrated, comparing them with a commercial chitosan dressing (Chitoderm®) and non-electrospun polysaccharidic membranes.

However, the polysaccharide-based matrix alone did not possess proper stability and consistency to be handled and applied to a wound.

For this reason, other polysaccharide-based electrospun systems have been designed, by exploiting two different strategies: i) the layer-by-layer deposition (here also referred to as "coating") of polysaccharides on a synthetic-based electrospun matrix (namely, polycaprolactone, PCL); ii) the production of a two-layer electrospun membrane with a mechanically stable PCL layer and a bioactive and fast releasing polysaccharide counterpart.

The two types of constructs have been characterized in terms of morphology, polysaccharide release kinetics, swelling capacity, and water vapor transmission ability. They revealed good biocompatibility and bioactivity towards human dermal fibroblasts, which showed enhanced healing ability in the presence of polysaccharide-endowed mats.

In addition, the antibiotic rifampicin has been added to the PCL layer, to confer the wound dressings antibacterial properties without compromising their biocompatibility. The antibiotic release as well as its inhibitory and bactericidal activity towards *Staphylococcus aureus*, *Staphylococcus epidermidis*, *Pseudomonas aeruginosa*, and *Escherichia coli* have been tested, with higher efficacy against Staphylococci and *Pseudomonas aeruginosa*.

SOMMARIO

Nella presente tesi di dottorato, i vantaggi offerti da matrici elettrofilate (come l'architettura biomimetica, l'elevata porosità e l'area superficiale) sono stati combinati con la bioattività dei polisaccaridi, in particolare con quella dell'acido ialuronico (naturalmente presente nella matrice extracellulare) e di un chitosano modificato con gruppi lattosidici (CTL), studiato per le sue proprietà bioattive, tra cui l'attività antiinfiammatoria nel microambiente della ferita, e qui usato per la prima volta per l'elettrofilatura di nanofibre.

Le limitazioni correlate all'elettrofilatura dei polisaccaridi sono state superate grazie all'aggiunta di un polimero sintetico (l'ossido di polietilene, PEO) e di un surfattante (il Tween® 20), utilizzato per ridurre la tensione superficiale in modo da ottenere nanofibre sottili, prive di difetti e con un diametro paragonabile a quello delle fibre di collagene della matrice extracellulare (50-500 nm). In seguito, l'attenzione si è spostata verso il passaggio più critico della stabilizzazione in acqua, poiché i prodotti elettrofilati a base di polisaccaridi vanno incontro ad una rapida dissoluzione, impedendone l'utilizzo quali medicazioni per ferite croniche. Per tale ragione, diversi metodi di reticolazione già studiati in letteratura sono stati testati (come EDC/NHS, glutaraldeide, genipina o trattamento al calore), rivelandosi tuttavia tutti infruttuosi a causa della natura fortemente idrofilica dell'acido ialuronico e del CTL. Pertanto, nuovi agenti reticolanti mai impiegati nel campo dell'elettrofilatura sono stati studiati; tra questi, il carbonildiimidazolo (CDI) ha dato i migliori risultati in termini di stabilità in acqua e mantenimento della morfologia fibrosa. Inoltre, è stata dimostrata la sorprendente abilità dei prodotti elettrofilati di trattenere grandi quantità di fluidi favorendo al contempo la permeazione del vapore acqueo, tramite una comparazione con una medicazione già presente in commercio a base di chitosano (il Chitoderm®) e con membrane polisaccaridiche non elettrofilate.

Nonostante ciò, la matrice a base di soli polisaccaridi non possiede una resistenza meccanica e consistenza che ne consentano la maneggiabilità e l'applicazione su una ferita.

Per questo motivo, sono stati disegnati altri sistemi elettrofilati a base di polisaccaridi, sfruttando due diverse strategie: i) la deposizione strato per strato (anche detta *coating*) dei polisaccaridi su una matrice elettrofilata a base sintetica costituita da policaprolattone (PCL); ii) la produzione di una membrana elettrofilata a due strati, formata da uno strato meccanicamente stabile di PCL e uno strato bioattivo e a rilascio rapido a base di polisaccaridi.

Queste due tipologie di strutture sono state caratterizzate per la loro morfologia, per le cinetiche di rilascio dei polisaccaridi, la capacità di assorbire fluidi e la permeabilità al vapore acqueo. Hanno, inoltre, rivelato una buona biocompatibilità e bioattività nei confronti di fibroblasti umani del derma, la cui capacità di rigenerazione era incentivata dalla presenza delle membrane contenenti polisaccaridi.

In aggiunta, l'antibiotico rifampicina è stato addizionato allo strato di PCL, per conferire a queste medicazioni anche proprietà antibatteriche, senza però alterarne la biocompatibilità. Il rilascio di antibiotico così come l'attività antibatterica contro *Staphylococcus aureus*, *Staphylococcus epidermidis*, *Pseudomonas aeruginosa* ed *Escherichia coli* sono stati testati, mostrando una maggiore efficacia nei confronti degli Stafilococchi e di *Pseudomonas aeruginosa*.

1. INTRODUCTION

1.1. Non-healing (chronic) wounds

The skin (**Figure 1**) is the largest organ of human body, acting as a barrier which limits its dehydration along with protecting it from external insults. Consequently, preserving the integrity of skin is of pivotal importance to maintain organism stability.[1]

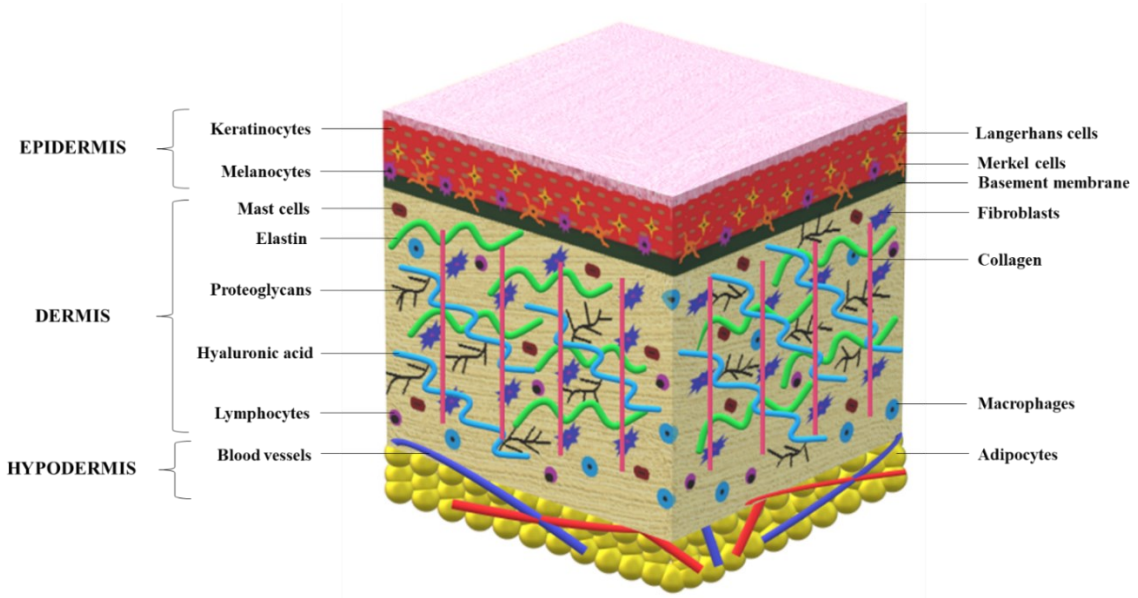

Figure 1. Schematic representation of skin anatomy with its main constituents.[2] Copyright (2021), with permission from Elsevier.

The presence of a skin damage (namely, a *wound*) in healthy patients activates a physiological healing path, which generally involves four subsequent stages: hemostasis, inflammation, proliferation, and remodeling (**Figure 2**).[3]

To prevent further blood loss from the injured site, platelets are immediately recruited in the ***i) hemostasis phase***, which results in the coagulation process. After that, platelets secrete cytokines (as the transforming growth factor-β, or TGF-β, and the platelet-derived growth factors, or PDGFs) which recall neutrophils to the site of damage, thus triggering the ***ii) inflammatory phase***. Neutrophils play a pivotal role in the healing process, since they exert an antimicrobial activity while secreting cytokines (as inteleukin-17, or IL-17) and growth factors (as vascular endothelial growth factor, or VEGF) with the function of recruiting inflammatory cells and stimulating keratinocyte, fibroblast,

and endothelial cell proliferation. Their action is carried out in 24 h, after which neutrophils undergo apoptosis. The ***iii) proliferation phase*** usually starts in 2-3 days with the deposition of granulation tissue. Meanwhile, the presence of procollagen, elastin, hyaluronic acid, and proteoglycans stimulates cell growth together with the formation of new blood vessels: on the one hand, keratinocyte proliferation strengthens the barrier function against external insults; on the other hand, vessel growth ensures oxygen supply and leukocyte migration towards the regenerating tissue. During the proliferation phase, even monocytes are recruited to the injured site by the cytokines secreted from apoptotic neutrophils and differentiate in macrophages to increase the resident macrophage population. By this point, macrophages switch from the proinflammatory phenotype (M1) to the anti-inflammatory one (M2) and the chemokines produced during this phenotypical change trigger the T cell response. The crosstalk between all the cell types is afterwards fundamental for the ***iv) remodelling phase***, in which extracellular matrix (ECM) deposition and angiogenesis go together with collagen deposition and the control of matrix metalloproteinases (MMPs) activity, whose deregulation hampers an adequate wound closure.[3–6]

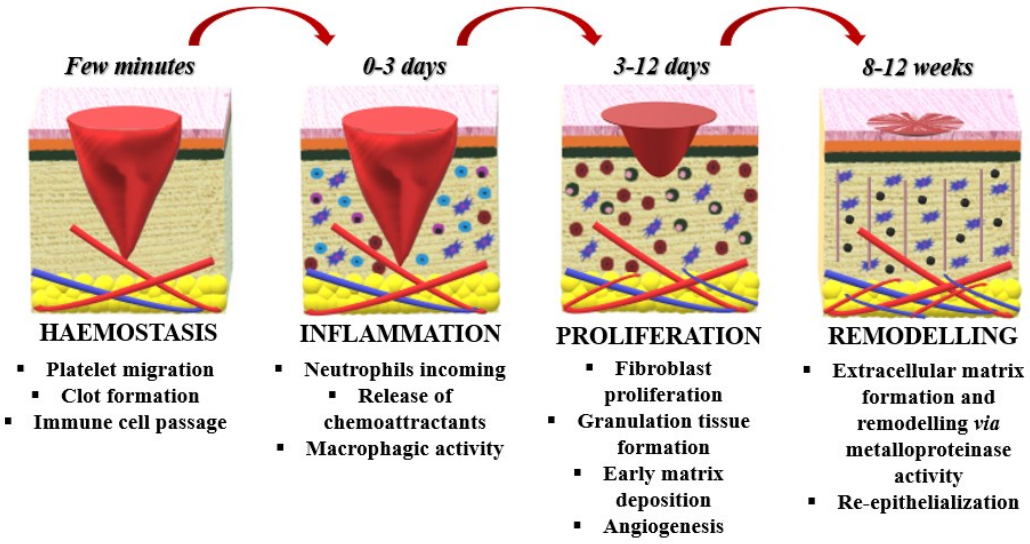

Figure 2. Schematization of the physiological healing path temporal progression.[2] Copyright (2021), with permission from Elsevier.

The ordered sequence of this phases represents the boundary line between acute and chronic (or non-healing) wounds. Depending on the extent of the damage, acute wounds (as skin abrasions, cuts,

burns, or surgical injuries) usually heal in 8-12 weeks following the physiological healing path in an orderly and timely manner.[7–9] Conversely, *chronic wounds* fail this healing timeline, stalling in a self-perpetuating inflammatory phase and provoking fibrosis, tissue loss and laceration besides increasing the risk of infections. This can be particularly ascribed to pre-existing pathological conditions (such as diabetes, autoimmune diseases, or venous stasis) which then cause a lower mitogenic activity, growth factor secretion, and angiogenesis along with increasing the production of proteases, cytokines, MMPs, and reactive oxygen species (ROS), which destroy the ECM.[10–15]

Based on their etiology, the Wound Healing Society classifies non-healing wounds in four main categories: i) pressure ulcers, ii) diabetic ulcers, iii) venous ulcers, and iv) arterial insufficiency ulcers. Chronic wounds may require also years or decades to completely heal, heavily affecting patient's quality of life, since they lead emotional and physical trauma which can sometimes evolve in permanent disability (as in the case of limb amputation).[16]

Chronic wounds also represent a significant economic burden for the medical system. For example, only in the US they weight on the national health system for 25 billion dollar per year, with a simultaneous increase of 6.5 million patients every year.[17] Similarly, in the UK, with a rate of 100000 ulcers diagnosed every year, chronic wounds involve the 3% of the total healthcare costs,[18] while in Europe they require the 2% of the total healthcare budget.[19]

Considering this scenario, the need for strategies able to improve non-healing wound management, treatment, and resolution is urgent to increase patients' life expectancy as well as ensuring an easier administration at the expense of the healthcare systems.

1.1.1. Wound dressings – definition

The standard clinical practice for wound management includes surgical debridement and negative pressure treatment to clean and prepare the wound bed, with the aim of stimulating the endogenous healing process and to accelerate the effectiveness of the adopted therapeutic measures. After that, a

wound dressing must be applied to protect wound microenvironment, which is intended as a protective device useful to accelerate the healing response and fasten its closure. The choice of the specific wound dressing is then based on the pathophysiological healing process as well as on the type of wound to be treated.[20,21]

There is no unanimity on the definition of the characteristics an ideal wound dressing should possess, but there are certainly some key factors influencing the goodness of the adopted device in favoring tissue regeneration (**Table 1**). Biocompatibility, antimicrobial, hemostatic, and anti-scarring potential, ability to absorb exudates and gas permeability while maintaining a moist environment, mimicking of the extracellular matrix structure and mechanical properties, biodegradability, and adaptability to the wound shape are among the most significant. They should also be designed to limit the frequency of dressing changes, which are associated to patient's discomfort and wound mechanical stresses.[22–31]

Particular attention must be paid to moisture retention capacity, as in 1962 Winter demonstrated that a moist environment accelerates epithelial healing compared to dry wounds exposed to air only.[32] Indeed, the moist environment seems to favor cell regeneration and motility allowing at the same time enzymatic activity, collagen deposition, and functionality of epidermal growth factor. For this reason, an effective wound dressing should ensure a proper equilibrium between moisture retention and gas permeability, thereby enhancing skin regeneration.[33,34]

Table 1. Main features required to an ideal wound dressing to enhance the healing process, re-epithelialization, and functional recovery, avoiding scar insurgence.[2] Copyright (2021), with permission from Elsevier.

Wound dressing properties	Relevance
Biocompatibility	It is the first prerequisite of material safeness
Biodegradability	A biodegradable material, which follows tissue regeneration, leaves space to the new healthy tissue also minimizing the need for dressing changes
Non-immunogenicity	No adverse immune response must be directed against the dressing selected
Conformability to the wound	A wound dressing which adapts its shape to the wound site allows an efficient covering and fluid retention. Conformability has not to be confused with sticking to the wound surface, which is not a favorable condition
Moisturizing ability	A moist environment, in which exudate absorption and water vapor/gaseous exchanges are allowed, favors cell viability and migration as well as the deposition of collagen and the functionality of growth factors and enzymes involved in the healing process
Haemostatic activity	Haemostatic wound dressings avoid excessive bleeding, allowing the activation of the coagulation cascade and the healing process
Stimulation of cell migration and proliferation	The simultaneous action of different cell types (as immune cells, endothelial cells, fibroblasts, keratinocytes) allows the regulation of the inflammatory response, the deposition of the extracellular matrix, and the formation of new tissue
Avoidance of pathogen infections	The contamination of the wound compromises the success of the healing process, leading to a chronicization of the inflammation state and to the formation of necrotic tissue
Mimicking of skin architecture and mechanical properties	A wound dressing which recalls native tissue enhances cell colonization, proliferation, and activity leading to re-epithelialization
Maintenance of proper tissue temperature	A decrease in wound bed temperature below normal body values impairs the healing process, due to a reduction in cell activity and consequent slow epithelial regeneration and collagen deposition
Minimization of dressing changes	Dressing changes are painful and, in some cases, could cause secondary tissue damage, lessening the healing process
Cost effectiveness	A manageable and cost-effective material has more chances to encounter the market demand

1.1.2. Wound dressings – classification

Wound dressings can be classified in two main categories, namely passive and active (**Figure 3**). Traditional passive wound dressings are, for example, gauzes, plasters, or cotton wools. However, they only have the function to protect the wound site from the external environment, but they often dry the wound bed, thus impairing wound closure without stimulating any regenerative response. Furthermore, they require frequent changes to limit the risk of infection and the wound adherence due to excessive exudate evaporation.[35]

For this reason, attention was focused on a new generation of materials (namely, the active wound dressings) that are able to actively interact with the surrounding damaged tissue, thereby being involved in the wound healing process. Indeed, active dressings are specifically designed to ensure proper moisture retention while acting as a barrier against pathogens and promoting tissue structural and functional recovery.

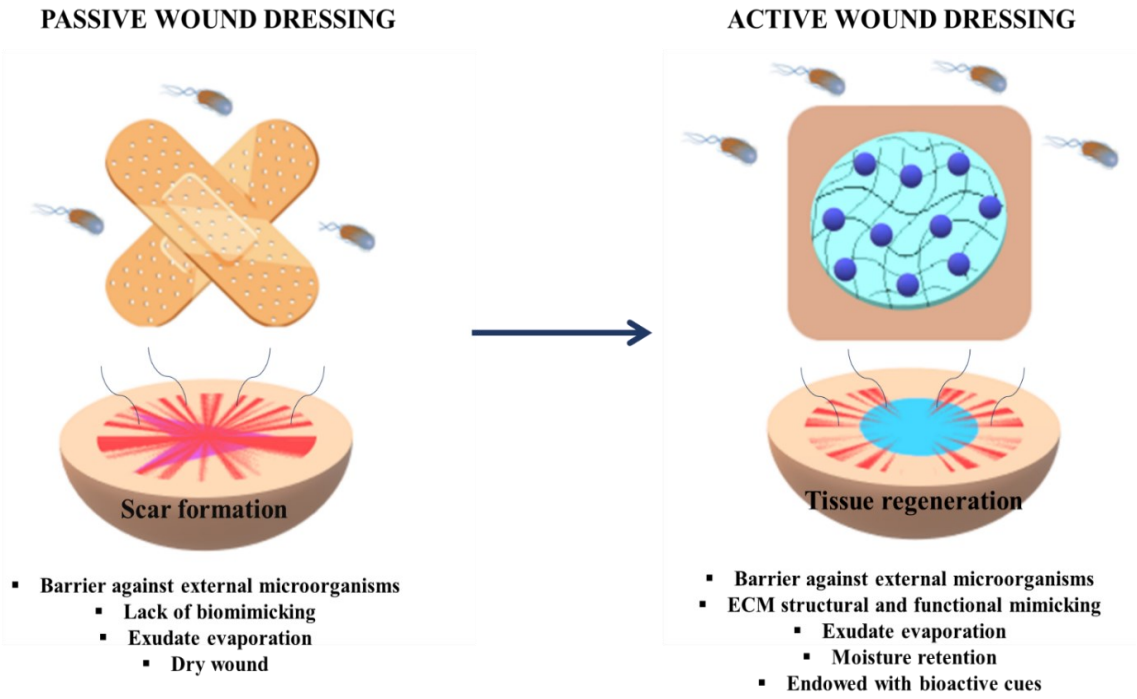

Figure 3. Schematization of the wound dressing main features, highlighting the advantages of using active wound dressings rather than passive ones.[2] Copyright (2021), with permission from Elsevier.

The main active dressings currently studied or used in the clinical practice can be divided in semi-permeable films, semi-permeable foams, hydrogels, hydrocolloids, alginate dressings, and bioactive dressings.[9,36,37]

Semi-permeable films were originally produced as nylon derivatives equipped with an adhesive polyethylene support. However, in this formulation they are occlusive and do not allow exudate absorption, leading to skin maceration and infection along with requiring frequent dressing changes.[38] For this reason, they were substituted with polyurethane-based dressings, able to adhere and adapt to the wound shape while promoting re-epithelialization. Indeed, they are occlusive for bacteria and water, but not for gases. This means that, in the presence of mild exudates, the exudate accumulation within the wound bed encounters its evaporation throughout the film dressing. Moreover, polyurethane films are transparent, allowing wound assessment and limiting dressing substitution.[39] Commercial semi-permeable films are, as few examples, Opsite™, Bioclusive™, or Tegaderm™, which differ for specific features, such as permeability, conformability to the wound, or adhesiveness.[40–42] These products are particularly indicated in case of superficial wounds with mild exudates, but they cannot maintain the moisture equilibrium over a certain amount of liquid. In addition, in some cases they can adhere and seal to the wound bed, causing skin laceration during dressing removal.[43,44]

Semi-permeable foams are typically made of polyurethane, but contrary to semi-permeable films they can be employed even in case of heavy exudating wounds. In addition, they act as a cushion over the wound, promoting autolytic debridement and gaseous exchanges. In some cases, they cannot well adapt to the wound, and are used together to secondary dressings to ensure their stabilization.[45] This is the case, for example, of Cutimed® Siltec, endowed with a silicon contact layer.[46] Even multilayer foam dressings have been commercialized, with the specific aim of avoiding wound adherence, possible infections, and patient's pain. Examples of this are Allevyn™ and Tielle™, structured in three distinct layers. The first one, comprises an outer impermeable polyurethane layer, a central

absorbent hydrocellular layer, and an inner porous layer designed to avoid epidermal cell migration into the dressing and allow an easy removal. The second one is divided in a polyurethane adhesive layer and a thin polyurethane foam membrane enriched with a central hydrophilic polyurethane foam layer which should prevent the dressing from completely drying out, to maintain a moist microenvironment, allowing non-traumatic removal and gaseous exchanges while blocking microorganisms entrance.[47,48] Nevertheless, foam dressings are not indicated for eschars or dry wounds since their high absorption capability could cause wound bed adherence with subsequent difficult and painful dressing removal.[49]

Hydrogels are crosslinked polymer-based three-dimensional matrices which can hold up to 90% of liquid (generally, water). Thanks to their water retention capacity, they can both provide water to dry wounds and absorb, on the other hand, moderate amount of exudate, thus maintaining a moist environment. Moreover, they promote necrotic debris removal, favor oxygen exchanges through the surface, and stimulate epithelial regeneration. The dressing changes are barely painful in the case of hydrogels and their features (as chemical, mechanical, physical properties as well as their flexibility) can be modulated in a precise manner, varying, for example, their composition or production method.[50–52] Several hydrogel-based commercial products (such as TegaGel®, Nu-Gel®, Carrasyn®Gel) have been made available over the years. However, they possess poor mechanical stability and cannot properly serve as bacterial barrier alone, requiring the addition of antimicrobials to avoid wound contamination. Further, the high-water content delivered to the injured site can provoke, in some cases, skin maceration and dressing immersion in the surrounding damaged tissue. For this reason, their employment must be considered on the basis of the amount of exudate a wound is able to secrete.[44,53]

Hydrocolloids are interactive absorbing dressings made of a hydrophobic pressure sensitive layer (continuous phase) and a hydrophilic filler (dispersed phase). This specific design enables self-adhesiveness and humidity regulation ensuring, at the same time, the absorption of fluids and the

autolytic debridement.[54,55] The continuous phase is often represented by elastomers or adhesives (as polyisobutylene and styrene-isoprene-styrene copolymer); the dispersive component is, instead, characterized by gel forming agents (as carboxymethylcellulose, gelatin, or pectin). In particular, the hydrophilic phase can absorb large amount of exudate turning into a hydrophilic gel, thereby eliminating the excess of fluid, and limiting skin desiccation. On the other hand, the hydrophobic layer acts to prevent bacterial infection and maintains proper wound temperature.[9,56,57] Hydrocolloids are largely employed wound dressings. Moreover, due to their ease and painless removal, they are particularly useful even for pediatric wounds (as in the case of DuoDERM®).[58] Nevertheless, their employment is not recommended when the damaged tissue is already infected, since the hypoxic and excessively moist environment could enhance necrotic tissue autolysis and facilitate microorganism proliferation.[53,59,60]

Alginate dressings are non-toxic, highly absorbing, non-adherent, and, in the presence of wound exudates, they can turn into highly hydrated gels. Their properties vary depending on their formulation, since they can be rich in mannuronic acid (as Sorbsan™ or Tegaderm™ Alginate Ag) or in guluronic acid (as Kaltostat™ or SeaSorb™). Indeed, alginate is a polysaccharide copolymer given by a linear repetition of (1 → 4)-linked β-D-mannuronic acid (M) and α-D-guluronic acid (G) residues. In the presence of divalent cations (especially Ca^{2+}) it undergoes ionotropic gelation, during which G residues reorganize in a specific structure, namely the "egg-box". Consequently, the guluronic acid-rich alginate dressings are stronger and less flexible than mannuronic-acid rich ones when hydrated and they differentially contribute to the healing response. Indeed, upon interaction with the wound bed, considerable quantities of calcium ions are substituted in time by sodium ions, leading to gel formation and creating an adequate moist environment which promote re-epithelialization. Moreover, this ion exchange plays an active role in the coagulation cascade, which employs calcium ions.[61–65] Alginate dressings have been produced in different forms, such as films, foams, fibers, hydrogels, and hydrocolloids, in view of skin regeneration.[66] Notwithstanding all their

advantages, alginate dressings should not be applied on dry wounds since their high fluid attraction ability could cause a burning sensation for the patient. Moreover, in these conditions an increased pressure could be exerted on the wound bed impairing the healing process and causing the formation of necrotic tissue.[67]

Bioactive dressings are an extended class of medical devices including all the biomaterials able to actively foster the wound healing response. This can be achieved by using naturally bioactive polymers or by endowing inert materials with bioactive moieties.[68] Indeed, many natural polymers (as chitosan, hyaluronic acid, collagen, to name some) possess intrinsic antimicrobial, hemostatic, anti-inflammatory, and other bioactive properties which make them suitable candidates in the field of wound care.[69–73] In other cases, the dressing materials can be enriched, for example, with antimicrobial compounds, growth factors, anti-inflammatory drugs, and other substances able to locally stimulate cellular activity while avoiding any pathogen infection and adverse responses. This confers bioactive dressings an additional asset over non-functionalized materials to support the reconstruction of tissue architecture and function.[74–76]

The strategies for clinical wound care currently include another class of biomaterials, namely **tissue engineered skin substitutes**, which not only assist skin regeneration, but have the specific function to substitute the missing tissue. Tissue engineered skin substitutes can be classified, considering their application, in permanent, semi-permanent, or temporary; considering the tissue to be treated, in dermal, epidermal, or composite; and, considering their origin, in biological (autogenous, allogeneic, xenogeneic) or alloplastic (synthetic, composed by biocompatible polymer matrices).[77] Acellular, synthetic skin substitutes are, for example, Biobrane™, Alloderm™, and Integra™;[78–80] on the other hand, Dermagraft®, Apligraf®, or OrCel™, to name some, are example of cell-containing grafts.[81–83] Thanks to the abundance of commercial products, tissue engineered skin substitutes are a good alternative in the treatment of unhealed skin injuries which fail the traditional wound care line.

Nonetheless, they still present substantial drawbacks, as they can induce scarring, immune rejection, and fail integration with the surrounding tissue along with precluding a correct revascularization, which leads to cell death. Added to this, they cannot exactly recreate the anatomy, physiology, biology, and aesthetic of the damaged skin besides requiring high production costs. Therefore, the research of new materials able to mimic the architecture and biology of natural human skin in a cost-effective and feasible way still represents an urgent medical need.[84–87]

1.2. Electrospinning

The extracellular matrix (ECM) can be considered as a natural scaffold, whose topology and geometry affects cell physiology and tissue remodelling.[88] Therefore, when considering biomaterials for tissue regeneration (as in the case of non-healing wounds) their ability to reproduce ECM structure is an important parameter that has to be examined in its complexity, since ECM is composed by interconnected fibrous structural proteins (collagen, elastin, laminin among the most abundant), polysaccharides (which include glycosaminoglycans, as hyaluronic acid), and proteoglycans (which are formed by glycosaminoglycans attached to ECM proteins, as chondroitin sulfate).[89,90]

In this context, electrospinning emerged as a simple and effective technique to produce biomimetic nanoscale/microscale fibrous scaffolds. It consists of an electro-hydrodynamic process exploited to synthetize membranes with thin polymeric fibers, a large surface area, and high porosity. The electrospinning benchtop apparatus (**Figure 4**) consists of a high voltage power supply, a spinneret (frequently, a needle-equipped syringe) located on a syringe pump, and a metallic collector. The polymers of choice are dissolved in their own solvent (or, sometimes, mixtures of solvents); then, the solution is loaded into the syringe and extruded through the needle, controlled by the syringe pump. In this process, a high voltage (generally, 5–30 kV) is applied on the polymeric solution to increase its surface charge density, leading to the formation of a cone-like drop (namely, "Taylor cone") at the tip of the needle; if the electric field applied overcomes the liquid surface tension, a continuous

filament is produced and accelerated towards the collector of opposite polarity. In the space between the needle and the collector, the polymer jet stretches and elongates, the solvents evaporate, and the polymers are deposited on the collector as non-woven ultra-fine fibers.[91–94]

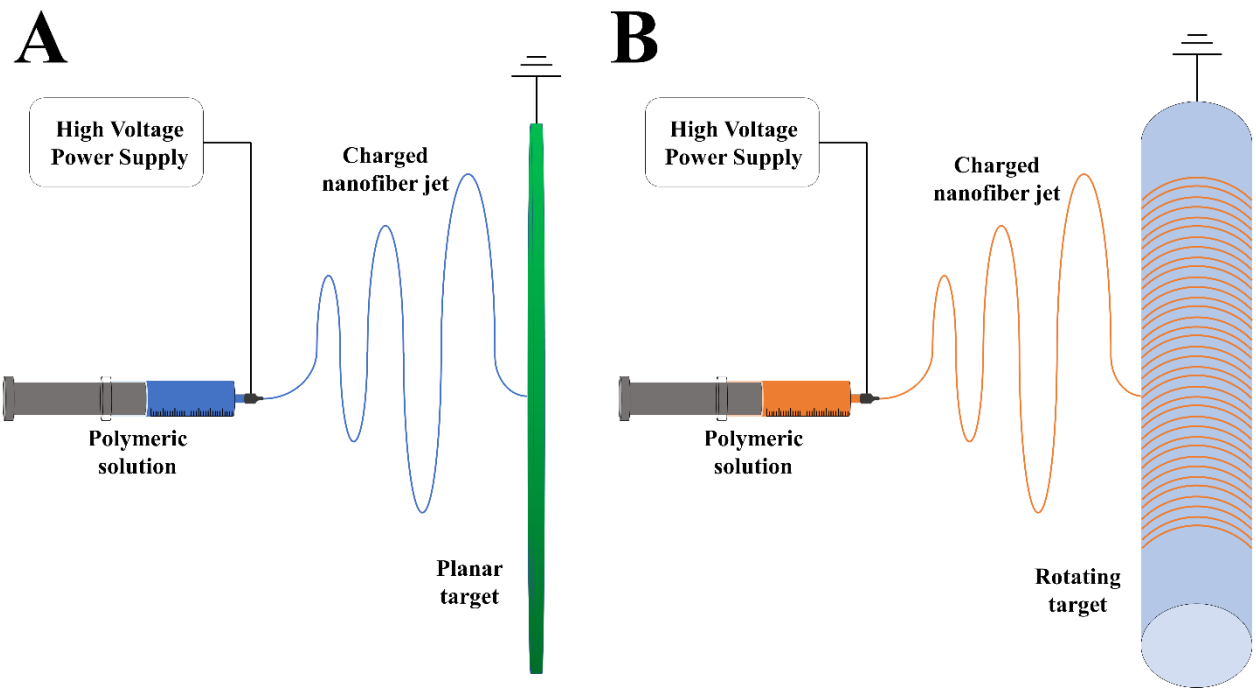

Figure 4. Schematization of the electrospinning apparatus. The high voltage power supply is connected both to the spinneret and the collector to overcome polymer surface tension at the tip of the needle and allow fiber deposition. Two types of setups are here illustrated: **A)** planar target for the preparation of planar membranes; **B)** rotating target (or mandrel) for the preparation of tubular scaffolds.[2] Copyright (2021), with permission from Elsevier.

The electrospinnability, intended as the ability to produce mats with a certain fiber diameter and porosity starting from a specific polymer solution, depends on several parameters, namely solution (concentration, viscosity, electrical conductivity, surface tension, polymer molecular weight), process (voltage, injection rate, needle-collector distance, type of collector), and environmental (temperature, relative humidity) parameters.[92,95,96]

The physical properties of the obtained fibers can be tailored by adjusting the electrospinning apparatus configuration (vertical or horizontal) or by modifying the geometry of the collector (for example, disks or mandrels). Moreover, basing on the spinneret (as in the case of coaxial needles) it is possible to ameliorate the ability to incorporate bioactive compounds and modulate their release in time, promoting tissue restoration.[97–102]

Looking at the versatility of the electrospinning technique, its success even in the field of wound care is noticeable. Indeed, the obtained nanofibrous matrices, with their interconnected porous structure, recall ECM architecture guiding cellular crosstalk between the dermal and epidermal layers. With a diameter falling in the range of collagen fibers (50–500 nm), electrospun nanofibers also provide mechanical and biochemical support and can be engineered with biological cues specifically selected to enhance tissue repair and/or prevent the insurgence of infections.[103] They provide a high contact surface area for exudate absorption and water vapor/gas exchanges, with a hemostatic and anti-scarring potential. In fact, the moisturizing ability accelerate tissue repair and wound closure, avoiding scar formation. Electrospun mats are even highly flexible and, when the tensile strength is high enough, they well adapt to the wound shape without the addition of secondary dressings. Besides, the wide variety of polymers to be used and combined allow the reproduction of the physiological microenvironment either from a structural and compositional perspective.[104–107]

1.2.1. From synthetic to natural polymers

The choice of the polymers to be used for electrospun membrane preparation is one of the most important factors to pursue a wide-ranging mimicking of the extracellular matrix (ECM). In fact, on the chemical nature of such polymers depends dressing degradability, resistance, mechanical properties, similarity to ECM components, and all that characteristics which define membrane architecture and conformability to the injured site along with its bioactivity and capability to recreate a suitable environment for tissue regeneration.[108–111]

The use of synthetic polymers has known a considerable increase in the last 15 years and most of them have been approved by the Food and Drug Administration (FDA) for clinical application. Indeed, many synthetic polymers (polyurethane, polyethylene oxide, poly(lactide-co-glycolide), poly(vinyl alcohol), poly- ε-caprolactone, to cite the most used) possess numerous features, such as mechanical strength and integrity, good degradation profile, possibility of surface modifications, or thermal stability, which allow them to be exploited for the synthesis of a wide range of medical

devices, as electrospun matrices and scaffolds.[112–114] Among them, **poly-ε-caprolactone (PCL)** (**Figure 5**) is one of the most employed due to its biocompatibility, long-term stability, and low-cost availability. It is a hydrophobic semicrystalline linear aliphatic polyester slowly degraded (2 - 4 years) upon hydrolysis of the ester bonds in physiological conditions, while preserving high mechanical properties.[115–117]

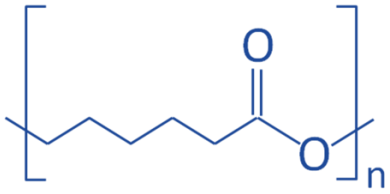

Figure 5. Chemical structure of poly-ε-caprolactone (PCL).

Polyethylene oxide (PEO) (**Figure 6**) is another frequently used FDA-approved synthetic polymer, thanks to its biocompatibility and water-solubility. It is a hydrophilic inert semicrystalline polyether with excellent thermal and mechanical stability, whose hydroxyl termination ensure a high water-absorption capacity. [118–120]

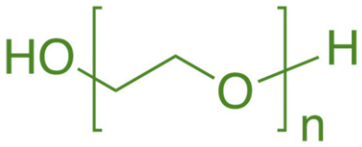

Figure 6. Chemical structure of polyethylene oxide (PEO).

Synthetic polymers can be used alone or can be mixed to synergistically combine their properties and control the release of bioactive compounds. As an example, Kim and co-workers mixed hydrophobic polymers (poly- ε-caprolactone [PCL], poly- L -lactic acid [PLLA], and poly(lactic-co-glycolic acid) [PLGA]) with the hydrophilic poly(ethylene oxide) [PEO] to selectively incorporate lysozyme in the electrospun mat and tune its release. The PCL/PEO blend revealed a better morphological stability in aqueous environment with respect to the other tested mixtures, with a sustained lysozyme release over time. In addition, as its release depended on the PEO degradation profile, it could be tuned by varying polymer ratio.[121]

Notwithstanding all the benefits offered by synthetic polymers in the fabrication of stable electrospun membranes, the basically hydrophobic nature of the majority of these polymers and the lack of biological signals which could induce cell attachment, growth, and differentiation often limit their employment.[122] For this reason, the attention moved towards natural polymers, namely proteins (as collagen, elastin, silk fibroin) and polysaccharides (as hyaluronic acid, chitosan, alginate). Indeed, some of them, as collagen or hyaluronic acid, are natural components of the ECM, thus allowing even a compositional mimicking of the natural microenvironment. Moreover, they are intrinsically biocompatible, hydrophilic, and possess biological cues recognized by cells, thus serving as tissue regeneration matrices (**Table 2**).[123–125]

Table 2. Summary of the main differences between synthetic and natural polymers basing on peculiar features in the field of wound healing.[2] Copyright (2021), with permission from Elsevier.

	Synthetic polymers	***Natural polymers***
Biocompatibility	Good	Excellent
Biodegradability	Low	Fast
Immunogenicity	Low	Absent
Hydrophilicity	Low	High
Thermal stability	High	Low
Mechanical strength	High	Low
Molecular interaction with cells	Absent	Present
Bioactive properties	Absent	Present

However, even the use of natural polymers brings some drawbacks, since they exhibit weak mechanical properties and their electrospinnability is hampered by their solubility and by the characteristics of the aqueous solutions of these polymers, such as their viscosity, conductivity, and surface tension. Thus, blending natural and synthetic polymers has been found to be an efficient strategy to combine the bioactive properties of the natural polymers with the mechanical strength and stability of synthetic ones.[126,127] Nevertheless, a successful blending entails the knowledge of polymer chemical properties since their miscibility depends on specific interactions between polymers chains.

In addition, once assessed the compatibility of such polymers, particular attention must be paid on the choice of the solvent to be used, since its evaporation rate affects fiber deposition and morphology as well as the porosity of the resulting nanofibrous matrix. It must also be considered that many synthetic and natural polymers are not water-soluble, hence organic solvents must be employed, such as acetic acid, trifluoroacetic acid, dimethylformamide, chloroform, formic acid, or solutions based on fluoroalcohols, whose toxicity must not be underestimated. These organic solvents are easily manageable due to their high volatility, and are used alone, or they can be properly mixed to improve polymer solubility.[114,128–136]

1.2.2. Polysaccharides

Among natural polymers, polysaccharides stand out in the field of wound care for their stunning properties as active healing promoters. Indeed, they favor tissue regeneration and restoration both from a structural and functional standpoint, recreating the physiological wound environment and guiding cellular response towards a traditional healing path.[137–139] Most of them are abundant in nature and, beyond their excellent biocompatibility, they even offer several advantages over other polymers, as antimicrobial, hemostatic, or anti-inflammatory properties along with the ability to reproduce extracellular matrix (ECM) architecture and composition. Moreover, due to their low immunogenicity, natural polysaccharides do not trigger adverse immunogenic responses, but rather interact with immune system components activating macrophages, which are active players in the wound healing process.[140]

Considering the wide variety of available polysaccharides (as hyaluronic acid, chitosan, alginate, cellulose, dextran, pectin, to name some),[141–147] hyaluronic acid and chitosan are amongst the most employed for wound healing purposes.

Hyaluronic acid (**Figure** 7) is one of the main ECM components, being particularly attractive in the design of medical devices for skin repair. It is a high molecular weight non-sulfated

glycosaminoglycan, structured in a linear repetition of (β1 → 4)-glucuronic acid and (β1 → 3)-N-acetyl-D-glucosamine residues.

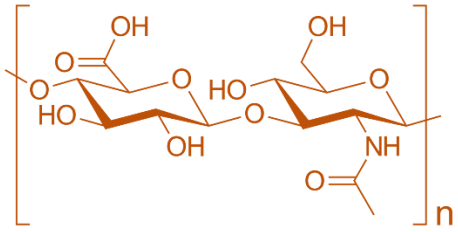

Figure 7. Hyaluronic acid chemical structure.

It is particularly abundant in the ECM of skin, which contains at least 50% of the hyaluronic acid total body amount, but it is also present in many connective tissues, as cartilage, vitreous body, or synovial fluid. Hyaluronic acid is essential in many biological processes, like tissue homeostasis, angiogenesis, tumor biology, and anti-apoptosis activity. All these features, together with its intrinsic biocompatibility, biodegradability, and viscoelasticity are of paramount relevance for wound healing applications.[148,149] In addition, hyaluronic acid high hydrophilicity along with its lubricant and moisturizing properties contribute to skin hydration and reduce the possibility of biofilm formation.[150,151] Hyaluronic acid is even recognized by cells through the membrane receptor CD44, where the molecular recognition promotes cell adhesion, proliferation, and differentiation.[152]
Considering its bioactive properties, hyaluronic acid has been studied for its anti-inflammatory and antioxidant abilities; indeed, it is involved in all phases of the inflammatory response: it regulates inflammatory cell migration, interacts with inflammatory elements, and performs a scavenging activity towards reactive oxygen species (ROS) and hydroxyl radicals. For all these reasons, it is largely employed as dermal filler, substrate for dermal regeneration, and in the production of wound dressing materials.[153,154]

Chitosan (**Figure 8**) is a high molecular weight polysaccharide composed by (β1 → 4)-linked glucosamine and N-acetylglucosamine residues, in variable percentage. It derives from the

deacetylation of chitin, a natural constituent of the exoskeleton of crustaceans, cuticles of insects, and cell walls of many fungi.

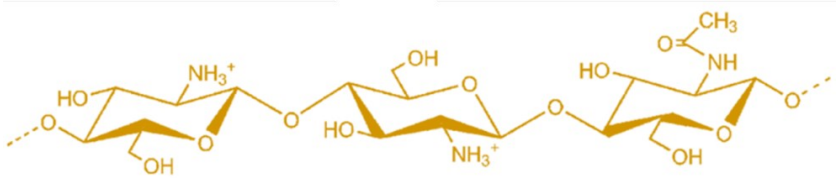

Figure 8. Chitosan chemical structure.

Thanks to its outstanding combination of properties, as biocompatibility, biodegradability, chemical and thermal stability, and cost-effectiveness, this polysaccharide has been widely exploited for biomedical purposes, from drug delivery to wound care. Indeed, it possesses also hemostatic and mucoadhesive properties; it supports the epithelialization process and reduces blood loss while promoting and strengthening blood clots, thus accelerating the healing process. Furthermore, chitosan even exerts an antimicrobial activity, protecting against a wide range of bacteria. Therefore, it is largely employed as hemostatic wound dressing as well as in the preparation of antiseptic bandages.[155–158] The ability of chitosan to favor the coagulation process relies on its polycationic nature since the positive charges interact with negatively charged red blood cell membranes, thus promoting platelet adhesion, activation, and aggregation as well as the adsorption of plasmatic fibrinogen, the increase of its local concentration, and complement activation. In addition, the activation of the healing process by means of chitosan-based materials depends on the surface available for the interaction with cells and coagulation factors, thus revealing the effectiveness of using electrospun dressings, in which the surface-to-volume ratio is maximized.[159] Thanks to the presence of numerous available amino groups, highly deacetylated chitosan can be exploited for the grafting of specific ligands, such as oligosaccharides.[160] Among them, ***CTL*** (1-deoxylactic-1-γ-L-chitosan) (**Figure 9**) is a hydrophilic lactose-modified chitosan obtained by reductive amination with the lactose aldehydic group.

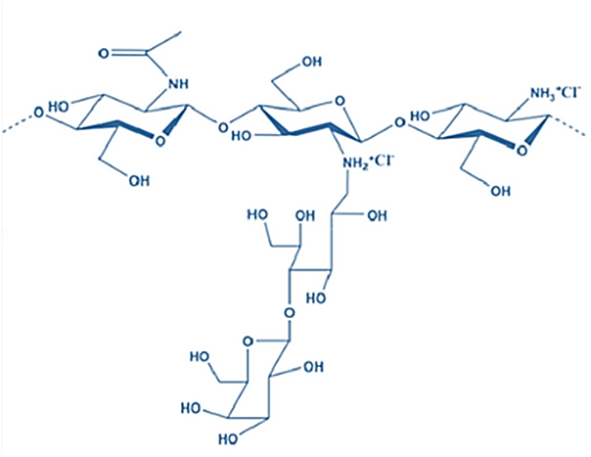

Figure 8. CTL chemical structure.

This confers CTL several chemical-physical advantages over chitosan, including the higher water solubility at neutral pH values,[161,162] allowing the employment of non-toxic solvents and increasing the biocompatibility of the final product. CTL even possesses bioactive properties; for example, it encourages the aggregation of articular chondrocytes by inducing the production of glycosaminoglycans and type-II collagen and interacting with Galectin-1[163] or it promotes the differentiation of multipotent stem cells (namely, human dental pulp stem cells) into an osteoblast phenotype.[164] More recently, even the anti-inflammatory properties of CTL on human dermal fibroblasts have been studied, revealing its ability (alone or in combination with hyaluronic acid) to counteract the oxidative damage and reduce the levels of inflammatory cytokines along with inhibiting the matrix metalloproteinase-3 (MMP-3) activity and exerting a pro-regenerative effect on the ECM.[165]

Consequently, the investigation of CTL as possible candidate in the production of electrospun matrices for wound dressing development should bring considerable advantages in the field of wound care.

1.3. Polysaccharide-based electrospun wound dressings

Polysaccharide-based electrospun wound dressings combine the innumerable benefits of electrospun nanofibrous biomimetic matrices with the potential of polysaccharides as wound healing promoters, even offering the possibility to incorporate additional bioactive compounds able to enhance and broaden the intrinsic bioactivity of carbohydrate polymers.[166–169] However, there are some critical issues to consider, particularly related polysaccharide electrospinnability, stability in water, and mechanical strength, which could hinder their employment in the development of devices and in the clinical practice.

1.3.1. Polysaccharide electrospinnability

As mentioned in *section 1.2.1*, the electrospinnability of polysaccharides alone brings some concerns due to their viscosity, surface tension, and electrical conductivity as well as their molecular weight and chain entanglement,[170–173] requiring the association with a synthetic and easily spinnable counterpart.[174–176]

Among the physicochemical features of the polysaccharidic solutions, the surface tension is an essential parameter to consider, since surface tension disruption at the tip of the needle is necessary to allow the formation of the filament during the electrospinning process and to control fiber morphology and diameter.[177,178] For this reason, not only mixtures of synthetic and natural polymers, but even the addition of surfactants as Tween® 20 has been proven to be an efficient strategy to decrease solution surface tension and conductivity, thus allowing polysaccharide spinnability and leading to the formation of thin and bead-free fibers.[179,180]

1.3.2. Stability and crosslinking

The electrospinning of polysaccharides also requires post-processing steps, due to the high hydrophilicity and instability in water of the obtained products. Indeed, considering their application

as wound dressings, the ability to resist in an aqueous environment as well as the swelling capacity and the possibility to absorb fluids is fundamental.[181,182]

Therefore, to avoid the rapid hydrolysis of polysaccharide-based electrospun wound dressings in an aqueous environment, an adequate crosslinking procedure must be carried out not only to stabilize the structure but also to preserve its fibrous matrix and mechanical properties.[183,184] Different strategies have been attempted over the years in order to crosslink natural polymer biomaterials, ranging from chemical to enzymatic to physical methods: chemical crosslinking involves the formation of covalent bonds between polymer chains, using coupling and crosslinking agents;[185] physical crosslinking includes strategies such as irradiation (γ-irradiation, UV irradiation, high-energy electron beam irradiation) or heat treatments;[186] enzymatic crosslinking considers the employment of specific enzymes (such as transglutaminase, oxidoreductases) to catalyze crosslinking chemical reactions.[187]

More in detail, the **chemical crosslinking** has been widely explored in the last ten years to realize natural polymer crosslinking. Among the various strategies attempted, glutaraldehyde has been largely employed as chemical crosslinking agent; however, its use is associated in some cases to by-product cytotoxicity and a low crosslinking reactivity.[188–191] On the other hand, despite its high cost, genipin has also been studied as crosslinker for biopolymers containing free primary amine groups since it exhibits lower toxicity after crosslinking if compared with glutaraldehyde.[192–194]

Likewise, carbodiimide-based crosslinkers are one of the most used classes of chemical crosslinkers and, among them, EDC and NHS (1-ethyl-3-(3-dimethylaminopropyl) carbodiimide – N-hydroxysuccinimide) are the most represented. Carbodiimide-based coupling agents have the advantage to be less toxic than glutaraldehyde, in addition to a high conversion efficiency and to the ability to act also in mild reaction conditions.[195–198]

Carbonyldiimidazole (CDI) (**Figure 9**) represents another effective carbodiimide coupling agent that mediates the formation of amide bonds between carboxyl- or hydroxyl-groups and aminic moieties without being incorporated.[199]

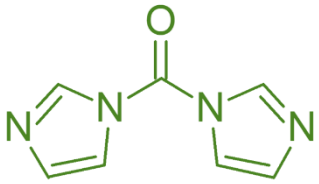

Figure 9. Carbonyldiimidazole (CDI) chemical structure.

For instance, CDI has been studied as covalent crosslinker to immobilize specific molecules on the surface of electrospun membranes, as reported by Bastürk and co-workers, which exploited CDI to covalently bind α-amylase on the surface of poly(vinyl alcohol)/poly(acrylic acid) (PVA/PAA) matrices.[200] It has also been employed as crosslinker in pullulan/gelatin hydrogels, with a "one-step" method employing aqueous DMSO as reaction solvent.[201] However, its use as coupling agent for electrospun nanofiber stabilization is not documented until 2022.

Physical crosslinking is mainly performed using UV irradiation, which, in the presence of a specific photoinitiator, allows radical formation, thus activating chemical groups on polymer chains and leading to the formation of a crosslinked network; however, despite its efficacy, it can cause a partial degradation of the polysaccharide contained into the membrane.[202,203] Methacrylic anhydride is a methacrylating agent often used to chemically modify polymer chains through the introduction of methacryloyl moieties, allowing thereafter the photo-crosslinking of the methacrylated polymers, without affecting the biocompatibility of the final product.[204–210]

As an alternative physical method, controlled thermal treatment has been attempted, because it induces the crystallization of the electrospun polymers, promoting chain entanglement and stabilizing the resultant structure.[211]

Despite the myriad of available crosslinking strategies, there is not absolute concert in the choice of the best crosslinker, since all the agents in use present both advantages and disadvantages, depending on the crosslinking mechanism as well as on the composition of the membrane itself, whose nanofibrous structure should be preserved since it confers electrospun matrices several advantages over the other types of wound dressings.

1.3.3. Mechanical support

The mechanical strength of polysaccharide-based electrospun membranes still represents a critical issue in defining the goodness of the final medical device. Indeed, polysaccharides possess poor mechanical properties, thereby requiring the association with the stronger synthetic polymers. Blending natural and synthetic polymers is the most common approach to improve both the electrospinnability and mechanical stability of polysaccharidic electrospun wound dressings.[212–214] However, even the production of multilayer electrospun matrices has been proven to be a valid method to obtain mechanically stable and easy to handle nanofibrous wound dressings.

This can be achieved by exploiting the layer-by-layer deposition of polysaccharidic coatings on synthetic-based electrospun products, thus combining in an ease and effective way the mechanical stability of the synthetic nanofibrous and highly porous matrices with polysaccharide bioactivity and ability to interact with the surrounding wound microenvironment.[215–218]

By following a different strategy, electrospun bilayer structures have been produced, with the purpose to closely mimic extracellular matrix (ECM) structure and composition: the synthetic part of the scaffolds is thought to provide mechanical support and stability, whereas the polysaccharide-based layer is functional to skin regeneration by maintaining proper wound bed hydration and quickly delivering bioactive polymers to the damaged tissue.[219–221]

Depending on the production method of such multilayer electrospun matrices, the availability and release of the polysaccharides can be tuned, thereby widening the range of applicability to different

types of wounds, whose treatment should be assessed each time even considering the extent of the damage.

1.3.4. Biofunctionalization

Although some polysaccharides own intrinsic biological properties, advanced wound dressings are often endowed with specific therapeutic agents, which can be topically released to further stimulate the progression of a normal healing path and promote total tissue recovery in an aseptic microenvironment. Thus, the implementation with bioactive compounds (also referred to as "biofunctionalization") which could exert an antimicrobial action as well as accelerate re-epithelialization and limit the pain associated to the wound and the inflammatory process is of great importance in the design of an electrospun wound dressing. [222–224] This implies the use of tailored incorporation strategies which do not alter solution parameters or the stability of the membrane to achieve a fine control of the functionalization efficiency and the degradation rate and tune the release profile of such compounds. [225,226]

The bioactive compounds that can be added to electrospun membranes and scaffolds can be chosen basing on their natural involvement in the healing process or according to their ability to assist this process. For example, growth factors are involved in angiogenesis, tissue regeneration and remodelling;[227,228] vitamins (as vitamin E, D, or C) seem to promote angiogenesis, re-epithelialization, and granulation tissue formation, while avoiding scar formation and exerting an anti-inflammatory and antioxidant activity;[229–231] anti-inflammatory, analgesics, and anesthetic drugs can be used to reduce patient's pain.[232–234] The wound site is often susceptible to infections, so measures to prevent the infiltration and growth of bacteria and other microorganisms are needed, paving the way for a variety of antimicrobic biohybrid dressings.[235] Indeed, electrospun matrices can be enriched with antibiotics, for example ciprofloxacin, metronidazole, and mafenide acetate, or antibacterial wide spectrum agents, such as silver nanoparticles, zinc oxide nanoparticles,

antimicrobial peptides. These compounds are already widely employed in case of infected wounds or are adopted to enhance the antimicrobial behavior of wound dressings.[131,236–239]

Among antibiotics, **rifampicin** (**Figure 10**) is one of the most effective broad-spectrum bactericidal antibiotics, which blocks the RNA-polymerase β subunit, inhibiting the transcription and subsequent bacterial protein synthesis.[240,241] Despite its large employment to treat *Mycobacterium tuberculosis* infections, it demonstrated its activity even against a wide range of both Gram-positive and Gram-negative bacteria, being particularly effective in the case of biofilm formation by Staphylococci.[242–244]

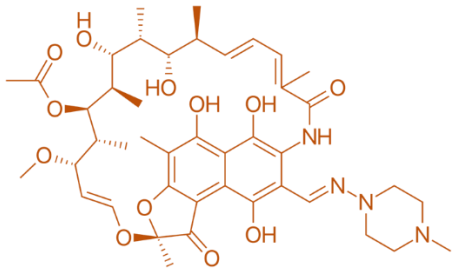

Figure 10. Chemical structure of rifampicin.

Several polymers, such as poly(lactic acid), poly(vinyl alcohol), or poly(lactic acid-co-glycolic acid) have already been combined with rifampicin to confer antibacterial properties to nanofibrous structures.[245–247] Among them, rifampicin-loaded PCL membranes for orthopedic application have been characterized, revealing their antibacterial effect against *Pseudomonas aeruginosa* and *Staphylococcus epidermidis* in the first 6 h.[248]

Hence, the porous and nanofibrous nature of electrospun wound dressings along with the high surface-to-volume ratio allow an efficient drug loading, whose release can be tuned by controlling fiber diameter, porosity, and surface area as well as using alternative electrospinning set-ups (as coaxial electrospinning).[107,249–252]

2. AIM OF THE STUDY

Notwithstanding the huge quantity of wound dressings already commercialized, the wound care practice still urgently needs new strategies to treat non-healing wounds, thus redirecting the abnormal wound healing process towards a physiological path and limiting undesirable outcomes for the patient.

In this context, the present thesis aims to produce a new class of bioactive wound dressings exploiting an advanced, simple, and effective technique, namely, electrospinning. Indeed, thanks to their ability to mimic the physical properties of extracellular matrix, with a highly interconnected porous structure and surface area, electrospun wound dressings appear to be particularly effective in promoting the healing process, while absorbing a large amount of exudate and maintaining a moist environment, and thereby avoiding scar formation. The use of natural polymers offers additional advantages to electrospun products, thanks to their bioactivity in a biomimetic approach which enhances wound closure.

The first aim of this thesis was the production of polysaccharide-based electrospun matrices using two different polysaccharides: i) hyaluronic acid, which is a natural component of the extracellular matrix; ii) a lactose-modified chitosan (CTL), which has never been electrospun before and has been studied for its anti-inflammatory properties in the wound microenvironment, among others.

The second aim of the present work was to stabilize the final structure of the polysaccharide membranes in aqueous environment, thus enabling their handling and employment as wound dressing materials while preserving the ability to absorb huge quantities of exudate and transmit water vapor throughout the wound.

Considering the mechanical weakness of polysaccharide-based electrospun products, the third aim of the work was to produce stable and easy-to-use electrospun matrices that can be applied to a wound.

To this end, two different strategies were investigated: i) the layer-by-layer (or coating) deposition of CTL and hyaluronic acid on an electrospun mat of the synthetic polymer polycaprolactone (PCL); ii) the synthesis of a two-layered electrospun system in which the polysaccharide layer is deposited on a PCL synthetic counterpart. This strategy should provide the final structure with adequate stability and mechanical strength thanks to the PCL layer, while at the same time endowing the matrix with bioactive polysaccharides differently released depending on the incorporation method.

Lastly, with the goal of ensuring a broad-spectrum activity against pathogens commonly present in the wound site, the wound dressing material obtained in this work was endowed with rifampicin, by loading it on the PCL film of the coated or bilayered structure.

3. MATERIALS AND METHODS

3.1. Materials

Hyaluronic acid (HA) (MW = 40–50 kDa; Batch N# 2018082984) and CTL hydrochloride (lactose-modified chitosan; Batch N# 350118) were provided by Sigea S.R.L. (Trieste, Italy) and BiopoLife S.r.l. (Trieste, Italy), respectively. CTL final composition, determined through 1H NMR, was as follow: glucosamine residue 27%, *N*-acetylglucosamine 18%, and 2-(lactit-1-yl)-glucosamine 55%; the calculated relative MW of CTL is around 1.5×10^3 kDa, as determined by viscometry.[164] Polyethylene oxide (PEO) (MW = 900 kDa), poly (ε-caprolactone) (PCL) (MW = 80 kDa), Tween® 20, dichloromethane (DCM), *N*,*N*-dimethylformamide (DMF), sodium hydroxide, methanol, acetone, dimethyl sulfoxide (DMSO), 1,1′-Carbonyldiimidazole (CDI), methacrylic anhydride, glutaraldehyde (25 wt% in water), 1-ethyl-3-(3-dimethylaminopropyl) carbodiimide (EDC), N-hydroxysuccinimide (NHS), sodium chloride, phosphate buffered saline (PBS), and the LB broth with agar were purchased from Sigma-Aldrich (Chemical Co. USA). Genipin (purity 98%) was acquired from Challenge Bioproducts Co., Ltd. (Yun- Lin Hsien, Taiwan). Rifampicin was purchased from EMD Millipore Corp. Fortuna Optima glass syringes (an inner diameter of 9 mm) were acquired from Sigma-Aldrich (USA). The D-ES30PN-20 W potential generator was purchased from Gamma High Voltage Research Inc. (Ormond Beach, FL, USA). The syringe pump, model KDS-100-CE, was acquired from KD Scientific (Holliston, MA, USA). Recombinant Trypsin−EDTA 1X, penicillin/streptomycin 100X, Fetal Bovine Serum (FBS), and Dulbecco's Modified Eagle Medium (DMEM) were purchased from Euroclone (Milan, Italy). Normal Human Dermal Fibroblasts, Fibroblast Growth Medium 2, and the Fibroblast Supplement Mix were acquired from PromoCell GmbH.

3.2. Membrane preparation

3.2.1. Monolayer wound dressings

3.2.1.1. Polysaccharide-based membranes

All the polysaccharide solutions were prepared by dissolving the polymers (HA, CTL, and PEO) separately in deionized water to combine them in binary and ternary mixtures.

The *CTL/PEO solution* was obtained by mixing the two polymers at the final concentrations of 1.25% (w/V) for CTL and 2.5% (w/V) for PEO. After 30 minutes of stirring, 1% (V/V) Tween® 20 was added as surfactant to reduce solution surface tension. The nanofibrous matrices were obtained with a custom-made horizontal electrospinning apparatus using the following parameters: voltage, 30 kV; distance between needle tip and the collector, 15 cm; flow rate, 1.2 mL/h; needle gauge, 23G; time, 60 minutes. The negative pole of the high voltage power supply was set over the collector.

Two types of *HA/PEO solutions* were produced, by combining 2.5% (w/V) PEO with 5% (w/V) and 6.5% (w/V) HA, respectively. In both cases, after 30 minutes, 1% (V/V) Tween® 20 was added to the solutions. The electrospun matrices were obtained as follows: voltage, 30 kV; distance between the needle tip and the collector, 20 cm; flow rate, 1.2 mL/h; needle gauge, 23 G; time, 60 minutes. In this case, the negative pole was set over the needle.

Finally, a *ternary mixture of HA, CTL, and PEO* was realized. After complete dissolution of polymers overnight (o/n), the pH of both HA and CTL solutions was adjusted to 7.5, with the aim to avoid the formation of complexes between the positively charged CTL and the negatively charged HA. CTL was then added to the PEO solution and stirred for 3 hours. Afterwards, HA was also added to obtain a ternary mixture with final concentrations of HA/CTL/PEO of 2% (w/V), 1% (w/V), 2% (w/V), respectively. After 30 minutes of equilibration, 1% (V/V) Tween® 20 was added and the mixture was stirred o/n at room temperature before electrospinning. The nanofibrous mats were manufactured with the following parameters: voltage, 30 kV; distance between the tip of the needle and the collector, 20 cm; flow rate, 1.2 mL/h; needle gauge, 23 G; time, 90 minutes. The negative pole of the high voltage

power supply was set over the collector. The same ternary solution used in the electrospinning procedure was cured in Petri dishes (diameter, 6 cm) and freeze-dried for 1 day (ALPHA 1–2 LD plus freeze-dryer, CHRIST, Osterode am Harz, Germany) to obtain non-fibrous membranes to be used as comparison.

3.2.1.2. PCL-based membranes

The PCL solution was prepared according to what reported by Porrelli and co-workers.[218] Briefly, 12% (w/V) PCL was solubilized in a DCM: DMF (7:3) mixture, by first dissolving PCL in DCM o/n, followed by the addition of DMF the day after. The membranes were obtained using the following parameters: voltage, 17 kV; distance between the tip of the needle and the collector, 25 cm; flow rate, 0.6 mL/h; needle gauge, 27 G; time, 60 minutes. The negative pole of the high voltage power supply was set over the collector. Some of the PCL mats were activated by air-plasma treatment, converting their basically hydrophobic behavior into a hydrophilic one. The process was carried out with a PDC 32-G Plasma Cleaner (Harrick Plasma, Ithaca, USA) used in low power mode (6.8 W) for 5 minutes, with a pressure of 0.1 mTorr. Activated PCL mats were even used to produce polysaccharide-coated PCL membranes. In this case, both HA and CTL were solubilized in deionized water at the final concentration of 0.2% (w/V) and their pH was adjusted to 7.2–7.4. CTL was first cured on PCL samples until complete adsorption and air-dried. Then, CTL-coated membranes were washed in deionized water and air-dried. Subsequently, HA was cured on the top of PCL-CTL samples, which were washed in deionized water and air-dried again.

3.2.2. Multilayer wound dressings

3.2.2.1. Bilayer electrospun membranes

The bilayer electrospun wound dressings (hereafter named "**PCL bilayer**") were obtained by combining PCL and polysaccharide-based monolayer matrices. In detail, the PCL basal layer was synthetized as described in *section 3.2.1.2.* The obtained PCL membrane was then activated for 1

minute by air-plasma treatment and mounted on the planar collector for the following electrospinning step. The ternary polysaccharidic solution of HA/CTL/PEO (*section 3.2.1.1.*) was chosen to realize the PCL bilayer membrane, which was obtained by electrospinning the polysaccharidic mixture on the PCL membrane with the same parameters described in *section 3.2.1.1.*, except for the time, which was of 60 minutes in this case.

To confer antibacterial properties to the PCL bilayer membranes, the rifampicin was incorporated into the PCL basal layer. In detail, 0.1% (w/V) rifampicin was solubilized in DMF, prior to the addition of DMF to the PCL in DCM solution. The obtained solution was then electrospun following the same experimental set-up employed for the non-functionalized membranes (*section 3.2.1.2.*). Once PCL/Rif membrane was produced, the bilayer was synthetized by activating for 1 minute the Rif-loaded matrix and electrospinning the polysaccharidic ternary mixture on the PCL/Rif mat, thus obtaining the "**Rif bilayer**" membrane. Considering rifampicin light sensitivity, all the procedure was executed under dark conditions.

3.2.2.2. Coated electrospun membranes

The coated electrospun wound dressings (hereinafter called "**PCL coating**") where realized with a procedure similar to that described in *section 3.2.1.2.* Briefly, CTL and HA were solubilized in deionized water at the final concentration of 0.6% (w/V) and their pH was adjusted to 7.2–7.4. The coating was then realized on a 1 minute-plasma treated PCL membrane by curing CTL and HA successively on the nanofibrous matrix, with a wash in deionized water after each layer deposition.

To impart antibacterial properties even to the PCL coating membranes, also in this case the rifampicin was added to the PCL layer as described above (*section 3.2.2.1.*), followed by the 1-minute activation and polysaccharide coating. The rifampicin-loaded PCL coating matrices will be named "**Rif coating**" from now on.

3.3. Crosslinking strategies

Due to the high instability and almost instantaneous dissolution of the monolayer polysaccharide-based membranes in aqueous environments, the resulting mats were subjected to various crosslinking treatments to stabilize them in water and ensure their applicability for biomedical purposes.

3.3.1. Glutaraldehyde vapor

Three Petri dishes (diameter, 6 mm) containing 25% glutaraldehyde in water were placed on the bottom of a vacuum chamber. The polysaccharidic membrane samples were stabilized on the grid of the sealed chamber and crosslinked under vacuum conditions for 4 hours or 2 hours. In this last case, the electrospun mats were subsequently heat treated for 24 hours at 60 °C to further stabilize the nanofibrous mesh.

3.3.2. EDC/NHS

EDC and NHS were added to the polymer solution 30 minutes before the electrospinning process at a final concentration of 2% (w/V) and 1% (w/V), respectively. In one case, the powder was directly added to the final polysaccharidic solution; alternatively, EDC/NHS were first dissolved in deionized water and then added to the electrospinning solution.

3.3.3. Genipin

Genipin crosslinking was executed according to two different procedures. In one case, genipin was directly added to the polymeric solution at a final concentration of 0.05% or 0.2% (w/V) 5 minutes before the electrospinning process. Once obtained, the nanofibrous matrices were placed at 37 °C for 24 hours to 7 days, with the purpose to promote genipin reaction. Otherwise, electrospun polysaccharidic mats were post-processing treated with 0.5% (w/V) genipin dissolved in ethanol for 15, 30, and 45 minutes, and then they were heated at 37 °C for 24 hours to activate genipin reaction.

3.3.4. Thermal treatment

The thermal treatment was performed by heating the polysaccharidic membranes in a convection oven at 80 °C for 4, 6, 8 hours. Alternatively, to mitigate the effect of humidity on the nanofibrous meshes, a vacuum oven was employed, by heating the samples for 1 hours (after equilibrating from 20 °C to 80 °C) or 1, 2, 3 hours at 80 °C.

3.3.5. Methacrylic anhydride

Pure methacrylic anhydride was employed, by gently curing it on HA/CTL/PEO samples until complete adsorption and air-drying. The matrices were subsequently washed with various solvents, namely deionized water, sodium hydroxide, methanol, acetone, and dimethylformamide, to determine the best washing method able to ensure nanofiber architecture maintenance.

3.3.6. Carbonyldiimidazole (CDI)

Different attempts were carried out with CDI, to find the optimal compromise between matrix water stability and nanofiber structure loss. The first crosslinking attempt was performed o/n in DMF by exploring several equivalents of coupling agent for mol of CTL glucosamine residues, namely 100, 50, 25, and 10 equivalents. Subsequently, other solvents than DMF were tested as better possible reaction media, namely dichloromethane, dimethyl sulfoxide, and tetrahydrofuran.

Then, in an effort to confer further stability to the chemically crosslinked membrane, the CDI crosslinking was coupled with the thermal treatment, by first crosslinking the polysaccharide matrices with 50 equivalents of CDI in DMF and subsequently heating them for 4 hours at 80 °C.

Finally, to find the best reaction times, the crosslinking with 50 equivalents of CDI in DMF was performed at different incubation times, namely 1, 2, 3, 4, 5, 7, 8 hours, and o/n.

In all cases, after the crosslinking step the membranes were quickly washed in ethanol and air-dried.

3.4. Scanning Electron Microscope (SEM) analysis

In all cases, dried membrane samples were placed on aluminum stubs covered with a double-sided carbon tape and sputter-coated with gold using a Sputter Coater K550X (Emitech, Quorum Technologies Ltd., UK). The morphological analysis was then performed with a scanning electron microscope (Quanta 250 SEM, FEI, Oregon, USA) working in secondary electron detection mode. The working distance was set at 10 mm to obtain the appropriate magnifications, and the acceleration voltage was set between 20 and 30 kV. Fiber diameters were calculated using Fiji software,[253] by randomly selecting 50 fibers on each sample.

3.5. Attenuated Total Reflectance – Fourier Transform Infrared (ATR-FTIR) spectroscopy

In the case of the monolayer matrices, ATR-FTIR was performed to assess the occurred crosslinking on samples treated o/n with 50 equivalents of CDI in DMF. HA/CTL/PEO membranes before and after CDI crosslinking were analyzed as well as HA, CTL, PEO, and CDI pure spectra as comparison. On the other hand, ATR-FTIR analysis was carried out on the multilayer membranes to evaluate the presence of both polysaccharides and rifampicin on the electrospun matrices, by comparing them with the pure spectra of the single membrane components (namely, PCL, rifampicin, HA, CTL, PEO). In all cases, IR spectra were recorded in transmittance mode with a Nicolet iS50 FT-IR spectrometer (Thermo Scientific, MI, Italy), within a wavenumber range of 4000–500 cm^{-1}. All the spectra were acquired with 32 scans and a resolution of 4 cm^{-1}.

3.6. Swelling tests

The swelling behavior was assessed in deionized water or saline solution (NaCl 150 mM) in the case of the monolayer matrices, while the multilayer membranes were tested in PBS. In all cases, the liquid retention ability was quantified after rehydration of the samples, by measuring the weight changes as a function of the immersion time. As regards the monolayer matrices, seven types of samples were

compared: CDI-crosslinked and methacrylic anhydride-crosslinked electrospun polysaccharidic mats, CDI-crosslinked freeze-dried polysaccharidic mats, PCL electrospun matrices (non-activated, activated, or coated with CTL/HA), and the commercial product Chitoderm® (Pietrasanta Pharma S.p.A.). Once measured dry weights, wet weights were determined at each timepoint (15, 30, 45 minutes and 1, 2, 3, 5, 7, 24 hours) by gentle blotting with a filter paper to remove the exceeding surface liquid.

The same procedure was followed for the multilayer matrices, in which case the swelling behavior of the PCL bilayer and PCL coating membranes was compared to the plasma-treated PCL mats and measured after 1, 4, 24, 96, 168 hours.

The swelling ratio was in either case calculated according to **Equation (1)**, as proposed by Porrelli and co-workers:[164]

$$\text{Swelling (\%)} = \left(\frac{(W_s - W_d)}{W_d}\right) \times 100 \quad \textbf{(1)}$$

where W_d and W_s are the weights of the samples in the dry and the swollen state, respectively. The results were taken as the mean values of four samples for each condition.

3.7. Degradation tests

The rate of degradation of the polysaccharide monolayer matrices was evaluated in water and saline solution (NaCl 150 mM) on the same samples which were tested for swelling behavior, namely CDI-crosslinked and methacrylic anhydride-crosslinked electrospun polysaccharidic mats, CDI-crosslinked freeze-dried polysaccharidic mats, PCL electrospun matrices (non-activated, activated, or coated with CTL/HA), and the Chitoderm® (Pietrasanta Pharma S.p.A.).

Their stability was evaluated after 1, 3, 5, 7 days of immersion at 37 °C. The wet weight was measured after 10 min equilibration and related to weight variations in time, which were calculated using **Equation (2)**, adapting the protocol proposed by Turco and co-workers:[254]

$$\text{Weight variation (\%)} = 1 - \left(\frac{W_{tn}}{W_{10\ min}}\right) \times 100 \quad \textbf{(2)}$$

where W_{tn} and W_{10min} are the wet weights of the samples at the defined timepoint and after 10 min of rehydration, respectively. Four replicates were analyzed for each condition.

3.8. Water Vapor Transmission Rate

The ability of membranes to transmit water vapor was assessed both for monolayer and multilayer matrices. In the first case, CDI-crosslinked polysaccharidic electrospun meshes, PCL electrospun mats (non-activated, activated, and coated with CTL/HA), and Chitoderm® (Pietrasanta Pharma S.p.A.) were analyzed; in the second case, PCL bilayer and PCL coating matrices were tested and compared to the plasma-treated PCL mats.

Glass vials with a top closure of 13 mm of diameter were filled with deionized water, leaving a 2 cm gap between the water and the sample, which was placed as a lid on the vial and sealed on the side with Parafilm®. The vials were then weighted and incubated at 37 °C for 24 and 48 hours (monolayer mats) or 24, 48, and 72 hours (multilayer mats), by measuring water loss at each timepoint. Uncapped vials and vials capped with Parafilm® were used as free evaporation and totally occlusive controls, respectively. The water vapor transmission rate was afterwards calculated using **Equation (3)**, as proposed by Tarusha and co-workers:[255]

$$\mathrm{WVTR}\left(\frac{g}{m^2 h}\right) = \left(\frac{(W_{tx} - W_{t0})}{A \times h}\right) \times 100 \quad \textbf{(3)}$$

where, W_{tx} is the weight after 24, 48, or 72 hours, W_{t0} is the initial weight of the vial, and A is the area of the top closure of the vial. Three replicates were analyzed per each sample.

3.9. Polysaccharide release

The release of fluorophore-conjugated polysaccharides from PCL bilayer and PCL coating membranes was monitored in PBS after 1, 4, 24, 96, and 168 hours, upon incubation at 37 °C in the dark. The labeled polysaccharides (CTL-FITC, HA-CF640R) were kindly provided by prof. Ivan Donati (University of Trieste, Trieste, Italy) and synthetized according to the procedures proposed by Sacco and co-workers[256] and Porrelli and co-workers.[164] The fluorescent matrices were prepared as

described in *section 3.2.2*, by substituting the non-fluorescent polysaccharides with the labeled ones. Once obtained the membranes, six disks (diameter, 13 mm) for each condition examined were placed in 24-wells culture plates, adding 1 mL of PBS in each well. At each timepoint, 200 µL of PBS were collected from each sample and transferred in a 96-well black plate for fluorescence reading (CTL-FITC excitation and emission wavelengths: 485 nm and 520 nm, respectively; HA-CF640R excitation and emission wavelengths: 642 nm and 662 nm, respectively) through a GloMax Multi+ Detection System (Promega corporation, Madison, USA). A calibration curve was used to relate fluorescence intensity to the amount of CTL and HA released. The residual PBS was then removed from the wells and substituted with fresh medium, to evaluate polysaccharide cumulative release. PCL electrospun samples were used as blanks.

3.10. Rifampicin release

The release of rifampicin from the Rif bilayer and Rif coating membranes was followed in time (1, 4, 24, 96, 168 hours) by immersing them in PBS and incubating at 37 °C in dark conditions. Six disks (diameter, 13 mm) for each kind of sample were placed in 24-wells culture plates, by adding 1 mL of PBS in each well. After each timepoint, 800 µL of release solution were collected from every sample for absorbance evaluation and the residual PBS was substituted with fresh medium, to evaluate antibiotic cumulative release. The released rifampicin was quantified by means of UV spectrophotometry (Ultraspec 2100 pro, Amersham Bioscience) at 475 nm and the Lambert-Beer equation was exploited, knowing that ε_{475nm} is equal to 15400. PCL electrospun samples were used as blanks.

To evaluate the influence of polysaccharide release kinetic from bilayer membranes on the antibiotic release, two disks (diameter, 13 mm) of PCL/Rif membranes were immersed in two different PBS solutions, enriched or not with CTL and HA (by estimating the amount of polysaccharide that would be released from a 13-mm PCL bilayer sample). After 1 hour of immersion, the absorbance at 475

nm of the two solutions was measured, estimating the rifampicin concentration thanks to the Lambert-Beer equation.

3.11. Contact angle and Surface Free Energy analyses

The wettability of the multilayer matrices with and without rifampicin was assessed through contact angle measurement, using the sessile drop method. Five samples (diameter, 6 mm) were examined for each condition, by using untreated and plasma-treated PCL and PCL/Rif membranes as comparison. The contact angle was measured on images acquired with a stereomicroscope (Leica MZ16) equipped with a 45° tilted mirror and a digital camera (Leica DFC 320), then connected to the software Image Pro 3D Suite. Membrane wettability was studied in the presence of three types of fluids, namely deionized water, deionized water + 10% FBS, and the cell culture medium DMEM. For each type of fluid, 4 µL were deposited on the sample and the images were acquired after 30 seconds, to allow drop stabilization on the surface. The obtained images were thereafter analyzed using the "contact angle" tool of Fiji software and the contact angle of each kind of sample exposed to the various types of fluids was calculated. Surface free energies were then evaluated using the Owens−Wendt method[257] adapted by Ren and co-workers[258] and Can-Herrera and co-workers.[259] Both deionized water and ethylene glycol (EG) contact angles (4 µL of fluid/sample) were analyzed to calculate the surface energy components: the polar/hydrophilic component (γ_s^p) and the dispersive/hydrophobic component (γ_s^d). The total surface free energy (γ_s) was, therefore, calculated according to **Equation 4**:

$$\gamma_s = \gamma_s^p + \gamma_s^d \quad \textbf{(4)}$$

3.12. Cell culture

NIH-3T3 murine fibroblasts (ATCC CRL-1658) were cultured in high-glucose DMEM supplemented with 10% FBS, 2mM L-glutamine, 100 U/mL penicillin, and 0.1 mg/mL streptomycin in humid

atmosphere conditions, at 37 °C and with 5% pCO_2. Cells were sub-cultured using trypsin 0.25% three times a week or at a confluence level of about 70-80%.

Normal Human Dermal Fibroblasts (NHDF) from adult donor were cultured under humid atmosphere at 37 °C and with 5% pCO_2 in their own Fibroblast Growth Medium 2, supplemented with 100 U/mL penicillin, 0.1 mg/mL streptomycin, and the related Fibroblast Growth Medium 2 Supplement Mix, which was stored in the dark. Cells were sub-cultured using 0.25% trypsin, when the confluence level was estimated at about 80%. Cells at the second passage of culture were used for the biological tests.

3.12.1. Biocompatibility assay

Considering the potentially cytotoxic effects of Tween® 20 employed for polysaccharide electrospinning, both PCL bilayer and Rif bilayer matrices were washed rapidly (2 minutes) in ethanol to remove the surfactant from the electrospun matrices without affecting their integrity. Hence, to first evaluate the efficacy of the ethanol washing in improving mat biocompatibility, PCL bilayer membranes, treated or not with ethanol, were tested on murine fibroblasts NIH-3T3, by using cells grown in plain medium as control. Both types of membranes tested were cut in disks (diameter, 6 mm) and sterilized under UV irradiation for 45 minutes. After that, 20'000 cells/well suspended in 1 mL of complete DMEM were seeded onto 24-well culture plate, considering five replicates for each condition. The culture plates were then incubated at 37 °C with 5% pCO_2 for 4 hours to allow cell adhesion on the bottom of the wells. Once adhered, two disks per type of sample were added to their respective wells and cell viability was assessed after 24 hours through a Resazurin Cell Viability Assay kit (Sigma Aldrich, St. Louis). In detail, the cell culture medium was removed from the wells and substituted with 400 µL of Resazurin solution (diluted 1:30 in DMEM). After 4 hours of incubation, 200 µL of the Resazurin solution were collected from each well and transferred to a 96-well black plate for fluorescence reading, which was performed using a spectrofluorometer GloMax Multi+ Detection System (Promega corporation, Madison, USA), with an excitation wavelength of 525 nm and an emission wavelength in the range of 580-640 nm.

Once the efficacy of the ethanol washing was assessed, the biocompatibility of all the multilayer matrices, loaded or not with rifampicin, was tested on NHDF. All types of membranes were cut in disks (diameter, 6 mm) and sterilized under UV irradiation for i) 45 minutes in the case of the membranes without rifampicin, ii) 10 minutes in the case of the antibiotic-enriched mats. Cells at a density of 20'000 cells/well were suspended in 500 µL of complete Fibroblast Growth Medium and seeded onto 24-well cell culture plates, considering five replicates for each condition. The cell culture plates were afterwards incubated at 37 °C with 5% pCO_2 for 4 hours, to ensure cell adhesion on the bottom of the wells. Subsequently, two disks per type of sample were added to the corresponding cell-containing well, to assess cell viability in the presence of the material. Cells seeded in the absence of the material and treated with PCL and PCL/Rif mats were used as controls, while empty wells with the culture medium only and with the culture medium treated with the different types of matrices to test were used as blanks. Cell proliferation was evaluated after 24, 48, and 72 hours using the Resazurin Cell Viability Assay kit (Sigma Aldrich, St. Louis). At each timepoint, the medium was removed from the wells and substituted with 400 µL of Resazurin solution (diluted 1:30 in the NHDF culture medium). After 4 hours of incubation, 200 µL of the Resazurin solution were collected from each well and transferred to a 96-well black plate for fluorescence reading. Meanwhile, each well was washed with PBS and replaced with 500 µL of fresh cell culture medium. The fluorescence was measured again through a spectrofluorometer GloMax Multi+ Detection System (Promega corporation, Madison, USA), with an excitation wavelength of 525 nm and an emission wavelength in the range of 580-640 nm.

3.12.2. Wound healing assay

The wound healing assay (also referred to as "scratch test") was performed to study *in vitro* the ability of the CTL and HA released from the PCL bilayer and PCL coating matrices to promote wound closure. To this aim, liquid extracts of the membranes were prepared. Specifically, 5x5 cm electrospun membranes (PCL, PCL bilayer, and PCL coating) were sterilized under UV irradiation

for 45 minutes and immersed in 10 mL of NHDF culture medium for 72 hours, after the PCL bilayer mats had previously been washed with ethanol (*section 3.10.1*). The membranes were then removed from the medium, which was stored at 4 °C in the dark. NHDFs were seeded on 6-well cell culture plates at a density of 250'000 cells/well considering two replicates for each condition and incubated o/n at 37 °C to allow cell adhesion. The day after, the culture medium was removed from each well and 3 mL of liquid extract of the membranes were added to the cells. Cells treated with plain culture medium were used as controls. After 24 hours, when cells reached at least 80% of confluency, the medium was removed from each well, stored in a Falcon tube, and replaced with PBS. A scratch was realized in each well using a 200 µL pipette tip, by gently impressing a first vertical scratch followed by a second scratch perpendicular to the first one. After the wounding was performed on the cell monolayer, PBS was removed and replaced with the previously stored conditioned medium. The scratch closure was followed over time through an optical microscope (Optech IB3 ICS) equipped with a Nikon D5200 and the images were captured at different timepoints (t_0, 2, 4, 6, 10, 24, 48 hours). The analysis was performed using the software ImageJ: the region of interest (ROI) was outlined per each scratch and the percentage of closure over time was plotted. In detail, for each type of sample, eight images were analyzed and the percentage of closure over time was calculated by relating the gap area at the defined timepoint to the gap area at t_0, thereby obtaining the percentage of closed area. The gap closure in time was then measured according to **Equation 5**:

$$\text{Gap closure (\%)} = 100\% - \text{\% closed area} \quad \textbf{(5)}$$

3.13. Antibacterial assays

Escherichia coli (ATCC 8739, hereinafter called *Escherichia coli**1***), *Escherichia coli* (ATCC 25922, hereafter named *Escherichia coli**2***), *Pseudomonas aeruginosa* (ATCC 27853), *Staphylococcus aureus* (ATCC 25923), and *Staphylococcus epidermidis* (ATCC 12228) were swiped on LB agar plates from a glycerol stock at -80 °C and grown o/n at 37°C. For liquid culture, some bacterial colonies were collected from the Petri plates and resuspended in 5 mL of LB medium. Each bacterial

inoculum was then incubated o/n at 37 °C under shaking conditions (140 rpm). The day after, a re-inoculum was prepared by diluting an aliquot of the o/n cultures (1 mL of each bacterial strain) in 5 mL of fresh LB medium, then incubating again at 37°C and 140 rpm for about 40 minutes (up to mid-log phase), to reach a final bacterial concentration of 10^6 CFU/mL. The bacterial concentration was determined upon optical density measurements (Ultraspec 2100 pro, Amersham Bioscience) at 600 nm (OD_{600nm}).

3.13.1. Growth inhibition assay

The growth inhibition assay was carried out to evaluate the ability of rifampicin-endowed multilayer matrices to inhibit bacterial growth even in a highly diluted environment, such as an exudating wound. To this aim, liquid extracts of the membranes (both Rif bilayer and Rif coating) were prepared in PBS, estimating in both cases an initial antibiotic concentration of about 10 µg/mL, measured by UV spectrophotometry (Ultraspec 2100 pro, Amersham Bioscience) at 475 nm using the Lambert-Beer equation (ε_{475nm} = 15400). In a 96-well plate, serial 1:2 dilutions of membrane extracts in LB medium were performed from an estimated initial concentration of 5 µg/ml to a final concentration of 0.3125 µg/mL. The test was performed in duplicate for each type of sample (Rif bilayer and Rif coating) in the presence of each bacterial strain (*Escherichia coli**1***, *Pseudomonas aeruginosa*, *Staphylococcus aureus*, *Staphylococcus epidermidis*). In detail, 100 µL of bacteria were added to each dilution; bacteria in LB medium only and exposed to membranes without antibiotic were used as growth control, whereas the medium without bacteria was selected as negative growth control. Subsequently, the 96-wells were placed in a plate reader at 37 °C (FLUOStar® Omega-BMG Labtech spectrophotometer) and the absorbance at 600 nm was measured for 20 hours (with 30 minutes intervals between each measure).

To assess the antibiotic sensitivity of the tested bacterial strains, they were exposed to free rifampicin (previously dissolved in DMSO) at different concentrations (from 40 µg/mL to 0.16 µg/mL) and incubated at 37 °C for 18 hours. After that, the bacterial growth was estimated again upon

spectroscopy measurement at 600 nm, to identify the minimum antibiotic concentration able to inhibit bacterial growth (MIC, minimum inhibitory concentration). [260,261]

3.13.2. Time killing test

The time killing test was performed to evaluate the ability of the released rifampicin to even exert a bactericidal activity. For this purpose, after re-inoculum, the bacteria were diluted at a final concentration of 10^7 CFU/mL. As a t_0 control, they were serially diluted in PBS from 10^{-1} to 10^4 and 50 µL of every dilution were spread on a LB agar plate and incubated at 37 °C o/n. Meanwhile, the bacteria (10^7 CFU/mL) were incubated at 37°C under agitation (140 rpm) in the presence of the rifampicin-endowed multilayer matrices, whereas the respective materials without antibiotic were used as growth control. In detail, 1.5 mL of each bacterial strain (*Escherichia coli**2***, *Pseudomonas aeruginosa*, *Staphylococcus aureus*, *Staphylococcus epidermidis*) were cultured in the presence of three disks (diameter, 13 mm) of each type of membrane (Rif bilayer, PCL bilayer, Rif coating, PCL coating). At the selected timepoints (30 minutes, 2 hours, 4 hours), 100 µL of each sample were serially diluted in PBS. 50 µL of each dilution were then spread on LB agar plates, which were incubated o/n at 37 °C. The day after, the colonies grown on the plates were counted and the CFU/mL per each timepoint were calculated based on the examined dilution.

4. RESULTS

4.1. Monolayer membranes

Monolayer electrospun membranes were designed with the aim to produce a polysaccharide-based wound dressing material. Different polysaccharide-based solutions were attempted to find the best polymer mixture to be electrospun, capable of producing thin and bead-free nanofibers in a reproducible manner. For this purpose, both binary and ternary mixtures of hyaluronic acid (HA), lactose-modified chitosan (CTL), and polyethylene oxide (PEO) were tested.

Non-fibrous polysaccharide membranes and synthetic-based electrospun meshes were used for comparison, also considering the functionalization of the synthetic membranes with a bioactive polysaccharidic coating.

4.1.1. Polysaccharide-based electrospun membranes

Binary mixtures of CTL/PEO and HA/PEO were examined. In the first case, CTL [1.25%] (w/V) and PEO [2.5%] (w/V) were independently dissolved in deionized water and then mixed with the addition of Tween® 20 as surfactant, to reduce the surface tension of the solution and to improve its electrospinnability. An analogue method was followed for HA/PEO solution preparation. However, in this second case two different concentrations of hyaluronic acid were tested, namely 5% (w/V) and 6.5% (w/V), while PEO concentration was the same in both cases, namely 2.5% (w/V).

The CTL/PEO solution exhibited high viscosity, being inhomogeneous and difficult to withdraw with the syringe for the electrospinning. It also presented some macroscopic complexes, which were probably due to chain entanglement between the two high molecular weight employed polymers. Moreover, a phase separation occurred after 30 minutes without stirring. So, this process exhibited high instability, inhomogeneous morphology of the electrospun fibers (**Figure 11A**), and uncertainty in fiber chemical composition.

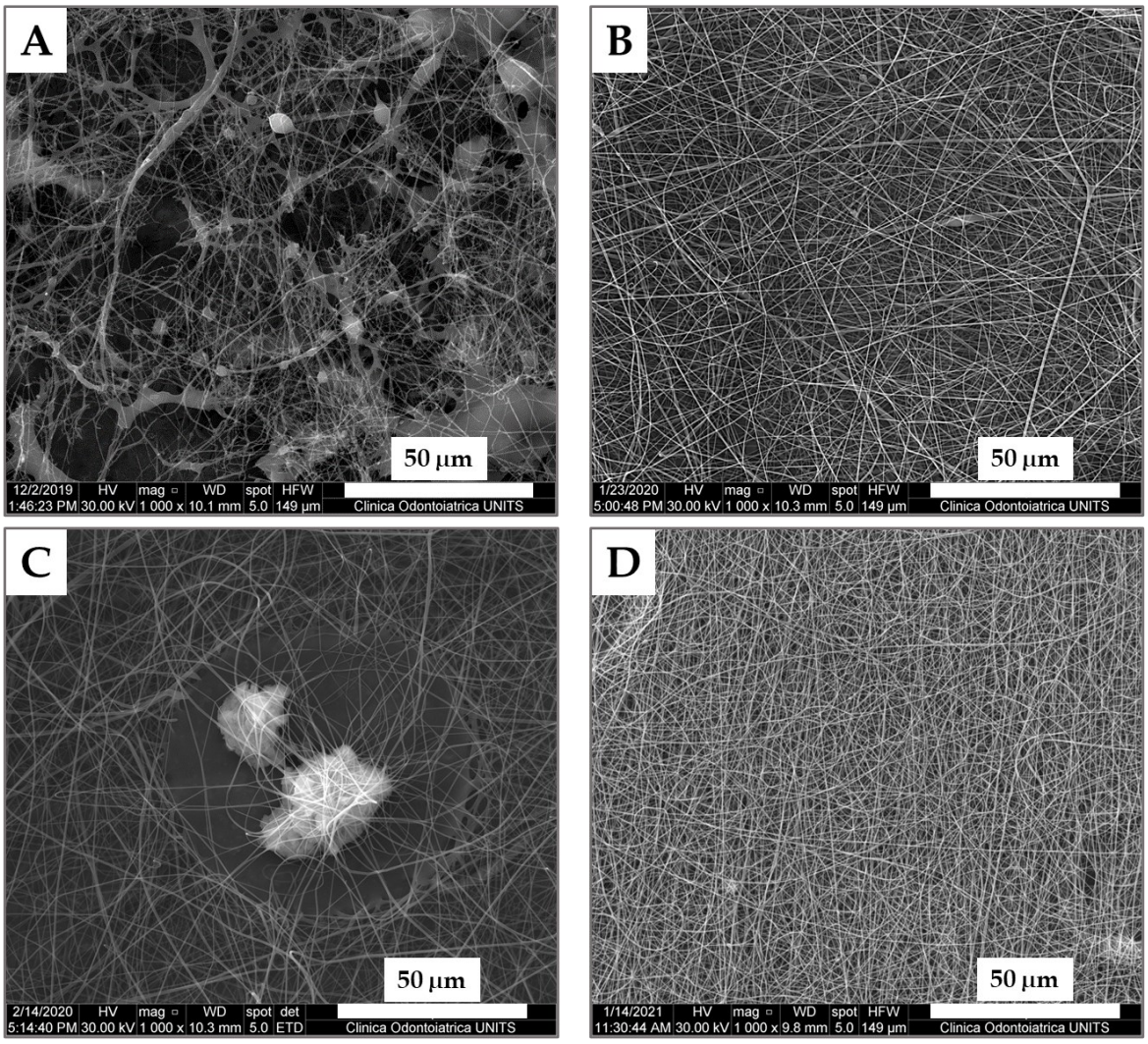

Figure 11. SEM micrographs of polysaccharide-based membranes, with the ternary mixture showing the best morphology, with thin and uniform fibers, devoid of defects or burns.
(A) CTL [1.25%] / PEO [2.5%]; **(B)** HA [5%] / PEO [2.5%]; **(C)** HA [6.5%] / PEO [2.5%]; **(D)** HA [2%] / CTL [1%] / PEO [2%]. All the concentrations are expressed as w/V.

On the other hand, the HA/PEO solutions seemed to be easier to treat due to their higher homogeneity and lower viscosity. Indeed, in the case of the HA [5%] (w/V)/ PEO [2.5%] (w/V) solution, more homogenous and defect-free nanofibers were obtained (**Figure 11B**). Nevertheless, even when the electrospinning time was increased, the membrane was very inconsistent and difficult to remove from the aluminum foil. For this reason, a higher concentration of hyaluronic acid was employed with the aim to improve membrane texture. Unfortunately, in this case membrane burning was observed (**Figure 11C**). Indeed, a current of 30 µA was registered during the electrospinning process, which, associated to the high voltage employed (30 kV), generated a heat of about 810 J.

To find the best combination between these polymers and produce a stable and spinnable solution, a ternary mixture of HA/CTL/PEO was prepared. The three polymers were separately dissolved in deionized water; then CTL and hyaluronic acid were added to the PEO solution, after 3 hours of equilibration between the two. Even in this case, Tween® 20 was included as a surfactant. The ternary mixture revealed the best viscosity to be withdrawn with the syringe and was visibly homogenous and devoid of macroscopic complexes between the polymers employed, so it proved to be the most promising candidate for the electrospinning step. As evidence, thin, homogenous, and bead-free fibers were observed with high reproducibility (**Figure 11D**). For this reason, HA/CTL/PEO matrices were selected for further characterization as candidate wound dressing material.

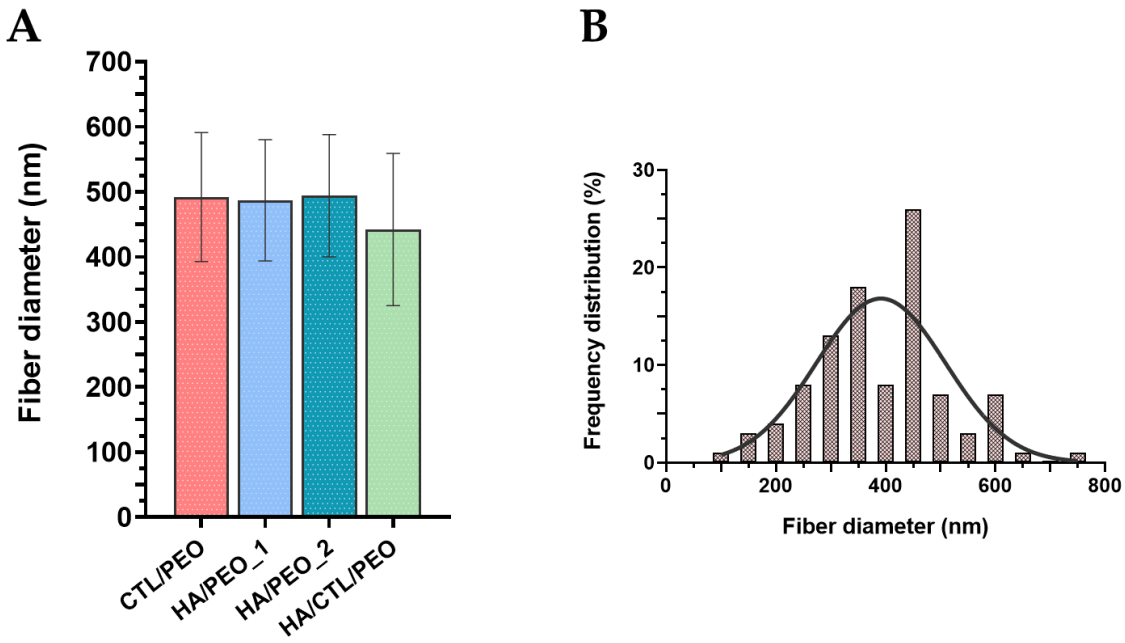

Figure 12. Dimensional analysis of polysaccharide-based electrospun membranes **(A)**, with particular attention to the ternary mixture, which showed optimal fiber diameter as well as a normal distribution of fiber diameter throughout the membranes **(B)**.
The acronyms HA/PEO_1 and HA/PEO_2 stand for HA [5%] / PEO [2.5%] and HA [6.5%] / PEO [2.5%], respectively. All the concentrations are expressed as w/V.

The fiber diameter was examined and compared between the different types of membranes. It was calculated using 50 randomly selected fibers and showed a similar trend in all types of membranes (**Figure 12A**), with the mean fiber diameter ranging from 492 ± 99 nm for CTL/PEO membranes to 442 ± 117 nm for the ternary mixture. Moreover, in this last case a normal distribution of the fibers

within the sample was observed (**Figure 12B**), confirming the correct setup of the electrospinning process.

4.1.2. Non-electrospun polysaccharide-based membranes

Freeze-dried membranes were produced from the same ternary solution employed for the synthesis of polysaccharide-based electrospun mats, to highlight the advantages of using a nanofibrous matrix over a conventional non-fibrous structure. As confirmed by SEM imaging (**Figure 13**), the freeze-drying process results in membranes characterized by an amorphous layer of the polymer blend and no organized fibrous structure. As another non-electrospun control, a commercial product, namely Chitoderm®, was analyzed for its composition and structure. It consists of an outer impermeable polyurethane layer which serves as protection against the external environment, and a lower chitosan pad with a macro-fibrous structure.

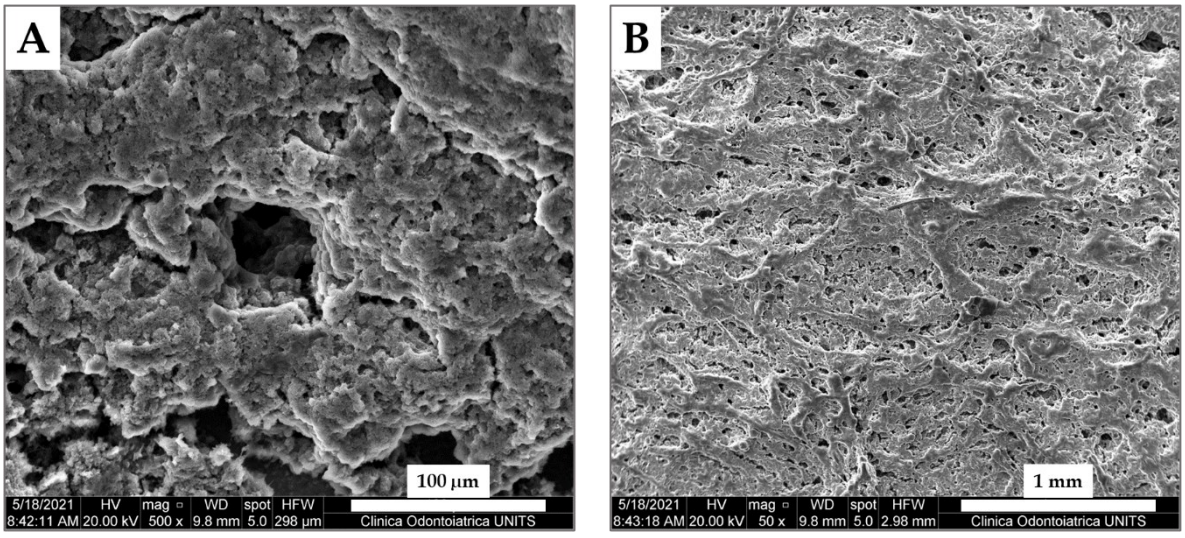

Figure 13. SEM micrographs of HA/CTL/PEO freeze-dried mats at different magnifications: **(A)** 500 X; **(B)** 50 X. The free-drying process does not allow to obtain any nanofibrous structure.

4.1.3. Synthetic-based electrospun membranes

The differences between electrospun matrices of different compositions were also analyzed. To this aim, three types of PCL membranes were produced for comparison, starting from the same electrospinning process: (i) untreated, non-activated PCL, (ii) air-plasma activated PCL, and (iii) PCL

coated with CTL/HA (both with a final concentration of 0.2% w/V). In all cases, a uniform distribution of fibers was observed, and the activation process did not cause significant changes in fiber morphology. On the other hand, the presence of the coating slightly alters the overall morphology and leads to a slight increase in fiber diameter due to rehydration, resulting in a statistically significant difference compared with pristine or activated PCL (**Figure 14**).

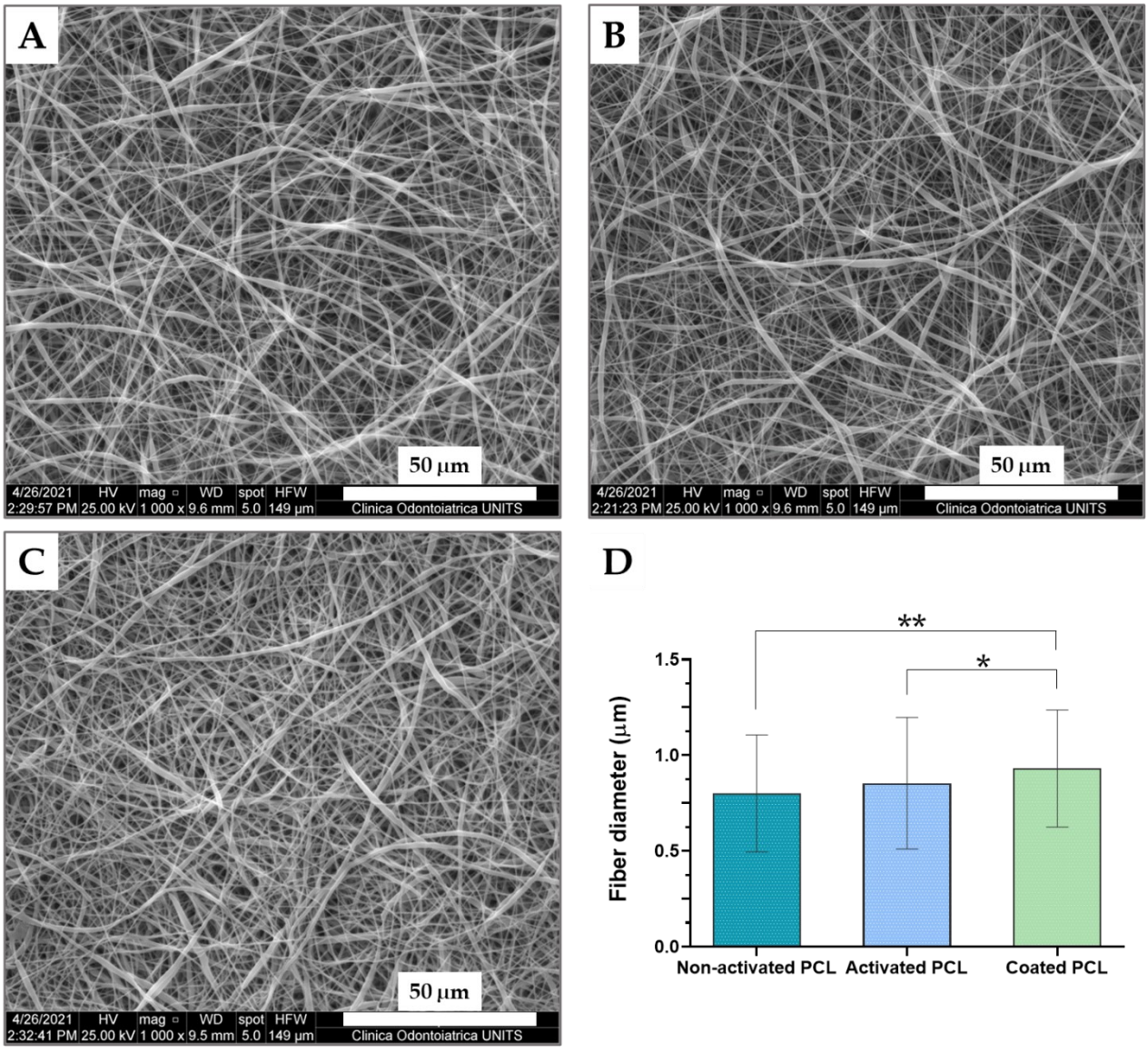

Figure 14. SEM micrographs of electrospun PCL matrices, namely **(A)** non-activated, **(B)** activated, and **(C)** polysaccharide-coated nanofibers. On the lower right, **(D)** a comparison of fiber diameters. Statistical analysis was performed with Kruskal-Wallis test and Mann–Whitney test for two-groups comparison, applying Bonferroni's correction. Statistically significant differences are indicated as asterisks (*).

4.1.4. Stability and crosslinking

As expected, the high degree of hydrophilicity of the polysaccharides used, combined with the large surface area characteristic of nanofiber structures, imparts considerable structural instability to polysaccharide-based electrospun membranes in aqueous environments. Indeed, the nanofibrous mesh collapses within seconds when exposed to water, resulting in the immediate dissolution of the biomaterial. For this reason, different crosslinking strategies were tried to impart water resistance to HA/CTL/PEO membranes while maintaining the fibrous structure, with different results depending on the strategy chosen (**Table 3**).

Table 3. Summary of the crosslinking strategies attempted on HA/CTL/PEO matrices and the effects on membrane stability, thought of as both water resistance and architecture maintenance.

Crosslinking treatment	***Outcome***
CDI	Partial fiber fusion, but optimal stability in water.
Methacrylic anhydride	Preservation of fibers after washing in dimethylformamide and acetone, despite rapid degradation if compared to CDI crosslinking.
Glutaraldehyde	No resistance in water. Fiber fusion or loss when coupled with thermal treatment.
EDC/NHS	Immediate gelation after crosslinker addition to the solution.
Genipin	Fiber loss and total instability in water, both when added before electrospinning or after membrane production.
Heat	Fiber loss and immediate dissolution in water.

4.1.4.1. Glutaraldehyde

Glutaraldehyde vapor was used as well-established crosslinker to stabilize polysaccharide-based nanofibers using two different procedures: i) 4 hours of crosslinking in a vacuum chamber and ii) 2 hours of crosslinking in a vacuum chamber combined with heat treatment (**Figure 15**).

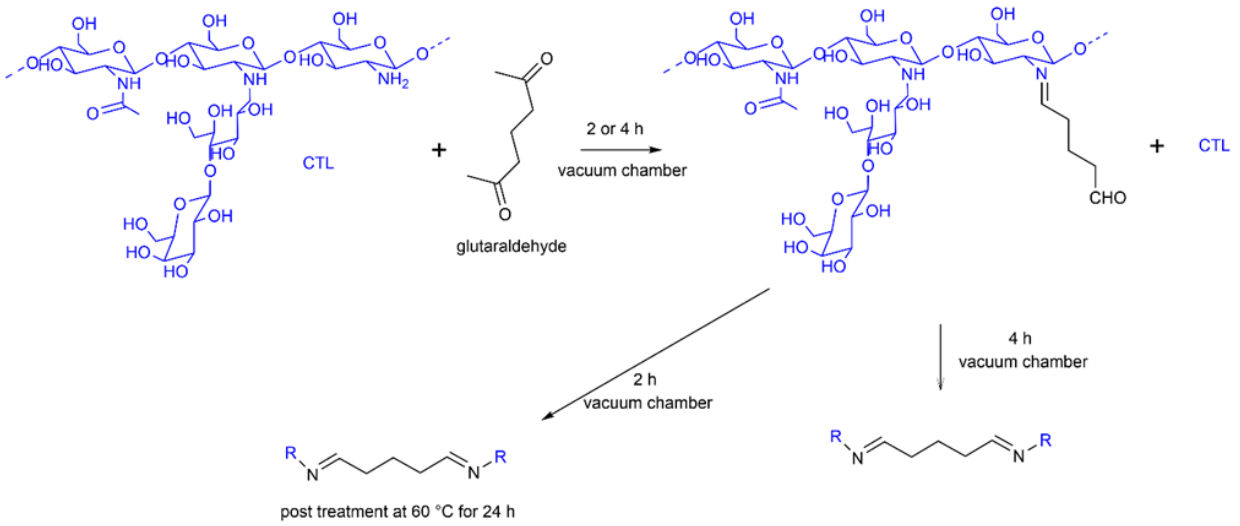

Figure 15. Glutaraldehyde-mediated crosslinking mechanism in the presence of HA/CTL/PEO membranes.

In the first case, a partial loss of the fibrous structure was observed, even though the overall architecture was still recognizable; on the other hand, after the heat treatment the nanofibrous architecture was completely lost (**Figure 16**). Nevertheless, aqueous stability was not achieved in either case.

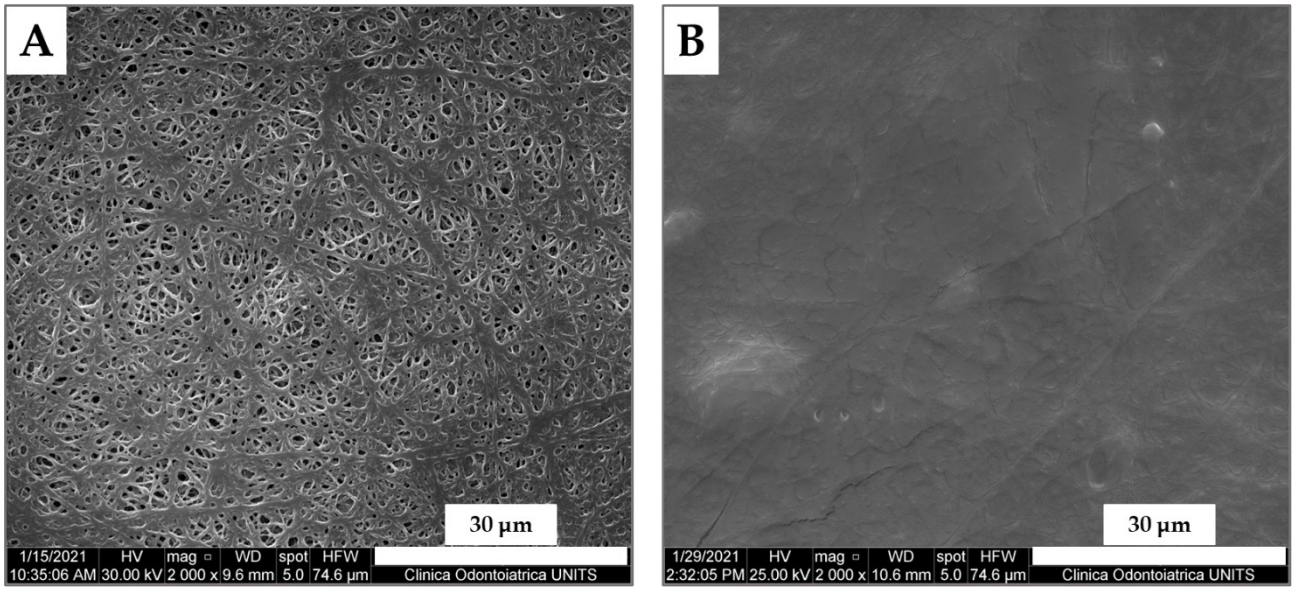

Figure 16. SEM images of HA/CTL/PEO mats crosslinked with glutaraldehyde (25% in water) vapor under vacuum conditions **(A)** for 4 hours and **(B)** for 2 hours followed by heat treatment, which finally destroys the nanofibrous architecture.

4.1.4.2. EDC/NHS

In the case of EDC/NHS, the crosslinkers were added to the polysaccharidic solution 30 minutes before the electrospinning process in powder form or after their solubilization in water (**Figure 17A**). Unfortunately, in both cases, the high reactivity of both CTL and hyaluronic acid induced an almost immediate gelation of the solution, hindering the electrospinning process (**Figure 17B-C**).

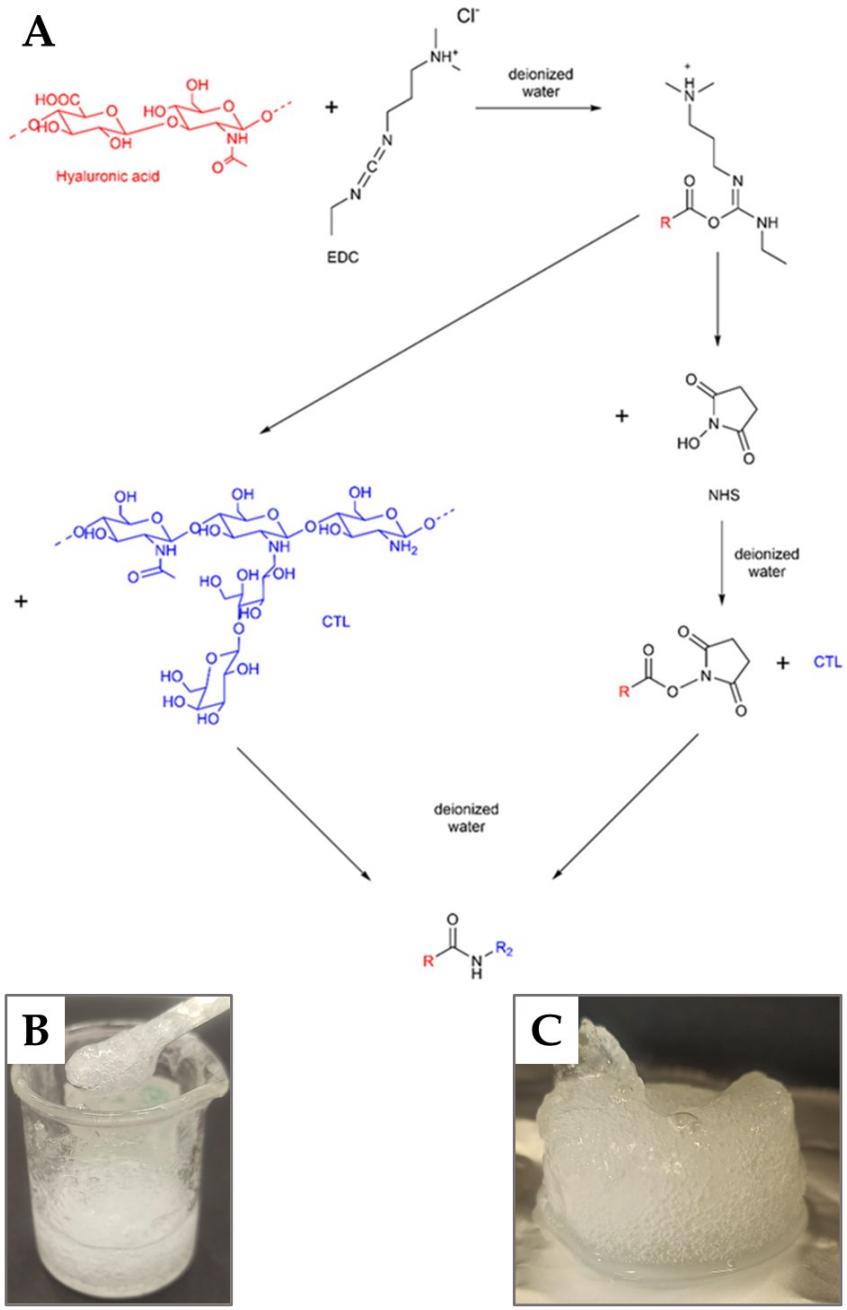

Figure 17. Crosslinking of HA/CTL/PEO mats by EDC/NHS. **(A)** EDC/NHS reaction mechanism within the electrospinning solution; **(B)** crosslinking by direct addition of EDC/NHS powder to the polysaccharidic solution; **(C)** crosslinking by EDC/NHS dissolution in water before mixing with HA/CTL/PEO solution.

4.1.4.3. Genipin

Genipin crosslinking was performed according to two different procedures: i) the crosslinker was electrospun with the polysaccharide solution or ii) the membranes were post-processed at different timepoints (15, 30, 45 minutes) with genipin dissolved in ethanol (**Figure 18**). In both cases, the samples were subjected to heat treatment at 37 °C to activate the genipin and promote crosslinking between fiber meshes. Nevertheless, crosslinking did not occur in any case, not even after 7 days, resulting in the complete membrane dissolution on contact with water (**Figure 19**).

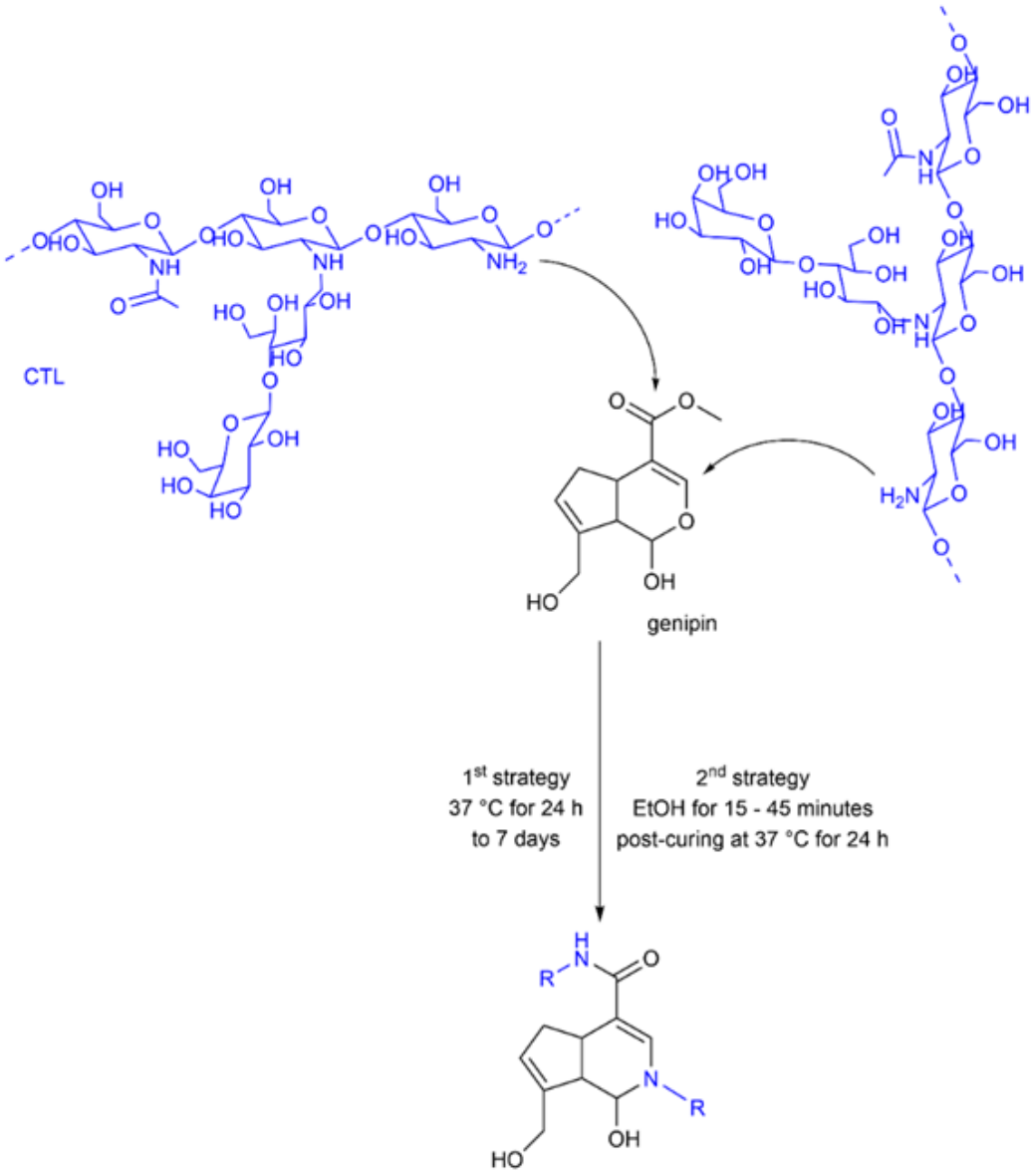

Figure 18. Genipin reaction mechanism in the electrospinning solution (first strategy) or in the presence of CTL aminic moieties on nanofiber backbone (second strategy).

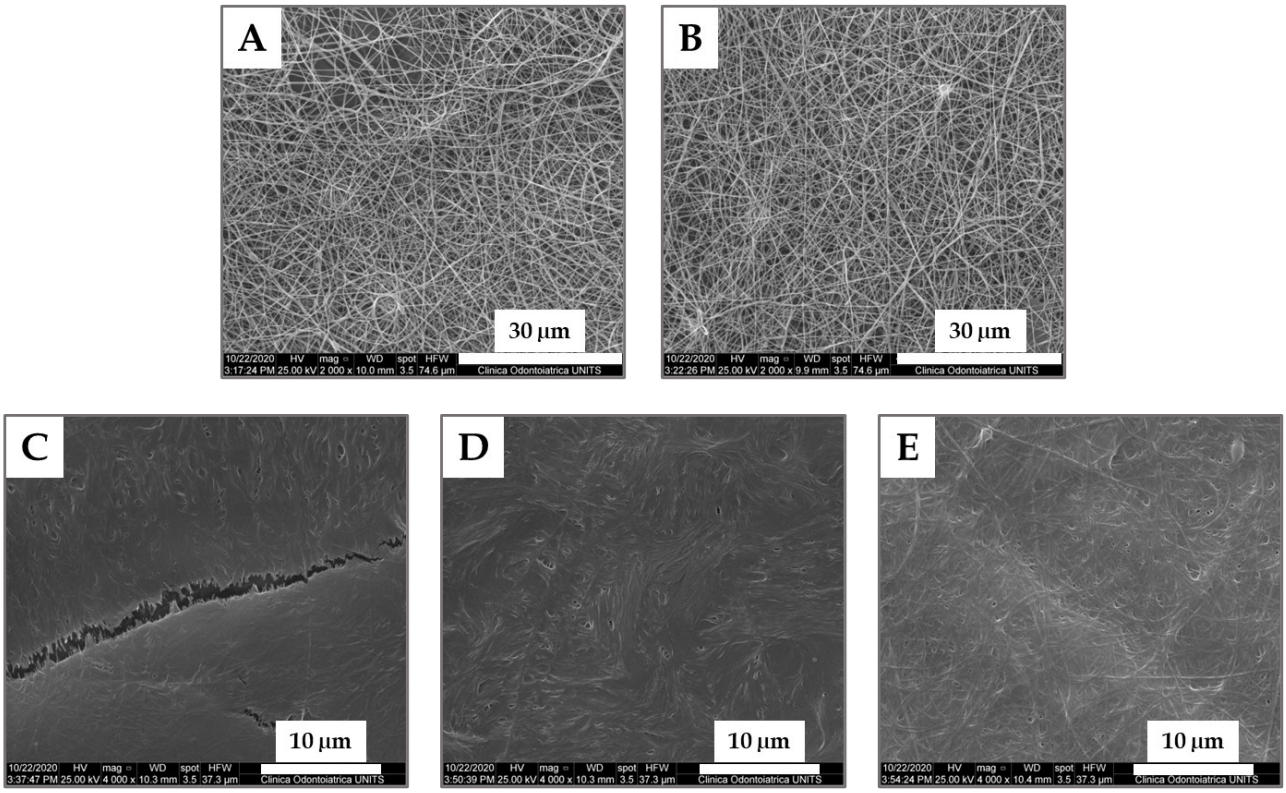

Figure 19. SEM micrographs of HA/CTL/PEO matrices electrospun after the addition of **(A)** 0.05% (w/V) and **(B)** 0.2% (w/V) genipin or treated after the electrospinning process with 0.5% (w/V) genipin in ethanol for **(C)** 15 minutes, **(D)** 30 minutes, **(E)** 45 minutes and then heated at 37 °C for 24 hours.

4.1.4.4. Thermal treatment

Thermal treatment was performed at 80 °C in a convection oven for 4, 6, and 8 hours, but the nanofibrous structure was lost after only 4 hours and the membranes showed absolute instability in water (**Figure 20A**). Therefore, with the aim of improving the thermal treatment procedure in a dry environment, the membranes were even crosslinked in a vacuum oven at 80 °C with different time settings. Nevertheless, in all cases neither the fibrous architecture was maintained nor the stability in water was achieved (**Figure 20B-E**), thereby demonstrating the ineffectiveness of this type of crosslinking in stabilizing the polysaccharidic structure, regardless of the environmental parameters.

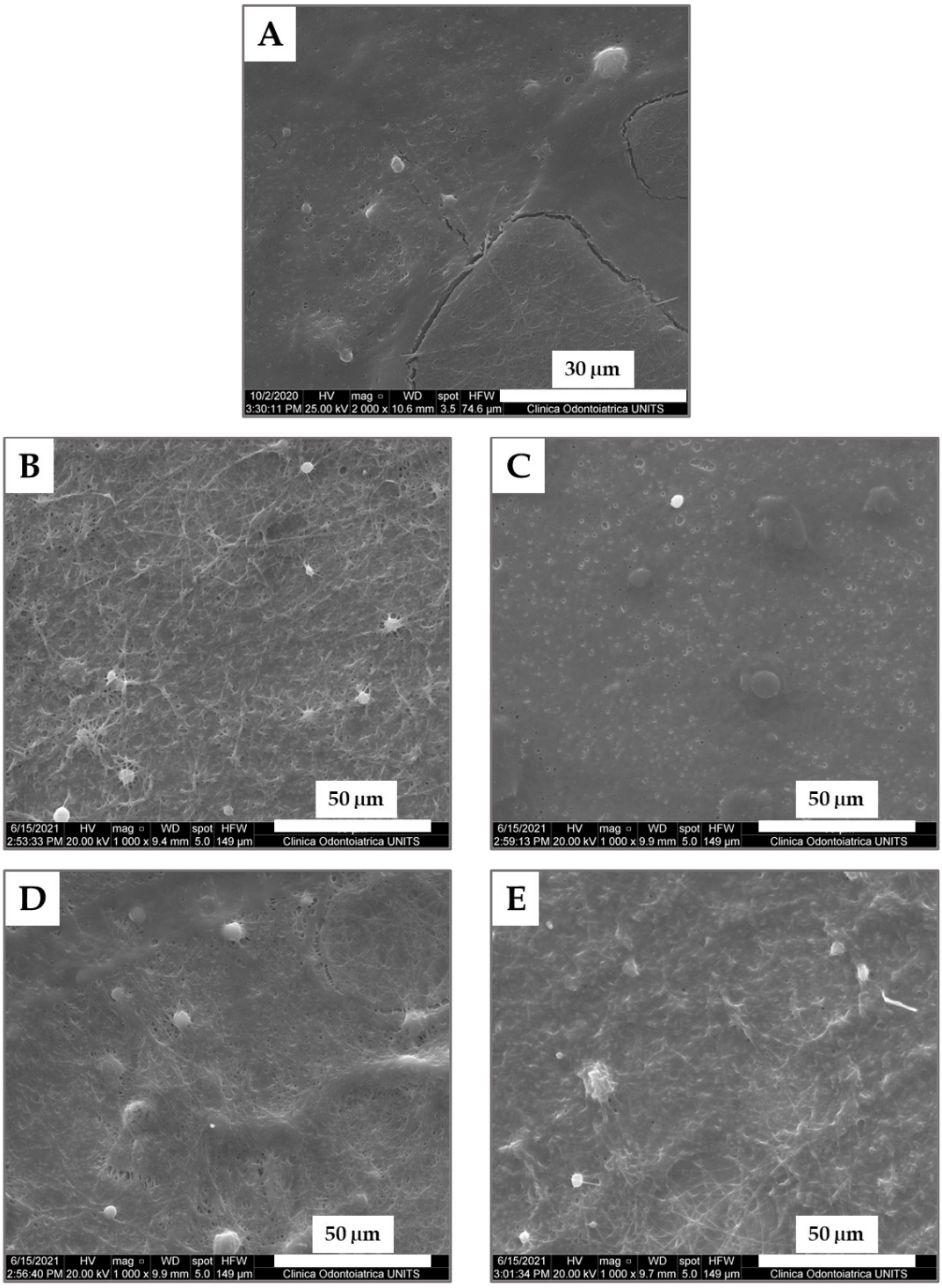

Figure 20. SEM images of the polysaccharide membranes after thermal treatment performed at 80 °C by **(A)** heating in a convection oven for 4 hours and in a vacuum oven for **(B)** 1 hour after equilibration from 20 °C to 80 °C; **(C)** 1 hour; **(D)** 2 hours; **(E)** 3 hours.

4.1.4.5. Methacrylic anhydride

Pure methacrylic anhydride was used to stabilize polysaccharide-based electrospun mats, exploiting the ability of this crosslinker to directly react with primary amines or hydroxyl groups (**Figure 21**).[262,263]

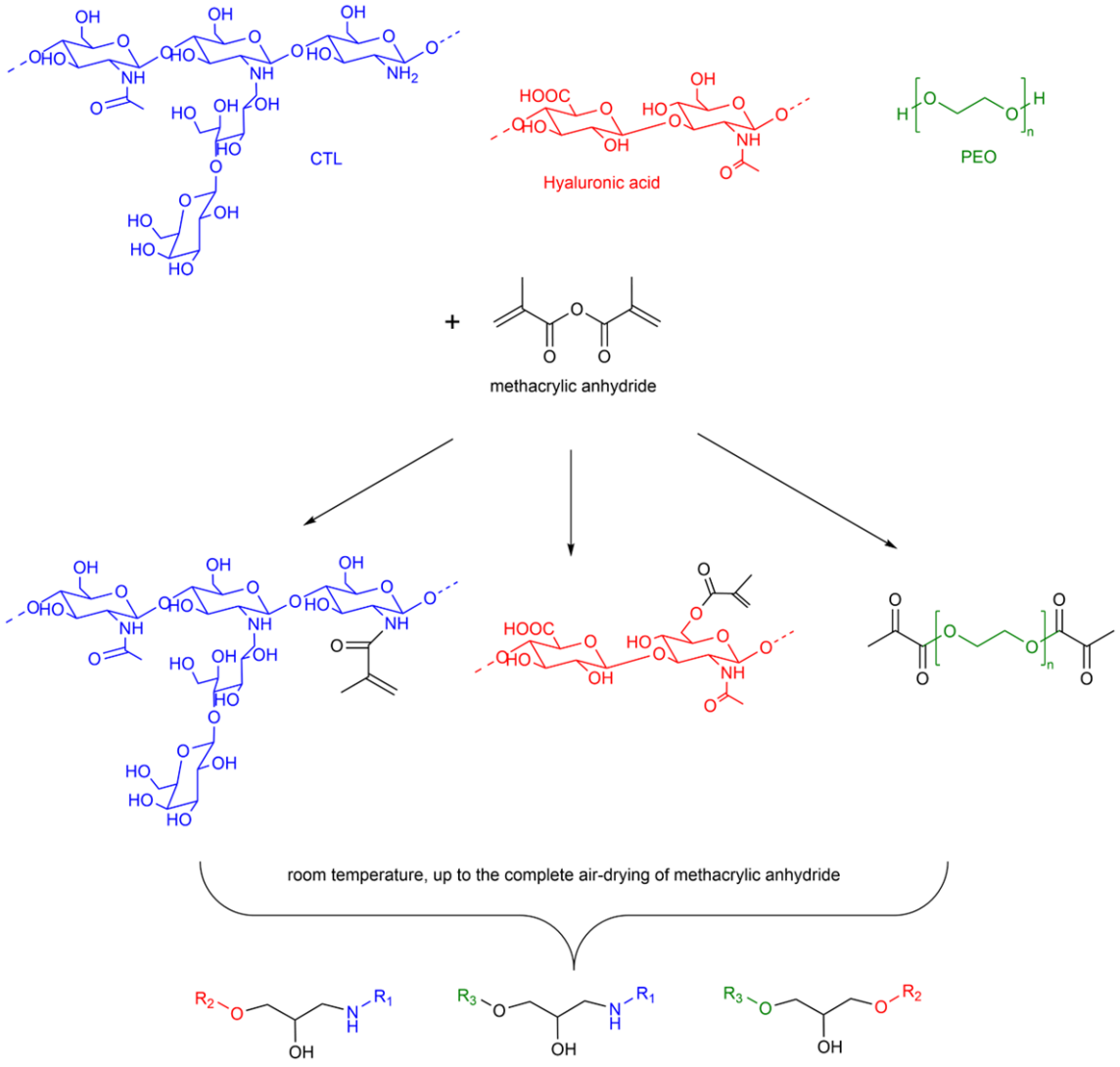

Figure 21. Methacrylic anhydride reaction mechanism in the presence of aminic moieties (CTL) or hydroxyl groups (hyaluronic acid, PEO).

After treatment with methacrylic anhydride, the membranes were subjected to an additional washing step to remove the excess methacrylic anhydride while retaining the nanofibrous architecture. To this aim, different solvents were tested, namely water, sodium hydroxide, methanol, acetone, and dimethylformamide. Of the different methods tested (**Figure 22 A-E**), only washings in acetone and

dimethylformamide gave satisfactory results in terms of structural integrity, with acetone being safer in terms of biocompatibility.

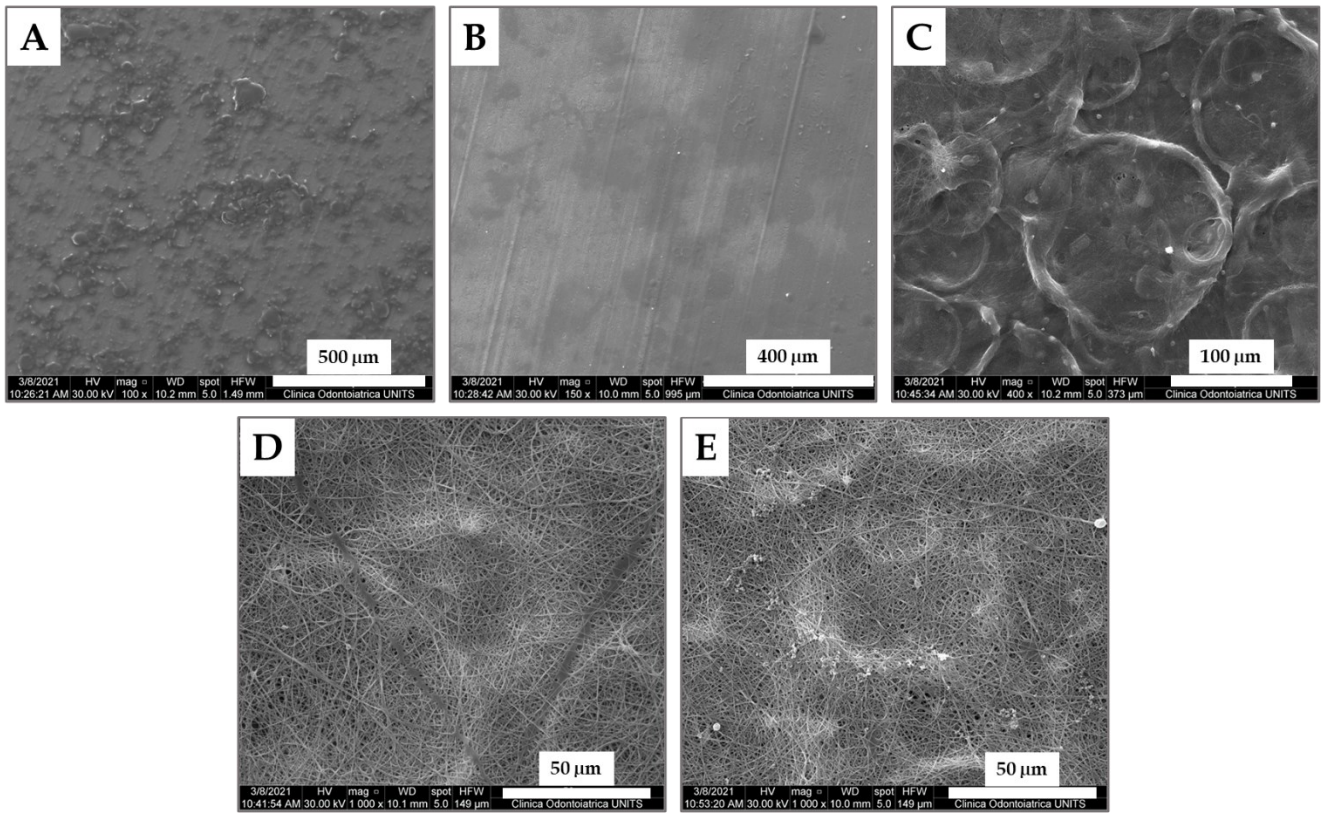

Figure 22. SEM micrographs of HA/CTL/PEO matrices stabilized with methacrylic anhydride e washed with **(A)** water, **(B)** sodium hydroxide, **(C)** methanol, **(D)** acetone, and **(E)** dimethylformamide.

4.1.4.6. Carbonyldiimidazole (CDI)

With the aim of finding the optimal reaction conditions to stabilize the polysaccharidic structure, CDI crosslinking was carried out with different amounts of crosslinker (namely, 100, 50, 25, 10 equivalents of CDI per mol of CTL glucosamine residues) overnight in DMF. Crosslinking with 100 and 25 equivalents of CDI allowed stability of membranes in water, but extremely changed the morphology of the nanofibers, while the crosslinking with 50 equivalents was the best compromise in terms of fiber preservation and water resistance (**Figure 22**). Indeed, in the presence of 100 equivalents the stability in water is guaranteed, but the treatment is too strong to preserve the nanofiber architecture. On the other hand, 25 equivalents allow the stabilization of the membrane, but

the crosslinking is too labile leading to fiber fusion. Finally, crosslinking with 10 equivalents caused the immediate dissolution of the nanofibrous matrix and was thus ineffective.

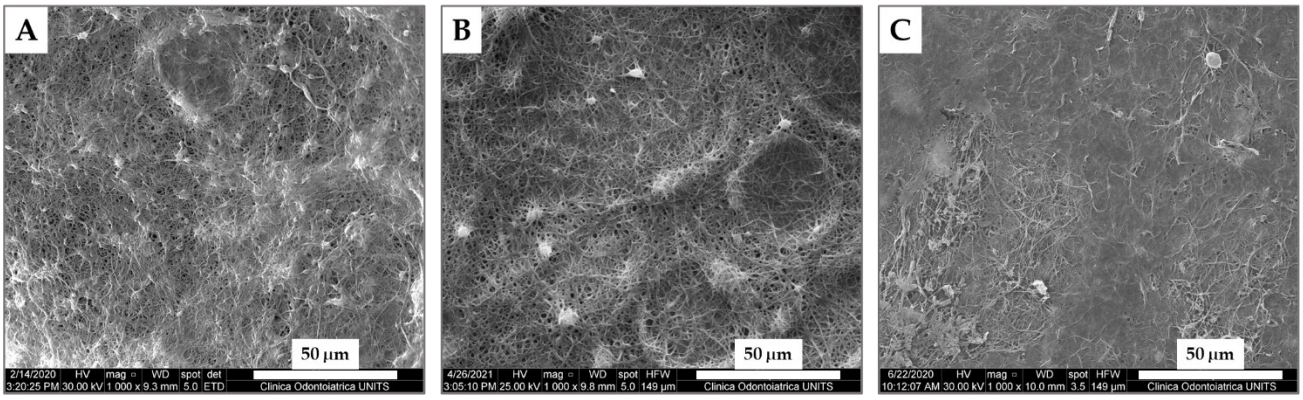

Figure 22. SEM images of HA/CTL/PEO matrices crosslinked with different equivalents of CDI per mol of CTL glucosamine residues: **(A)** 100 equivalents, **(B)** 50 equivalents, **(C)** 25 equivalents. The crosslinking with 50 equivalents is the best compromise which allows to partially retain the nanofibrous structure while ensuring matrix water resistance.

Different solvents (namely, dichloromethane, dimethyl sulfoxide, and tetrahydrofuran) were tested to analyze the effects of the reaction medium on the goodness of the crosslinking (**Figure 23**). Despite the stability of the matrices in aqueous environment, the nanofibrous architecture was completely lost in all cases, with evident fiber fusion and polymer precipitation.

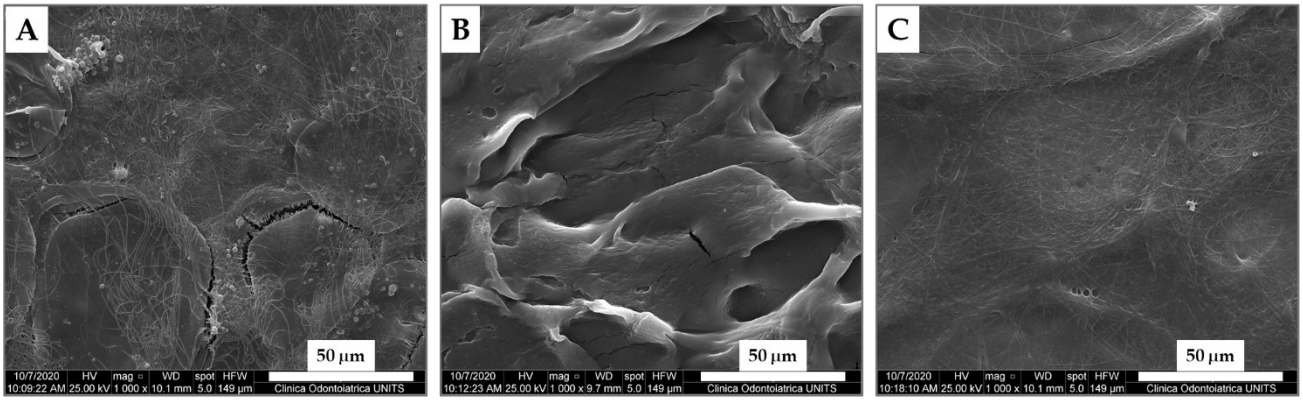

Figure 23. SEM micrographs of HA/CTL/PEO matrices crosslinked with 50 equivalents of CDI in different solvents: **(A)** DCM, **(B)** DMSO, **(C)** THF. In all cases, the nanofibrous structure is significantly altered by the chemical treatment.

Therefore, DMF confirmed to be the best reaction solvent with the proposed mechanism illustrated in **Figure 24**.

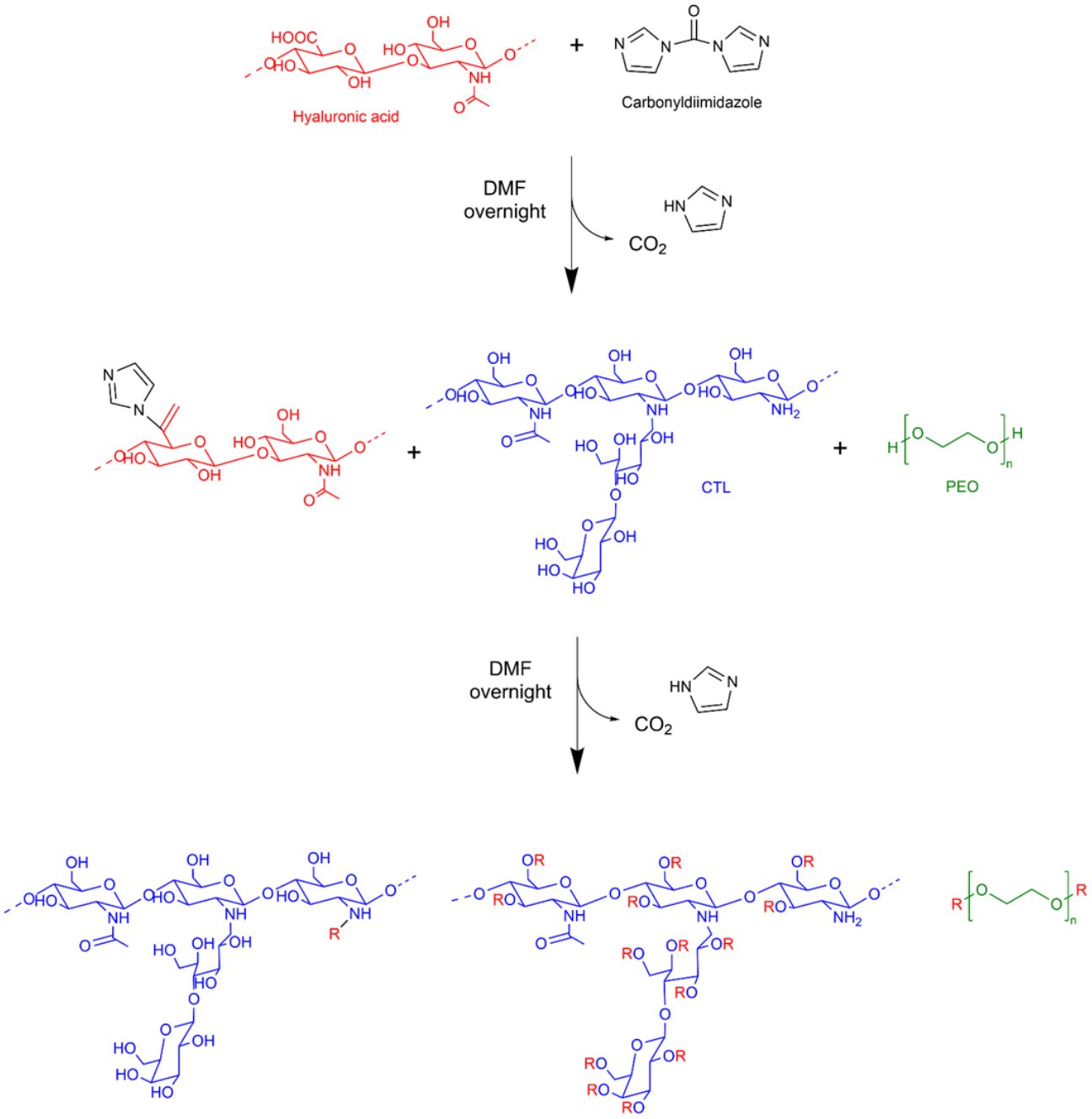

Figure 24. Schematic representation of the proposed reaction mechanism of CDI in the presence of hyaluronic acid, CTL, and PEO chains.

In an attempt to improve the long-term membrane stability, the chemical crosslinking was combined with thermal treatment, by heating the CDI-crosslinked polysaccharide matrices. However, even in this case thermal treatment led to unsatisfactory results, as it affected the nanofiber morphology and made the membrane unstable (**Figure 25**).

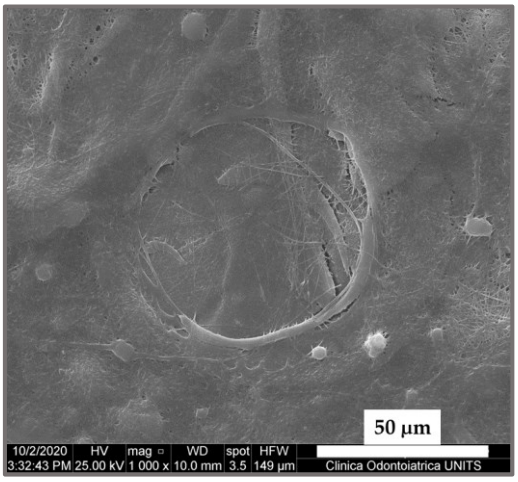

Figure 25. SEM representation of a polysaccharidic membrane chemically crosslinked with 50 equivalents of CDI and post-treated by heating at 80 °C. The thermal treatment considerably alters matrix architecture, destabilizing it.

Finally, to find the best reaction time, CDI crosslinking was performed at different timepoints, namely 1, 2, 3, 4, 5, 6, 7, 8 hours, and overnight (**Figure 26-27**). By comparing the morphology of the crosslinked mats before and after immersion in water, it was observed that the overall nanofibrous architecture was slightly affected after the crosslinking step, with a kind of partial fiber fusion. The best results were, by the way, obtained after overnight incubation, since the slight morphological alteration was compensated by the optimal water resistance.

Therefore, overnight crosslinking with 50 equivalents of CDI in DMF was selected for further membrane characterization.

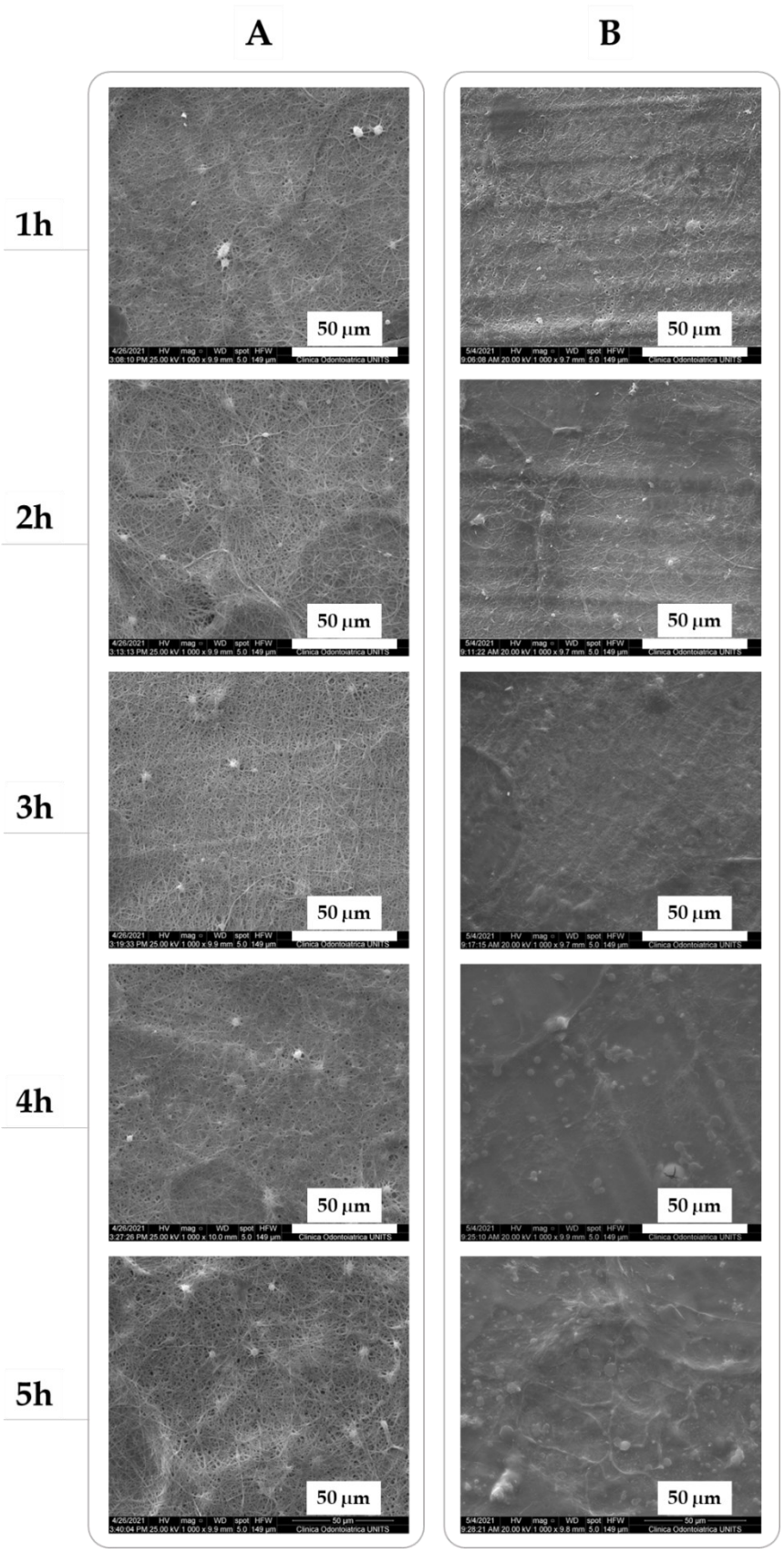

Figure 26. SEM micrographs of HA/CTL/PEO matrices crosslinked with 50 equivalents of CDI at different timepoints (**from 1 hour to 5 hours**), by comparing the structure before (**Panel A**) and after (**Panel B**) immersion in water. The comparison between crosslinked mats before and after immersion in aqueous environment shows the additional changes in their morphology caused by water.

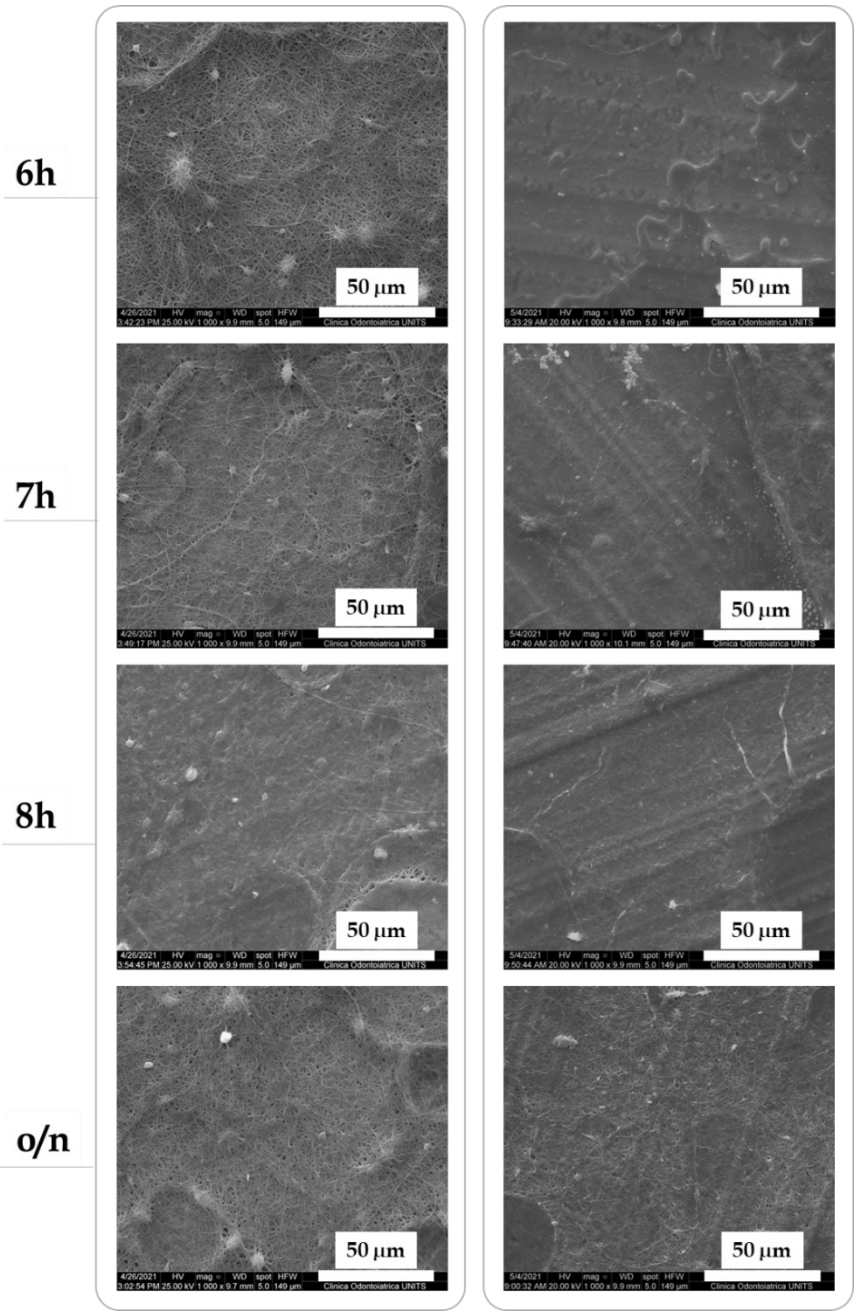

Figure 27. SEM micrographs of HA/CTL/PEO matrices crosslinked with 50 equivalents of CDI at different timepoints (**from 6 hours to the overnight treatment**), by comparing the structure before (**Panel A**) and after (**Panel B**) immersion in water. The comparison between crosslinked mats before and after immersion in aqueous environment shows the additional changes in their morphology caused by water.

4.1.5. Physicochemical characterization

4.1.5.1. Membrane characterization by attenuated Total Reflectance – Fourier Transform Infrared (ATR-FTIR) spectroscopy (4000-500 cm^{-1})

After determining that CDI-mediated crosslinking was the best among the other methods tested, with an adequate equilibrium between fiber loss and aqueous resistance, ATR-FTIR spectroscopy was exploited to study the formation of amide bond within the HA/CTL/PEO chains in the nanofibrous mat after overnight treatment with CDI, as reported in **Figure 28**. The spectra of uncrosslinked and crosslinked membrane were compared with the spectra of their individual components (namely, hyaluronic acid, CTL, PEO) and of CDI, with the characteristic bands being distinguishable within the spectra. However, no CDI signals were detected in the case of CDI-crosslinked meshes, since CDI is the coupling agent that only mediates the formation of the amide bond without being incorporated into the structure.[264] On the other hand, the signal related to the amide bond formation was superimposed on the IR signals of carbonyl (C=O) and carboxylic (-COOH) groups, which hindered the identification of its band.

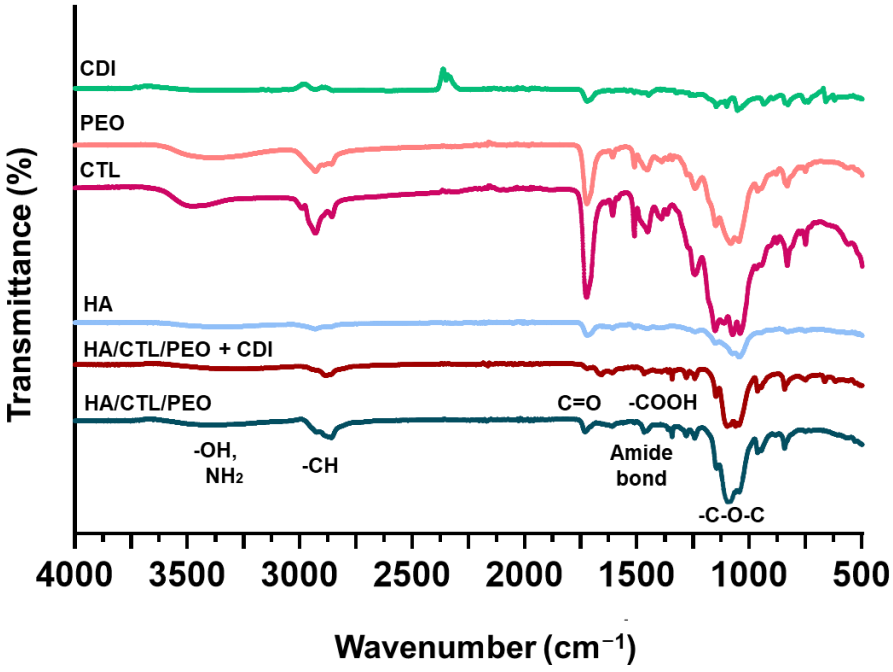

Figure 28. ATR-FTIR spectra of CDI-crosslinked and un-crosslinked polysaccharidic mats, compared with the spectra of the single membrane constituents (that are hyaluronic acid, CTL, PEO) and of CDI (in the case of crosslinked mats).

4.1.5.2. Swelling behavior

The swelling behavior of CDI- and methacrylic anhydride-crosslinked matrices was evaluated in both water and saline solution (NaCl 150 mM), chosen to reproduce physiological conditions.[265–267] Polysaccharide matrices were compared with : i) non-electrospun products, namely CDI-crosslinked freeze-dried membranes obtained from the same solution used to produce HA/CTL/PEO electrospun mats together with the commercial product Chitoderm®; ii) synthetic-based electrospun mats as non-activated, activated, and CTL/HA-coated PCL matrices. As can be seen in **Figure 29**, the nanofibrous structure together with the great hydrophilicity of the polysaccharides employed in the CDI-crosslinked electrospun membranes have a strong influence on the swelling capacity of the matrix in both water and saline solution. For similar reasons, plasma-activated PCL membranes showed a remarkable increase in swelling ratio up to 24 hours compared to non-activated PCL and polysaccharide-coated mats (**Figure 29B**). Considering the high hydrophilicity of both the CTL and hyaluronic acid mentioned above, the lower swelling capacity registered in the presence of the polysaccharidic coating could be explained by the rapid formation of a hydrated uniform layer, which affects membrane porosity and reduces the absorption capacity of the material. On the other hand, CDI-crosslinked electrospun polysaccharidic membranes possessed a swelling behavior close to that of activated PCL ones. This indicates that these membranes retain a high swelling capacity, despite the partial loss of the fibrous structure induced by the crosslinking step. In contrast, the membranes crosslinked with methacrylic anhydride were not able to retain large amounts of liquid as they started dissolving within the first hour of immersion. Furthermore, notwithstanding the high stability of the commercial product Chitoderm®, its ability to retain water was about 3 times lower at 24 hours than CDI-crosslinked electrospun mats (**Figure 29A**). A similar trend was observed with non-electrospun polysaccharidic membranes, thus confirming the crucial role played by the nanofibrous structure in determining the ability of the device to absorb a huge quantity of fluid. The high hydrophilicity of CDI-crosslinked polysaccharide membranes and of activated PCL membranes, their marked swelling

behavior and, thus, the large amount of absorbed fluid are responsible for the higher variability of the results compared to other materials.

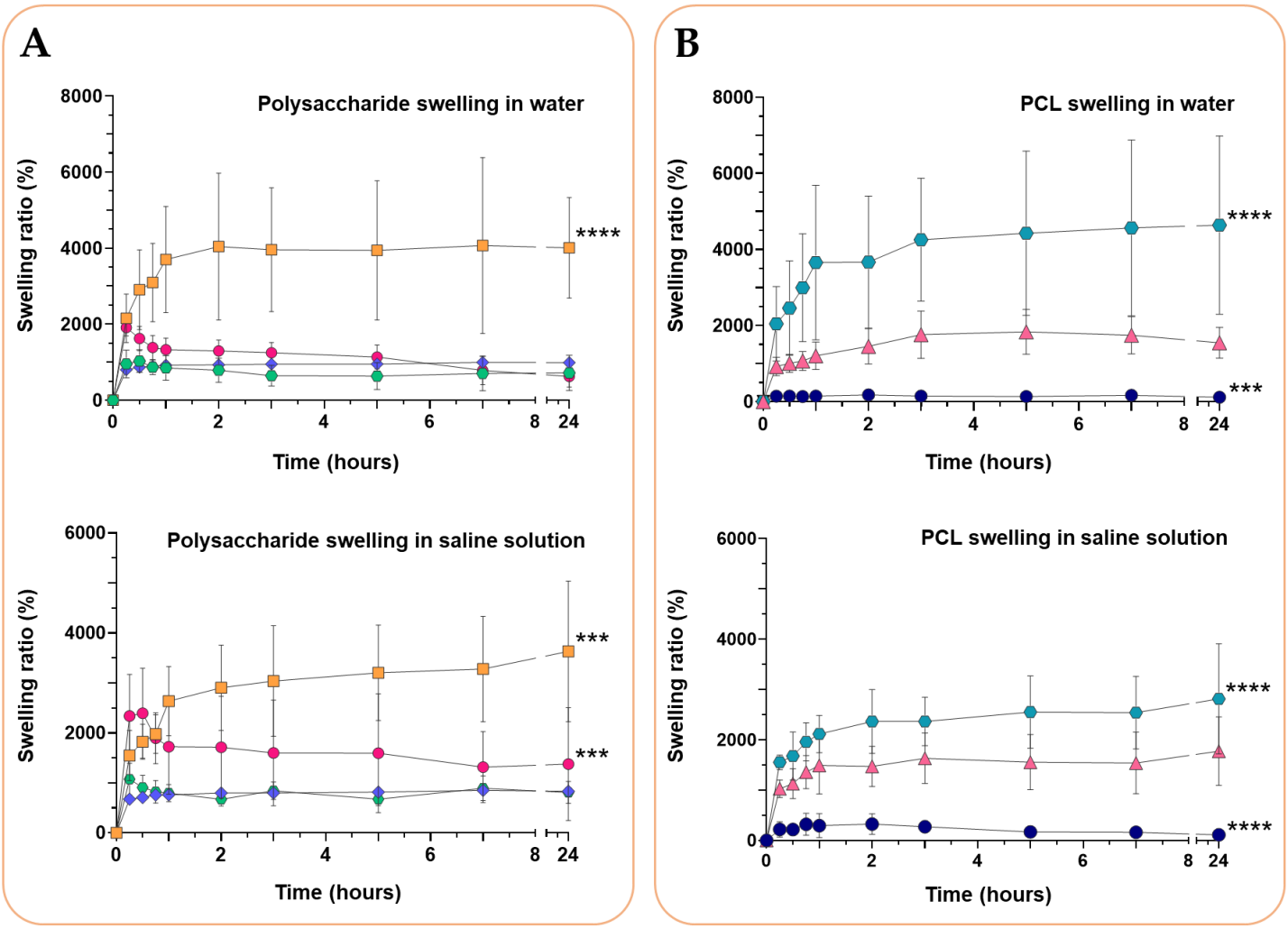

Figure 29. Swelling behavior in water and saline solution (NaCl 150 mM) of electrospun and non-electrospun membranes expressed as swelling ratio (%) as a function of the immersion time.

Panel A: swelling capacity of (■) polysaccharide-based electrospun membranes crosslinked with CDI or (●) methacrylic anhydride, (⬣) polysaccharide-based freeze-dried membranes and (◆) Chitoderm®.

Panel B: swelling capacity of (●) non-activated, (⬣) activated, and (▲) polysaccharide-coated PCL membranes.

In the case of polysaccharides in water, statistical analysis was performed with Kruskal-Wallis test and Mann-Whitney test for two-groups comparison, applying Bonferroni's correction. In the case of polysaccharides in saline solution, PCL in water, and PCL in saline solution, statistical analysis was performed with ANOVA test, applying Bonferroni's correction. Statistically significant differences are indicated with asterisks (*). *** = $p < 0.001$.

4.1.5.3. Degradation tests

Considering the frequency of dressing changes and the importance of maintaining a suitable architecture compatible with dressing removal,[268–270] the stability of the electrospun membranes was followed up to 7 days in both water and saline solution, by measuring the weight variation over time (**Figure 30**). Polysaccharide-based matrices crosslinked with CDI and methacrylic anhydride were compared to PCL membranes (non-activated, activated, and polysaccharide coated), Chitoderm®, and freeze-dried polysaccharidic membranes crosslinked with CDI. The results confirmed the overall stability of all the PCL-based membranes, even in the presence of the coating. However, in this last case a slight degradation behavior was observed, maybe due to the coating desorption in the aqueous environment after 1 to 3 days of immersion, depending on the tested fluid. On the other hand, the efficacy of the CDI crosslinking was assessed by comparing it with methacrylic anhydride crosslinking. In this case the membranes displayed a progressive degradation behavior after only 1 day, leading to matrix rupture. On the other hand, CDI-crosslinked mats revealed an optimal stability in water until day 7, while they were stable in saline solution for up to 3 days. After that, a slight degradation trend was noticeable even if affected by some fluctuation on the measure, possibly caused by the presence of salts destabilizing the polysaccharidic structure. At the same time, CDI-crosslinked membranes obtained by freeze-drying underwent a mild degradation between 1 and 3 days in water or saline solution, respectively, without showing any degradation in the next timepoints; in contrast, Chitoderm® samples were stable over time regardless of the tested fluid.

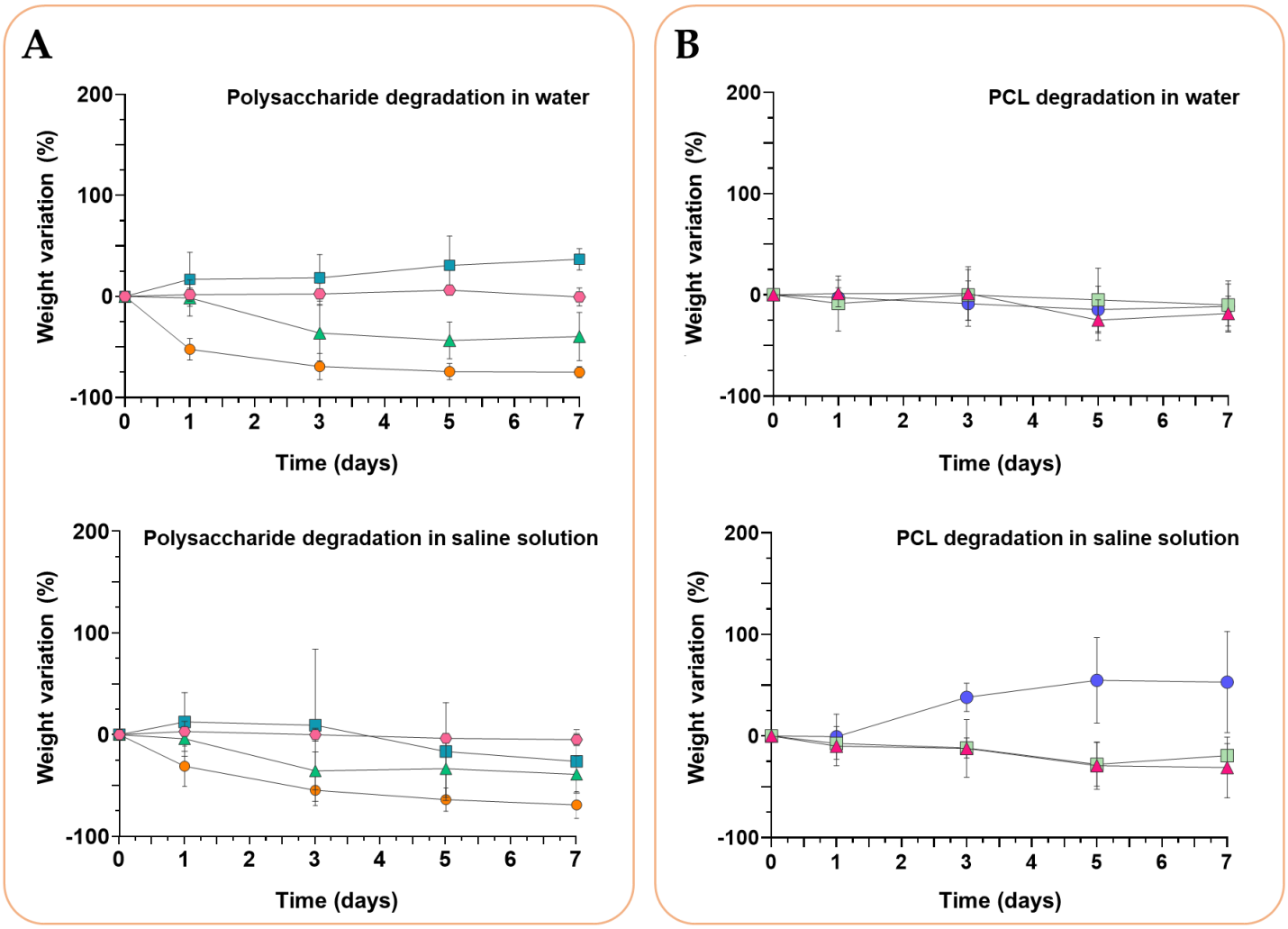

Figure 30. Degradation behavior in water and saline solution (NaCl 150 mM) of electrospun and non-electrospun membranes expressed as weight variation (%) in time.

Panel A: degradation of (■) polysaccharide-based electrospun membranes crosslinked with CDI or (●) methacrylic anhydride, (▲) polysaccharide-based freeze-dried membranes and (⬣) Chitoderm®.

Panel B: degradation of (●) non-activated, (■) activated, and (▲) coated with polysaccharides PCL membranes.

In all cases, statistical analysis was performed with Kruskal-Wallis test and Mann-Whitney test for two-groups comparison, applying Bonferroni's correction; no statistical differences were found.

4.1.5.4. Membrane permeability

The ability to transmit water vapor was assessed on electrospun membranes crosslinked with CDI, which were compared with three types of electrospun PCL membranes (namely, non-activated, activated, or coated with CTL/HA) and Chitoderm®. Parafilm® was used as a control for non-permeability; unsealed vials were tested as control for total evaporation. The results (**Figure 31**) indicated an optimal water vapor permeability for PCL membranes, which all showed similar results. CDI-crosslinked polysaccharide mats revealed a similar trend to PCL mats after 24 hours, but the transmission rate was lower than PCL after 48 hours. This could be due to the composition of the membrane itself, which is based on highly hydrophilic polymers. Due to its polysaccharidic nature, its great ability to retain water could result in water being trapped in the nanofibrous structure, leading to a weight increase when measuring the amount of residual water in the system. Nevertheless, the water vapor permeability of polysaccharidic electrospun mats was still higher than that of Chitoderm®, in which case the outer polyurethane layer shields pathogen entry but reduces at the same time water evaporation.

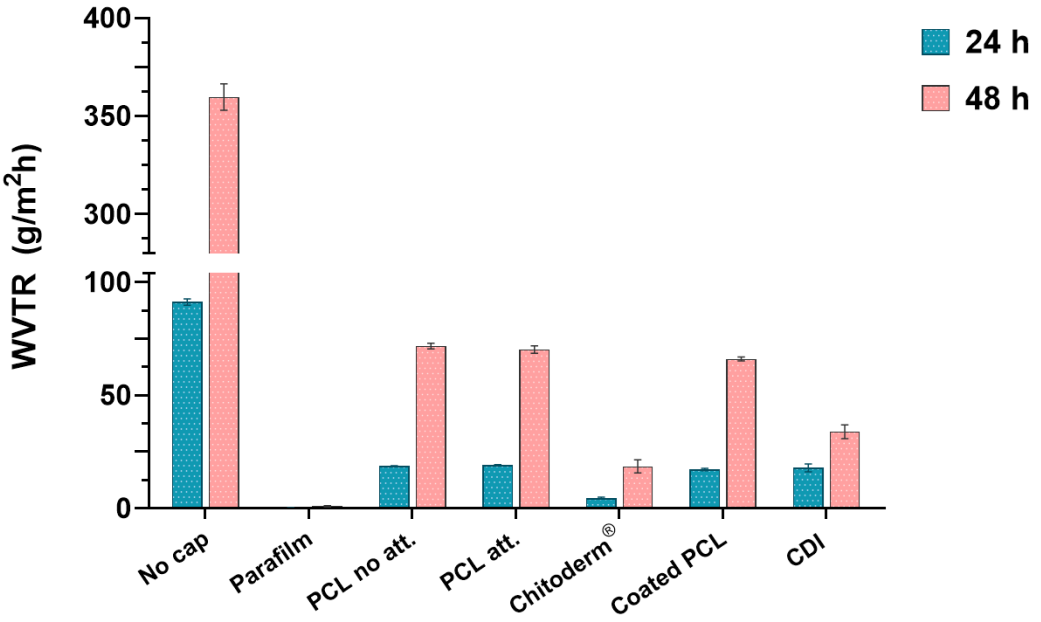

Figure 31. Water vapor transmission ability of PCL (non-activated, activated, coated) mats, CDI-crosslinked polysaccharidic membranes, and Chitoderm® after 24 hours and 48 hours. All the electrospun products present a suitable permeability to water vapor, with a midway behavior between the total evaporation or the absence of transmission.

4.2. Multilayer membranes

Despite the promising results obtained with monolayer polysaccharide-based electrospun membranes, their handling and adaptability to the wound could be a critical issue hindering their applicability on the wound bed. For this reason, two types of multilayer systems were considered : i) a fully electrospun system (hereafter referred to as "**PCL bilayer**") obtained by combining the polysaccharidic matrix with a synthetic PCL counterpart, resulting in a bilayer membrane with a protective and easy to handle synthetic layer and a bioactive inner layer; ii) a polysaccharide-functionalized PCL membrane (hereinafter referred to as "**PCL coating**") realized by layer-by-layer deposition of CTL and hyaluronic acid on an electrospun PCL matrix. In addition, considering the need for antibacterial wound dressings able to prevent and control bacterial infections at the wound site, the PCL layer was even exploited to introduce a broad-spectrum antibiotic, namely rifampicin (Rif), to synthetize rifampicin-loaded PCL bilayer and PCL coating membranes, henceforth called "**Rif bilayer**" and "**Rif coating**", respectively.

4.2.1. Bilayer and coated matrices

The synthetic PCL membrane employed to produce the multilayer systems was that used for comparison in the monolayer membrane characterization (*section 4.1.3*), as it was easy to manufacture and had good morphology with uniform and defect-free fibers. In particular, the activated PCL matrix was chosen (**Figure 32A**), to allow a closer interaction with the polysaccharides, both in the case of the bilayer and coated matrices.

The coating was performed by layer-by-layer deposition of both CTL and hyaluronic acid at a final concentration of 0.6% (w/V) (**Figure 32B**). Even in this case, homogeneous, randomly oriented fibers were obtained, with the coating not affecting the goodness of the membrane. The higher polysaccharide concentration compared to the previously analyzed coated membranes (s*ection 4.1.3*) was chosen to increase the bioactivity of the final product.

The PCL bilayer system (**Figure 32C-D**) was, on the other side, realized by electrospinning the HA/CTL/PEO solution on a plasma-treated PCL matrix. In this case, it was possible to observe two uniform and superimposed matrices: i) the thicker PCL fibers in the rear region; ii) the thinner HA/CTL/PEO nanofibers in the front region (**Figure 32C**). Moreover, by observing the matrix from a side view, the two layers were clearly distinguishable (**Figure 32D**).

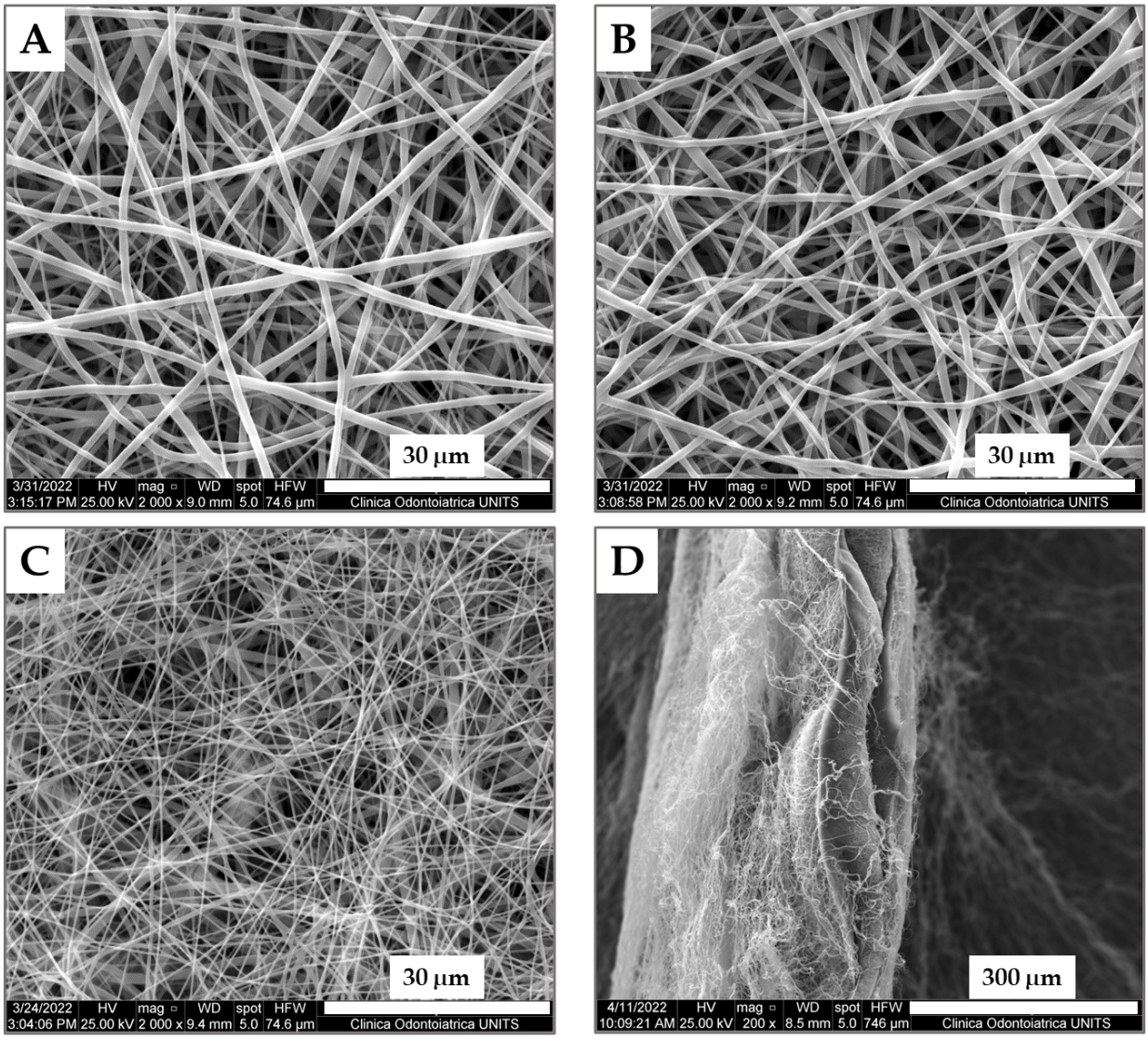

Figure 32. SEM micrographs of the multilayer matrices and their controls, namely **(A)** plasma-treated PCL, **(B)** PCL coating, PCL bilayer in **(C)** front view and **(D)** cross section.

The dimensional analysis (**Figure 33**) revealed that the presence of the coating slightly alters the fiber diameter compared to the PCL alone, which is due to partial fiber rehydration. Meanwhile, the lower fiber diameter calculated in the case of the bilayer which is associated to a higher standard deviation

could be due to the dual nature of the membrane: PCL on one side and polysaccharides on the other. Indeed, by analyzing the fiber diameter distribution in the three types of membranes, a homogenous distribution was observed in the case of PCL alone (**Figure 33B**) and PCL coating (**Figure 33C**), while the PCL bilayer showed an inhomogeneous distribution of fiber diameter, which was overcome by separating the two contributions given by the synthetic and polysaccharidic layers (**Figure 33D**).

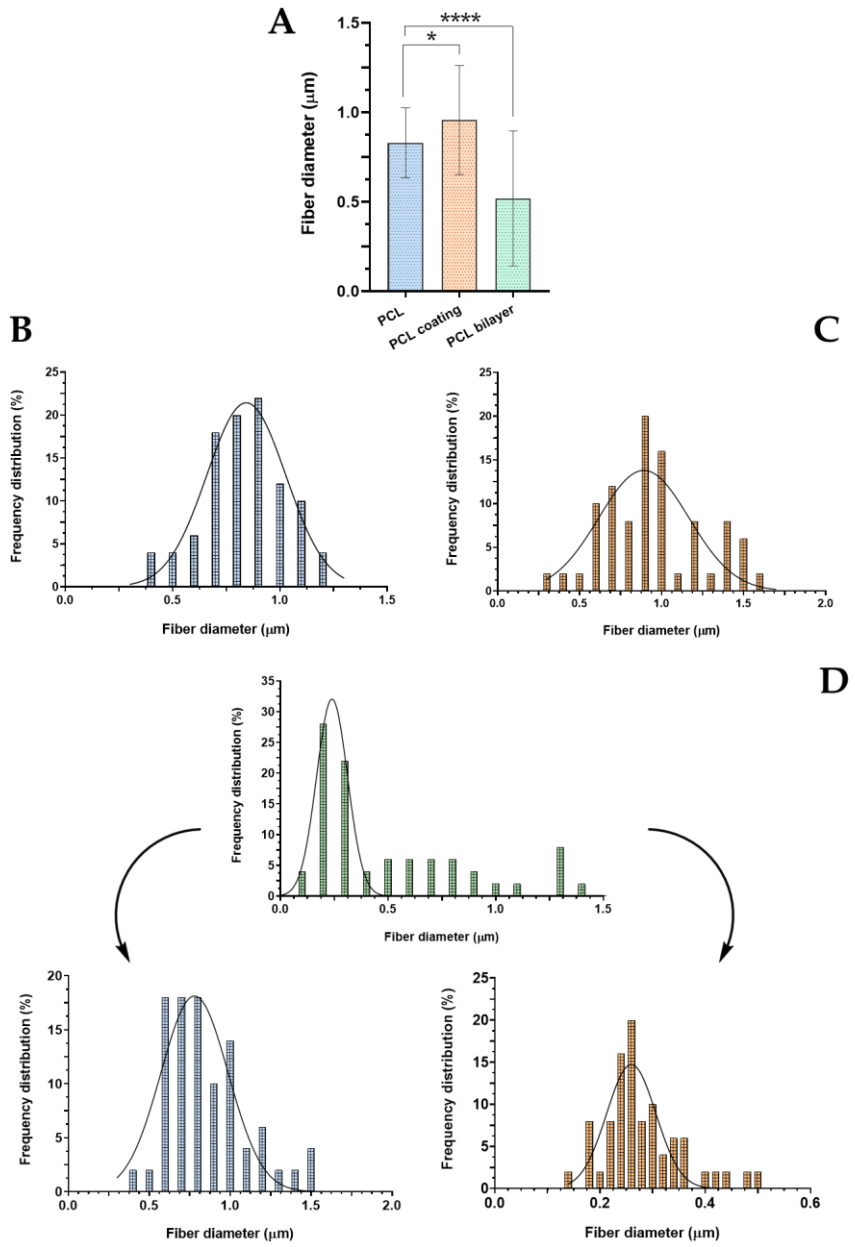

Figure 33. Dimensional analysis **(A)** of the PCL and multilayer systems and comparison of the fiber diameter distribution between **(B)** PCL, **(C)** PCL coating, and **(D)** PCL bilayer. In the case of the bilayer, the inhomogeneous distribution is explained by the distinct contribution of the PCL (lower left) and polysaccharides (lower right). Statistical analysis was performed with Kruskal-Wallis test and Mann-Whitney test for two-groups comparison, applying Bonferroni's correction. Statistically significant differences are indicated with asterisks (*). **** = $p < 0.0001$.

4.2.1.1. Rifampicin-loaded membranes

The multilayer systems were even endowed with an antibiotic agent, rifampicin, to confer them antibacterial properties. The antibiotic was added directly to the PCL electrospinning solution and thus integrated into the fibrous mesh. The resulting matrices (**Figure 34A-C**) showed no significant morphological changes compared to the non-functionalized matrices, with the typical homogeneous, defect-free, and randomly oriented fibers. Furthermore, the dimensional analysis (**Figure 34D**) revealed similar results to the rifampicin-free membranes. Even the statistical differences between the different types of membranes analyzed were comparable to the non-functionalized matrices, proving the goodness of the functionalization process, which does not alter the overall morphology.

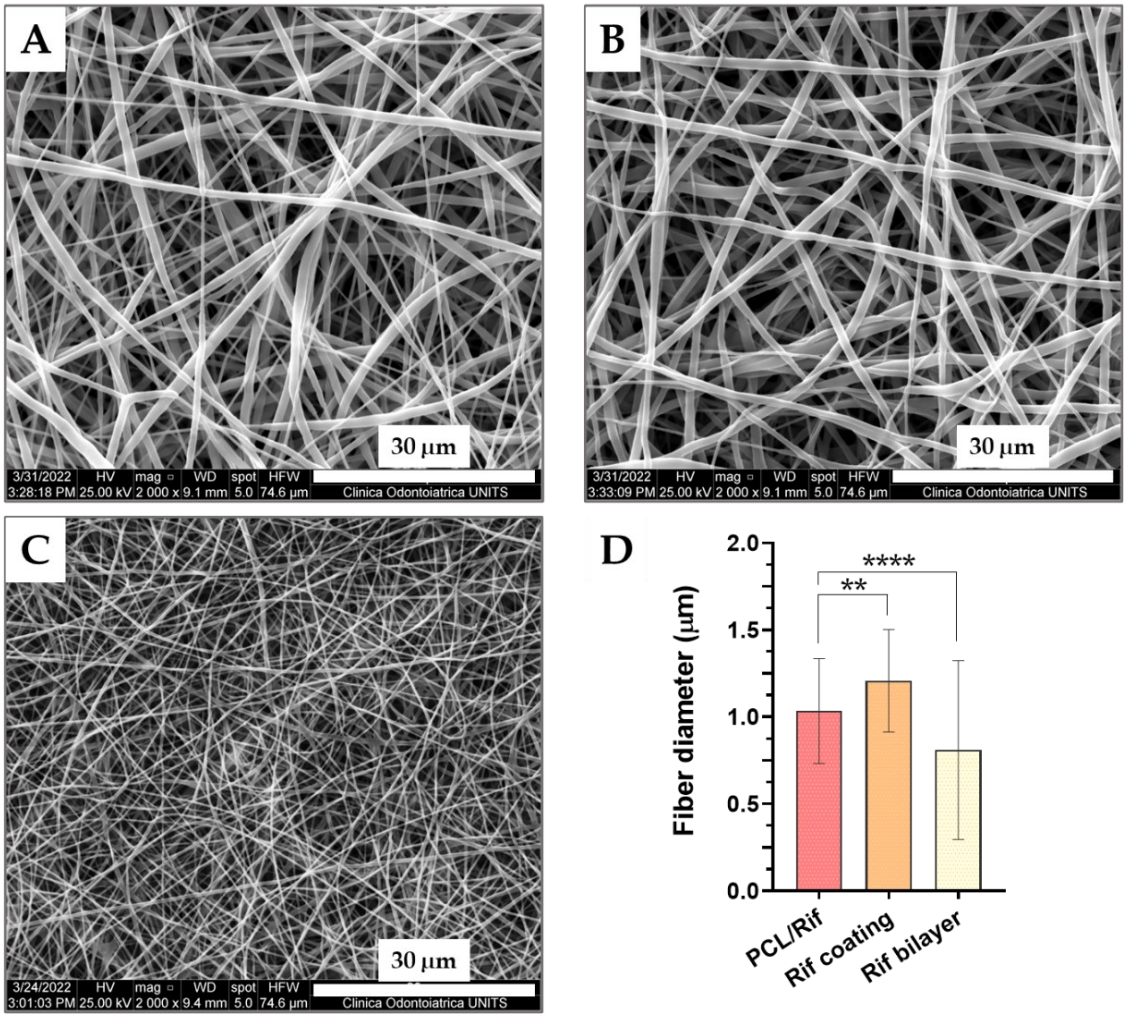

Figure 34. SEM micrographs of rifampicin-loaded membranes, namely **(A)** PCL/Rif, **(B)** Rif coating, and **(C)** Rif bilayer. On the lower right, **(D)** a comparison of fiber diameters. Statistical analysis was performed with Kruskal-Wallis test and Mann–Whitney test for two-groups comparison, applying Bonferroni's correction. Statistically significant differences are indicated as asterisks (*). **** = $p < 0.0001$.

4.2.2. Physicochemical characterization

4.2.2.1. Membrane characterization by Attenuated Total Reflectance – Fourier Transform Infrared (ATR-FTIR) spectroscopy (4000-500 cm^{-1})

ATR-FTIR spectroscopy was employed to assess the presence of polysaccharides and rifampicin on both the bilayer structure and on the coated matrices (**Figure 35**). The spectra of all the devices were compared with the spectra of their individual components. In the case of the bilayer, the presence of the polysaccharides was clearly indicated by the -OH band, which was even marked with respect to the polymers alone due to the combined effect of CTL, hyaluronic acid, and PEO. On the other hand, the same band was less pronounced in the coated membranes, probably due to the lower concentration of the polysaccharides and to the absence of PEO, when compared to the bilayer.

As regards the PCL basal layer, it was detectable in both the bilayer and the coated matrices thanks to the -CH and C=O bands, while the rifampicin could not be identified in the final structure since its signal overlapped with that of the other polymers.

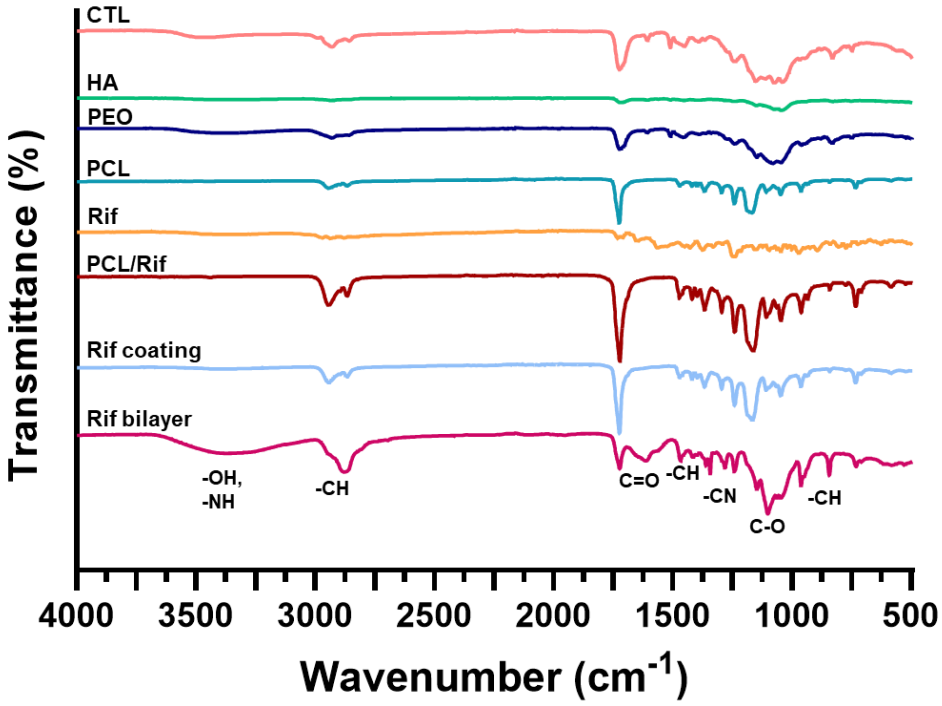

Figure 35. ATR-FTIR spectra of Rif coating and Rif bilayer matrices, compared with the spectra of the single membrane components (namely, CTL, HA, PEO, Rifampicin, PCL) and of the basal PCL/Rif membrane.

4.2.2.2. Swelling behavior

The swelling behavior of the PCL bilayer and PCL coating mats was evaluated in PBS, which is a fluid largely employed to study the water uptake capacity of wound dressing devices.[271–275]

The polysaccharide-based matrices were here compared with the PCL alone and their water uptake capacity was followed for up to 7 days. As can be observed in **Figure 36**, the swelling behavior of PCL bilayer was comparable to that of the pure plasma-treated PCL membrane, which reached a swelling ratio of about 4000% after 7 days. This demonstrates again the great advantage of using electrospun devices for wound care management, where the high porosity and available surface area allow to retain a considerable amount of exudate. On the other hand, the lower ability of PCL coating to absorb fluid was in line with the previous experiments (*section 4.1.5.2.*) and could be explained by the rapid hydration of the coating in the aqueous environment, which shields the porosity of the membrane and affects the swelling capacity of the material, although it still exhibits a high swelling ratio (about 1500%).

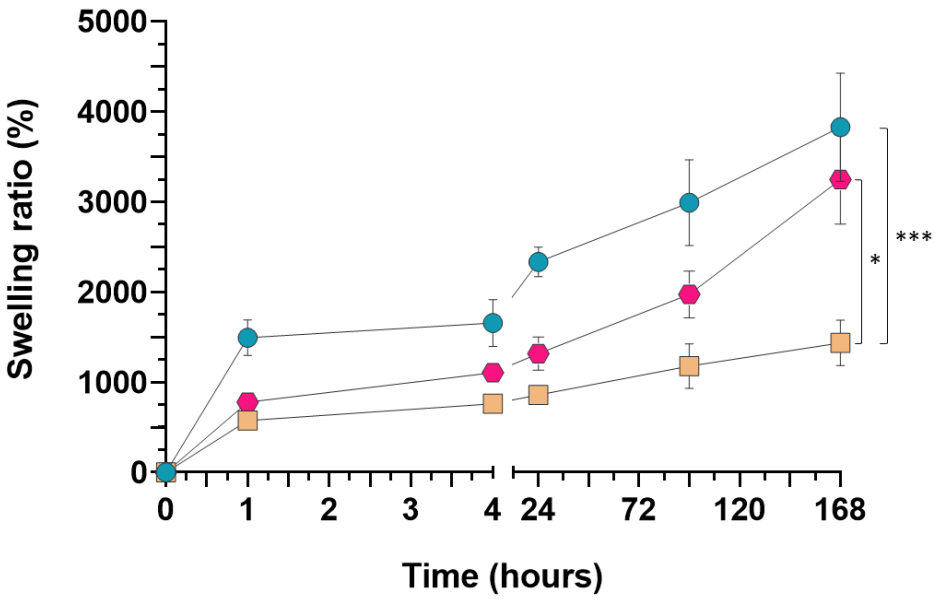

Figure 36. Swelling behavior in PBS of PCL bilayer (⬣) and PCL coating (■) matrices, compared with plasma-treated PCL mats (●).
The statistical analysis was performed with ANOVA test, applying Bonferroni's correction. Statistically significant differences are indicated with asterisks (*). *** = $p < 0.0001$.

4.2.2.3. Membrane permeability

Water vapor permeability and, thus, the ability to promote gas exchanges was assessed up to 72 hours on PCL bilayer and PCL coating mats, using plasma-treated PCL membranes as controls. On the other hand, Parafilm® was used as a control for non-permeability, while unsealed vials were tested as control for total evaporation. Consistent with what observed for the monolayer polysaccharide-based membrane (*section 4.1.5.4.*), the results (**Figure 37**) revealed an optimal ability of all types of the tested membranes to transmit water vapor, with an evaporation efficiency halfway between the total evaporation and the lack of transmission. Moreover, this behavior was sustained until 72 hours, revealing the effectiveness of these electrospun devices to preserve the proper moist environment at the wound site.

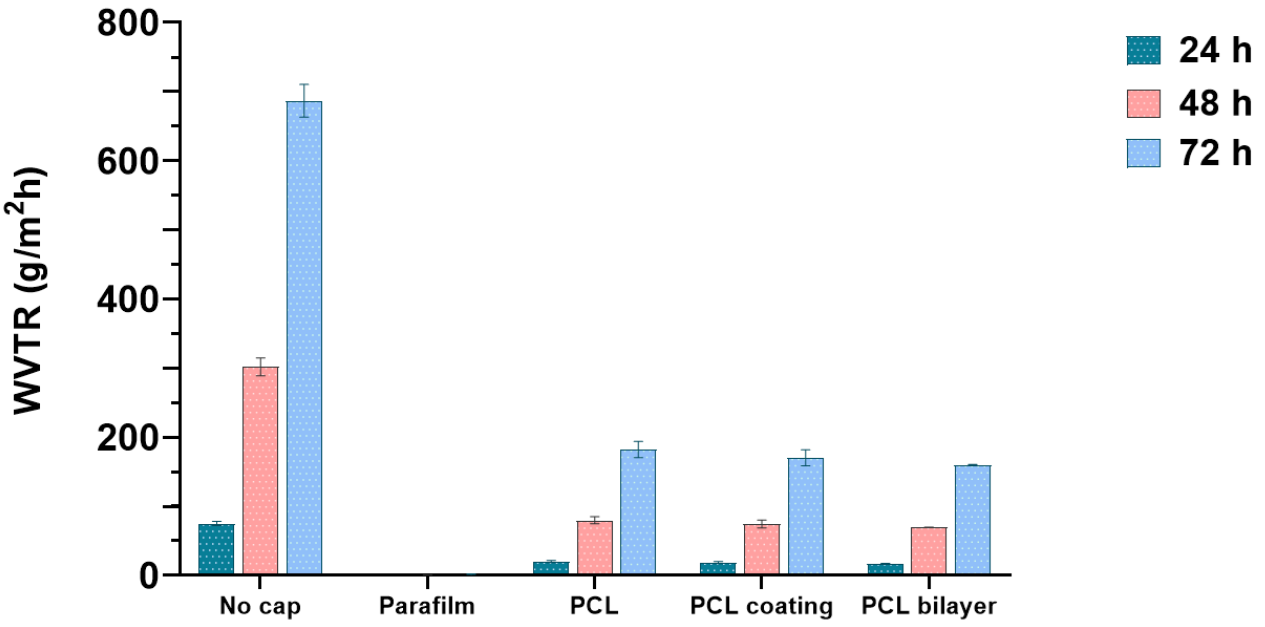

Figure 37. Water vapor transmission rate of plasma-treated PCL mats and of polysaccharide-enriched electrospun matrices (PCL coating and PCL bilayer). Even after 72 hours, all the electrospun products retain an appropriate permeability to water vapor, with a midway behavior between the total evaporation or the absence of evaporation.

4.2.2.4. Membrane wettability and surface free energy

The wettability of all types of electrospun membranes, namely PCL, PCL coating, and PCL bilayer, was examined using contact angle measurements. The same samples, but with rifampicin added, were also analyzed to evaluate how the presence of rifampicin affects the surface properties of the membranes. In particular, in the case of PCL alone, both not-treated and plasma-treated mats were tested to examine the effectiveness of air-plasma treatment in increasing the hydrophilicity of PCL-based membranes. The wettability measurements were carried out in the presence of three types of fluids: i) water; ii) water additioned with 10% fetal bovine serum (FBS), to evaluate any possible interaction with serum proteins; iii) Dulbecco's Modified Eagle Medium (DMEM), to assess membrane behavior in an *in vitro* cellular environment.

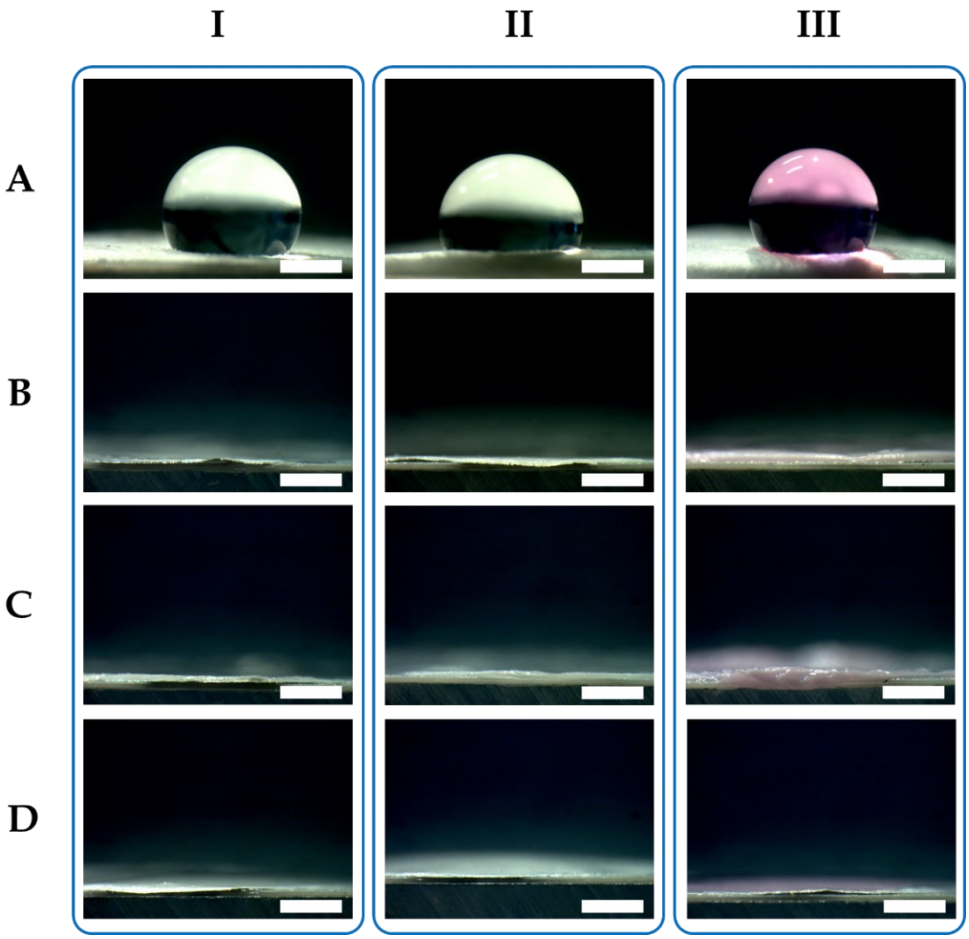

Figure 38. Contact angle images of **(A)** not-treated PCL, **(B)** plasma-treated PCL, **(C)** PCL coating, and **(D)** PCL bilayer matrices in the presence of **(I)** water, **(II)** water + FBS, and **(III)** DMEM. The absence of the drop is due to its complete spreading on the surface. Scale bar: 1 mm.

The membranes without rifampicin (**Figure 38**) revealed a highly hydrophilic behavior, with a complete fluid spreading on their surface in all cases, except for not-treated PCL, which showed to be non wettable with all types of medium tested, thus confirming how the air-plasma treatment impacts on membrane hydrophilicity. Similar wetting behavior was observed with the rifampicin-loaded mats (**Figure 39**), with drops spreading completely on the surface of both plasma-treated PCL and polysaccharide-endowed PCL. However, as far as the non-activated PCL is concerned, the expected hydrophobic behavior was retained in the presence of water and turned into a hydrophilic one in the case of water + FBS and DMEM. This can be attributed to the presence of rifampicin, which interacts with serum proteins and thereby increases hydrophilicity of the membrane.

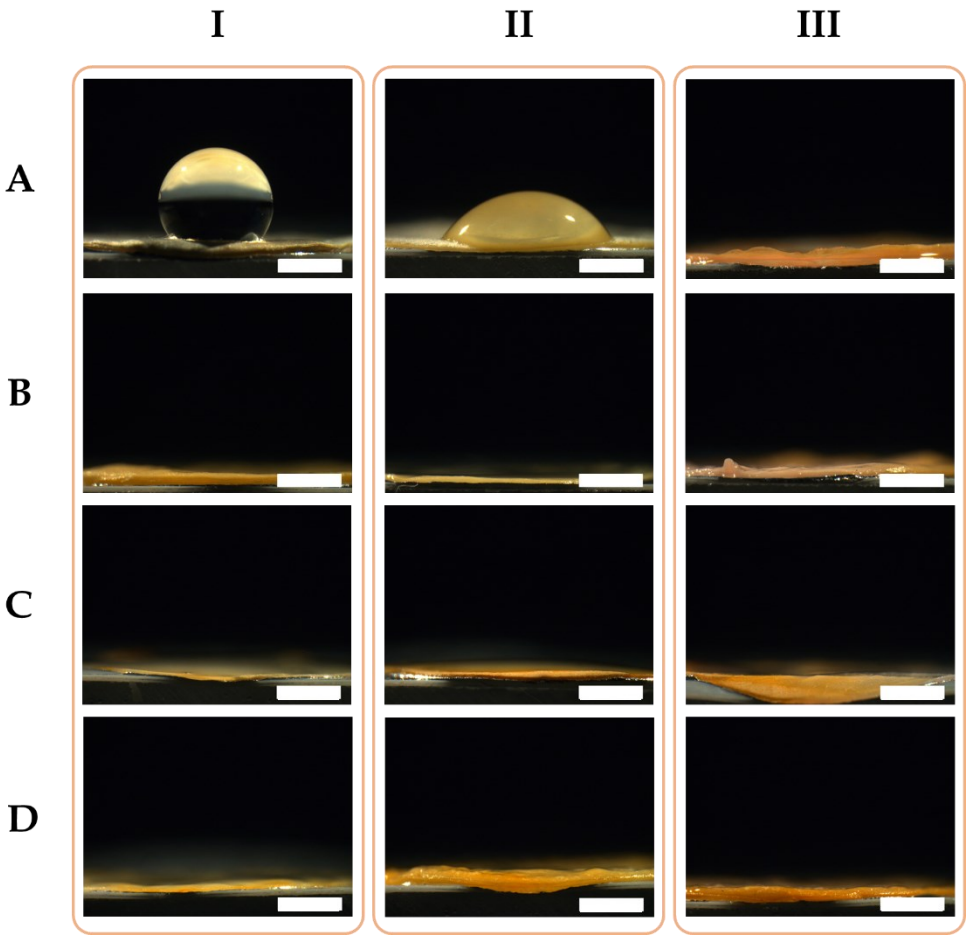

Figure 39. Contact angle images of Rif-loaded membranes: **(A)** not-treated PCL, **(B)** plasma-treated PCL, **(C)** PCL coating, and **(D)** PCL bilayer matrices in the presence of **(I)** water, **(II)** water + FBS, and **(III)** DMEM. The absence of the drop is due to its complete spreading on the surface. Scale bar: 1 mm.

Surface free energy of the samples was evaluated according to the Owens-Wendt method, by using the contact angle of water to calculate the polar/hydrophilic component (γ_s^p) and the contact angle of ethylene glycol to estimate the dispersive/hydrophobic component (γ_s^d). The analysis was performed both for both non-functionalized and rifampicin-loaded membranes (**Table 4**). The high contact angle values of the non-activated PCL membranes (> 90°) together with the low values of the polar component (γ_s^p) confirmed their basically hydrophobic behavior. On the other hand, in the presence of rifampicin, the contact angles of not-treated PCL membranes were < 90° for water + FBS and DMEM, leading to an increase of the polar component, evidence of the augmented hydrophilicity. In all other cases, contact angles equal to 0° were registered, with the polar component (γ_s^p) higher than not-treated membranes, confirming membrane hydrophilicity.

Table 4. Mean values of the contact angle measurements and surface free energy components for non-functionalized and Rif-loaded membranes. The contact angle values of ethylene glycol were all equal to 0°.

	Contact angle H_20 [deg]	Contact angle H_20 + FBS [10%] [deg]	Contact angle DMEM [deg]	γ_s^d [mJ/m²]	γ_s^p [mJ/m²]	γ_s [mJ/m²]
Not-treated PCL	124.9 ± 1.6	113.2 ± 2.5	119.5 ± 7.9	79.5 ± 0.1	13.3 ± 0.8	92.8 ± 0.8
Plasma-treated PCL	0.0 ± 0.1	0.0 ± 0.1	0.0 ± 0.1	79.5 ± 0.1	19.1 ± 0.1	98.5 ± 0.1
PCL coating	0.0 ± 0.1	0.0 ± 0.1	0.0 ± 0.1	79.5 ± 0.1	19.1 ± 0.1	98.5 ± 0.1
PCL bilayer	0.0 ± 0.1	0.0 ± 0.1	0.0 ± 0.1	79.5 ± 0.1	19.1 ± 0.1	98.5 ± 0.1
Not-treated PCL/Rif	126.0 ± 3.9	57.3 ± 4.5	0.0 ± 0.1	79.5 ± 0.1	13.9 ± 2.1	93.4 ± 2.1
Plasma-treated PCL/Rif	0.0 ± 0.1	0.0 ± 0.1	0.0 ± 0.1	79.5 ± 0.1	19.1 ± 0.1	98.5 ± 0.1
Rif coating	0.0 ± 0.1	0.0 ± 0.1	0.0 ± 0.1	79.5 ± 0.1	19.1 ± 0.1	98.5 ± 0.1
Rif bilayer	0.0 ± 0.1	0.0 ± 0.1	0.0 ± 0.1	79.5 ± 0.1	19.1 ± 0.1	98.5 ± 0.1

4.2.2.5. Polysaccharide release

The stability of polysaccharides on the bilayer and coated PCL matrices was studied exploiting a fluorescein-labeled CTL (CTL-FITC) and a CF640R-labeled hyaluronic acid (HA-CF640R) for membrane synthesis. The cumulative release of the labeled polysaccharides in PBS was followed for up to 7 days by spectrofluorimety. In the case of the PCL bilayer matrix, the fluorescence was estinguished after only 1 hour, with null fluorescence values in the next timepoints. This is due to the high solubility of both CTL and hyaluronic acid in aqueous environments, which is further enhanced by the high-surface electrospun architecture, making them even more available after immersion in water or aqueous solvents. In the presence of the coating, however, a different behavior was observed (**Figure 40**).

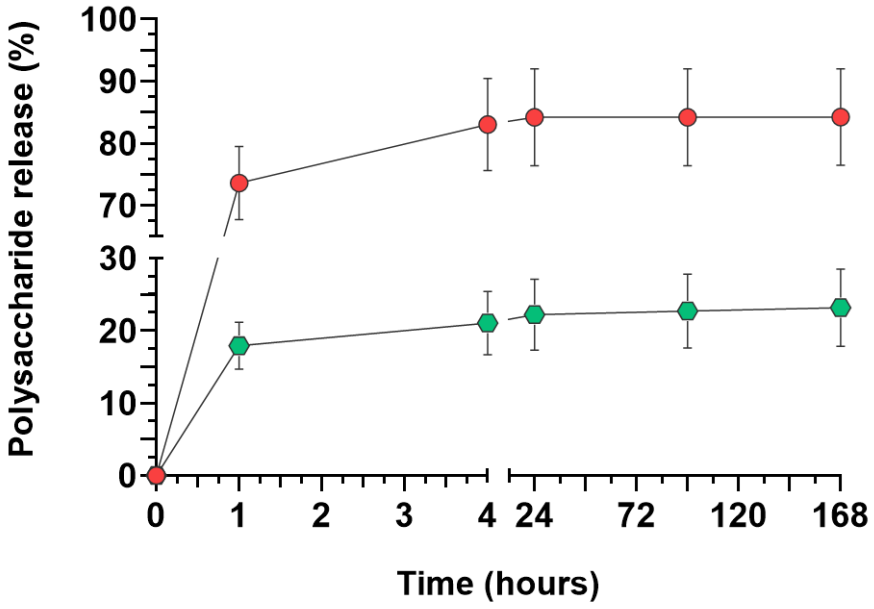

Figure 40. Cumulative release of polysaccharides from PCL coating membranes expressed as percentage of CTL-FITC (⬢) and HA-CF640R (●) detected in the PBS medium.

Indeed, the outer hyaluronic acid layer was almost completely released after 24 hours (≈ 85%), then the release kinetic stabilized and reached a plateau; meanwhile, the inner CTL layer was slowly released in the medium, with a release of ≈ 25% after 7 days. This may be attributed to the stronger binding with the underlying plasma-treated PCL matrix, which interacts with the CTL chains and

retain them on the structure. At the same time, the outer hyaluronic acid layer is feebly connected to the CTL, mainly through weak electrostatic interaction between the residues charges on the two polymers, and is thus immediately available in the medium. Therefore, the PCL bilayer could be useful for a stronger and immediate release of the polysaccharides, which is particularly beneficial for wound dressings that need to be frequently changed, whilst the PCL coating membranes could be beneficial for longer treatment times or for skin grafts application.

4.2.2.6. Rifampicin release

The cumulative release of rifampicin from the Rif bilayer and the Rif coating membranes was evalutated in PBS for 7 days by UV-visible spectroscopy and compared with the rifampicin release from plasma-treated and not-treated PCL mats, to analyze the influence of the air-plasma activation on rifampicin integrity. The results (**Figure 41**) revealed a significantly higher antibiotic release in the case of the non-activated PCL membranes. This is probably due to a lower amount of intact rifampicin within the nanofibrous mesh after the activation process, as this type of treatment seems to partially degrade the drug, resulting in a significantly lower release in time. Meanwhile, a significant difference was observed between the Rif bilayer and Rif coating meshes. Despite the identical PCL/Rif base layer, the diverse release can be explained by the different preparation method used to add CTL and hyaluronic acid to the PCL matrix. Indeed, in the case of Rif coating, the antibiotic loaded in the PCL mesh is partially solubilized during the layer-by-layer deposition, thus is trapped in the polysaccharide layer, and follows the slower polysaccharide release. On the other hand, in the case of Rif bilayer, the polysaccharides are immediately solubilized and readily available in the medium, thus moving the antibiotic release equilibrium towards the medium. This has been demonstrated by immersing two identical PCL/Rif membranes in two different media (namely, PBS and PBS enriched with polysaccharides) and evaluating the difference in the antibiotic release. In the first case, 1.96 μg/mL of rifampicin were released, while in the presence of the polysaccharides the

antibiotic release was of 2.59 µg/mL, revealing how the polysaccharides present in the medium affect the release equilibrium.

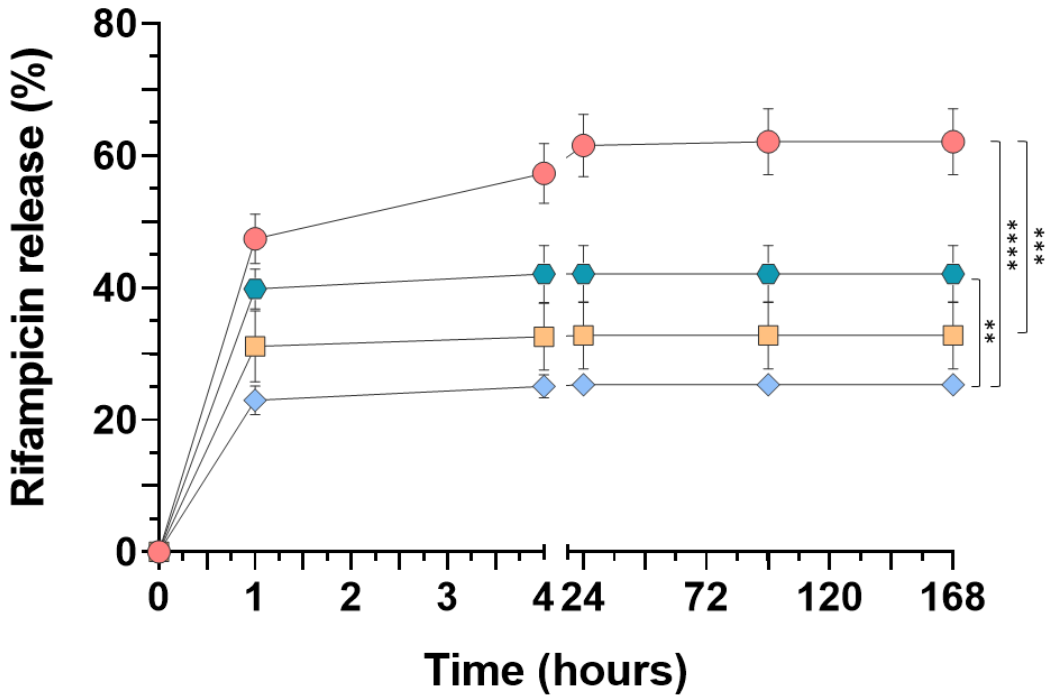

Figure 41. Cumulative rifampicin release in PBS from non-activated (●) and plasma-treated PCL mats (■), Rif bilayer (⬢), and Rif coating (◆) electrospun matrices.
The statistical analysis was performed with ANOVA test, applying Bonferroni's correction. Statistically significant differences are indicated with asterisks (*). **** = $p < 0.0001$.

4.2.3. Biological characterization

4.2.3.1. Membrane biocompatibility

Membrane biocompatibility was first tested on the murine NIH-3T3 cell line, to evaluate the potential cytotoxic effect of the Tween® 20 employed for the PCL bilayer production. For this reason, the PCL bilayer matrices were washed in ethanol for 2 minutes to assess the effectiveness of ethanol in extracting the residual surfactant from the polysaccharidic layer without affecting polysaccharide availability. As can be seen in **Figure 42A**, the cells exposed to the PCL bilayer suffered from the release of Tween® 20, while, after washing with ethanol, they showed comparable behavior to the

untreated controls. Once the need for this post-processing step was established, the biocompatibility of all types of matrices (namely control PCL, PCL coating, and PCL bilayer with or without rifampicin) was studied using human dermal fibroblasts (HDF). The results (**Figure 42B**) showed a similar trend in all cases, indicating that all the fibrous structures tested were biocompatible regardless of the preparation method and even in the presence of the antibiotic.

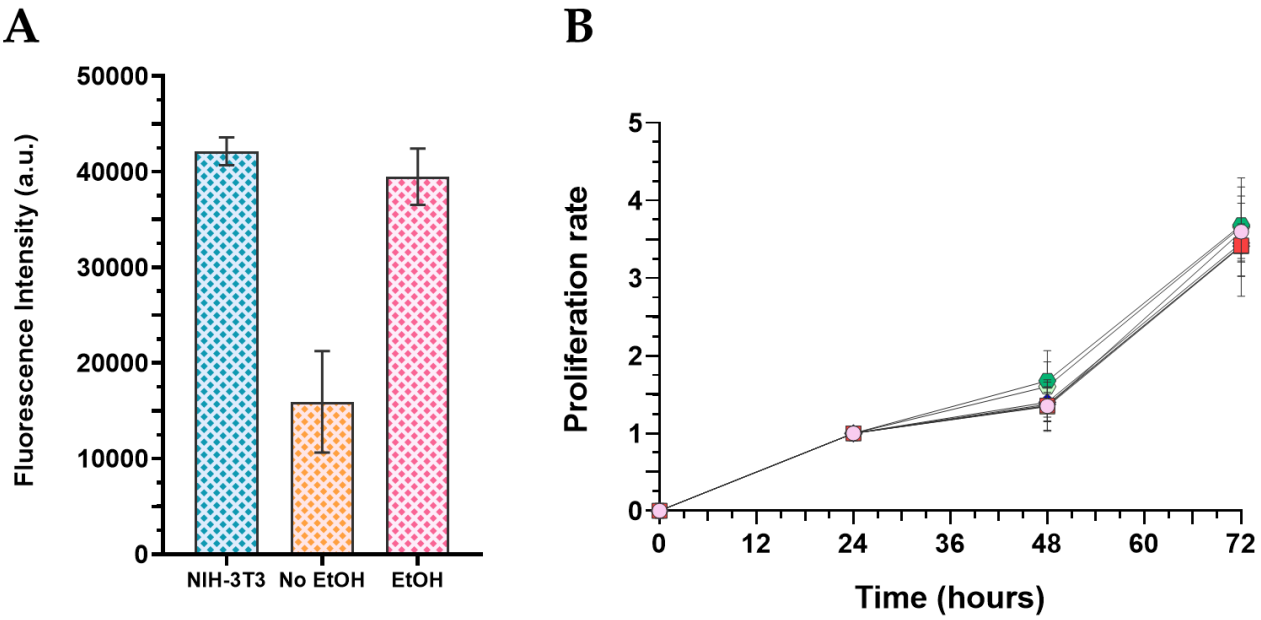

Figure 42. Multilayer matrices biocompatibility assessed through Alamar Blue Assay. **(A)** Evaluation of NIH-3T3 cells viability in the presence of PCL bilayer membranes treated (EtOH) or not (No EtOH) with ethanol to extract Tween®20 residues. **(B)** Biocompatibility towards human dermal fibroblasts of PCL (■) and PCL/Rif (■), PCL coating (◆) and Rif coating (◆), PCL bilayer (⬢) and Rif bilayer (⬢) membranes. The control cells are indicated as pink circles (●).
The statistical analysis was performed with ANOVA test, applying Bonferroni's correction. No statistically significant differences were found.

4.2.3.2. Membrane bioactivity

The bioactivity of the polysaccharides released from the PCL bilayer and PCL coating matrices was tested on human dermal fibroblasts using a wound healing assay, which consists in inducing a scratch on a cell monolayer to then follow cell migration and proliferation until gap closure.[276,277] Untreated and PCL-treated cells were used as controls. As can be seen from both the graph (**Figure 43**) and the images (**Figure 44-45**), the gap closed faster already at earlier timepoints (2 hours) in the presence of

the polysaccharide-endowed matrices and this trend was even more visible at longer timepoints (6-10 hours). Even after 24 hours the scratch was still partially visible in the controls, whereas it was clearly completely closed in the case of PCL coating and PCL bilayer membranes. After 48 hours, the wound was finally closed in the controls too. On the other hand, despite the slight divergence between the PCL bilayer and the PCL coating mats, the latter being slightly slower in promoting gap closure, no significant differences were detected between the two. Considering the differential polysaccharide release between the two types of matrices, such behavior suggests that the burst release of hyaluronic acid from the PCL coating mesh combined with even lower amounts of CTL is already sufficient to exert a bioactive effect, thus inducing wound closure.

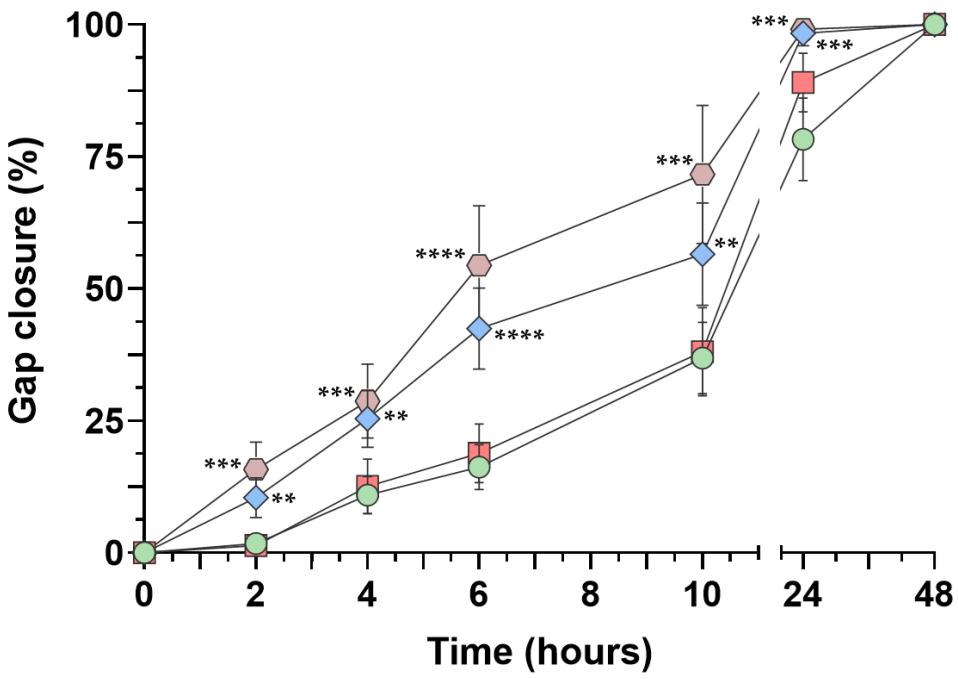

Figure 43. Wound healing assay on human dermal fibroblast, performed by following gap closure in time in the presence of different treatments, namely PCL bilayer (●) and PCL coating (◆). The controls are represented by untreated cells (●) and cell treated with polysaccharide-free PCL membranes (■).
The statistical analysis was performed with ANOVA test, applying Bonferroni's correction. Statistically significant differences are indicated with asterisks (*). **** = $p < 0.0001$.

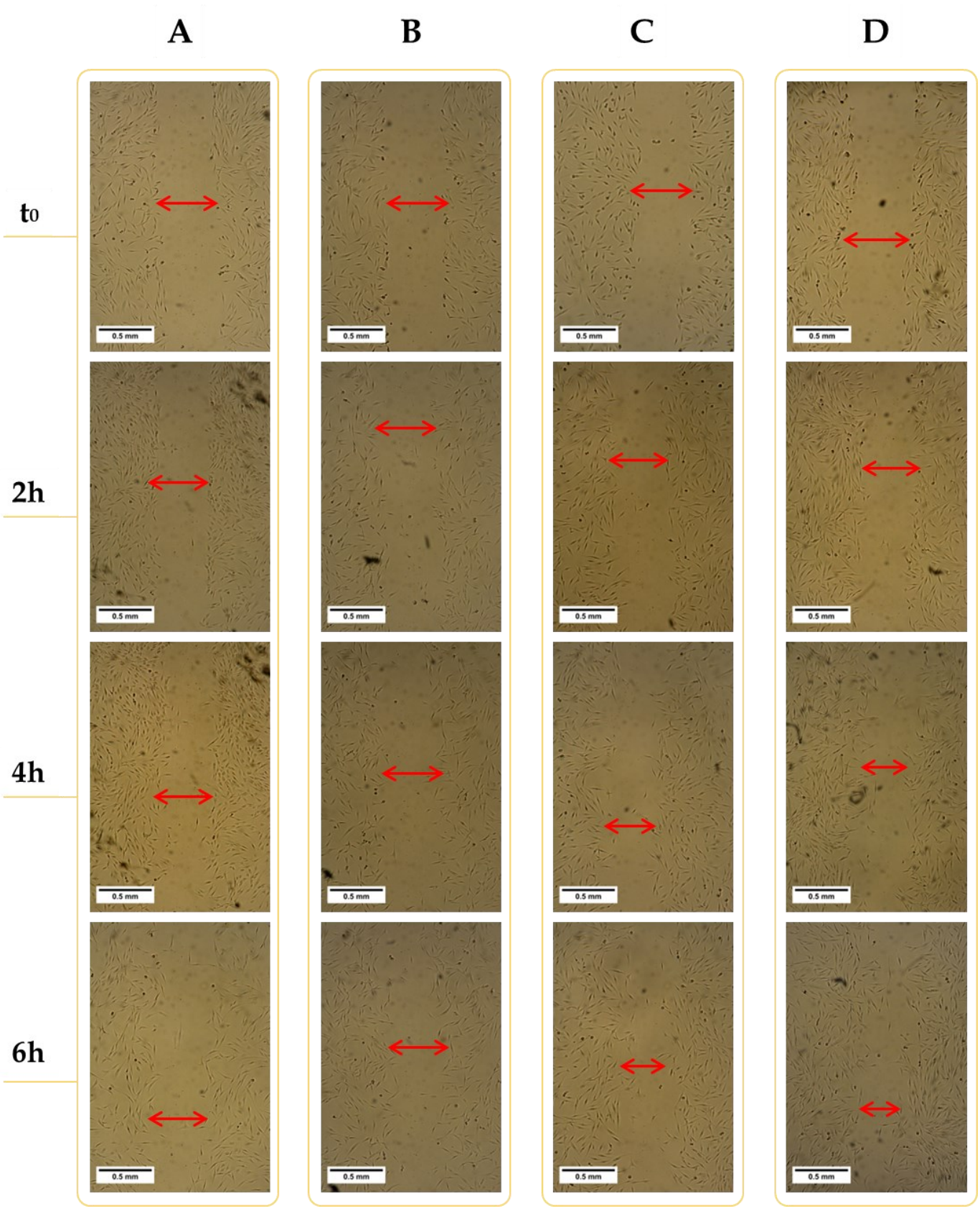

Figure 44. Wound healing assay on human dermal fibroblast, performed by following gap closure (**from t_0 to 6 hours**) in the presence of untreated cells **(A)** and PCL-treated cells **(B)** as well as in the case of polysaccharide-delivering matrices, namely PCL coating **(C)** and PCL bilayer **(D)**. The red arrows mark the extension of the already existing scratch on the cell monolayer.

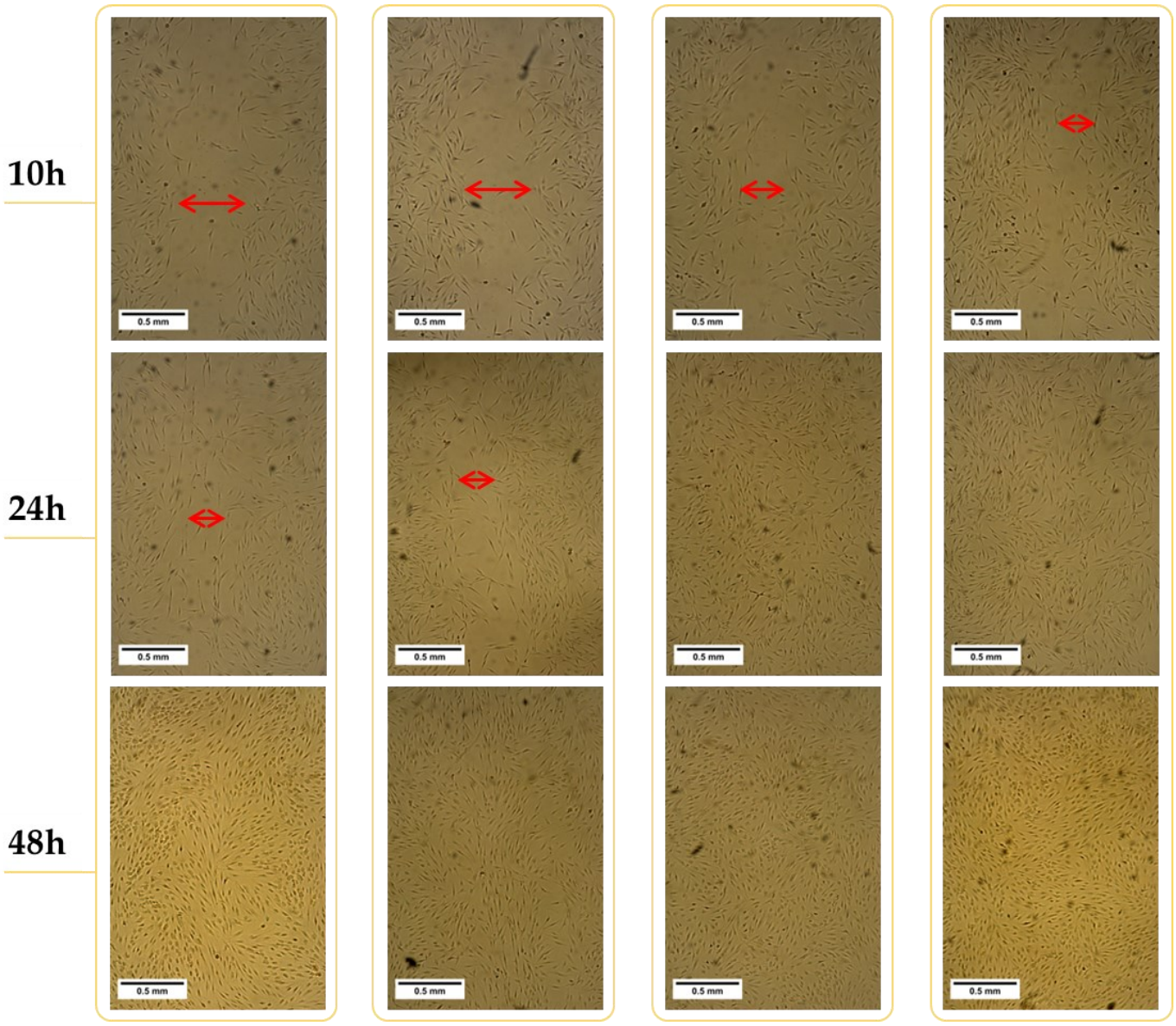

Figure 45. Wound healing assay on human dermal fibroblast, performed by following gap closure (**from 10 hours to 48 hours**) in the presence of untreated cells **(A)** and PCL-treated cells **(B)** as well as in the case of polysaccharide-delivering matrices, namely PCL coating **(C)** and PCL bilayer **(D)**. The red arrows mark the extension of the already existing scratch on the cell monolayer. Images without red arrows represent a complete wound healing.

4.2.4. Microbiological characterization

4.2.4.1. Bacterial growth inhibition

The ability of Rif bilayer and Rif coating membranes to inhibit the growth of bacteria was assessed using four bacterial strains that commonly infect the wound site: the Gram-negatives *Escherichia coli* and *Pseudomonas aeruginosa* and the Gram-positives *Staphylococcus aureus* and *Staphylococcus epidermidis*. To test the inhibitory activity of rifampicin, liquid extracts of both types of membranes were prepared. An estimated initial rifampicin concentration of 10 µg/mL was obtained and added to the bacteria to reach a final antibiotic concentration of 5 µg/mL. The extracts were then serially diluted to 0.3125 µg/mL. Bacteria treated with antibiotic were then incubated at 37 °C for 20 hours and the bacterial growth was monitored by measuring absorbance at 600 nm every 30 minutes. The results (**Figure 46**) revealed an optimal inhibitory effect of the rifampicin released from the fibrous mats (both bilayer and coated matrices) in the case of the Gram-positive bacteria, being effective even at low concentrations. Similar results were obtained against the Gram-negative *Pseudomonas aeruginosa*. Unfortunately, the sensitivity of *Escherichia coli* to the concentrations of rifampicin tested was not as high as that of the other bacteria studied. At the highest concentration tested (5 µg/mL), the inhibitory effect was only slight after 5 hours. Therefore, to assess the actual sensitivity of the bacterial strains analyzed, they were treated with free rifampicin at different concentrations (from 40 µg/mL to 0.16 µg/mL) and the bacterial growth was evaluated after 18 hours upon spectroscopy measurements, The following minimum inhibitory concentrations (MICs) were obtained: 40 µg/mL for *Escherichia coli*, 1.25 µg/mL for *Staphylococcus aureus*, 0.16 µg/mL for *Staphylococcus epidermidis*, 0.625 µg/mL for *Pseudomonas aeruginosa*. To further confirm the resistance of the *Escherichia coli* strain examined, another strain was tested (*Escherichia coli* ATCC 25922), revealing a MIC value of 5 µg/mL.

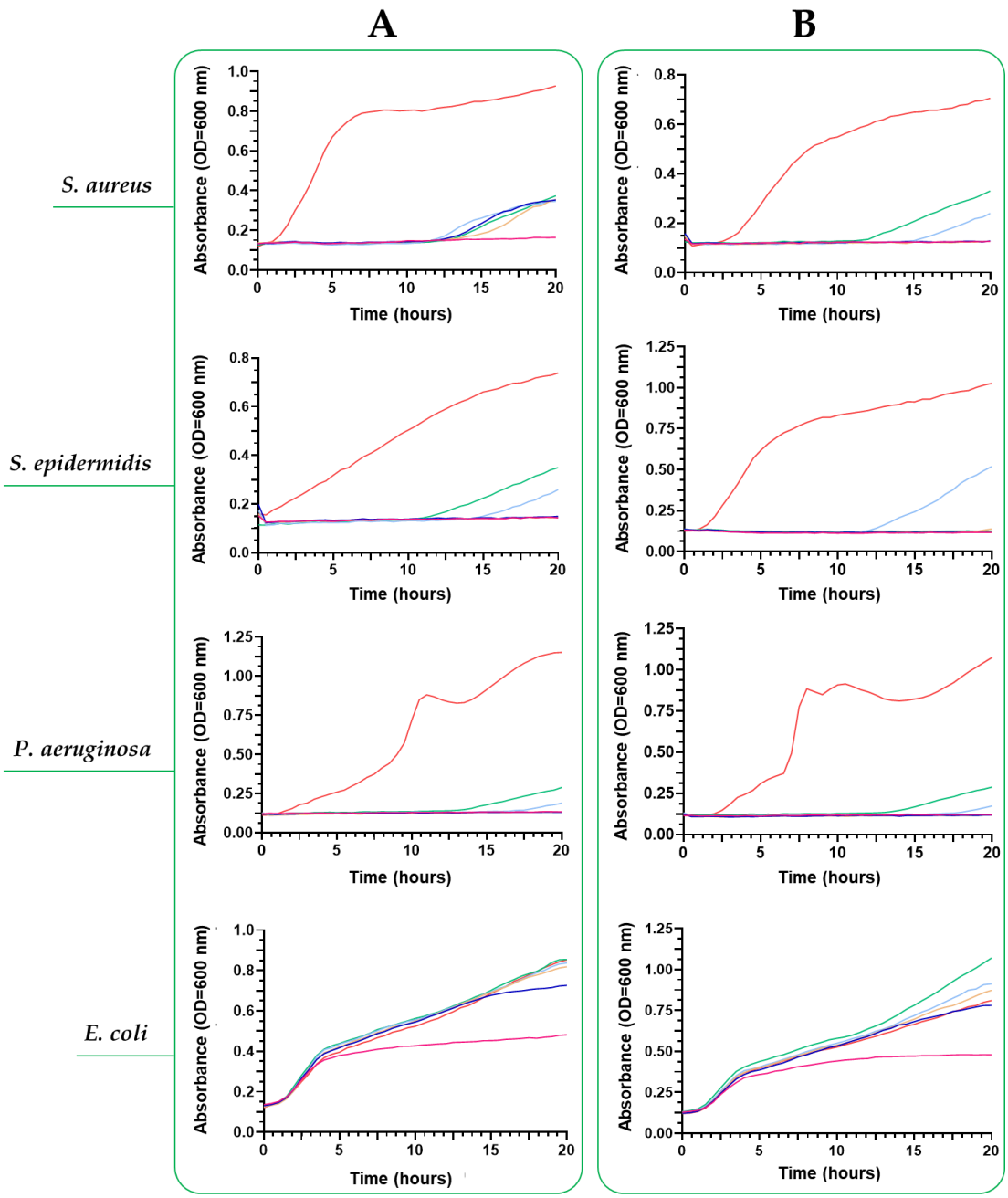

Figure 46. Bacterial growth inhibition curves of the **(A)** Rif coating and **(B)** Rif bilayer matrices in the presence of four different bacterial strains (*Staphylococcus aureus*, *Staphylococcus epidermidis*, *Pseudomonas aeruginosa*, *Escherichia coli*). The red line indicates the control without antibiotic. Then, different rifampicin concentrations were tested: 5 µg/mL (pink line), 2.5 µg/mL (blue line), 1.25 µg/mL (yellow line), 0.625 µg/mL (light blue line), 0.3125 µg/mL (green line).

4.2.4.2. Time killing

The bactericidal effect of the Rif coating and Rif bilayer membranes was tested on the same bacterial strains, namely *Staphylococcus aureus, Staphylococcus epidermidis*, *Pseudomonas aeruginosa*, and *Escherichia coli*, by using the more sensitive *Escherichia coli* strain. In this case, the bacteria were

grown in the presence of the membranes and non-functionalized matrices were used as controls. At different timepoints (t_0, 30 minutes, 2 hours, 4 hours) serial dilutions of the bacteria were spread on LB agar plates and incubated overnight at 37 °C. The next day, the number of colonies was counted, and the CFU/mL were estimated, to assess the ability of the antibiotic membranes to kill the selected bacteria over time. As can be seen in **Figure 47**, the rifampicin-loaded matrices showed a bactericidal effect on all strains tested, with *Staphylococcus epidermidis* being the most sensitive and *Escherichia coli* the most resistant. This was in accordance with what observed in the growth inhibition test, where the amount of rifampicin required to inhibit *Escherichia coli* growth was significantly higher than for the other bacterial strains.

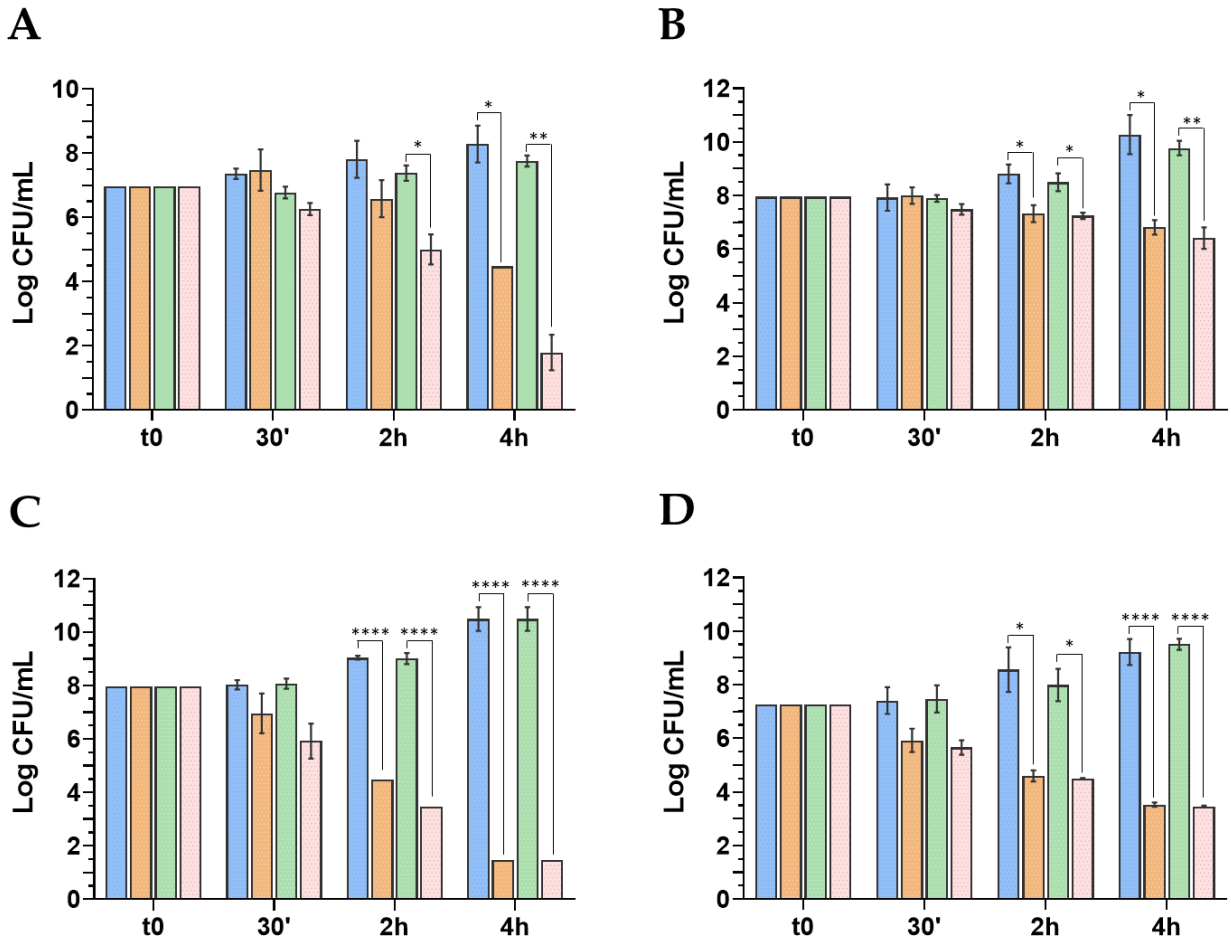

Figure 47. Bactericidal effect of the rifampicin-loaded matrices over time, tested towards **(A)** *Staphylococcus aureus*, **(B)** *Escherichia coli*, **(C)** *Staphylococcus epidermidis*, and **(D)** *Pseudomonas aeruginosa*. The Rif coating and Rif bilayer samples are represented in the orange and light pink bars, respectively. The controls of PCL coating and PCL bilayer are indicated as blue and green bars, respectively. The statistical analysis was performed with ANOVA test, applying Bonferroni's correction. Statistically significant differences are indicated with asterisks (*). **** = $p < 0.0001$

5. DISCUSSION

Given the compelling need for wound dressings able of mimicking the architecture and composition of the extracellular matrix (ECM), absorbing the exceeding exudates, and providing a large surface area for water vapor and gas exchange,[107,278,279] the current thesis initially focused on the synthesis and characterization of **monolayer electrospun nanofibrous wound dressings** based on two different polysaccharides, namely hyaluronic acid (HA) and a bioactive lactose derivative of chitosan (CTL). The combined presence of these two polysaccharides should greatly benefit the wound healing process. Hyaluronic acid, a natural component of ECM, is indeed widely used, as it provides excellent biomimicry and is recognized by cells, while exerting an anti-inflammatory activity. On the other hand, CTL offers the enormous advantage of being water soluble at neutral pH, combining the properties of chitosan with the possibility to use aqueous, non-toxic solvents for its employment. Its bioactivity has been studied in numerous fields, such as osteochondral or neuronal regeneration.[164,280,281] Recently, the anti-inflammatory properties of CTL, alone or in combination with hyaluronic acid, have also been investigated, revealing its ability to modulate the expression of pro-inflammatory cytokines (such as, IL-1β, TNF-α) and MMP-3.[165] As chitosan derivative , it should even provide some of the advantages given by chitosan itself, such as hemostatic or antibacterial activity, due to the presence of positive charges along the polymer chains that bind negatively charged bacterial cell walls.[282,283] Moreover, CTL can be easily functionalized to increase its bioactive properties. For example, Porrelli and co-workers enriched CTL with nAg (CTL-nAg) to produce PCL-based antibacterial electrospun membranes coated with CTL-nAg, to enhance their antibacterial potential.[218]

Given the need to combine polysaccharides with synthetic polymers and surfactants, capable of improving their electrospinnability and reducing the surface tension of the solution to support the extrusion of the filament,[284–287] hyaluronic acid and CTL were combined with polyethylene oxide (PEO), while Tween® 20 was used as a surfactant. After several attempts, monolayer electrospun

matrices were produced, with the best results obtained from a ternary mixture of HA/CTL/PEO. In this way, a CTL-based nanofibrous mesh, with homogeneous, uniform, and defect-free nanofibers, in a diameter range corresponding to the size of natural collagen nanofibers (50–500 nm), could be produced for the first time.[103] Not only is the electrospinning process challenging, but even the post-processing stabilization of the polysaccharidic matrices presents some criticalities. Indeed, due to their high hydrophilicity combined with a large surface area available, polysaccharide membranes are extremely soluble in aqueous environments, hindering their employment for biomedical purposes, where the medical device is expected to interact with biological fluids.[184,194,288] In the case of HA/CTL/PEO mats, both hyaluronic acid and CTL are highly hydrophilic polysaccharides combined with another hydrophilic synthetic polymer, leading to the immediate dissolution of the synthetized membranes upon contact with water. For this reason, inspired by the numerous available literature examples,[2,289–291] different crosslinking strategies have been tested in this work to face the considerable instability of the monolayer polysaccharidic membranes, namely physical (heat treatment) and chemical (glutaraldehyde, genipin, EDC/NHS, methacrylic anhydride, carbonyldiimidazole) methods. The use of carbodiimide-based coupling agents, such as EDC/NHS, is well documented,[292–294] as they react with carboxylic groups, whose activation promotes the amide bond formation. Indeed, in the presence of amino- or alcohol groups, a nucleophilic attack on the activated moieties unseat the crosslinker, mediating the amide bond creation without incorporating the reactive adduct.[295] In this context, Séon-Lutz and co-workers produced and stabilized an electrospun wound dressing based on hyaluronic acid and polyvinyl alcohol by EDC/NHS crosslinking. They obtained stable and only partially fused nanofibers at various relative humidity levels (up to 90%); moreover, they tested EDC/NHS cytotoxicity, not observing any adverse effect.[296] Following these observations, in the present work, HA/CTL/PEO nanofibers were crosslinked by adding EDC/NHS directly to the electrospinning solution, both in powder form and previously dissolved in water. Unfortunately, regardless of the addition method, there was immediate gelation

in the solution, which hindered its electrospinning. This could be due to an increased reactivity given by the presence of hyaluronic acid and CTL, whose combination hinders the maintenance of the solution state after crosslinker addition. Alongside EDC/NHS, glutaraldehyde is an efficient and widely employed aldehydic chemical crosslinker.[297–300] Glutaraldehyde mediates the formation of imminic bonds (C≡N) exploiting a Shiff's base reaction between glutaraldehyde aldehydic groups and free amino groups.[301] Given the free amino groups of CTL, it should potentially interact with glutaraldehyde, to form a mesh able to entangle hyaluronic acid and PEO chains. Glutaraldehyde treatments reported in the literature follow a wide range of timepoints, from 4 hours to 12–16 hours to 3 days.[166,302,303] Here, two different approaches were attempted by testing glutaraldehyde vapor crosslinking at different times, namely 4 hours and 2 hours. In the latter case, membranes were further heat treated to additionally stabilize the final structure. Prolonged reaction times were not possible due to the partial fiber fusion observed upon exposure to glutaraldehyde vapor; on the other hand, the architecture was completely lost after heat treatment. According to Ahmadi and co-workers, this could be explained by the release of water as a by-product of the reaction, which could be entrapped into polymer chains, leading to swelling of the fibers and morphology alteration.[304] Hence, considering the presence of the highly hydrophilic hyaluronic acid and CTL in the produced electrospun mats, this swelling phenomenon is particularly pronounced, hampering polysaccharidic matrices exposure to a wet environment for extended times. On the other hand, the heat treatment would be too strong, irreparably destroying the nanofibrous architecture. In any case, the membranes were completely unstable in water, and dissolved within a few seconds, thus revealing the ineffectiveness of glutaraldehyde in crosslinking HA/CTL/PEO membranes. Furthermore, the potentially toxic effects of glutaraldehyde must be considered. For this reason, novel approaches have been suggested and investigated over the years, such as the use genipin,[192,288] which has been successfully employed instead of glutaraldehyde for the production of biocompatible chitosan-based biomaterials.[305] Genipin crosslinking reaction entails the nucleophilic substitution of the genipin ester

function by primary amines to form secondary amides or the nucleophilic attack on genipin dihydropyran ring, creating a six membered nitrogen heterocycle.[306] To obtain genipin-crosslinked nanofibrous devices, genipin can be directly added to the polymeric solution or it can be used in a post-processing step by dissolution in ethanol or PBS and immersion of the electrospun matrices in the crosslinking solution.[194,289,307] For instance, Panzavolta and co-workers stabilized gelatin-based electrospun meshes both by adding genipin to the electrospinning solution 30 minutes before the process and post-treating the matrices with a genipin-based ethanolic solution up to 7 days.[308] In the present thesis, both approaches were tried. As described for glutaraldehyde, genipin could react with amino groups of CTL to form an entangled nanofibrous matrix which entraps hyaluronic acid and PEO chains. In our case, the presence of genipin as crosslinker did not alter the polysaccharide solution properties, ensuring the production of optimal nanofibers, with a surface free of defects. The obtained matrices were then heated at 37 °C for 24 hours to 7 days, to trigger genipin reaction and assist the crosslinking between the polymer nanofibers. Unfortunately, the reaction did not occur and even after 7 days of incubation the membranes were completely unable to resist in an aqueous environment. This could be due to the dry environment offered by electrospun devices, which is not a suitable condition to guarantee genipin activity. Indeed, during the electrospinning process the solvent evaporates and the fibers are deposited on the collector as ideally solvent-free fibers. On the other hand, the post-electrospinning crosslinking was performed by dissolving genipin in ethanol and embedding the polysaccharidic membranes for different times. The matrices were then heated to support genipin reactivity, but even this approach was unsuccessful, leading to the loss of the nanofibrous structure. In fact, the prolonged exposure to ethanol affects the nanofibrous morphology and the thermal treatment seemed to further worsen the already altered architecture. Consequently, with the aim of investigating the effects of the thermal treatment alone on the nanofibrous mat, heat was used as potential crosslinking strategy. Indeed, as mentioned earlier (*section 1.3.1.*), the thermal crosslinking is a physical method that can induce crystallization of the electrospun polymers and

stabilize the resultant structure.[211] Two different methods were here adopted: membranes were heated at 80 °C in a convection oven or in a vacuum oven. Membrane burning was here observed above 80 °C, despite the higher temperatures successfully tested in the literature.[211,309,310] Moreover, the heated membranes were completely unstable in water, quickly losing their nanostructured feature. Thus, in an attempt to stabilize the final polysaccharidic structure, the thermal treatment was combined with a chemical treatment with carbonyldiimidazole (CDI), which was both coupled with the physical crosslinking or used alone. As explained in *section 1.3.1.*, CDI is a carbodiimide coupling agent able to mediate amide bond formation between carboxyl- or hydroxyl-groups and aminic moieties without being incorporated,[199] as shown by the analysis of ATR-FTIR. In fact, CDI signal was not detectable in the spectrum of CDI-crosslinked mats, which was comparable to that of not-crosslinked ones. In the presence of the characteristic carbonyl (C=O) and carboxyl (-COOH) bands, the amide bond IR spectrum could not be distinguished because of band overlap, thereby requiring further characterization of the reaction mechanism by 1H NMR. CDI has been investigated in literature as covalent crosslinker in various fields, as covalent immobilization on electrospun surfaces, polymer grafting, or hydrogels and nanosponges stabilization.[200,201,311–313] However, to the best of our knowledge, the use of CDI as a coupling agent for electrospun nanofibers, therefore leading to polymeric chain entanglement through amide bond formation, has not been documented yet. Nevertheless, the best crosslinking results were obtained with CDI in the case of HA/CTL/PEO membranes, representing a suitable compromise between mat aqueous stability and nanofiber architecture maintenance. Indeed, despite some unavoidable architecture alteration, the morphological characterization of the membranes revealed a partial retention of the nanofibrous morphology. Meanwhile, they were particularly stable in aqueous environment, preserving their macroscopic integrity. This was confirmed by the swelling and degradation studies, which revealed the high absorption potential of CDI-crosslinked mats as well as their optimal stability in water and saline solution. Indeed, the ability to absorb and retain exudates is of remarkable importance when

considering the efficacy of wound dressings and their potential application in mild and highly exudating wounds.[314,315] A comparison with polycaprolactone (PCL) electrospun membranes was useful to evaluate the behavior and efficacy of an electrospun nanofibrous matrix. Indeed, PCL is a well-established polymer in numerous fields, including wound management; several PCL wound dressings have been synthetized over the years, with *in vitro* and *in vivo* studies supporting their usefulness in wound management.[316–319] However, one of the major drawbacks of PCL lies in its hydrophobicity, which could affect its interaction with biological environments. To overcome this issue, it can be associated with hydrophilic polymers, or subjected to a surface modification that increases material hydrophilicity.[320–322] In this direction, Porrelli and co-workers produced a hydrophilic PCL-based nanofibrous scaffold by using an air-plasma treatment as a surface modification approach, thus increasing membrane wettability and favoring the interaction with cells.[218] In this study, PCL membranes were employed as pristine (non-activated matrices), air-plasma activated membranes, and coated with a double polysaccharide layer of CTL and hyaluronic acid (to compare the presence of a polysaccharide coating with the use of polysaccharides as nanofiber constituents themselves). Notably, the swelling behavior of the activated PCL membranes was similar to that of the CDI-crosslinked polysaccharide mats, indicating that the high surface area and porosity offered by the nanofibrous architecture combined with a strong hydrophilicity enables a considerable fluid retention ability. On the other hand, the polysaccharide coating of the PCL membranes slightly altered membrane ability to absorb fluids, perhaps because the rapid hydration of the polysaccharidic layer limits the porosity of the underlying electrospun mesh, thereby hindering the water uptake capacity of these matrices. The advantage of using electrospun wound dressings was further proven by the comparison with a commercial product, namely the Chitoderm®, and CDI-crosslinked membranes produced through the freeze-drying technique. In both cases, the fluid retention ability was significantly less than that of electrospun products, despite their proved stability in both water and saline solution. Overall, the swelling capacity was slightly lower in saline solution compared to

water. This could be attributed to the osmotic pressure created by the mobile ions between the saline solvent and the nanofibrous network. Donnan's equilibrium theory establishes that the ionic forces are determined by the counterions present in the solvent and the ionizable chemical groups on the material. In the presence of free sodium cations, a charge-screening effect could occur, consequently reducing the osmotic pressure and turning the absorbed solution back towards the medium.[323,324] The stability of CDI crosslinking became even more evident when compared to the last crosslinking method tested, which was based on methacrylic anhydride. Methacrylic anhydride is a methacrylate agent commonly used to chemically modify polymer chains thanks to the introduction of methacryloyl moieties that allow the photo-crosslinking of the methacrylated polymers, without affecting the biocompatibility of the final product.[204–209,325] Here, the ability of this crosslinker to directly react with primary amines and hydroxyl groups was exploited, using pure methacrylic anhydride as post-electrospinning treatment on HA/CTL/PEO membranes. Nevertheless, despite the good morphology displayed by the crosslinked membranes washed in acetone or dimethylformamide, the use of methacrylic anhydride alone was not sufficient to pursue a long-term stabilization of the polysaccharidic mats, resulting in their degradation already after few hours. Probably, the interaction between the methacrylate moieties introduced after the electrospinning process caused a weak and temporary stabilization of the nanofibrous network, subsequently leading to its rapid degradation. On the contrary, CDI-crosslinked mats were stable up to 7 days in water, while in saline a mild degradation behavior was observed after 3 days. As described above, a change in the osmotic pressure could induce membrane shrinkage in the presence of salts, a phenomenon that varies depending on the composition of the material considered. Nevertheless, the frequency of dressings changes must be considered, which is approximately 2–3 times per week, depending on the type of wound to be treated.[326–328] Furthermore, the advantages of a local release of the polysaccharides employed to favor wound closure and tissue regeneration should not be neglected.[329–333] Hence, the degradation behavior exhibited by CDI-crosslinked mats after 3 days of immersion in saline solution should not affect the

quality of the final product but should rather be an added value in promoting skin regeneration. Another important parameter to consider when producing wound dressing materials is their ability to transmit water vapor and favor gaseous exchanges to ensure moisture retention at the wound site, in line with Winter's findings.[334–336] As discussed in *section 1.1.1*., in 1962 Winter demonstrated that in the presence of a dry environment, where the wound is covered by a superficial scab, the regeneration process is delayed if compared to a wound maintained in a moist environment, which instead prevents the formation of the scab.[32] Consequently, an ideal wound dressing should ensure the maintenance of the proper equilibrium between the evaporation rate, which, if too high, would hamper moisture retention, and a barrier behavior, which, if too occlusive, would not allow an adequate drainage of fluids, leading to skin maceration and paving the way for infections.[337,338] After evaluating the goodness of CDI crosslinking among the different strategies attempted, the water vapor permeability was tested by a comparison with PCL electrospun membranes (pristine, plasma-treated, or polysaccharide coated) and Chitoderm®. The water vapor transmission rate of electrospun products was higher than that of the commercial product, due to the outer polyurethan layer of Chitoderm®, which acts as a barrier against microorganism being impermeable. On the other hand, the evaporation rate of CDI-crosslinked matrices was lower than that of the electrospun PCL products after 48 hours, possibly due to their higher hydrophilicity and thus greater efficiency in trapping water molecules. In fact, the water vapor transmission ability also depends on the diffusivity of the water molecules within the polymer meshes;[339] consequently, the presence of hyaluronic acid and CTL, with their considerable hydrophilicity, should cause a slight water retention on the nanofibrous mat after 48 hours. Nevertheless, the water vapor permeability of electrospun devices is well halfway between the complete evaporation and total impermeability, as expected from an ideal wound dressing.

Based on these considerations, the present monolayer polysaccharidic matrices should be a good starting point to produce electrospun dressing devices, despite all the critical aspects related to the crosslinking with the numerous approaches currently available. However, the mechanical stability of

such products could be a critical issue since handling and the adaptability to the wound bed concur in defining the goodness of the final product.

To this end, the synthesis of **multilayer electrospun matrices** should be of great advantage to obtain stable and easy to handle devices, which could induce wound closure by releasing polysaccharides in the wound. In fact, multilayer nanofibers are often characterized by better mechanical properties and volume expansion if compared to monolayer matrices, which could favor blood clot formation. Moreover, they can be easily functionalized with bioactive and antibacterial agents to further stimulate wound closure as well as protect it from infections.[340–343] The current thesis project presents two types of multilayer mats, in particular: i) a fully electrospun dressing obtained by electrospinning the ternary polysaccharidic mixture used to produce the monolayer meshes on a plasma-treated PCL membrane (named, "**PCL bilayer**"); ii) a PCL mat activated by air-plasma treatment and subsequently coated by layer-by-layer deposition of CTL and hyaluronic acid (called, "**PCL coating**"). The concentration of the polysaccharides was increased in this case with respect to the polysaccharide-coated PCL mats used as comparison in the characterization of the monolayer membranes, with the aim of improving the potential bioactivity of the final dressing. Considering the increased risk of infection at the wound site, which could further worsen and discourage the regeneration process,[344–346] the multilayer structure was exploited to even confer antibacterial properties to the obtained electrospun matrices; in fact, a broad-spectrum antibiotic drug (namely, the rifampicin) already studied, among others, in the dermatology field[347–349] was loaded on the basal PCL layer of both the PCL bilayer and PCL coating membranes, obtaining the so-called "**Rif bilayer**" and "**Rif coating**" matrices. In all cases, an optimal morphology was displayed, with randomly oriented, homogeneous, and defect-free fibers. In detail, the dual nature of the PCL bilayer membranes is noteworthy, as it was possible to appreciate the presence and contribution of the underlying thicker PCL layer and of the thinner polysaccharidic nanofibers uniformly deposited above. Meanwhile, the presence of the rifampicin did neither alter the PCL solution properties and

the electrospinning process nor the goodness of membrane architecture. On the other hand, the ATR-FTIR analysis allowed to detect slight differences in the spectra of the Rif coating and Rif bilayer mats due to the different polysaccharidic functionalization. In fact, in the case of the bilayer matrices, the higher CTL and hyaluronic acid concentrations combined with the addition of PEO to ensure polysaccharide electrospinnability determined a more pronounced -OH band with respect to the coated membranes, where the only -OH source is represented by CTL and hyaluronic acid used at lower concentrations. The differences between the two types of multilayer matrices became even more evident by the characterization of their swelling capacity, which is a fundamental parameter to evaluate based on the need to absorb wound exudates. Indeed, as well known, the presence of exceeding exudates causes skin maceration, fibroblast inactivity, and the extension of the inflammatory phase, which is responsible for the self-perpetuation of the chronic wound, thus complicating patient's treatment and increasing its morbidity.[350–352] The comparison between the PCL control membrane and the multilayer structures revealed in all cases an optimal swelling behavior in phosphate buffered saline solution (PBS); however, albeit still considerable, the fluid retention ability of the PCL coating mats was significantly lower than that of PCL and PCL bilayer membranes. As hypothesized in the monolayer matrix characterization, where the PCL membranes coated with a lower polysaccharide concentration were used as a comparison, this is likely due to the rapid hydration of the coating which masks the underlying PCL porosity, thus reducing the ability of the coated network to absorb fluids. Despite the alteration in the swelling behavior, the water vapor permeability was not influenced by the different polysaccharide loading. Indeed, as observed for the monolayer structures, all the electrospun products were able to maintain a proper moisture equilibrium, being halfway between the total water evaporation and the absence of transmission. Moreover, the water vapor transmission ability was followed up to 72 hours in this case, in line with the frequency of dressing changes,[326–328] demonstrating an optimal permeability trend even at prolonged timepoints.

All types of matrices activated by air-plasma exposure were also fully wettable in the presence of several fluids, namely, water, water supplemented with fetal bovine serum (FBS), and a traditional cell culture medium (the DMEM medium). The study of the different types of liquids was devoted to exploring the behavior of the membranes in the presence of serum proteins, which are present both in the physiological and *in vitro* microenvironment and whose interaction could determine changes in matrix hydrophilicity. In fact, in the presence of not-treated PCL/Rif membranes a hydrophilic behavior (measured by means of sessile contact angle) was observed in the presence of FBS-supplemented deionized water ($\theta = 57.35°$) and DMEM ($\theta = 0°$), demonstrating the already known ability of rifampicin to interact with serum proteins.[353–356] This represents a relevant result as a hydrophobic behavior (independently of the employed fluid) was expected in the case of membranes not subjected to air-plasma treatment, due to the basal un-wettable PCL layer. It must be pointed out that if on the one hand the interaction with the biological environment is of pivotal importance for the success of a biomaterial, on the other hand the non-specific protein adsorption could possibly trigger a foreign body reaction, thus impairing biomaterial function and biocompatibility.[357] According to the Berg's limit, which gives a quantitative definition to the hydrophobic and hydration forces driving protein adsorption, a contact angle $\theta < 65°$ defines a hydrophilic surface which avoids non-specific adsorption of proteins, since they are not able to displace water from the hydrophilic surface, while an opposite behavior is registered for $\theta > 65°$.[358–360] However, this model presents some limitations, as it underestimates the mutual protein interactions during adsorption as well as it relies on large scale interactions on ideally flat surfaces, not considering what happens at the nanometer scale. In this sense, Whitesides and co-workers analyzed the structure-property relationship of different self-assembled monolayers to study at the molecular level those factors which could avoid the non-specific protein interactions, finding the so called "Whitesides rules" whereby the non-specific protein adsorption is determined by: i) the presence of a hydrophilic surface; ii) the presence of hydrogen bond acceptors; iii) the absence of hydrogen bond donors; iv) the absence of

net charge.[361,362] Basing on these considerations, the presence of polymeric coatings could satisfy many of these rules. In the specific case of the non-functionalized multilayer matrices here synthetized, the non-specific protein adsorption should be overcome, since the air-plasma treatment combined with the addition of polysaccharides, whose pH is moreover finely regulated, determines a considerable shift of the material towards a hydrophilic behavior with total drop spreading, which enhances its biocompatibility, not considering the bioactive properties of the polysaccharide employed. The change in the biomaterial surface properties is even confirmed by the surface free energy examination, performed through the Owens−Wendt method, which specifically relates the surface free energy of a material with the polar and dispersive interactions between the solid and the respective liquid under examination.[257,363] The analysis revealed an increase in the polar component in the case of all the air-plasma treated membranes as well as in the case of not-treated rifampicin-loaded membranes exposed to FBS-supplemented water and DMEM, thus confirming the surface modification occurred on the analyzed matrices.

Once assessed the surface properties of the multilayer fibrous matrices, their stability had to be evaluated, highlighting the effects of the differential polysaccharide incorporation. In detail, membrane stability was characterized both in terms of polysaccharide and rifampicin release. In the first case, the polysaccharides were immediately released from the PCL bilayer upon medium contact because of their high hydrophilicity combined with the elevated surface area offered by the nanofibrous architecture. Indeed, being a not-crosslinked entirely electrospun architecture, the polysaccharide dissolution was almost instantaneous, with the PCL bottom layer always staying intact. Considering the application as wound dressing materials, which are frequently replaced,[364,365] the local delivery and immediate availability of anti-inflammatory and pro-regenerative agents (as the polysaccharides employed are) in the injured site could be particularly advantageous to stimulate wound response[165,366–369] while maintaining an outer PCL fibrous layer able to protect the wound from external abrasions, absorb the produced exudate, and favor the gaseous exchanges.[370,371] On the

other hand, in the case of the PCL coating a burst release of the hyaluronic acid was registered in the first 4 hours, while the CTL was more stable and slowly released in time, reaching a ≈ 25% of release after one week. This could be attributed to the sequential coating procedure, which consists in a first CTL layer followed by hyaluronic acid deposition. Therefore, the hyaluronic acid, which is the outer coating layer, is rapidly released from the matrix, while the inner CTL layer is strictly interconnected with the underlying activated PCL matrix, thus being more stable in time. This could open new perspectives for the application of the PCL coating membranes not only as wound dressing materials, but also as skin substitutes, which must lie in the injured site for a prolonged timespan following tissue regeneration. Thus, even a controlled and prolonged release of the bioactive agents, compatible with the treatment times, could represent a plus to employ electrospun materials for chronic wound care.[372–374] Meanwhile, the stability of the loaded rifampicin was evaluated too, by comparing not-treated and plasma-treated membranes. As a matter of fact, the activation procedure affected rifampicin integrity thus reducing its availability in time. On the other hand, by comparing the multilayer matrices with the plasma-treated PCL/Rif control membranes, a higher rifampicin release was detected in the case of the Rif bilayer, even if the basal PCL/Rif mat is the same in all cases. It was hypothesized, and then experimentally validated, that the immediate polysaccharide dissolution in the medium from the bilayer shifts the release equilibrium towards the medium, driving the rifampicin out of the membrane. Indeed, the high affinity of polysaccharides with water allowed them to expand in the medium, which was a PBS solution, thus absorbing solvent molecules between the polymer chains and increasing the local salt concentration.[375] Then, according to the Donnan's equilibrium, as explained above in reference to the differential behavior of monolayer matrices in water and saline solution, a membrane shrinkage occurs due to the change in the osmotic pressure, thereby forcing the rifampicin towards the medium. On the contrary, in the case of the PCL coating, the antibiotic is partially solubilized and trapped within the first coating layer, reducing the percentage of release in time.

Once the physicochemical performance of the multilayer matrices was studied, their biological evaluation has been investigated, first considering their composition. Indeed, the presence of the surfactant in the polysaccharide layer of the PCL bilayer meshes could significantly impair the biocompatibility of the device.[376,377] Due to the ability of high ethanol concentrations to solubilize Tween® 20,[378,379] but not polysaccharides,[380,381] an additional ethanol wash (of only few minutes, so as not to destroy the nanofibrous architecture) was included in the preparation protocol, with the aim of washing out any residual surfactant. In fact, this post-processing procedure ensured the biocompatibility of the PCL bilayer membranes towards murine fibroblasts. Subsequently, taking into account the release of polysaccharides and rifampicin from the multilayer matrices, their biocompatibility was assessed towards human dermal fibroblasts, to exclude any possible acute toxicity of the final biomaterial. In no case was cell proliferation affected by the presence of the biomaterial, with a similar trend between all the types of treatments, which were moreover comparable to the controls of not-treated fibroblasts. This demonstrated the safety of the polysaccharidic multilayer matrices with or without antibiotic and their potential applicability on the wound site, where the fibroblast proliferation is essential to ensure the repair of the damaged tissue. Indeed, chronic wounds affect a deeper portion of skin, including not only the epidermal layer, but even the underlying dermis. Here the fibroblasts should proliferate and migrate towards the wound bed, reconstructing the ECM, promoting granulation tissue formation, and offering a support for the migration of inflammatory cells as well as secreting cytokines, chemokines, and growth factors which guide cell response and survival at the wound site. Unfortunately, the stress induced by the uncontrolled inflammatory phase of chronic wounds, can induce premature senescence of fibroblasts. Therefore, strategies need to be developed to protect the wound from the external environment while stimulating tissue regeneration and remodelling.[382–385] In this sense, the bioactivity of both PCL coating and PCL bilayer membranes was tested by a wound healing assay, with the purpose to study the influence of the polysaccharide released in stimulate wound closure. Therefore, human dermal

fibroblasts were also selected in this case and untreated and PCL-treated cells were used as controls. Both types of polysaccharide-based matrices revealed their bioactivity, inducing a significantly faster gap closure already at the earlier timepoints. Even after 24 hours, the scratch was still partially visible in the controls, while it was completely closed in the presence of the polysaccharides. On the other hand, no significant differences were detected between the PCL coating and PCL bilayer mats, despite a slightly faster scratch closure in the presence of the PCL bilayer, which could be attributed to the faster polysaccharide release in the short term. In the future, a comparative study could be carried out on the synergistic effect of the CTL and hyaluronic acid released from the material in inducing tissue response and regeneration with regard to wound closure, also considering the already proven ability of both polysaccharides to play an active role in modulating the inflammatory and remodelling phases, while exerting an antioxidant and pro-regenerative potential.[165]

Finally, in view of the urgent need for wound dressings and skin substitutes that can also counteract and prevent wound infections, the antibacterial efficacy of the rifampicin released from the antibiotic-enriched matrices was tested against four bacterial strains commonly infecting the wound site, namely the two Gram-positives *Staphylococcus aureus* and *Staphylococcus epidermidis* and the two Gram-negatives *Escherichia coli* and *Pseudomonas aeruginosa*. [386–389] The inhibitory activity was first assessed, by exposing the bacteria for 20 hours to rifampicin extracts obtained from the Rif coating and Rif bilayer membranes, which were serially diluted to test a wide range of concentrations (from 5 μg/mL to 0.3125 μg/mL). The antibiotic thus showed efficacy in inhibiting Gram-positives growth as well as *Pseudomonas aeruginosa*. However, the same efficacy was not observed in the presence of *Escherichia coli*, which seemed to be resistant also at the higher drug concentration analyzed. Perhaps, the *Escherichia coli* strain adopted developed resistance to rifampicin thanks to a mutation in the β subunit of the bacterial RNA polymerase, as systematically discussed by Goldstein in his review on the mechanisms underlying rifampicin resistance.[390] For this reason, the minimum inhibitory concentration of the antibiotic drug was evaluated on all bacteria strains, including an

additional *Escherichia coli* strain which revealed a higher sensitivity (5 µg/mL with respect to the 40 µg/mL of the first strain employed) though it was less sensitive with respect to the other bacteria under investigation. Based on these considerations, the bactericidal activity of rifampicin was tested in the presence of the four bacterial strains, this time using the more sensitive *Escherichia coli*. The antibiotic revealed its bactericidal activity over time towards all the bacteria tested, with *Staphylococcus epidermidis* being the most affected and *Escherichia coli* suffering the least under the influence of rifampicin, which is consistent with the inhibitory activity studied. Therefore, the antibiotic-endowed matrices (both Rif coating and Rif bilayer mats) have demonstrated their ability to prevent bacterial infections caused by *Staphylococcus aureus*, *Staphylococcus epidermidis*, and *Pseudomonas aeruginosa*. On the other hand, a lower antibacterial efficacy was observed in the case of *Escherichia coli*, due to possible antibiotic resistance. Nonetheless, even the limitations encountered in the antibacterial activity can be overcome by loading different antibiotic drugs on the fibrous surface, as the combination of antibiotics is well exploited in clinical practice to achieve higher antibacterial efficacy.[391–393]

As a matter of fact, the employment of the multilayer matrices revealed numerous advantages because: i) they are easy to handle; ii) they possess suitable physicochemical properties; iii) they are able to deliver bioactive polysaccharides locally with different feed rate depending on the synthesis method (thus extending their application not only as wound dressings but also as skin substitutes); iv) they can be easily functionalized with further bioactive, anti-inflammatory, or antibacterial moieties to reach the final goal of wound closure, tissue regeneration, and remodelling, reducing patient's pain and unwanted scarring as much as possible.

6. CONCLUSIONS

Exploring new strategies to treat non-healing (or chronic) wounds is of pivotal importance in the wound care practice, as there is an urgent medical need worldwide. In this scenario, the electrospinning technique could be a valid alternative approach, since it allows the production of nanofibrous extracellular matrix (ECM)-like membranes, with a large surface area and porosity which favor fluid drainage and gas permeation besides exerting an anti-scarring and hemostatic potential. Depending on the polymers employed, it is then possible to mimic ECM composition other than its architecture. The present thesis proposes the exploitation of the electrospinning technique to produce biomimetic and bioactive polysaccharide-based nanofibrous scaffolds to be used as wound dressing materials, endowed with antibacterial properties. In detail, two main work section can be distinguished: i) the synthesis, stabilization, and physicochemical characterization of polysaccharidic monolayer membranes; ii) the production and physicochemical, biological, and microbiological characterization of multilayer polysaccharide-based matrices endowed or not with a broad-spectrum antibiotic, the rifampicin.

In the first part of the project, the monolayer dressing was produced starting from two different polysaccharides, namely a lactose-modified chitosan (CTL, known for its bioactive and anti-inflammatory properties) and hyaluronic acid (HA, which is a natural component of the ECM). Considering that the polysaccharides are non-spinnable alone, due to their unfavorable solution properties, they were combined with a synthetic polymer (the polyethylene oxide, PEO) and a surfactant (the Tween® 20), able to reduce solution surface tension. After several combinations (HA/PEO, CTL/PEO, HA/CTL/PEO), the best results in terms of solution and electrospinning process stability as well as nanofiber morphology were obtained with a ternary mixture of HA/CTL/PEO. Unfortunately, given the high hydrophilicity of the chosen polymers and the elevated surface-to-volume ratio, the membranes immediately dissolved in water, hampering their application as wound dressing materials. For this reason, an additional crosslinking step was needed and different

approaches were explored, ranging from strategies already reported in the literature (EDC/NHS, glutaraldehyde vapor, genipin, thermal treatment) to unexplored methods (carbonyldiimidazole, or CDI, and an alternative use of methacrylic anhydride). However, only the CDI and methacrylic anhydride crosslinking produced satisfactory results, representing a compromise between nanofiber architecture maintenance and water resistance. In view of their potential use as wound dressings, both CDI- and methacrylic anhydride-crosslinked mats were compared to synthetic electrospun matrices and non electrospun products. In the first case, polycaprolactone (PCL) subjected or not to air-plasma treatment (to increase membrane hydrophilicity) and coated with CTL and hyaluronic acid was chosen; in the second case, a freeze-dried matrix obtained with the same ternary polysaccharide mixture used for the electrospun membranes and a commercial product, the Chitoderm®, were selected. The swelling capacity of the nanofibrous matrices was significantly higher than that of non-electrospun ones, regardless of their composition. On the other hand, the CDI-crosslinked matrices revealed a better ability to retain fluids with respect to that treated with methacrylic anhydride, which rather showed a degradation behavior in the first hours of immersion. The study of the degradation rate of all the analyzed membranes confirmed what seen during the swelling analysis. Moreover, the CDI-crosslinked mats revealed their stability in water for up to 7 days, while their started to partially degrade after 3 days in saline solution, being anyway compatible with the times of dressing substitution. Electrospun products also demonstrated an optimal water vapor permeability, with an intermediate behavior between the total evaporation and the absence of transmission. Although the promising physicochemical features, the polysaccharide-based meshes were not stable and handleable as the synthetic matrices. Consequently, synthetic polymers and polysaccharides were combined to produce two types of easy-to-handle multilayer matrices: i) an entirely electrospun product made of a PCL basal layer and a HA/CTL/PEO upper layer (named "**PCL bilayer**"); ii) a CTL/HA coated PCL membrane (called "**PCL coating**"). The multilayer structure was even exploited to functionalize the dressings, by introducing an antibiotic (namely, rifampicin) into the PCL layer,

resulting in the so-called "**Rif bilayer**" and "**Rif coating**" membranes. In order to improve the bonding between the PCL and polysaccharides (electrospun or layer-by-layer deposited), the PCL-based nanofibrous network was activated by air-plasma treatment, ensuring a high wettability of the surface. On the other hand, the multilayer matrices showed satisfactory results in terms of swelling capacity and water vapor permeability, in line with what observed in the case of the monolayer membranes. In addition, the different synthesis method was strictly correlated with different release of both polysaccharides and rifampicin from the nanofibrous structures. Indeed, both CTL and hyaluronic acid were immediately released from the PCL bilayer, due to the combination of polymer hydrophilicity and large surface area of the electrospun products. This could be greatly advantageous in the case of a wound dressing material, which needs to be frequently changed and rapidly release the loaded bioactive agents. On the other side, in the case of the PCL coating, the outer hyaluronic acid layer was immediately released in the first 4 hours, while the inner CTL layer was more interconnected with the underlying PCL matrix, being more stable and slowly released over time. Such behavior suggests that PCL coating mats can be used as skin substitutes, which must resist in the tissue for a longer period, thus requiring a prolonged release of the bioactive components too. In any case, no acute cytotoxicity was observed on human dermal fibroblasts (HDFs), while a bioactivity of the polysaccharidic membranes was observed by wound healing assay. Indeed, the closure of the scratch on HDFs was significantly higher when treated with the PCL bilayer and PCL coating matrices compared to the control, reaching complete healing after 24 hours.

Likewise, with respect to the antibiotic, the immediate polysaccharide release from the PCL bilayer caused an osmotic imbalance which forced the rifampicin out of the membranes, thus resulting in a faster drug release kinetic with respect to the PCL coating. In this sense, it must be anyway considered the effect of the air-plasma treatment, which partially affects rifampicin integrity. Nevertheless, the antibacterial efficacy against *Staphylococcus aureus*, *Staphylococcus epidermidis*, and *Pseudomonas aeruginosa* was not impaired, both in terms of inhibitory and bactericidal activity. However, the

membranes were partially effective in the case of *Escherichia coli*, which showed resistance to the antibiotic. A mild bactericidal activity was observed in the presence of a more sensitive strain, despite always lower than the other bacterial strains tested.

In view of these results, the polysaccharide-based electrospun nanofibrous dressings developed in this work, should be highly advantageous as wound dressing materials, from both a structural and compositional point of view, and even open up new sceneries in the field of skin substitutes. The bioactivity of these devices should be further investigated at the molecular level, to analyze the effects of the polysaccharide presence in the wound healing process. On the other hand, the versatility of the multilayer matrices offers the possibility to incorporate a variety of compounds, ranging from antibacterial, anti-inflammatory, anesthetics, or bioactive moieties, being therefore even modulable and designed for different types of wounds. Both the bioactivity and antibacterial properties of the final product should be finally tested through *in vivo* wound models (such as rats or rabbits) to evaluate the clinical performance of the device in a microenvironment as close as possible to that of humans. This should include the ability to stimulate wound closure and dermal regeneration and prevent scar formation as well as its ability to prevent the occurrence of infections at the wound site.

REFERENCES

(1) Zhao, R.; Liang, H.; Clarke, E.; Jackson, C.; Xue, M. Inflammation in Chronic Wounds. *International Journal of Molecular Sciences* **2016**, *17* (12), 2085. https://doi.org/10.3390/ijms17122085.

(2) Gruppuso, M.; Turco, G.; Marsich, E.; Porrelli, D. Polymeric Wound Dressings, an Insight into Polysaccharide-Based Electrospun Membranes. *Applied Materials Today* **2021**, *24*, 101148. https://doi.org/10.1016/j.apmt.2021.101148.

(3) Xue, M.; Jackson, C. J. Extracellular Matrix Reorganization During Wound Healing and Its Impact on Abnormal Scarring. *Advances in Wound Care* **2015**, *4* (3), 119–136. https://doi.org/10.1089/wound.2013.0485.

(4) Larouche, J.; Sheoran, S.; Maruyama, K.; Martino, M. M. Immune Regulation of Skin Wound Healing: Mechanisms and Novel Therapeutic Targets. *Advances in Wound Care* **2018**, *7* (7), 209–231. https://doi.org/10.1089/wound.2017.0761.

(5) Frykberg, R. G.; Banks, J. Challenges in the Treatment of Chronic Wounds. *Advances in Wound Care* **2015**, *4* (9), 560–582. https://doi.org/10.1089/wound.2015.0635.

(6) Zhang, K.; Lui, V. C. H.; Chen, Y.; Lok, C. N.; Wong, K. K. Y. Delayed Application of Silver Nanoparticles Reveals the Role of Early Inflammation in Burn Wound Healing. *Scientific Reports* **2020**, *10* (1), 6338. https://doi.org/10.1038/s41598-020-63464-z.

(7) Kuhlmann, M.; Wigger-Alberti, W.; Mackensen, Y. v.; Ebbinghaus, M.; Williams, R.; Krause-Kyora, F.; Wolber, R. Wound Healing Characteristics of a Novel Wound Healing Ointment in an Abrasive Wound Model: A Randomised, Intra-Individual Clinical Investigation. *Wound Medicine* **2019**, *24* (1), 24–32. https://doi.org/10.1016/j.wndm.2019.02.002.

(8) Chen, Z.; Hu, Y.; Li, J.; Zhang, C.; Gao, F.; Ma, X.; Zhang, J.; Fu, C.; Geng, F. A Feasible Biocompatible Hydrogel Film Embedding Periplaneta Americana Extract for Acute Wound Healing. *International Journal of Pharmaceutics* **2019**, *571*, 118707. https://doi.org/10.1016/j.ijpharm.2019.118707.

(9) Dhivya, S.; Padma, V. V.; Santhini, E. Wound Dressings – a Review. *BioMedicine* **2015**, *5* (4), 22. https://doi.org/10.7603/s40681-015-0022-9.

(10) Liao, X.; Liang, J.-X.; Li, S.-H.; Huang, S.; Yan, J.-X.; Xiao, L.-L.; Song, J.-X.; Liu, H.-W. Allogeneic Platelet-Rich Plasma Therapy as an Effective and Safe Adjuvant Method for Chronic Wounds. *Journal of Surgical Research* **2020**, *246*, 284–291. https://doi.org/10.1016/j.jss.2019.09.019.

(11) Martinengo, L.; Olsson, M.; Bajpai, R.; Soljak, M.; Upton, Z.; Schmidtchen, A.; Car, J.; Järbrink, K. Prevalence of Chronic Wounds in the General Population: Systematic Review and Meta-Analysis of Observational Studies. *Annals of Epidemiology* **2019**, *29*, 8–15. https://doi.org/10.1016/j.annepidem.2018.10.005.

(12) Marfia, G.; Navone, S. E.; Di Vito, C.; Ughi, N.; Tabano, S.; Miozzo, M.; Tremolada, C.; Bolla, G.; Crotti, C.; Ingegnoli, F.; Rampini, P.; Riboni, L.; Gualtierotti, R.; Campanella, R.

Mesenchymal Stem Cells: Potential for Therapy and Treatment of Chronic Non-Healing Skin Wounds. *Organogenesis* **2015**, *11* (4), 183–206. https://doi.org/10.1080/15476278.2015.1126018.

(13) Morton, L. M.; Phillips, T. J. Wound Healing and Treating Wounds. *Journal of the American Academy of Dermatology* **2016**, *74* (4), 589–605. https://doi.org/10.1016/j.jaad.2015.08.068.

(14) Tort, S.; Demiröz, F. T.; Coşkun Cevher, Ş.; Sarıbaş, S.; Özoğul, C.; Acartürk, F. The Effect of a New Wound Dressing on Wound Healing: Biochemical and Histopathological Evaluation. *Burns* **2020**, *46* (1), 143–155. https://doi.org/10.1016/j.burns.2019.02.013.

(15) Das, A.; Abas, M.; Biswas, N.; Banerjee, P.; Ghosh, N.; Rawat, A.; Khanna, S.; Roy, S.; Sen, C. K. A Modified Collagen Dressing Induces Transition of Inflammatory to Reparative Phenotype of Wound Macrophages. *Scientific Reports* **2019**, *9* (1), 14293. https://doi.org/10.1038/s41598-019-49435-z.

(16) Järbrink, K.; Ni, G.; Sönnergren, H.; Schmidtchen, A.; Pang, C.; Bajpai, R.; Car, J. The Humanistic and Economic Burden of Chronic Wounds: A Protocol for a Systematic Review. *Systematic Reviews* **2017**, *6* (1), 15. https://doi.org/10.1186/s13643-016-0400-8.

(17) Han, G.; Ceilley, R. Chronic Wound Healing: A Review of Current Management and Treatments. *Advances in Therapy* **2017**, *34* (3), 599–610. https://doi.org/10.1007/s12325-017-0478-y.

(18) Phillips, C. J.; Humphreys, I.; Fletcher, J.; Harding, K.; Chamberlain, G.; Macey, S. Estimating the Costs Associated with the Management of Patients with Chronic Wounds Using Linked Routine Data: Costs of Wounds Using Routine Data. *International Wound Journal* **2016**, *13* (6), 1193–1197. https://doi.org/10.1111/iwj.12443.

(19) Graves, N.; Phillips, C. j.; Harding, K. A Narrative Review of the Epidemiology and Economics of Chronic Wounds. *British Journal of Dermatology* **2022**, *187* (2), 141–148. https://doi.org/10.1111/bjd.20692.

(20) Schultz, G. S.; Sibbald, R. G.; Falanga, V.; Ayello, E. A.; Dowsett, C.; Harding, K.; Romanelli, M.; Stacey, M. C.; Teot, L.; Vanscheidt, W. Wound Bed Preparation: A Systematic Approach to Wound Management. *Wound Repair and Regeneration* **2003**, *11* (s1), S1–S28. https://doi.org/10.1046/j.1524-475X.11.s2.1.x.

(21) Khandelwal, P.; Das, A.; Sen, C. K.; Srinivas, S. P.; Roy, S.; Khanna, S. A Surfactant Polymer Wound Dressing Protects Human Keratinocytes from Inducible Necroptosis. *Scientific Reports* **2021**, *11* (1), 4357. https://doi.org/10.1038/s41598-021-82260-x.

(22) Wiegand, C.; Abel, M.; Hipler, U.-C.; Elsner, P. Effect of Non-Adhering Dressings on Promotion of Fibroblast Proliferation and Wound Healing in Vitro. *Scientific Reports* **2019**, *9* (1), 4320. https://doi.org/10.1038/s41598-019-40921-y.

(23) Wang, Y.-H.; Liu, C.-C.; Cherng, J.-H.; Fan, G.-Y.; Wang, Y.-W.; Chang, S.-J.; Hong, Z.-J.; Lin, Y.-C.; Hsu, S.-D. Evaluation of Chitosan-Based Dressings in a Swine Model of Artery-Injury-Related Shock. *Scientific Reports* **2019**, *9* (1), 14608. https://doi.org/10.1038/s41598-019-51208-7.

(24) Xu, R.; Xia, H.; He, W.; Li, Z.; Zhao, J.; Liu, B.; Wang, Y.; Lei, Q.; Kong, Y.; Bai, Y.; Yao, Z.; Yan, R.; Li, H.; Zhan, R.; Yang, S.; Luo, G.; Wu, J. Controlled Water Vapor Transmission Rate Promotes Wound-Healing via Wound Re-Epithelialization and Contraction Enhancement. *Scientific Reports* **2016**, *6* (1), 24596. https://doi.org/10.1038/srep24596.

(25) Thangavel, P.; Ramachandran, B.; Chakraborty, S.; Kannan, R.; Lonchin, S.; Muthuvijayan, V. Accelerated Healing of Diabetic Wounds Treated with L-Glutamic Acid Loaded Hydrogels Through Enhanced Collagen Deposition and Angiogenesis: An In Vivo Study. *Scientific Reports* **2017**, *7* (1), 10701. https://doi.org/10.1038/s41598-017-10882-1.

(26) Shyna, S.; Shantikrishna, A.; Nair, P.; Velutheril Thomas, L. A Nonadherent Chitosan-Polyvinyl Alcohol Absorbent Wound Dressing Prepared via Controlled Freeze-Dry Technology. *International Journal of Biological Macromolecules* **2020**, *150*, 129–140. https://doi.org/10.1016/j.ijbiomac.2020.01.292.

(27) Chanmugam, A.; Langemo, D.; Thomason, K.; Haan, J.; Altenburger, E. A.; Tippett, A.; Henderson, L.; Zortman, T. A. Relative Temperature Maximum in Wound Infection and Inflammation as Compared with a Control Subject Using Long-Wave Infrared Thermography. *Advances in Skin & Wound Care* **2017**, *30* (9), 406–414. https://doi.org/10.1097/01.ASW.0000522161.13573.62.

(28) McGuiness, W.; Vella, E.; Harrison, D. Influence of Dressing Changes on Wound Temperature. *Journal of Wound Care* **2004**, *13* (9), 383–385. https://doi.org/10.12968/jowc.2004.13.9.26702.

(29) He, J.; Liang, Y.; Shi, M.; Guo, B. Anti-Oxidant Electroactive and Antibacterial Nanofibrous Wound Dressings Based on Poly(ε-Caprolactone)/Quaternized Chitosan-Graft-Polyaniline for Full-Thickness Skin Wound Healing. *Chemical Engineering Journal* **2020**, *385*, 123464. https://doi.org/10.1016/j.cej.2019.123464.

(30) Daristotle, J. L.; Lau, L. W.; Erdi, M.; Hunter, J.; Djoum, A.; Srinivasan, P.; Wu, X.; Basu, M.; Ayyub, O. B.; Sandler, A. D.; Kofinas, P. Sprayable and Biodegradable, Intrinsically Adhesive Wound Dressing with Antimicrobial Properties. *Bioengineering & Translational Medicine* **2020**, *5* (1), e10149. https://doi.org/10.1002/btm2.10149.

(31) Jang, L. K.; Fletcher, G. K.; Monroe, M. B. B.; Maitland, D. J. Biodegradable Shape Memory Polymer Foams with Appropriate Thermal Properties for Hemostatic Applications. *Journal of Biomedical Materials Research Part A* **2020**, *108* (6), 1281–1294. https://doi.org/10.1002/jbm.a.36901.

(32) Winter, G. D. Formation of the Scab and the Rate of Epithelization of Superficial Wounds in the Skin of the Young Domestic Pig. *Nature* **1962**, *193*, 293–294. https://doi.org/10.1038/193293a0.

(33) Ma, M.; Zhong, Y.; Jiang, X. Thermosensitive and PH-Responsive Tannin-Containing Hydroxypropyl Chitin Hydrogel with Long-Lasting Antibacterial Activity for Wound Healing. *Carbohydrate Polymers* **2020**, *236*, 116096. https://doi.org/10.1016/j.carbpol.2020.116096.

(34) Rudolph, D. Standards of Care for Venous Leg Ulcers: Compression Therapy and Moist Wound Healing. *Journal of Vascular Nursing* **2001**, *19* (1), 20–27. https://doi.org/10.1067/mvn.2001.113987.

(35) Farahani, M.; Shafiee, A. Wound Healing: From Passive to Smart Dressings. *Advanced Healthcare Materials* **2021**, *10* (16), 2100477. https://doi.org/10.1002/adhm.202100477.

(36) Boateng, J. S.; Matthews, K. H.; Stevens, H. N. E.; Eccleston, G. M. Wound Healing Dressings and Drug Delivery Systems: A Review. *Journal of Pharmaceutical Sciences* **2008**, *97* (8), 2892–2923. https://doi.org/10.1002/jps.21210.

(37) Liang, Y.; He, J.; Guo, B. Functional Hydrogels as Wound Dressing to Enhance Wound Healing. *ACS Nano* **2021**, *15* (8), 12687–12722. https://doi.org/10.1021/acsnano.1c04206.

(38) Mayet, N.; Choonara, Y. E.; Kumar, P.; Tomar, L. K.; Tyagi, C.; Du Toit, L. C.; Pillay, V. A Comprehensive Review of Advanced Biopolymeric Wound Healing Systems. *Journal of Pharmaceutical Sciences* **2014**, *103* (8), 2211–2230. https://doi.org/10.1002/jps.24068.

(39) Smith, D.; Peterson, L. J. Treatment of Skin Graft Donor Sites with a Semipermeable Polyurethane Dressing. *Journal of Oral and Maxillofacial Surgery* **1983**, *41* (1), 61–65. https://doi.org/10.1016/S0278-2391(83)80034-2.

(40) Zhao, X.; Wang, L.; Gao, J.; Chen, X.; Wang, K. Hyaluronic Acid/Lysozyme Self-Assembled Coacervate to Promote Cutaneous Wound Healing. *Biomaterials Science* **2020**, *8* (6), 1702–1710. https://doi.org/10.1039/C9BM01886G.

(41) Sato, A. C.; Bosch, R. V.; Will, S. E. A.; Alvarez-Flores, M. P.; Goldfeder, M. B.; Pasqualoto, K. F. M.; da Silva, B. A. V. G.; de Andrade, S. A.; Chudzinski-Tavassi, A. M. Exploring the in Vivo Wound Healing Effects of a Recombinant Hemolin from the Caterpillar Lonomia Obliqua. *Journal of Venomous Animals and Toxins including Tropical Diseases* **2016**, *22* (1), 36. https://doi.org/10.1186/s40409-016-0093-4.

(42) Dijksteel, G. S.; Ulrich, M. M. W.; Vlig, M.; Nibbering, P. H.; Cordfunke, R. A.; Drijfhout, J. W.; Middelkoop, E.; Boekema, B. K. H. L. Potential Factors Contributing to the Poor Antimicrobial Efficacy of SAAP-148 in a Rat Wound Infection Model. *Annals of Clinical Microbiology and Antimicrobials* **2019**, *18* (1), 38. https://doi.org/10.1186/s12941-019-0336-7.

(43) Lei, J.; Sun, L.; Li, P.; Zhu, C.; Lin, Z.; Mackey, V.; Coy, D. H.; He, Q. The Wound Dressings and Their Applications in Wound Healing and Management. *Health Science Journal* **2019**, *13*, 1–8.

(44) Ilenghoven, D.; Chan, C. Y.; Wan Ahmad Kamal, W.; MohdYussof, S.; Ibrahim, S. A Review of Wound Dressing Practices. *Clinical Dermatology* **2017**, *2* (6), 1–12. https://doi.org/10.23880/CDOAJ-16000133.

(45) Kirwan, H.; Pignataro, R. The Skin and Wound Healing, in *Pathology and Intervention in Musculoskeletal Rehabilitation, Second, Elsevier Inc.* **2016**, 25–62. https://doi.org/10.1016/B978-0-323-31072-7.00002-6.

(46) Braunwarth, H.; Brill, F. H. H. Antimicrobial Efficacy of Modern Wound Dressings: Oligodynamic Bactericidal versus Hydrophobic Adsorption Effect. *Wound Medicine* **2014**, *5*, 16–20. https://doi.org/10.1016/j.wndm.2014.04.003.

(47) Carter, K. Hydropolymer Dressings in the Management of Wound Exudate. *British Journal of Community Nursing* **2003**, *8* (S9), S10–S16. https://doi.org/10.12968/bjcn.2003.8.Sup3.11579.

(48) Atherton, D.; Sreetharan, V.; Mosahebi, A.; Prior, S.; Willis, J.; Bishop, J.; Dziewulski, P. A Randomised Controlled Trial of a Double Layer of Allevyn™ Compared to Jellonet and Proflavin as a Tie-over Dressing for Small Skin Grafts. *Journal of Plastic, Reconstructive & Aesthetic Surgery* **2008**, *61* (5), 535–539. https://doi.org/10.1016/j.bjps.2007.01.004.

(49) Chaganti, P.; Gordon, I.; Chao, J. H.; Zehtabchi, S. A Systematic Review of Foam Dressings for Partial Thickness Burns. *The American Journal of Emergency Medicine* **2019**, *37* (6), 1184–1190. https://doi.org/10.1016/j.ajem.2019.04.014.

(50) Tao, G.; Wang, Y.; Cai, R.; Chang, H.; Song, K.; Zuo, H.; Zhao, P.; Xia, Q.; He, H. Design and Performance of Sericin/Poly(Vinyl Alcohol) Hydrogel as a Drug Delivery Carrier for Potential Wound Dressing Application. *Materials Science and Engineering: C* **2019**, *101*, 341–351. https://doi.org/10.1016/j.msec.2019.03.111.

(51) Nešović, K.; Janković, A.; Radetić, T.; Vukašinović-Sekulić, M.; Kojić, V.; Živković, L.; Perić-Grujić, A.; Rhee, K. Y.; Mišković-Stanković, V. Chitosan-Based Hydrogel Wound Dressings with Electrochemically Incorporated Silver Nanoparticles – In Vitro Study. *European Polymer Journal* **2019**, *121*, 109257. https://doi.org/10.1016/j.eurpolymj.2019.109257.

(52) Kim, M.-S.; Oh, G.-W.; Jang, Y.-M.; Ko, S.-C.; Park, W.-S.; Choi, I.-W.; Kim, Y.-M.; Jung, W.-K. Antimicrobial Hydrogels Based on PVA and Diphlorethohydroxycarmalol (DPHC) Derived from Brown Alga Ishige Okamurae: An in Vitro and in Vivo Study for Wound Dressing Application. *Materials Science and Engineering: C* **2020**, *107*, 110352. https://doi.org/10.1016/j.msec.2019.110352.

(53) Kamoun, E. A.; Kenawy, E.-R. S.; Chen, X. A Review on Polymeric Hydrogel Membranes for Wound Dressing Applications: PVA-Based Hydrogel Dressings. *Journal of Advanced Research* **2017**, *8* (3), 217–233. https://doi.org/10.1016/j.jare.2017.01.005.

(54) Límová, M.; Troyer-Caudle, J. Controlled, Randomized Clinical Trial of 2 Hydrocolloid Dressings in the Management of Venous Insufficiency Ulcers. *Journal of Vascular Nursing* **2002**, *20* (1), 22–33. https://doi.org/10.1067/mvn.2002.121907.

(55) Kong, D.; Zhang, Q.; You, J.; Cheng, Y.; Hong, C.; Chen, Z.; Jiang, T.; Hao, T. Adhesion Loss Mechanism Based on Carboxymethyl Cellulose-Filled Hydrocolloid Dressings in Physiological Wounds Environment. *Carbohydrate Polymers* **2020**, *235*, 115953. https://doi.org/10.1016/j.carbpol.2020.115953.

(56) Thu, H.-E.; Zulfakar, M. H.; Ng, S.-F. Alginate Based Bilayer Hydrocolloid Films as Potential Slow-Release Modern Wound Dressing. *International Journal of Pharmaceutics* **2012**, *434* (1–2), 375–383. https://doi.org/10.1016/j.ijpharm.2012.05.044.

(57) Jin, S. G.; Yousaf, A. M.; Kim, K. S.; Kim, D. W.; Kim, D. S.; Kim, J. K.; Yong, C. S.; Youn, Y. S.; Kim, J. O.; Choi, H.-G. Influence of Hydrophilic Polymers on Functional Properties and Wound Healing Efficacy of Hydrocolloid Based Wound Dressings. *International Journal of Pharmaceutics* **2016**, *501* (1–2), 160–166. https://doi.org/10.1016/j.ijpharm.2016.01.044.

(58) Martin, F. T.; O'Sullivan, J. B.; Regan, P. J.; McCann, J.; Kelly, J. L. Hydrocolloid Dressing in Pediatric Burns May Decrease Operative Intervention Rates. *Journal of Pediatric Surgery* **2010**, *45* (3), 600–605. https://doi.org/10.1016/j.jpedsurg.2009.09.037.

(59) Vowden, K.; Vowden, P. Wound Dressings: Principles and Practice. *Surgery (Oxford)* **2014**, *32* (9), 462–467. https://doi.org/10.1016/j.mpsur.2014.07.001.

(60) Skórkowska-Telichowska, K.; Czemplik, M.; Kulma, A.; Szopa, J. The Local Treatment and Available Dressings Designed for Chronic Wounds. *Journal of the American Academy of Dermatology* **2013**, *68* (4), e117–e126. https://doi.org/10.1016/j.jaad.2011.06.028.

(61) Lalzawmliana, V.; Anand, A.; Mukherjee, P.; Chaudhuri, S.; Kundu, B.; Nandi, S. K.; Thakur, N. L. Marine Organisms as a Source of Natural Matrix for Bone Tissue Engineering. *Ceramics International* **2019**, *45* (2, Part A), 1469–1481. https://doi.org/10.1016/j.ceramint.2018.10.108.

(62) Forster, R. E. J.; Thürmer, F.; Wallrapp, C.; Lloyd, A. W.; Macfarlane, W.; Phillips, G. J.; Boutrand, J.-P.; Lewis, A. L. Characterisation of Physico-Mechanical Properties and Degradation Potential of Calcium Alginate Beads for Use in Embolisation. *Journal of Materials Science: Materials in Medicine* **2010**, *21* (7), 2243–2251. https://doi.org/10.1007/s10856-010-4080-y.

(63) Qin, Y. The Gel Swelling Properties of Alginate Fibers and Their Applications in Wound Management. *Polymers for Advanced Technologies* **2008**, *19* (1), 6–14. https://doi.org/10.1002/pat.960.

(64) Raman, S. P.; Keil, C.; Dieringer, P.; Hübner, C.; Bueno, A.; Gurikov, P.; Nissen, J.; Holtkamp, M.; Karst, U.; Haase, H.; Smirnova, I. Alginate Aerogels Carrying Calcium, Zinc and Silver Cations for Wound Care: Fabrication and Metal Detection. *The Journal of Supercritical Fluids* **2019**, *153*, 104545. https://doi.org/10.1016/j.supflu.2019.104545.

(65) Momoh, F. U.; Boateng, J. S.; Richardson, S. C. W.; Chowdhry, B. Z.; Mitchell, J. C. Development and Functional Characterization of Alginate Dressing as Potential Protein Delivery System for Wound Healing. *International Journal of Biological Macromolecules* **2015**, *81*, 137–150. https://doi.org/10.1016/j.ijbiomac.2015.07.037.

(66) Varaprasad, K.; Jayaramudu, T.; Kanikireddy, V.; Toro, C.; Sadiku, E. R. Alginate-Based Composite Materials for Wound Dressing Application: A Mini Review. *Carbohydrate Polymers* **2020**, *236*, 116025. https://doi.org/10.1016/j.carbpol.2020.116025.

(67) Hampton, S. The Role of Alginate Dressings in Wound Healing. *The Diabetic Foot Journal* **2004**, *7*, 4–7.

(68) Colobatiu, L.; Gavan, A.; Potarniche, A.-V.; Rus, V.; Diaconeasa, Z.; Mocan, A.; Tomuta, I.; Mirel, S.; Mihaiu, M. Evaluation of Bioactive Compounds-Loaded Chitosan Films as a Novel

and Potential Diabetic Wound Dressing Material. *Reactive and Functional Polymers* **2019**, *145*, 104369. https://doi.org/10.1016/j.reactfunctpolym.2019.104369.

(69) Vasconcelos, A.; Gomes, A. C.; Cavaco-Paulo, A. Novel Silk Fibroin/Elastin Wound Dressings. *Acta Biomaterialia* **2012**, *8* (8), 3049–3060. https://doi.org/10.1016/j.actbio.2012.04.035.

(70) Sharma, S.; Swetha, K. L.; Roy, A. Chitosan-Chondroitin Sulfate Based Polyelectrolyte Complex for Effective Management of Chronic Wounds. *International Journal of Biological Macromolecules* **2019**, *132*, 97–108. https://doi.org/10.1016/j.ijbiomac.2019.03.186.

(71) Fu, R.; Li, C.; Yu, C.; Xie, H.; Shi, S.; Li, Z.; Wang, Q.; Lu, L. A Novel Electrospun Membrane Based on Moxifloxacin Hydrochloride/Poly(Vinyl Alcohol)/Sodium Alginate for Antibacterial Wound Dressings in Practical Application. *Drug Delivery* **2016**, *23* (3), 818–829. https://doi.org/10.3109/10717544.2014.918676.

(72) Abednejad, A.; Ghaee, A.; Morais, E. S.; Sharma, M.; Neves, B. M.; Freire, M. G.; Nourmohammadi, J.; Mehrizi, A. A. Polyvinylidene Fluoride–Hyaluronic Acid Wound Dressing Comprised of Ionic Liquids for Controlled Drug Delivery and Dual Therapeutic Behavior. *Acta Biomaterialia* **2019**, *100*, 142–157. https://doi.org/10.1016/j.actbio.2019.10.007.

(73) Lin, Z.; Wu, T.; Wang, W.; Li, B.; Wang, M.; Chen, L.; Xia, H.; Zhang, T. Biofunctions of Antimicrobial Peptide-Conjugated Alginate/Hyaluronic Acid/Collagen Wound Dressings Promote Wound Healing of a Mixed-Bacteria-Infected Wound. *International Journal of Biological Macromolecules* **2019**, *140*, 330–342. https://doi.org/10.1016/j.ijbiomac.2019.08.087.

(74) Yang, Y.; Liang, Y.; Chen, J.; Duan, X.; Guo, B. Mussel-Inspired Adhesive Antioxidant Antibacterial Hemostatic Composite Hydrogel Wound Dressing via Photo-Polymerization for Infected Skin Wound Healing. *Bioactive Materials* **2022**, *8*, 341–354. https://doi.org/10.1016/j.bioactmat.2021.06.014.

(75) Hao, Y.; Zhao, W.; Zhang, H.; Zheng, W.; Zhou, Q. Carboxymethyl Chitosan-Based Hydrogels Containing Fibroblast Growth Factors for Triggering Diabetic Wound Healing. *Carbohydrate Polymers* **2022**, *287*, 119336. https://doi.org/10.1016/j.carbpol.2022.119336.

(76) Li, A.; Li, L.; Zhao, B.; Li, X.; Liang, W.; Lang, M.; Cheng, B.; Li, J. Antibacterial, Antioxidant and Anti-Inflammatory PLCL/Gelatin Nanofiber Membranes to Promote Wound Healing. *International Journal of Biological Macromolecules* **2022**, *194*, 914–923. https://doi.org/10.1016/j.ijbiomac.2021.11.146.

(77) Horch, R. E.; Kopp, J.; Kneser, U.; Beier, J.; Bach, A. D. Tissue Engineering of Cultured Skin Substitutes. *Journal of Cellular and Molecular Medicine* **2005**, *9* (3), 592–608. https://doi.org/10.1111/j.1582-4934.2005.tb00491.x.

(78) Austin, R. E.; Merchant, N.; Shahrokhi, S.; Jeschke, M. G. A Comparison of Biobrane™ and Cadaveric Allograft for Temporizing the Acute Burn Wound: Cost and Procedural Time. *Burns* **2015**, *41* (4), 749–753. https://doi.org/10.1016/j.burns.2014.10.003.

(79) Gravvanis, A. I.; Tsoutsos, D. A.; Iconomou, T.; Gremoutis, G. The Use of Integra Artificial Dermis to Minimize Donor-Site Morbidity after Suprafascial Dissection of the Radial Forearm Flap. *Microsurgery* **2007**, *27* (7), 583–587. https://doi.org/10.1002/micr.20406.

(80) Callcut, R. A.; Schurr, M. J.; Sloan, M.; Faucher, L. D. Clinical Experience with Alloderm: A One-Staged Composite Dermal/Epidermal Replacement Utilizing Processed Cadaver Dermis and Thin Autografts. *Burns* **2006**, *32* (5), 583–588. https://doi.org/10.1016/j.burns.2005.12.002.

(81) Omar, A. A.; Mavor, A. I. D.; Jones, A. M.; Homer-Vanniasinkam, S. Treatment of Venous Leg Ulcers with Dermagraft®. *European Journal of Vascular and Endovascular Surgery* **2004**, *27* (6), 666–672. https://doi.org/10.1016/j.ejvs.2004.03.001.

(82) Zaulyanov, L.; Kirsner, R. S. A Review of a Bi-Layered Living Cell Treatment (Apligraf®) in the Treatment of Venous Leg Ulcers and Diabetic Foot Ulcers. *Clinical Interventions in Aging* **2007**, *2* (1), 93–98. https://doi.org/10.2147/ciia.2007.2.1.93.

(83) Still, J.; Glat, P.; Silverstein, P.; Griswold, J.; Mozingo, D. The Use of a Collagen Sponge/Living Cell Composite Material to Treat Donor Sites in Burn Patients. *Burns* **2003**, *29* (8), 837–841. https://doi.org/10.1016/S0305-4179(03)00164-5.

(84) Varkey, M.; Ding, J.; Tredget, E. Advances in Skin Substitutes—Potential of Tissue Engineered Skin for Facilitating Anti-Fibrotic Healing. *Journal of Functional Biomaterials* **2015**, *6* (3), 547–563. https://doi.org/10.3390/jfb6030547.

(85) Vig, K.; Chaudhari, A.; Tripathi, S.; Dixit, S.; Sahu, R.; Pillai, S.; Dennis, V.; Singh, S. Advances in Skin Regeneration Using Tissue Engineering. *International Journal of Molecular Sciences* **2017**, *18* (4), 789. https://doi.org/10.3390/ijms18040789.

(86) Huang, S.; Fu, X. Tissue-Engineered Skin: Bottleneck or Breakthrough. *International Journal of Burns and Trauma* **2011**, *1* (1), 1–10.

(87) Haldar, S.; Sharma, A.; Gupta, S.; Chauhan, S.; Roy, P.; Lahiri, D. Bioengineered Smart Trilayer Skin Tissue Substitute for Efficient Deep Wound Healing. *Materials Science and Engineering: C* **2019**, *105*, 110140. https://doi.org/10.1016/j.msec.2019.110140.

(88) Han, D.; Gouma, P.-I. Electrospun Bioscaffolds That Mimic the Topology of Extracellular Matrix. *Nanomedicine: Nanotechnology, Biology and Medicine* **2006**, *2* (1), 37–41. https://doi.org/10.1016/j.nano.2006.01.002.

(89) Wu, J.; Pan, Z.; Zhao, Z.-Y.; Wang, M.-H.; Dong, L.; Gao, H.-L.; Liu, C.-Y.; Zhou, P.; Chen, L.; Shi, C.-J.; Zhang, Z.-Y.; Yang, C.; Yu, S.-H.; Zou, D.-H. Anti-Swelling, Robust, and Adhesive Extracellular Matrix-Mimicking Hydrogel Used as Intraoral Dressing. *Advanced Materials* **2022**, *34* (20), 2200115. https://doi.org/10.1002/adma.202200115.

(90) Zhang, X.; Chen, X.; Hong, H.; Hu, R.; Liu, J.; Liu, C. Decellularized Extracellular Matrix Scaffolds: Recent Trends and Emerging Strategies in Tissue Engineering. *Bioactive Materials* **2022**, *10*, 15–31. https://doi.org/10.1016/j.bioactmat.2021.09.014.

(91) Aoki, H.; Miyoshi, H.; Yamagata, Y. Electrospinning of Gelatin Nanofiber Scaffolds with Mild Neutral Cosolvents for Use in Tissue Engineering. *Polymer Journal* **2015**, *47* (3), 267–277. https://doi.org/10.1038/pj.2014.94.

(92) Angel, N.; Guo, L.; Yan, F.; Wang, H.; Kong, L. Effect of Processing Parameters on the Electrospinning of Cellulose Acetate Studied by Response Surface Methodology. *Journal of Agriculture and Food Research* **2020**, *2*, 100015. https://doi.org/10.1016/j.jafr.2019.100015.

(93) Sonntag, M.; Cimino, A.; Rajapaksha, M.; Thomas, J. Improved Control over Polymer Nanofiber Deposition with a Programmable 3-Axis Electrospinning Apparatus. *Journal of Electrostatics* **2020**, *103*, 103406. https://doi.org/10.1016/j.elstat.2019.103406.

(94) Mele, E. Electrospinning of Natural Polymers for Advanced Wound Care: Towards Responsive and Adaptive Dressings. *Journal of Materials Chemistry B* **2016**, *4* (28), 4801–4812. https://doi.org/10.1039/C6TB00804F.

(95) Tripathi, M.; Parthasarathy, S.; Roy, P. K. Mechanically Robust Polyurea Nanofibers Processed through Electrospinning Technique. *Materials Today Communications* **2020**, *22*, 100771. https://doi.org/10.1016/j.mtcomm.2019.100771.

(96) Kopp, A.; Smeets, R.; Gosau, M.; Kröger, N.; Fuest, S.; Köpf, M.; Kruse, M.; Krieger, J.; Rutkowski, R.; Henningsen, A.; Burg, S. Effect of Process Parameters on Additive-Free Electrospinning of Regenerated Silk Fibroin Nonwovens. *Bioactive Materials* **2020**, *5* (2), 241–252. https://doi.org/10.1016/j.bioactmat.2020.01.010.

(97) Yang, C.; Jia, Z.; Xu, Z.; Wang, K.; Guan, Z.; Wang, L. Comparisons of Fibers Properties between Vertical and Horizontal Type Electrospinning Systems, in *2009 IEEE Conference on Electrical Insulation and Dielectric Phenomena* **2009**, 204–207. https://doi.org/10.1109/CEIDP.2009.5377758.

(98) Niu, C.; Meng, J.; Wang, X.; Han, C.; Yan, M.; Zhao, K.; Xu, X.; Ren, W.; Zhao, Y.; Xu, L.; Zhang, Q.; Zhao, D.; Mai, L. General Synthesis of Complex Nanotubes by Gradient Electrospinning and Controlled Pyrolysis. *Nature Communications* **2015**, *6* (1), 7402. https://doi.org/10.1038/ncomms8402.

(99) Nagiah, N.; Murdock, C. J.; Bhattacharjee, M.; Nair, L.; Laurencin, C. T. Development of Tripolymeric Triaxial Electrospun Fibrous Matrices for Dual Drug Delivery Applications. *Scientific Reports* **2020**, *10* (1), 609. https://doi.org/10.1038/s41598-020-57412-0.

(100) Yoon, J.; Yang, H.-S.; Lee, B.-S.; Yu, W.-R. Recent Progress in Coaxial Electrospinning: New Parameters, Various Structures, and Wide Applications. *Advanced Materials* **2018**, *30* (42), 1704765. https://doi.org/10.1002/adma.201704765.

(101) Mi, H.-Y.; Jing, X.; Yu, E.; Wang, X.; Li, Q.; Turng, L.-S. Manipulating the Structure and Mechanical Properties of Thermoplastic Polyurethane/Polycaprolactone Hybrid Small Diameter Vascular Scaffolds Fabricated via Electrospinning Using an Assembled Rotating Collector. *Journal of the Mechanical Behavior of Biomedical Materials* **2018**, *78*, 433–441. https://doi.org/10.1016/j.jmbbm.2017.11.046.

(102) Gutierrez-Gonzalez, J.; Garcia-Cela, E.; Magan, N.; Rahatekar, S. S. Electrospinning Alginate/Polyethylene Oxide and Curcumin Composite Nanofibers. *Materials Letters* **2020**, *270*, 127662. https://doi.org/10.1016/j.matlet.2020.127662.

(103) Xue, J.; Wu, T.; Dai, Y.; Xia, Y. Electrospinning and Electrospun Nanofibers: Methods, Materials, and Applications. *Chemical Reviews* **2019**, *119* (8), 5298–5415. https://doi.org/10.1021/acs.chemrev.8b00593.

(104) Surendranath, M.; Rajalekshmi, R.; Ramesan, R. M.; Nair, P.; Parameswaran, R. UV-Crosslinked Electrospun Zein/PEO Fibroporous Membranes for Wound Dressing. *ACS Applied Bio Materials* **2022**, *5* (4), 1538–1551. https://doi.org/10.1021/acsabm.1c01293.

(105) Bozkaya, O.; Arat, E.; Gün Gök, Z.; Yiğitoğlu, M.; Vargel, İ. Production and Characterization of Hybrid Nanofiber Wound Dressing Containing Centella Asiatica Coated Silver Nanoparticles by Mutual Electrospinning Method. *European Polymer Journal* **2022**, *166*, 111023. https://doi.org/10.1016/j.eurpolymj.2022.111023.

(106) Valachová, K.; El Meligy, M. A.; Šoltés, L. Hyaluronic Acid and Chitosan-Based Electrospun Wound Dressings: Problems and Solutions. *International Journal of Biological Macromolecules* **2022**, *206*, 74–91. https://doi.org/10.1016/j.ijbiomac.2022.02.117.

(107) Ekambaram, R.; Dharmalingam, S. Fabrication and Evaluation of Electrospun Biomimetic Sulphonated PEEK Nanofibrous Scaffold for Human Skin Cell Proliferation and Wound Regeneration Potential. *Materials Science and Engineering: C* **2020**, *115*, 111150. https://doi.org/10.1016/j.msec.2020.111150.

(108) Sun, L.; Song, L.; Zhang, X.; Zhou, R.; Yin, J.; Luan, S. Poly(γ-Glutamic Acid)-Based Electrospun Nanofibrous Mats with Photodynamic Therapy for Effectively Combating Wound Infection. *Materials Science and Engineering: C* **2020**, *113*, 110936. https://doi.org/10.1016/j.msec.2020.110936.

(109) Balakrishnan, S. B.; Thambusamy, S. Preparation of Silver Nanoparticles and Riboflavin Embedded Electrospun Polymer Nanofibrous Scaffolds for in Vivo Wound Dressing Application. *Process Biochemistry* **2020**, *88*, 148–158. https://doi.org/10.1016/j.procbio.2019.09.033.

(110) Naseri-Nosar, M.; Ziora, Z. M. Wound Dressings from Naturally-Occurring Polymers: A Review on Homopolysaccharide-Based Composites. *Carbohydrate Polymers* **2018**, *189*, 379–398. https://doi.org/10.1016/j.carbpol.2018.02.003.

(111) Zahedi, P.; Rezaeian, I.; Ranaei-Siadat, S.-O.; Jafari, S.-H.; Supaphol, P. A Review on Wound Dressings with an Emphasis on Electrospun Nanofibrous Polymeric Bandages. *Polymers for Advanced Technologies* **2010**, *21* (2), 77–95. https://doi.org/10.1002/pat.1625.

(112) Kai, D.; Liow, S. S.; Loh, X. J. Biodegradable Polymers for Electrospinning: Towards Biomedical Applications. *Materials Science and Engineering: C* **2014**, *45*, 659–670. https://doi.org/10.1016/j.msec.2014.04.051.

(113) Baker, S. R.; Banerjee, S.; Bonin, K.; Guthold, M. Determining the Mechanical Properties of Electrospun Poly-ε-Caprolactone (PCL) Nanofibers Using AFM and a Novel Fiber

Anchoring Technique. *Materials Science and Engineering: C* **2016**, *59*, 203–212. https://doi.org/10.1016/j.msec.2015.09.102.

(114) Miguel, S. P.; Figueira, D. R.; Simões, D.; Ribeiro, M. P.; Coutinho, P.; Ferreira, P.; Correia, I. J. Electrospun Polymeric Nanofibres as Wound Dressings: A Review. *Colloids and Surfaces B: Biointerfaces* **2018**, *169*, 60–71. https://doi.org/10.1016/j.colsurfb.2018.05.011.

(115) Reddy, M. S. B.; Ponnamma, D.; Choudhary, R.; Sadasivuni, K. K. A Comparative Review of Natural and Synthetic Biopolymer Composite Scaffolds. *Polymers* **2021**, *13* (7), 1105. https://doi.org/10.3390/polym13071105.

(116) Mohammadalizadeh, Z.; Bahremandi-Toloue, E.; Karbasi, S. Synthetic-Based Blended Electrospun Scaffolds in Tissue Engineering Applications. *Journal of Materials Science* **2022**, *57* (6), 4020–4079. https://doi.org/10.1007/s10853-021-06826-w.

(117) Pinar, E.; Sahin, A.; Unal, S.; Gunduz, O.; Harman, F.; Kaptanoglu, E. The Effect of Polycaprolactone/Graphene Oxide Electrospun Scaffolds on the Neurogenic Behavior of Adipose Stem Cells. *European Polymer Journal* **2022**, *165*, 111000. https://doi.org/10.1016/j.eurpolymj.2022.111000.

(118) Menazea, A. A.; Ibrahium, H. A.; Awwad, N. S.; Moustapha, M. E.; Farea, M. O.; Bajaber, M. A. Facile Synthesis and High-Performance Dielectric Properties of Polyethylene Oxide-Chitosan- Iron Oxide Nano-Composite for Electrical Applications. *Journal of Materials Research and Technology* **2022**, *18*, 2273–2281. https://doi.org/10.1016/j.jmrt.2022.03.058.

(119) Johari, S. N. 'Afini M.; Tajuddin, N. A.; Hanibah, H.; Deraman, S. K. A Review: Ionic Conductivity of Solid Polymer Electrolyte Based Polyethylene Oxide. *International Journal of Electrochemical Science* **2021**, *16*, 211049. https://doi.org/10.20964/2021.10.53.

(120) Wang, Y.; Zhou, Y.; Xie, G.; Li, J.; Wang, Y.; Liu, X.; Zang, Z. Dual Resistance and Impedance Investigation: Ultrasensitive and Stable Humidity Detection of Molybdenum Disulfide Nanosheet-Polyethylene Oxide Hybrids. *ACS Applied Materials & Interfaces* **2021**, *13* (21), 25250–25259. https://doi.org/10.1021/acsami.1c02119.

(121) Kim, T. G.; Lee, D. S.; Park, T. G. Controlled Protein Release from Electrospun Biodegradable Fiber Mesh Composed of Poly(ε-Caprolactone) and Poly(Ethylene Oxide). *International Journal of Pharmaceutics* **2007**, *338* (1–2), 276–283. https://doi.org/10.1016/j.ijpharm.2007.01.040.

(122) Ghosal, K.; Agatemor, C.; Špitálsky, Z.; Thomas, S.; Kny, E. Electrospinning Tissue Engineering and Wound Dressing Scaffolds from Polymer-Titanium Dioxide Nanocomposites. *Chemical Engineering Journal* **2019**, *358*, 1262–1278. https://doi.org/10.1016/j.cej.2018.10.117.

(123) Ajmal, G.; Bonde, G. V.; Mittal, P.; Khan, G.; Pandey, V. K.; Bakade, B. V.; Mishra, B. Biomimetic PCL-Gelatin Based Nanofibers Loaded with Ciprofloxacin Hydrochloride and Quercetin: A Potential Antibacterial and Anti-Oxidant Dressing Material for Accelerated Healing of a Full Thickness Wound. *International Journal of Pharmaceutics* **2019**, *567*, 118480. https://doi.org/10.1016/j.ijpharm.2019.118480.

(124) Zhang, D.; Li, L.; Shan, Y.; Xiong, J.; Hu, Z.; Zhang, Y.; Gao, J. In Vivo Study of Silk Fibroin/Gelatin Electrospun Nanofiber Dressing Loaded with Astragaloside IV on the Effect of Promoting Wound Healing and Relieving Scar. *Journal of Drug Delivery Science and Technology* **2019**, *52*, 272–281. https://doi.org/10.1016/j.jddst.2019.04.021.

(125) Sridhar, R.; Lakshminarayanan, R.; Madhaiyan, K.; Amutha Barathi, V.; Lim, K. H. C.; Ramakrishna, S. Electrosprayed Nanoparticles and Electrospun Nanofibers Based on Natural Materials: Applications in Tissue Regeneration, Drug Delivery and Pharmaceuticals. *Chemical Society Reviews* **2015**, *44* (3), 790–814. https://doi.org/10.1039/C4CS00226A.

(126) Eskandarinia, A.; Kefayat, A.; Agheb, M.; Rafienia, M.; Amini Baghbadorani, M.; Navid, S.; Ebrahimpour, K.; Khodabakhshi, D.; Ghahremani, F. A Novel Bilayer Wound Dressing Composed of a Dense Polyurethane/Propolis Membrane and a Biodegradable Polycaprolactone/Gelatin Nanofibrous Scaffold. *Scientific Reports* **2020**, *10* (1), 3063. https://doi.org/10.1038/s41598-020-59931-2.

(127) Lima, L. L.; Taketa, T. B.; Beppu, M. M.; Sousa, I. M. de O.; Foglio, M. A.; Moraes, Â. M. Coated Electrospun Bioactive Wound Dressings: Mechanical Properties and Ability to Control Lesion Microenvironment. *Materials Science and Engineering: C* **2019**, *100*, 493–504. https://doi.org/10.1016/j.msec.2019.03.005.

(128) Movahedi, M.; Asefnejad, A.; Rafienia, M.; Khorasani, M. T. Potential of Novel Electrospun Core-Shell Structured Polyurethane/Starch (Hyaluronic Acid) Nanofibers for Skin Tissue Engineering: In Vitro and in Vivo Evaluation. *International Journal of Biological Macromolecules* **2020**, *146*, 627–637. https://doi.org/10.1016/j.ijbiomac.2019.11.233.

(129) Li, L.; Qian, Y.; Jiang, C.; Lv, Y.; Liu, W.; Zhong, L.; Cai, K.; Li, S.; Yang, L. The Use of Hyaluronan to Regulate Protein Adsorption and Cell Infiltration in Nanofibrous Scaffolds. *Biomaterials* **2012**, *33* (12), 3428–3445. https://doi.org/10.1016/j.biomaterials.2012.01.038.

(130) Ehterami, A.; Salehi, M.; Farzamfar, S.; Vaez, A.; Samadian, H.; Sahrapeyma, H.; Mirzaii, M.; Ghorbani, S.; Goodarzi, A. In Vitro and in Vivo Study of PCL/COLL Wound Dressing Loaded with Insulin-Chitosan Nanoparticles on Cutaneous Wound Healing in Rats Model. *International Journal of Biological Macromolecules* **2018**, *117*, 601–609. https://doi.org/10.1016/j.ijbiomac.2018.05.184.

(131) Li, H.; Zhang, Z.; Godakanda, V. U.; Chiu, Y.-J.; Angkawinitwong, U.; Patel, K.; Stapleton, P. G.; de Silva, R. M.; de Silva, K. M. N.; Zhu, L.-M.; Williams, G. R. The Effect of Collection Substrate on Electrospun Ciprofloxacin-Loaded Poly(Vinylpyrrolidone) and Ethyl Cellulose Nanofibers as Potential Wound Dressing Materials. *Materials Science and Engineering: C* **2019**, *104*, 109917. https://doi.org/10.1016/j.msec.2019.109917.

(132) Shi, R.; Geng, H.; Gong, M.; Ye, J.; Wu, C.; Hu, X.; Zhang, L. Long-Acting and Broad-Spectrum Antimicrobial Electrospun Poly (ε-Caprolactone)/Gelatin Micro/Nanofibers for Wound Dressing. *Journal of Colloid and Interface Science* **2018**, *509*, 275–284. https://doi.org/10.1016/j.jcis.2017.08.092.

(133) Mahmoodi, N. M.; Oveisi, M.; Taghizadeh, A.; Taghizadeh, M. Synthesis of Pearl Necklace-like ZIF-8@chitosan/PVA Nanofiber with Synergistic Effect for Recycling Aqueous Dye Removal. *Carbohydrate Polymers* **2020**, *227*, 115364. https://doi.org/10.1016/j.carbpol.2019.115364.

(134) Sionkowska, A. Current Research on the Blends of Natural and Synthetic Polymers as New Biomaterials: Review. *Progress in Polymer Science* **2011**, *36* (9), 1254–1276. https://doi.org/10.1016/j.progpolymsci.2011.05.003.

(135) Liu, Y.; Zhou, S.; Gao, Y.; Zhai, Y. Electrospun Nanofibers as a Wound Dressing for Treating Diabetic Foot Ulcer. *Asian Journal of Pharmaceutical Sciences* **2019**, *14* (2), 130–143. https://doi.org/10.1016/j.ajps.2018.04.004.

(136) Ma, G.; Liu, Y.; Peng, C.; Fang, D.; He, B.; Nie, J. Paclitaxel Loaded Electrospun Porous Nanofibers as Mat Potential Application for Chemotherapy against Prostate Cancer. *Carbohydrate Polymers* **2011**, *86* (2), 505–512. https://doi.org/10.1016/j.carbpol.2011.04.082.

(137) Aragão-Neto, A. C.; Soares, P. A. G.; Lima-Ribeiro, M. H. M.; Carvalho, E. J. A.; Correia, M. T. S.; Carneiro-da-Cunha, M. G. Combined Therapy Using Low Level Laser and Chitosan-Policaju Hydrogel for Wound Healing. *International Journal of Biological Macromolecules* **2017**, *95*, 268–272. https://doi.org/10.1016/j.ijbiomac.2016.11.019.

(138) Albuquerque, P. B. S.; Cerqueira, M. A.; Vicente, A. A.; Teixeira, J. A.; Carneiro-da-Cunha, M. G. Immobilization of Bioactive Compounds in Cassia Grandis Galactomannan-Based Films: Influence on Physicochemical Properties. *International Journal of Biological Macromolecules* **2017**, *96*, 727–735. https://doi.org/10.1016/j.ijbiomac.2016.12.081.

(139) Luo, Y.; Diao, H.; Xia, S.; Dong, L.; Chen, J.; Zhang, J. A Physiologically Active Polysaccharide Hydrogel Promotes Wound Healing. *Journal of Biomedical Materials Research Part A* **2010**, *94*, 193–204.

(140) Aduba, D.; Yang, H. Polysaccharide Fabrication Platforms and Biocompatibility Assessment as Candidate Wound Dressing Materials. *Bioengineering* **2017**, *4* (4), 1. https://doi.org/10.3390/bioengineering4010001.

(141) Zhao, Y.; Jalili, S. Dextran, as a Biological Macromolecule for the Development of Bioactive Wound Dressing Materials: A Review of Recent Progress and Future Perspectives. *International Journal of Biological Macromolecules* **2022**, *207*, 666–682. https://doi.org/10.1016/j.ijbiomac.2022.02.114.

(142) Bostancı, N. S.; Büyüksungur, S.; Hasirci, N.; Tezcaner, A. PH Responsive Release of Curcumin from Photocrosslinked Pectin/Gelatin Hydrogel Wound Dressings. *Biomaterials Advances* **2022**, *134*, 112717. https://doi.org/10.1016/j.msec.2022.112717.

(143) Das, M.; Zandraa, O.; Mudenur, C.; Saha, N.; Sáha, P.; Mandal, B.; Katiyar, V. Composite Scaffolds Based on Bacterial Cellulose for Wound Dressing Application. *ACS Applied Bio Materials* **2022**, *5* (8), 3722–3733. https://doi.org/10.1021/acsabm.2c00226.

(144) Zheng, Z.; Qi, J.; Hu, L.; Ouyang, D.; Wang, H.; Sun, Q.; Lin, L.; You, L.; Tang, B. A Cannabidiol-Containing Alginate Based Hydrogel as Novel Multifunctional Wound Dressing for Promoting Wound Healing. *Biomaterials Advances* **2022**, *134*, 112560. https://doi.org/10.1016/j.msec.2021.112560.

(145) Peng, W.; Li, D.; Dai, K.; Wang, Y.; Song, P.; Li, H.; Tang, P.; Zhang, Z.; Li, Z.; Zhou, Y.; Zhou, C. Recent Progress of Collagen, Chitosan, Alginate and Other Hydrogels in Skin Repair

and Wound Dressing Applications. *International Journal of Biological Macromolecules* **2022**, *208*, 400–408. https://doi.org/10.1016/j.ijbiomac.2022.03.002.

(146) Mirhaj, M.; Tavakoli, M.; Varshosaz, J.; Labbaf, S.; Salehi, S.; Talebi, A.; Kazemi, N.; Haghighi, V.; Alizadeh, M. Preparation of a Biomimetic Bi-Layer Chitosan Wound Dressing Composed of A-PRF/Sponge Layer and L-Arginine/Nanofiber. *Carbohydrate Polymers* **2022**, *292*, 119648. https://doi.org/10.1016/j.carbpol.2022.119648.

(147) Rusu, A. G.; Chiriac, A. P.; Nita, L. E.; Ghilan, A.; Rusu, D.; Simionescu, N.; Tartau, L. M. Nanostructured Hyaluronic Acid-Based Hydrogels Encapsulating Synthetic/ Natural Hybrid Nanogels as Promising Wound Dressings. *Biochemical Engineering Journal* **2022**, *179*, 108341. https://doi.org/10.1016/j.bej.2022.108341.

(148) Makvandi, P.; Ali, G. W.; Della Sala, F.; Abdel-Fattah, W. I.; Borzacchiello, A. Biosynthesis and Characterization of Antibacterial Thermosensitive Hydrogels Based on Corn Silk Extract, Hyaluronic Acid and Nanosilver for Potential Wound Healing. *Carbohydrate Polymers* **2019**, *223*, 115023. https://doi.org/10.1016/j.carbpol.2019.115023.

(149) Tokudome, Y.; Komi, T.; Omata, A.; Sekita, M. A New Strategy for the Passive Skin Delivery of Nanoparticulate, High Molecular Weight Hyaluronic Acid Prepared by a Polyion Complex Method. *Scientific Reports* **2018**, *8* (1), 2336. https://doi.org/10.1038/s41598-018-20805-3.

(150) Barroso, N.; Guaresti, O.; Pérez-Álvarez, L.; Ruiz-Rubio, L.; Gabilondo, N.; Vilas-Vilela, J. L. Self-Healable Hyaluronic Acid/Chitosan Polyelectrolyte Complex Hydrogels and Multilayers. *European Polymer Journal* **2019**, *120*, 109268. https://doi.org/10.1016/j.eurpolymj.2019.109268.

(151) Duan, Y.; Li, K.; Wang, H.; Wu, T.; Zhao, Y.; Li, H.; Tang, H.; Yang, W. Preparation and Evaluation of Curcumin Grafted Hyaluronic Acid Modified Pullulan Polymers as a Functional Wound Dressing Material. *Carbohydrate Polymers* **2020**, *238*, 116195. https://doi.org/10.1016/j.carbpol.2020.116195.

(152) Kwon, M. Y.; Wang, C.; Galarraga, J. H.; Puré, E.; Han, L.; Burdick, J. A. Influence of Hyaluronic Acid Modification on CD44 Binding towards the Design of Hydrogel Biomaterials. *Biomaterials* **2019**, *222*, 119451. https://doi.org/10.1016/j.biomaterials.2019.119451.

(153) Ke, C.; Sun, L.; Qiao, D.; Wang, D.; Zeng, X. Antioxidant Acitivity of Low Molecular Weight Hyaluronic Acid. *Food and Chemical Toxicology* **2011**, *49* (10), 2670–2675. https://doi.org/10.1016/j.fct.2011.07.020.

(154) Gocmen, G.; Gonul, O.; Oktay, N. S.; Yarat, A.; Goker, K. The Antioxidant and Anti-Inflammatory Efficiency of Hyaluronic Acid after Third Molar Extraction. *Journal of Cranio-Maxillofacial Surgery* **2015**, *43* (7), 1033–1037. https://doi.org/10.1016/j.jcms.2015.04.022.

(155) El-Kased, R. F.; Amer, R. I.; Attia, D.; Elmazar, M. M. Honey-Based Hydrogel: In Vitro and Comparative In Vivo Evaluation for Burn Wound Healing. *Scientific Reports* **2017**, *7* (1), 9692. https://doi.org/10.1038/s41598-017-08771-8.

(156) Taheri, P.; Jahanmardi, R.; Koosha, M.; Abdi, S. Physical, Mechanical and Wound Healing Properties of Chitosan/Gelatin Blend Films Containing Tannic Acid and/or Bacterial

Nanocellulose. *International Journal of Biological Macromolecules* **2020**, *154*, 421–432. https://doi.org/10.1016/j.ijbiomac.2020.03.114.

(157) Vijayan, A.; A., S.; Kumar, G. S. V. PEG Grafted Chitosan Scaffold for Dual Growth Factor Delivery for Enhanced Wound Healing. *Scientific Reports* **2019**, *9* (1), 19165. https://doi.org/10.1038/s41598-019-55214-7.

(158) Leonhardt, E. E.; Kang, N.; Hamad, M. A.; Wooley, K. L.; Elsabahy, M. Absorbable Hemostatic Hydrogels Comprising Composites of Sacrificial Templates and Honeycomb-like Nanofibrous Mats of Chitosan. *Nature Communications* **2019**, *10* (1), 2307. https://doi.org/10.1038/s41467-019-10290-1.

(159) Hickman, D. A.; Pawlowski, C. L.; Sekhon, U. D. S.; Marks, J.; Gupta, A. S. Biomaterials and Advanced Technologies for Hemostatic Management of Bleeding. *Advanced Materials* **2018**, *30* (4), 1700859. https://doi.org/10.1002/adma.201700859.

(160) Donati, I.; Haug, I. J.; Scarpa, T.; Borgogna, M.; Draget, K. I.; Skjåk-Bræk, G.; Paoletti, S. Synergistic Effects in Semidilute Mixed Solutions of Alginate and Lactose-Modified Chitosan (Chitlac). *Biomacromolecules* **2007**, *8* (3), 957–962. https://doi.org/10.1021/bm060856h.

(161) Cok, M.; Sacco, P.; Porrelli, D.; Travan, A.; Borgogna, M.; Marsich, E.; Paoletti, S.; Donati, I. Mimicking Mechanical Response of Natural Tissues. Strain Hardening Induced by Transient Reticulation in Lactose-Modified Chitosan (Chitlac). *International Journal of Biological Macromolecules* **2018**, *106*, 656–660. https://doi.org/10.1016/j.ijbiomac.2017.08.059.

(162) Donati, I.; Borgogna, M.; Turello, E.; Cesàro, A.; Paoletti, S. Tuning Supramolecular Structuring at the Nanoscale Level: Nonstoichiometric Soluble Complexes in Dilute Mixed Solutions of Alginate and Lactose-Modified Chitosan (Chitlac). *Biomacromolecules* **2007**, *8* (5), 1471–1479. https://doi.org/10.1021/bm0610828.

(163) Marcon, P.; Marsich, E.; Vetere, A.; Mozetic, P.; Campa, C.; Donati, I.; Vittur, F.; Gamini, A.; Paoletti, S. The Role of Galectin-1 in the Interaction between Chondrocytes and a Lactose-Modified Chitosan. *Biomaterials* **2005**, *26* (24), 4975–4984. https://doi.org/10.1016/j.biomaterials.2005.01.044.

(164) Porrelli, D.; Gruppuso, M.; Vecchies, F.; Marsich, E.; Turco, G. Alginate Bone Scaffolds Coated with a Bioactive Lactose Modified Chitosan for Human Dental Pulp Stem Cells Proliferation and Differentiation. *Carbohydrate Polymers* **2021**, *273*, 118610. https://doi.org/10.1016/j.carbpol.2021.118610.

(165) Donato, A.; Belluzzi, E.; Mattiuzzo, E.; Venerando, R.; Cadamuro, M.; Ruggieri, P.; Vindigni, V.; Brun, P. Anti-Inflammatory and Pro-Regenerative Effects of Hyaluronan-Chitlac Mixture in Human Dermal Fibroblasts: A Skin Ageing Perspective. *Polymers* **2022**, *14* (9), 1817. https://doi.org/10.3390/polym14091817.

(166) Ali, I. H.; Ouf, A.; Elshishiny, F.; Taskin, M. B.; Song, J.; Dong, M.; Chen, M.; Siam, R.; Mamdouh, W. Antimicrobial and Wound-Healing Activities of Graphene-Reinforced Electrospun Chitosan/Gelatin Nanofibrous Nanocomposite Scaffolds. *ACS Omega* **2022**, *7* (2), 1838–1850. https://doi.org/10.1021/acsomega.1c05095.

(167) Karizmeh, M. S.; Poursamar, S. A.; Kefayat, A.; Farahbakhsh, Z.; Rafienia, M. An in Vitro and in Vivo Study of PCL/Chitosan Electrospun Mat on Polyurethane/Propolis Foam as a Bilayer Wound Dressing. *Materials Science and Engineering: C* **2022**, 112667. https://doi.org/10.1016/j.msec.2022.112667.

(168) Alavi, M.; Nokhodchi, A. Antimicrobial and Wound Healing Activities of Electrospun Nanofibers Based on Functionalized Carbohydrates and Proteins. *Cellulose* **2022**, *29* (3), 1331–1347. https://doi.org/10.1007/s10570-021-04412-6.

(169) Xu, H.; Wu, Z.; Zhao, D.; Liang, H.; Yuan, H.; Wang, C. Preparation and Characterization of Electrospun Nanofibers-Based Facial Mask Containing Hyaluronic Acid as a Moisturizing Component and Huangshui Polysaccharide as an Antioxidant Component. *International Journal of Biological Macromolecules* **2022**, *214*, 212–219. https://doi.org/10.1016/j.ijbiomac.2022.06.047.

(170) Bazmandeh, A. Z.; Mirzaei, E.; Fadaie, M.; Shirian, S.; Ghasemi, Y. Dual Spinneret Electrospun Nanofibrous/Gel Structure of Chitosan-Gelatin/Chitosan-Hyaluronic Acid as a Wound Dressing: In-Vitro and in-Vivo Studies. *International Journal of Biological Macromolecules* **2020**, *162*, 359–373. https://doi.org/10.1016/j.ijbiomac.2020.06.181.

(171) Deshawar, D.; Gupta, K.; Chokshi, P. Electrospinning of Polymer Solutions: An Analysis of Instability in a Thinning Jet with Solvent Evaporation. *Polymer* **2020**, *202*, 122656. https://doi.org/10.1016/j.polymer.2020.122656.

(172) Rošic, R.; Pelipenko, J.; Kocbek, P.; Baumgartner, S.; Bešter-Rogač, M.; Kristl, J. The Role of Rheology of Polymer Solutions in Predicting Nanofiber Formation by Electrospinning. *European Polymer Journal* **2012**, *48* (8), 1374–1384. https://doi.org/10.1016/j.eurpolymj.2012.05.001.

(173) Nasouri, K.; Shoushtari, A. M.; Mojtahedi, M. R. M. Effects of Polymer/Solvent Systems on Electrospun Polyvinylpyrrolidone Nanofiber Morphology and Diameter. *Polymer Science Series A* **2015**, *57* (6), 747–755. https://doi.org/10.1134/S0965545X15060164.

(174) Wang, S.; Yan, F.; Ren, P.; Li, Y.; Wu, Q.; Fang, X.; Chen, F.; Wang, C. Incorporation of Metal-Organic Frameworks into Electrospun Chitosan/Poly (Vinyl Alcohol) Nanofibrous Membrane with Enhanced Antibacterial Activity for Wound Dressing Application. *International Journal of Biological Macromolecules* **2020**, *158*, 9–17. https://doi.org/10.1016/j.ijbiomac.2020.04.116.

(175) Ahmed, R.; Tariq, M.; Ali, I.; Asghar, R.; Noorunnisa Khanam, P.; Augustine, R.; Hasan, A. Novel Electrospun Chitosan/Polyvinyl Alcohol/Zinc Oxide Nanofibrous Mats with Antibacterial and Antioxidant Properties for Diabetic Wound Healing. *International Journal of Biological Macromolecules* **2018**, *120*, 385–393. https://doi.org/10.1016/j.ijbiomac.2018.08.057.

(176) Najafiasl, M.; Osfouri, S.; Azin, R.; Zaeri, S. Alginate-Based Electrospun Core/Shell Nanofibers Containing Dexpanthenol: A Good Candidate for Wound Dressing. *Journal of Drug Delivery Science and Technology* **2020**, *57*, 101708. https://doi.org/10.1016/j.jddst.2020.101708.

(177) Mosayebi, V.; Fathi, M.; Shahedi, M.; Soltanizadeh, N.; Emam-Djomeh, Z. Fast-Dissolving Antioxidant Nanofibers Based on Spirulina Protein Concentrate and Gelatin Developed Using Needleless Electrospinning. *Food Bioscience* **2022**, *47*, 101759. https://doi.org/10.1016/j.fbio.2022.101759.

(178) Angel, N.; Li, S.; Yan, F.; Kong, L. Recent Advances in Electrospinning of Nanofibers from Bio-Based Carbohydrate Polymers and Their Applications. *Trends in Food Science & Technology* **2022**, *120*, 308–324. https://doi.org/10.1016/j.tifs.2022.01.003.

(179) Kriegel, C.; Kit, K. M.; McClements, D. J.; Weiss, J. Electrospinning of Chitosan–Poly(Ethylene Oxide) Blend Nanofibers in the Presence of Micellar Surfactant Solutions. *Polymer* **2009**, *50* (1), 189–200. https://doi.org/10.1016/j.polymer.2008.09.041.

(180) Liu, S.; Su, Y.; Chen, Y. Fabrication, Surface Properties and Protein Encapsulation/Release Studies of Electrospun Gelatin Nanofibers. *Journal of Biomaterials Science, Polymer Edition* **2011**, *22* (7), 945–955. https://doi.org/10.1163/092050610X496585.

(181) Rashtchian, M.; Hivechi, A.; Bahrami, S. H.; Milan, P. B.; Simorgh, S. Fabricating Alginate/Poly(Caprolactone) Nanofibers with Enhanced Bio-Mechanical Properties via Cellulose Nanocrystal Incorporation. *Carbohydrate Polymers* **2020**, *233*, 115873. https://doi.org/10.1016/j.carbpol.2020.115873.

(182) İnal, M.; Mülazımoğlu, G. Production and Characterization of Bactericidal Wound Dressing Material Based on Gelatin Nanofiber. *International Journal of Biological Macromolecules* **2019**, *137*, 392–404. https://doi.org/10.1016/j.ijbiomac.2019.06.119.

(183) Zhang, H.; Cui, S.; Lv, H.; Pei, X.; Gao, M.; Chen, S.; Hu, J.; Zhou, Y.; Liu, Y. A Crosslinking Strategy to Make Neutral Polysaccharide Nanofibers Robust and Biocompatible: With Konjac Glucomannan as an Example. *Carbohydrate Polymers* **2019**, *215*, 130–136. https://doi.org/10.1016/j.carbpol.2019.03.075.

(184) Li, M.; Mondrinos, M. J.; Chen, X.; Lelkes, P. I. Electrospun Blends of Natural and Synthetic Polymers as Scaffolds for Tissue Engineering. *Conference proceedings: Annual International Conference of the IEEE Engineering in Medicine and Biology Society* **2005**, *2005*, 5858–5861. https://doi.org/10.1109/IEMBS.2005.1615822.

(185) Meng, L.; Arnoult, O.; Smith, M.; Wnek, G. E. Electrospinning of in Situ Crosslinked Collagen Nanofibers. *Journal of Materials Chemistry* **2012**, *22* (37), 19412. https://doi.org/10.1039/c2jm31618h.

(186) Koosha, M.; Raoufi, M.; Moravvej, H. One-Pot Reactive Electrospinning of Chitosan/PVA Hydrogel Nanofibers Reinforced by Halloysite Nanotubes with Enhanced Fibroblast Cell Attachment for Skin Tissue Regeneration. *Colloids and Surfaces B: Biointerfaces* **2019**, *179*, 270–279. https://doi.org/10.1016/j.colsurfb.2019.03.054.

(187) Hu, Q.; Wu, C.; Zhang, H. Preparation and Optimization of a Gelatin-Based Biomimetic Three-Layered Vascular Scaffold. *Journal of Biomaterials Applications* **2019**, *34* (3), 431–441. https://doi.org/10.1177/0885328219851224.

(188) Li, Z.; Pan, T.; Wu, Y.; Kang, W.; Liu, Y. Preparation and Characterization of Long-Term Stable Pullulan Nanofibers via in Situ Cross-Linking Electrospinning. *Adsorption Science & Technology* **2019**, *37* (5–6), 401–411. https://doi.org/10.1177/0263617418813018.

(189) Nicknejad, E. T.; Ghoreishi, S. M.; Habibi, N. Electrospinning of Cross-Linked Magnetic Chitosan Nanofibers for Protein Release. *AAPS PharmSciTech* **2015**, *16* (6), 1480–1486. https://doi.org/10.1208/s12249-015-0336-7.

(190) Kim, K.-O.; Akada, Y.; Kai, W.; Kim, B.-S.; Kim, I.-S. Cells Attachment Property of PVA Hydrogel Nanofibers Incorporating Hyaluronic Acid for Tissue Engineering. *Journal of Biomaterials and Nanobiotechnology* **2011**, *2* (4), 353–360. https://doi.org/10.4236/jbnb.2011.24044.

(191) Wang, W.; Jin, X.; Zhu, Y.; Zhu, C.; Yang, J.; Wang, H.; Lin, T. Effect of Vapor-Phase Glutaraldehyde Crosslinking on Electrospun Starch Fibers. *Carbohydrate Polymers* **2016**, *140*, 356–361. https://doi.org/10.1016/j.carbpol.2015.12.061.

(192) Lau, Y.-T.; Kwok, L.-F.; Tam, K.-W.; Chan, Y.-S.; Shum, D. K.-Y.; Shea, G. K.-H. Genipin-Treated Chitosan Nanofibers as a Novel Scaffold for Nerve Guidance Channel Design. *Colloids and Surfaces B: Biointerfaces* **2018**, *162*, 126–134. https://doi.org/10.1016/j.colsurfb.2017.11.061.

(193) Frohbergh, M. E.; Katsman, A.; Botta, G. P.; Lazarovici, P.; Schauer, C. L.; Wegst, U. G. K.; Lelkes, P. I. Electrospun Hydroxyapatite-Containing Chitosan Nanofibers Crosslinked with Genipin for Bone Tissue Engineering. *Biomaterials* **2012**, *33* (36), 9167–9178. https://doi.org/10.1016/j.biomaterials.2012.09.009.

(194) Li, Q.; Wang, X.; Lou, X.; Yuan, H.; Tu, H.; Li, B.; Zhang, Y. Genipin-Crosslinked Electrospun Chitosan Nanofibers: Determination of Crosslinking Conditions and Evaluation of Cytocompatibility. *Carbohydrate Polymers* **2015**, *130*, 166–174. https://doi.org/10.1016/j.carbpol.2015.05.039.

(195) Liu, R.; Ming, J.; Zhang, H.; Zuo, B. EDC/NHS Crosslinked Electrospun Regenerated Tussah Silk Fibroin Nanofiber Mats. *Fibers and Polymers* **2012**, *13* (5), 613–617. https://doi.org/10.1007/s12221-012-0613-y.

(196) Yang, X.; Wang, X.; Yu, F.; Ma, L.; Pan, X.; Luo, G.; Lin, S.; Mo, X.; He, C.; Wang, H. Hyaluronic Acid/EDC/NHS-Crosslinked Green Electrospun Silk Fibroin Nanofibrous Scaffolds for Tissue Engineering. *RSC Advances* **2016**, *6* (102), 99720–99728. https://doi.org/10.1039/C6RA13713J.

(197) Jia, W.; Li, M.; Kang, L.; Gu, G.; Guo, Z.; Chen, Z. Fabrication and Comprehensive Characterization of Biomimetic Extracellular Matrix Electrospun Scaffold for Vascular Tissue Engineering Applications. *Journal of Materials Science* **2019**, *54* (15), 10871–10883. https://doi.org/10.1007/s10853-019-03667-6.

(198) Zhou, M.; Khen, K.; Wang, T.; Hu, Q.; Xue, J.; Luo, Y. Chemical Crosslinking Improves the Gastrointestinal Stability and Enhances Nutrient Delivery Potentials of Egg Yolk LDL/Polysaccharide Nanogels. *Food Chemistry* **2018**, *239*, 840–847. https://doi.org/10.1016/j.foodchem.2017.07.019.

(199) Woodman, E. K.; Chaffey, J. G. K.; Hopes, P. A.; Hose, D. R. J.; Gilday, J. P. N,N′-Carbonyldiimidazole-Mediated Amide Coupling: Significant Rate Enhancement Achieved by Acid Catalysis with Imidazole·HCl. *Organic Process Research & Development* **2009**, *13* (1), 106–113. https://doi.org/10.1021/op800226b.

(200) Baştürk, E.; Demir, S.; Danış, Ö.; Kahraman, M. V. Covalent Immobilization of α-Amylase onto Thermally Crosslinked Electrospun PVA/PAA Nanofibrous Hybrid Membranes. *Journal of Applied Polymer Science* **2013**, *127* (1), 349–355. https://doi.org/10.1002/app.37901.

(201) Han, Y.; Lv, S. Synthesis of Chemically Crosslinked Pullulan/Gelatin-Based Extracellular Matrix-Mimetic Gels. *International Journal of Biological Macromolecules* **2019**, *122*, 1262–1270. https://doi.org/10.1016/j.ijbiomac.2018.09.080.

(202) Kianfar, P.; Vitale, A.; Dalle Vacche, S.; Bongiovanni, R. Photo-Crosslinking of Chitosan/Poly(Ethylene Oxide) Electrospun Nanofibers. *Carbohydrate Polymers* **2019**, *217*, 144–151. https://doi.org/10.1016/j.carbpol.2019.04.062.

(203) Zhao, W.; Li, Y.; Zhang, X.; Zhang, R.; Hu, Y.; Boyer, C.; Xu, F.-J. Photo-Responsive Supramolecular Hyaluronic Acid Hydrogels for Accelerated Wound Healing. *Journal of Controlled Release* **2020**, *323*, 24–35. https://doi.org/10.1016/j.jconrel.2020.04.014.

(204) Joshi, P.; Ahmed, M. S. U.; Vig, K.; Vega Erramuspe, I. B.; Auad, M. L. Synthesis and Characterization of Chemically Crosslinked Gelatin and Chitosan to Produce Hydrogels for Biomedical Applications. *Polymers for Advanced Technologies* **2021**, *32* (5), 2229–2239. https://doi.org/10.1002/pat.5257.

(205) Nazir, F.; Ashraf, I.; Iqbal, M.; Ahmad, T.; Anjum, S. 6-Deoxy-Aminocellulose Derivatives Embedded Soft Gelatin Methacryloyl (GelMA) Hydrogels for Improved Wound Healing Applications: In Vitro and in Vivo Studies. *International Journal of Biological Macromolecules* **2021**, *185*, 419–433. https://doi.org/10.1016/j.ijbiomac.2021.06.112.

(206) Samani, S.; Bonakdar, S.; Farzin, A.; Hadjati, J.; Azami, M. A Facile Way to Synthesize a Photocrosslinkable Methacrylated Chitosan Hydrogel for Biomedical Applications. *International Journal of Polymeric Materials and Polymeric Biomaterials* **2021**, *70* (10), 730–741. https://doi.org/10.1080/00914037.2020.1760274.

(207) Seo, J. W.; Shin, S. R.; Lee, M.-Y.; Cha, J. M.; Min, K. H.; Lee, S. C.; Shin, S. Y.; Bae, H. Injectable Hydrogel Derived from Chitosan with Tunable Mechanical Properties via Hybrid-Crosslinking System. *Carbohydrate Polymers* **2021**, *251*, 117036. https://doi.org/10.1016/j.carbpol.2020.117036.

(208) Skardal, A.; Zhang, J.; McCoard, L.; Xu, X.; Oottamasathien, S.; Prestwich, G. D. Photocrosslinkable Hyaluronan-Gelatin Hydrogels for Two-Step Bioprinting. *Tissue Engineering. Part A* **2010**, *16* (8), 2675–2685. https://doi.org/10.1089/ten.TEA.2009.0798.

(209) Zhang, Q.; Wei, X.; Ji, Y.; Yin, L.; Dong, Z.; Chen, F.; Zhong, M.; Shen, J.; Liu, Z. Adjustable and Ultrafast Light-Cured Hyaluronic Acid Hydrogel: Promoting Biocompatibility and Cell Growth. *Journal of Materials Chemistry B* **2020**, *8* (25), 5441–5450. https://doi.org/10.1039/C9TB02796C.

(210) Zhu, L.; Bratlie, K. M. pH Sensitive Methacrylated Chitosan Hydrogels with Tunable Physical and Chemical Properties. *Biochemical Engineering Journal* **2018**, *132*, 38–46. https://doi.org/10.1016/j.bej.2017.12.012.

(211) Sarhan, W. A.; Azzazy, H. M. E. High Concentration Honey Chitosan Electrospun Nanofibers: Biocompatibility and Antibacterial Effects. *Carbohydrate Polymers* **2015**, *122*, 135–143. https://doi.org/10.1016/j.carbpol.2014.12.051.

(212) Maeda, N.; Miao, J.; Simmons, T. J.; Dordick, J. S.; Linhardt, R. J. Composite Polysaccharide Fibers Prepared by Electrospinning and Coating. *Carbohydrate Polymers* **2014**, *102*, 950–955. https://doi.org/10.1016/j.carbpol.2013.10.038.

(213) Mahdavi, M.; Mahmoudi, N.; Rezaie Anaran, F.; Simchi, A. Electrospinning of Nanodiamond-Modified Polysaccharide Nanofibers with Physico-Mechanical Properties Close to Natural Skins. *Marine Drugs* **2016**, *14* (7), 128. https://doi.org/10.3390/md14070128.

(214) Dierings de Souza, E. J.; Kringel, D. H.; Guerra Dias, A. R.; da Rosa Zavareze, E. Polysaccharides as Wall Material for the Encapsulation of Essential Oils by Electrospun Technique. *Carbohydrate Polymers* **2021**, *265*, 118068. https://doi.org/10.1016/j.carbpol.2021.118068.

(215) Bazmandeh, A. Z.; Mirzaei, E.; Ghasemi, Y.; Kouhbanani, M. A. J. Hyaluronic Acid Coated Electrospun Chitosan-Based Nanofibers Prepared by Simultaneous Stabilizing and Coating. *International Journal of Biological Macromolecules* **2019**, *138*, 403–411. https://doi.org/10.1016/j.ijbiomac.2019.07.107.

(216) Croisier, F.; Atanasova, G.; Poumay, Y.; Jérôme, C. Polysaccharide-Coated PCL Nanofibers for Wound Dressing Applications. *Advanced Healthcare Materials* **2014**, *3* (12), 2032–2039. https://doi.org/10.1002/adhm.201400380.

(217) Deng, H.; Zhou, X.; Wang, X.; Zhang, C.; Ding, B.; Zhang, Q.; Du, Y. Layer-by-Layer Structured Polysaccharides Film-Coated Cellulose Nanofibrous Mats for Cell Culture. *Carbohydrate Polymers* **2010**, *80* (2), 474–479. https://doi.org/10.1016/j.carbpol.2009.12.004.

(218) Porrelli, D.; Mardirossian, M.; Musciacchio, L.; Pacor, M.; Berton, F.; Crosera, M.; Turco, G. Antibacterial Electrospun Polycaprolactone Membranes Coated with Polysaccharides and Silver Nanoparticles for Guided Bone and Tissue Regeneration. *ACS Applied Materials & Interfaces* **2021**, *13* (15), 17255–17267. https://doi.org/10.1021/acsami.1c01016.

(219) Chanda, A.; Adhikari, J.; Ghosh, A.; Chowdhury, S. R.; Thomas, S.; Datta, P.; Saha, P. Electrospun Chitosan/Polycaprolactone-Hyaluronic Acid Bilayered Scaffold for Potential Wound Healing Applications. *International Journal of Biological Macromolecules* **2018**, *116*, 774–785. https://doi.org/10.1016/j.ijbiomac.2018.05.099.

(220) Figueira, D. R.; Miguel, S. P.; de Sá, K. D.; Correia, I. J. Production and Characterization of Polycaprolactone- Hyaluronic Acid/Chitosan- Zein Electrospun Bilayer Nanofibrous Membrane for Tissue Regeneration. *International Journal of Biological Macromolecules* **2016**, *93*, 1100–1110. https://doi.org/10.1016/j.ijbiomac.2016.09.080.

(221) Golchin, A.; Nourani, M. R. Effects of Bilayer Nanofibrillar Scaffolds Containing Epidermal Growth Factor on Full-Thickness Wound Healing. *Polymers for Advanced Technologies* **2020**, *31* (11), 2443–2452. https://doi.org/10.1002/pat.4960.

(222) Afsharian, Y. P.; Rahimnejad, M. Bioactive Electrospun Scaffolds for Wound Healing Applications: A Comprehensive Review. *Polymer Testing* **2021**, *93*, 106952. https://doi.org/10.1016/j.polymertesting.2020.106952.

(223) Arampatzis, A. S.; Kontogiannopoulos, K. N.; Theodoridis, K.; Aggelidou, E.; Rat, A.; Willems, A.; Tsivintzelis, I.; Papageorgiou, V. P.; Kritis, A.; Assimopoulou, A. N. Electrospun Wound Dressings Containing Bioactive Natural Products: Physico-Chemical Characterization and Biological Assessment. *Biomaterials Research* **2021**, *25* (1), 23. https://doi.org/10.1186/s40824-021-00223-9.

(224) Khan, A. ur R.; Huang, K.; Khalaji, M. S.; Yu, F.; Xie, X.; Zhu, T.; Morsi, Y.; Jinzhong, Z.; Mo, X. Multifunctional Bioactive Core-Shell Electrospun Membrane Capable to Terminate Inflammatory Cycle and Promote Angiogenesis in Diabetic Wound. *Bioactive Materials* **2021**, *6* (9), 2783–2800. https://doi.org/10.1016/j.bioactmat.2021.01.040.

(225) García-Salinas, S.; Gámez, E.; Asín, J.; de Miguel, R.; Andreu, V.; Sancho-Albero, M.; Mendoza, G.; Irusta, S.; Arruebo, M. Efficiency of Antimicrobial Electrospun Thymol-Loaded Polycaprolactone Mats In Vivo. *ACS Applied Bio Materials* **2020**, *3* (5), 3430–3439. https://doi.org/10.1021/acsabm.0c00419.

(226) Jiang, S.; Ma, B. C.; Reinholz, J.; Li, Q.; Wang, J.; Zhang, K. A. I.; Landfester, K.; Crespy, D. Efficient Nanofibrous Membranes for Antibacterial Wound Dressing and UV Protection. *ACS Applied Materials & Interfaces* **2016**, *8* (44), 29915–29922. https://doi.org/10.1021/acsami.6b09165.

(227) Xie, Z.; Paras, C. B.; Weng, H.; Punnakitikashem, P.; Su, L.-C.; Vu, K.; Tang, L.; Yang, J.; Nguyen, K. T. Dual Growth Factor Releasing Multi-Functional Nanofibers for Wound Healing. *Acta Biomaterialia* **2013**, *9* (12), 9351–9359. https://doi.org/10.1016/j.actbio.2013.07.030.

(228) Bertoncelj, V.; Pelipenko, J.; Kristl, J.; Jeras, M.; Cukjati, M.; Kocbek, P. Development and Bioevaluation of Nanofibers with Blood-Derived Growth Factors for Dermal Wound Healing. *European Journal of Pharmaceutics and Biopharmaceutics* **2014**, *88* (1), 64–74. https://doi.org/10.1016/j.ejpb.2014.06.001.

(229) Fan, L.; Wang, H.; Zhang, K.; Cai, Z.; He, C.; Sheng, X.; Mo, X. Vitamin C-Reinforcing Silk Fibroin Nanofibrous Matrices for Skin Care Application. *RSC Advances* **2012**, *2* (10), 4110. https://doi.org/10.1039/c2ra20302b.

(230) Jiang, J.; Zhang, Y.; Indra, A. K.; Ganguli-Indra, G.; Le, M. N.; Wang, H.; Hollins, R. R.; Reilly, D. A.; Carlson, M. A.; Gallo, R. L.; Gombart, A. F.; Xie, J. 1α,25-Dihydroxyvitamin D3-Eluting Nanofibrous Dressings Induce Endogenous Antimicrobial Peptide Expression. *Nanomedicine* **2018**, *13* (12), 1417–1432. https://doi.org/10.2217/nnm-2018-0011.

(231) Zahid, S.; Khalid, H.; Ikram, F.; Iqbal, H.; Samie, M.; Shahzadi, L.; Shah, A. T.; Yar, M.; Chaudhry, A. A.; Awan, S. J.; Khan, A. F.; Rehman, I. ur. Bi-Layered α-Tocopherol Acetate

Loaded Membranes for Potential Wound Healing and Skin Regeneration. *Materials Science and Engineering: C* **2019**, *101*, 438–447. https://doi.org/10.1016/j.msec.2019.03.080.

(232) Abid, S.; Hussain, T.; Nazir, A.; Zahir, A.; Khenoussi, N. Acetaminophen Loaded Nanofibers as a Potential Contact Layer for Pain Management in Burn Wounds. *Materials Research Express* **2018**, *5* (8), 085017. https://doi.org/10.1088/2053-1591/aad2eb.

(233) Basar, A. O.; Castro, S.; Torres-Giner, S.; Lagaron, J. M.; Turkoglu Sasmazel, H. Novel Poly(ε-Caprolactone)/Gelatin Wound Dressings Prepared by Emulsion Electrospinning with Controlled Release Capacity of Ketoprofen Anti-Inflammatory Drug. *Materials Science and Engineering: C* **2017**, *81*, 459–468. https://doi.org/10.1016/j.msec.2017.08.025.

(234) Kharaghani, D.; Gitigard, P.; Ohtani, H.; Kim, K. O.; Ullah, S.; Saito, Y.; Khan, M. Q.; Kim, I. S. Design and Characterization of Dual Drug Delivery Based on In-Situ Assembled PVA/PAN Core-Shell Nanofibers for Wound Dressing Application. *Scientific Reports* **2019**, *9* (1), 12640. https://doi.org/10.1038/s41598-019-49132-x.

(235) Homaeigohar, S.; Boccaccini, A. R. Antibacterial Biohybrid Nanofibers for Wound Dressings. *Acta Biomaterialia* **2020**, *107*, 25–49. https://doi.org/10.1016/j.actbio.2020.02.022.

(236) Alipour, R.; Khorshidi, A.; Shojaei, A. F.; Mashayekhi, F.; Moghaddam, M. J. M. Skin Wound Healing Acceleration by Ag Nanoparticles Embedded in PVA/PVP/Pectin/Mafenide Acetate Composite Nanofibers. *Polymer Testing* **2019**, *79*, 106022. https://doi.org/10.1016/j.polymertesting.2019.106022.

(237) Zupančič, Š.; Potrč, T.; Baumgartner, S.; Kocbek, P.; Kristl, J. Formulation and Evaluation of Chitosan/Polyethylene Oxide Nanofibers Loaded with Metronidazole for Local Infections. *European Journal of Pharmaceutical Sciences* **2016**, *95*, 152–160. https://doi.org/10.1016/j.ejps.2016.10.030.

(238) Li, Z.; Liu, X.; Li, Y.; Lan, X.; Leung, P. H.; Li, J.; Li, G.; Xie, M.; Han, Y.; Lin, X. Composite Membranes of Recombinant Silkworm Antimicrobial Peptide and Poly (L-Lactic Acid) (PLLA) for Biomedical Application. *Scientific Reports* **2016**, *6* (1), 31149. https://doi.org/10.1038/srep31149.

(239) Sacco, P.; Sechi, A.; Trevisan, A.; Picotti, F.; Gianni, R.; Stucchi, L.; Fabbian, M.; Bosco, M.; Paoletti, S.; Marsich, E. A Silver Complex of Hyaluronan–Lipoate (SHLS12): Synthesis, Characterization and Biological Properties. *Carbohydrate Polymers* **2016**, *136*, 418–426. https://doi.org/10.1016/j.carbpol.2015.09.057.

(240) Campbell, E. A.; Korzheva, N.; Mustaev, A.; Murakami, K.; Nair, S.; Goldfarb, A.; Darst, S. A. Structural Mechanism for Rifampicin Inhibition of Bacterial RNA Polymerase. *Cell* **2001**, *104* (6), 901–912. https://doi.org/10.1016/S0092-8674(01)00286-0.

(241) Lee, Y.; Kim, S. S.; Choi, S.-M.; Bae, C.-J.; Oh, T.-H.; Kim, S. E.; Kim, U. J.; Kang, S.-J.; Jung, S.-I.; Park, K.-H. Rifamycin Resistance, RpoB Gene Mutation and Clinical Outcomes of Staphylococcus Species Isolates from Prosthetic Joint Infections in Republic of Korea. *Journal of Global Antimicrobial Resistance* **2022**, *28*, 43–48. https://doi.org/10.1016/j.jgar.2021.12.005.

(242) Kranthi Kiran, A. S.; Kizhakeyil, A.; Ramalingam, R.; Verma, N. K.; Lakshminarayanan, R.; Kumar, T. S. S.; Doble, M.; Ramakrishna, S. Drug Loaded Electrospun Polymer/Ceramic Composite Nanofibrous Coatings on Titanium for Implant Related Infections. *Ceramics International* **2019**, *45* (15), 18710–18720. https://doi.org/10.1016/j.ceramint.2019.06.097.

(243) Widmer, A. F.; Gaechter, A.; Ochsner, P. E.; Zimmerli, W. Antimicrobial Treatment of Orthopedic Implant-Related Infections with Rifampin Combinations. *Clinical Infectious Diseases* **1992**, *14* (6), 1251–1253. https://doi.org/10.1093/clinids/14.6.1251.

(244) Coiffier, G.; Albert, J.-D.; Arvieux, C.; Guggenbuhl, P. Optimizing Combination Rifampin Therapy for Staphylococcal Osteoarticular Infections. *Joint Bone Spine* **2013**, *80* (1), 11–17. https://doi.org/10.1016/j.jbspin.2012.09.008.

(245) Song, X.; Gao, Z.; Ling, F.; Chen, X. Controlled Release of Drug via Tuning Electrospun Polymer Carrier. *Journal of Polymer Science Part B: Polymer Physics* **2012**, *50* (3), 221–227. https://doi.org/10.1002/polb.23005.

(246) Shaikh, R. P.; Kumar, P.; Choonara, Y. E.; Toit, L. C. du; Pillay, V. Crosslinked Electrospun PVA Nanofibrous Membranes: Elucidation of Their Physicochemical, Physicomechanical and Molecular Disposition. *Biofabrication* **2012**, *4* (2), 025002. https://doi.org/10.1088/1758-5082/4/2/025002.

(247) Gilchrist, S. E.; Lange, D.; Letchford, K.; Bach, H.; Fazli, L.; Burt, H. M. Fusidic Acid and Rifampicin Co-Loaded PLGA Nanofibers for the Prevention of Orthopedic Implant Associated Infections. *Journal of Controlled Release* **2013**, *170* (1), 64–73. https://doi.org/10.1016/j.jconrel.2013.04.012.

(248) Ruckh, T. T.; Oldinski, R. A.; Carroll, D. A.; Mikhova, K.; Bryers, J. D.; Popat, K. C. Antimicrobial Effects of Nanofiber Poly(Caprolactone) Tissue Scaffolds Releasing Rifampicin. *Journal of Materials Science: Materials in Medicine* **2012**, *23* (6), 1411–1420. https://doi.org/10.1007/s10856-012-4609-3.

(249) Fahimirad, S.; Ajalloueian, F. Naturally-Derived Electrospun Wound Dressings for Target Delivery of Bio-Active Agents. *International Journal of Pharmaceutics* **2019**, *566*, 307–328. https://doi.org/10.1016/j.ijpharm.2019.05.053.

(250) Patiño Vidal, C.; Velásquez, E.; Galotto, M. J.; López de Dicastillo, C. Development of an Antibacterial Coaxial Bionanocomposite Based on Electrospun Core/Shell Fibers Loaded with Ethyl Lauroyl Arginate and Cellulose Nanocrystals for Active Food Packaging. *Food Packaging and Shelf Life* **2022**, *31*, 100802. https://doi.org/10.1016/j.fpsl.2021.100802.

(251) Viscusi, G.; Lamberti, E.; Vittoria, V.; Gorrasi, G. Coaxial Electrospun Membranes of Poly(ε-Caprolactone)/Poly(Lactic Acid) with Reverse Core-Shell Structures Loaded with Curcumin as Tunable Drug Delivery Systems. *Polymers for Advanced Technologies* **2021**, *32* (10), 4005–4013. https://doi.org/10.1002/pat.5404.

(252) Joy, N.; Venugopal, D.; Samavedi, S. Robust Strategies to Reduce Burst and Achieve Tunable Control over Extended Drug Release from Uniaxially Electrospun Composites. *European Polymer Journal* **2022**, *168*, 111102. https://doi.org/10.1016/j.eurpolymj.2022.111102.

(253) Schindelin, J.; Arganda-Carreras, I.; Frise, E.; Kaynig, V.; Longair, M.; Pietzsch, T.; Preibisch, S.; Rueden, C.; Saalfeld, S.; Schmid, B.; Tinevez, J.-Y.; White, D. J.; Hartenstein, V.; Eliceiri, K.; Tomancak, P.; Cardona, A. Fiji: An Open-Source Platform for Biological-Image Analysis. *Nature Methods* **2012**, *9* (7), 676–682. https://doi.org/10.1038/nmeth.2019.

(254) Turco, G.; Marsich, E.; Bellomo, F.; Semeraro, S.; Donati, I.; Brun, F.; Grandolfo, M.; Accardo, A.; Paoletti, S. Alginate/Hydroxyapatite Biocomposite For Bone Ingrowth: A Trabecular Structure With High And Isotropic Connectivity. *Biomacromolecules* **2009**, *10* (6), 1575–1583. https://doi.org/10.1021/bm900154b.

(255) Tarusha, L.; Paoletti, S.; Travan, A.; Marsich, E. Alginate Membranes Loaded with Hyaluronic Acid and Silver Nanoparticles to Foster Tissue Healing and to Control Bacterial Contamination of Non-Healing Wounds. *Journal of Materials Science: Materials in Medicine* **2018**, *29* (2), 22. https://doi.org/10.1007/s10856-018-6027-7.

(256) Sacco, P.; Decleva, E.; Tentor, F.; Menegazzi, R.; Borgogna, M.; Paoletti, S.; Kristiansen, K. A.; Vårum, K. M.; Marsich, E. Butyrate-Loaded Chitosan/Hyaluronan Nanoparticles: A Suitable Tool for Sustained Inhibition of ROS Release by Activated Neutrophils. *Macromolecular Bioscience* **2017**, *17* (11), 1700214. https://doi.org/10.1002/mabi.201700214.

(257) Owens, D. K.; Wendt, R. C. Estimation of the Surface Free Energy of Polymers. *Journal of Applied Polymer Science* **1969**, *13* (8), 1741–1747. https://doi.org/10.1002/app.1969.070130815.

(258) Ren, Z.; Chen, G.; Wei, Z.; Sang, L.; Qi, M. Hemocompatibility Evaluation of Polyurethane Film with Surface-Grafted Poly(Ethylene Glycol) and Carboxymethyl-Chitosan. *Journal of Applied Polymer Science* **2013**, *127* (1), 308–315. https://doi.org/10.1002/app.37885.

(259) Can-Herrera, L. A.; Ávila-Ortega, A.; de la Rosa-García, S.; Oliva, A. I.; Cauich-Rodríguez, J. V.; Cervantes-Uc, J. M. Surface Modification of Electrospun Polycaprolactone Microfibers by Air Plasma Treatment: Effect of Plasma Power and Treatment Time. *European Polymer Journal* **2016**, *84*, 502–513. https://doi.org/10.1016/j.eurpolymj.2016.09.060.

(260) Henderson, A.; Paterson, D. L.; Chatfield, M. D.; Tambyah, P. A.; Lye, D. C.; De, P. P.; Lin, R. T. P.; Chew, K. L.; Yin, M.; Lee, T. H.; Yilmaz, M.; Cakmak, R.; Alenazi, T. H.; Arabi, Y. M.; Falcone, M.; Bassetti, M.; Righi, E.; Rogers, B. A.; Kanj, S. S.; Bhally, H.; Iredell, J.; Mendelson, M.; Boyles, T. H.; Looke, D. F. M.; Runnegar, N. J.; Miyakis, S.; Walls, G.; Khamis, M. A. I.; Zikri, A.; Crowe, A.; Ingram, P. R.; Daneman, N.; Griffin, P.; Athan, E.; Roberts, L.; Beatson, S. A.; Peleg, A. Y.; Cottrell, K.; Bauer, M. J.; Tan, E.; Chaw, K.; Nimmo, G. R.; Harris-Brown, T.; Harris, P. N. A.; MERINO Trial Investigators and the Australasian Society for Infectious Disease Clinical Research Network (ASID-CRN); Newton, P.; Wren, H.; Graham, M.; Korman, T.; Aljohani, S. M.; Alalwan, B.; Sultana, K.; Sartor, A.; Welch, D.; Kahlmeter, G. Association Between Minimum Inhibitory Concentration, Beta-Lactamase Genes and Mortality for Patients Treated With Piperacillin/Tazobactam or Meropenem From the MERINO Study. *Clinical Infectious Diseases* **2021**, *73* (11), e3842–e3850. https://doi.org/10.1093/cid/ciaa1479.

(261) Kowalska-Krochmal, B.; Dudek-Wicher, R. The Minimum Inhibitory Concentration of Antibiotics: Methods, Interpretation, Clinical Relevance. *Pathogens* **2021**, *10* (2), 165. https://doi.org/10.3390/pathogens10020165.

(262) Li, C.; Mu, C.; Lin, W. Novel Hemocompatible Nanocomposite Hydrogels Crosslinked with Methacrylated Gelatin. *RSC Advances* **2016**, *6* (49), 43663–43671. https://doi.org/10.1039/C6RA04609F.

(263) Yue, K.; Li, X.; Schrobback, K.; Sheikhi, A.; Annabi, N.; Leijten, J.; Zhang, W.; Zhang, Y. S.; Hutmacher, D. W.; Klein, T. J.; Khademhosseini, A. Structural Analysis of Photocrosslinkable Methacryloyl-Modified Protein Derivatives. *Biomaterials* **2017**, *139*, 163–171. https://doi.org/10.1016/j.biomaterials.2017.04.050.

(264) Vaidyanathan, R.; Kalthod, V. G.; Ngo, D. P.; Manley, J. M.; Lapekas, S. P. Amidations Using N,N ‘-Carbonyldiimidazole: Remarkable Rate Enhancement by Carbon Dioxide. *The Journal of Organic Chemistry* **2004**, *69* (7), 2565–2568. https://doi.org/10.1021/jo049949k.

(265) Chen, S.; Wang, H.; Jian, Z.; Fei, G.; Qian, W.; Luo, G.; Wang, Z.; Xia, H. Novel Poly(Vinyl Alcohol)/Chitosan/Modified Graphene Oxide Biocomposite for Wound Dressing Application. *Macromolecular Bioscience* **2020**, *20* (3), 1900385. https://doi.org/10.1002/mabi.201900385.

(266) Oliveira, R. N.; Rouzé, R.; Quilty, B.; Alves, G. G.; Soares, G. D. A.; Thiré, R. M. S. M.; McGuinness, G. B. Mechanical Properties and in Vitro Characterization of Polyvinyl Alcohol-Nano-Silver Hydrogel Wound Dressings. *Interface Focus* **2014**, *4* (1), 20130049. https://doi.org/10.1098/rsfs.2013.0049.

(267) Sharma, S.; Dua, A.; Malik, A. Biocompatible Stimuli Responsive Superabsorbent Polymer for Controlled Release of GHK-Cu Peptide for Wound Dressing Application. *Journal of Polymer Research* **2017**, *24* (7), 104. https://doi.org/10.1007/s10965-017-1254-z.

(268) Joy, H.; Bielby, A.; Searle, R. A Collaborative Project to Enhance Efficiency through Dressing Change Practice. *Journal of Wound Care* **2015**, *24* (7), 312–317. https://doi.org/10.12968/jowc.2015.24.7.312.

(269) Timsit, J.-F.; Schwebel, C.; Bouadma, L.; Geffroy, A.; Garrouste-Orgeas, M.; Pease, S.; Herault, M.-C.; Haouache, H.; Calvino-Gunther, S.; Gestin, B.; Armand-Lefevre, L.; Leflon, V.; Chaplain, C.; Benali, A.; Francais, A.; Adrie, C.; Zahar, J.-R.; Thuong, M.; Arrault, X.; Croize, J.; Lucet, J.-C.; Dressing Study Group. Chlorhexidine-Impregnated Sponges and Less Frequent Dressing Changes for Prevention of Catheter-Related Infections in Critically Ill Adults: A Randomized Controlled Trial. *The Journal of the American Medical Association* **2009**, *301* (12), 1231–1241. https://doi.org/10.1001/jama.2009.376.

(270) Tiscar-González, V.; Menor-Rodríguez, M. J.; Rabadán-Sainz, C.; Fraile-Bravo, M.; The Life Group; Styche, T.; Valenzuela-Ocaña, F. J.; Muñoz-García, L. Clinical and Economic Impact of Wound Care Using a Polyurethane Foam Multilayer Dressing. *Advances in Skin & Wound Care* **2021**, *34* (1), 23–30. https://doi.org/10.1097/01.ASW.0000722744.20511.71.

(271) Trinca, R. B.; Westin, C. B.; da Silva, J. A. F.; Moraes, Â. M. Electrospun Multilayer Chitosan Scaffolds as Potential Wound Dressings for Skin Lesions. *European Polymer Journal* **2017**, *88*, 161–170. https://doi.org/10.1016/j.eurpolymj.2017.01.021.

(272) Oh, G.-W.; Nam, S. Y.; Heo, S.-J.; Kang, D.-H.; Jung, W.-K. Characterization of Ionic Cross-Linked Composite Foams with Different Blend Ratios of Alginate/Pectin on the Synergistic

Effects for Wound Dressing Application. *International Journal of Biological Macromolecules* **2020**, *156*, 1565–1573. https://doi.org/10.1016/j.ijbiomac.2019.11.206.

(273) Khan, M. U. A.; Raza, M. A.; Razak, S. I. A.; Abdul Kadir, M. R.; Haider, A.; Shah, S. A.; Mohd Yusof, A. H.; Haider, S.; Shakir, I.; Aftab, S. Novel Functional Antimicrobial and Biocompatible Arabinoxylan/Guar Gum Hydrogel for Skin Wound Dressing Applications. *Journal of Tissue Engineering and Regenerative Medicine* **2020**, *14* (10), 1488–1501. https://doi.org/10.1002/term.3115.

(274) Minsart, M.; Van Vlierberghe, S.; Dubruel, P.; Mignon, A. Commercial Wound Dressings for the Treatment of Exuding Wounds: An in-Depth Physico-Chemical Comparative Study. *Burns & Trauma* **2022**, *10*, tkac024. https://doi.org/10.1093/burnst/tkac024.

(275) Kumar, P. T. S.; Abhilash, S.; Manzoor, K.; Nair, S. V.; Tamura, H.; Jayakumar, R. Preparation and Characterization of Novel β-Chitin/Nanosilver Composite Scaffolds for Wound Dressing Applications. *Carbohydrate Polymers* **2010**, *80* (3), 761–767. https://doi.org/10.1016/j.carbpol.2009.12.024.

(276) Bagheri, M.; Validi, M.; Gholipour, A.; Makvandi, P.; Sharifi, E. Chitosan Nanofiber Biocomposites for Potential Wound Healing Applications: Antioxidant Activity with Synergic Antibacterial Effect. *Bioengineering & Translational Medicine* **2022**, *7* (1), e10254. https://doi.org/10.1002/btm2.10254.

(277) Guan, G.; Qizhuang Lv; Liu, S.; Jiang, Z.; Zhou, C.; Liao, W. 3D-Bioprinted Peptide Coupling Patches for Wound Healing. *Materials Today Bio* **2022**, *13*, 100188. https://doi.org/10.1016/j.mtbio.2021.100188.

(278) Luan, Z.; Zhang, H.; Hu, J.; Zhang, J.; Liu, Y. Crosslinked Carboxymethyl Starch Nanofiber Mats: Preparation, Water Resistance and Exudates Control Ability. *European Polymer Journal* **2021**, *154*, 110568. https://doi.org/10.1016/j.eurpolymj.2021.110568.

(279) Zheng, Y.; Zhang, K.; Yao, Y.; Li, X.; Yu, J.; Ding, B. Bioinspired Sequentially Crosslinked Nanofibrous Hydrogels with Robust Adhesive and Stretchable Capability for Joint Wound Dressing. *Composites Communications* **2021**, *26*, 100785. https://doi.org/10.1016/j.coco.2021.100785.

(280) Donati, I.; Stredanska, S.; Silvestrini, G.; Vetere, A.; Marcon, P.; Marsich, E.; Mozetic, P.; Gamini, A.; Paoletti, S.; Vittur, F. The Aggregation of Pig Articular Chondrocyte and Synthesis of Extracellular Matrix by a Lactose-Modified Chitosan. *Biomaterials* **2005**, *26* (9), 987–998. https://doi.org/10.1016/j.biomaterials.2004.04.015.

(281) Medelin, M.; Porrelli, D.; Aurand, E. R.; Scaini, D.; Travan, A.; Borgogna, M. A.; Cok, M.; Donati, I.; Marsich, E.; Scopa, C.; Scardigli, R.; Paoletti, S.; Ballerini, L. Exploiting Natural Polysaccharides to Enhance in Vitro Bio-Constructs of Primary Neurons and Progenitor Cells. *Acta Biomaterialia* **2018**, *73*, 285–301. https://doi.org/10.1016/j.actbio.2018.03.041.

(282) Hu, B.; Gao, M.; Boakye-Yiadom, K. O.; Ho, W.; Yu, W.; Xu, X.; Zhang, X.-Q. An Intrinsically Bioactive Hydrogel with On-Demand Drug Release Behaviors for Diabetic Wound Healing. *Bioactive Materials* **2021**, *6* (12), 4592–4606. https://doi.org/10.1016/j.bioactmat.2021.04.040.

(283) Sharifi, E.; Chehelgerdi, M.; Fatahian-Kelishadrokhi, A.; Yazdani-Nafchi, F.; Ashrafi-Dehkordi, K. Comparison of Therapeutic Effects of Encapsulated Mesenchymal Stem Cells in Aloe Vera Gel and Chitosan-Based Gel in Healing of Grade-II Burn Injuries. *Regenerative Therapy* **2021**, *18*, 30–37. https://doi.org/10.1016/j.reth.2021.02.007.

(284) Fahimirad, S.; Abtahi, H.; Satei, P.; Ghaznavi-Rad, E.; Moslehi, M.; Ganji, A. Wound Healing Performance of PCL/Chitosan Based Electrospun Nanofiber Electrosprayed with Curcumin Loaded Chitosan Nanoparticles. *Carbohydrate Polymers* **2021**, *259*, 117640. https://doi.org/10.1016/j.carbpol.2021.117640.

(285) Rezaei, M.; Nikkhah, M.; Mohammadi, S.; Bahrami, S. H.; Sadeghizadeh, M. Nano-curcumin/Graphene Platelets Loaded on Sodium Alginate/Polyvinyl Alcohol Fibers as Potential Wound Dressing. *Journal of Applied Polymer Science* **2021**, *138* (35), 50884. https://doi.org/10.1002/app.50884.

(286) Facchi, D. P.; Facchi, S. P.; Souza, P. R.; Bonafé, E. G.; Popat, K. C.; Kipper, M. J.; Martins, A. F. Composite Filter with Antimicrobial and Anti-Adhesive Properties Based on Electrospun Poly(Butylene Adipate-Co-Terephthalate)/Poly(Acid Lactic)/Tween 20 Fibers Associated with Silver Nanoparticles. *Journal of Membrane Science* **2022**, *650*, 120426. https://doi.org/10.1016/j.memsci.2022.120426.

(287) Ziani, K.; Henrist, C.; Jérôme, C.; Aqil, A.; Maté, J. I.; Cloots, R. Effect of Nonionic Surfactant and Acidity on Chitosan Nanofibers with Different Molecular Weights. *Carbohydrate Polymers* **2011**, *83* (2), 470–476. https://doi.org/10.1016/j.carbpol.2010.08.002.

(288) Mirzaei, E.; Faridi-Majidi, R.; Shokrgozar, M. A.; Asghari Paskiabi, F. Genipin Cross-Linked Electrospun Chitosan-Based Nanofibrous Mat as Tissue Engineering Scaffold. *Nanomedicine Journal* **2014**, *1* (3), 137–146. https://doi.org/10.7508/nmj.2014.03.003.

(289) Mak, Y. W.; Leung, W. W.-F. Crosslinking of Genipin and Autoclaving in Chitosan-Based Nanofibrous Scaffolds: Structural and Physiochemical Properties. *Journal of Materials Science* **2019**, *54* (15), 10941–10962. https://doi.org/10.1007/s10853-019-03649-8.

(290) Dodero, A.; Scarfi, S.; Mirata, S.; Sionkowska, A.; Vicini, S.; Alloisio, M.; Castellano, M. Effect of Crosslinking Type on the Physical-Chemical Properties and Biocompatibility of Chitosan-Based Electrospun Membranes. *Polymers* **2021**, *13* (5), 831. https://doi.org/10.3390/polym13050831.

(291) Lin, C.-M.; Chang, Y.-C.; Cheng, L.-C.; Liu, C.-H.; Chang, S. C.; Hsien, T.-Y.; Wang, D.-M.; Hsieh, H.-J. Preparation of Graphene-Embedded Hydroxypropyl Cellulose/Chitosan/Polyethylene Oxide Nanofiber Membranes as Wound Dressings with Enhanced Antibacterial Properties. *Cellulose* **2020**, *27* (5), 2651–2667. https://doi.org/10.1007/s10570-019-02940-w.

(292) Castro, K. C.; Campos, M. G. N.; Mei, L. H. I. Hyaluronic Acid Electrospinning: Challenges, Applications in Wound Dressings and New Perspectives. *International Journal of Biological Macromolecules* **2021**, *173*, 251–266. https://doi.org/10.1016/j.ijbiomac.2021.01.100.

(293) Federico, S.; Pitarresi, G.; Palumbo, F. S.; Fiorica, C.; Yang, F.; Giammona, G. Hyaluronan Alkyl Derivatives-Based Electrospun Membranes for Potential Guided Bone Regeneration:

Fabrication, Characterization and in Vitro Osteoinductive Properties. *Colloids and Surfaces B: Biointerfaces* **2021**, *197*, 111438. https://doi.org/10.1016/j.colsurfb.2020.111438.

(294) Keshvardoostchokami, M.; Majidi, S. S.; Huo, P.; Ramachandran, R.; Chen, M.; Liu, B. Electrospun Nanofibers of Natural and Synthetic Polymers as Artificial Extracellular Matrix for Tissue Engineering. *Nanomaterials* **2021**, *11* (1), 21. https://doi.org/10.3390/nano11010021.

(295) Khunmanee, S.; Jeong, Y.; Park, H. Crosslinking Method of Hyaluronic-Based Hydrogel for Biomedical Applications. *Journal of Tissue Engineering* **2017**, *8*, 204173141772646. https://doi.org/10.1177/2041731417726464.

(296) Séon-Lutz, M.; Couffin, A.-C.; Vignoud, S.; Schlatter, G.; Hébraud, A. Electrospinning in Water and in Situ Crosslinking of Hyaluronic Acid / Cyclodextrin Nanofibers: Towards Wound Dressing with Controlled Drug Release. *Carbohydrate Polymers* **2019**, *207*, 276–287. https://doi.org/10.1016/j.carbpol.2018.11.085.

(297) Ardekani, N. T.; Khorram, M.; Zomorodian, K.; Yazdanpanah, S.; Veisi, H.; Veisi, H. Evaluation of Electrospun Poly (Vinyl Alcohol)-Based Nanofiber Mats Incorporated with Zataria Multiflora Essential Oil as Potential Wound Dressing. *International Journal of Biological Macromolecules* **2019**, *125*, 743–750. https://doi.org/10.1016/j.ijbiomac.2018.12.085.

(298) Chen, X.; Meng, J.; Xu, H.; Shinoda, M.; Kishimoto, M.; Sakurai, S.; Yamane, H. Fabrication and Properties of Electrospun Collagen Tubular Scaffold Crosslinked by Physical and Chemical Treatments. *Polymers* **2021**, *13* (5), 755. https://doi.org/10.3390/polym13050755.

(299) Darbasizadeh, B.; Fatahi, Y.; Feyzi-barnaji, B.; Arabi, M.; Motasadizadeh, H.; Farhadnejad, H.; Moraffah, F.; Rabiee, N. Crosslinked-Polyvinyl Alcohol-Carboxymethyl Cellulose/ZnO Nanocomposite Fibrous Mats Containing Erythromycin (PVA-CMC/ZnO-EM): Fabrication, Characterization and in-Vitro Release and Anti-Bacterial Properties. *International Journal of Biological Macromolecules* **2019**, *141*, 1137–1146. https://doi.org/10.1016/j.ijbiomac.2019.09.060.

(300) Mistry, P.; Chhabra, R.; Muke, S.; Narvekar, A.; Sathaye, S.; Jain, R.; Dandekar, P. Fabrication and Characterization of Starch-TPU Based Nanofibers for Wound Healing Applications. *Materials Science and Engineering: C* **2021**, *119*, 111316. https://doi.org/10.1016/j.msec.2020.111316.

(301) Vondran, J. L.; Sun, W.; Schauer, C. L. Crosslinked, Electrospun Chitosan–Poly(Ethylene Oxide) Nanofiber Mats. *Journal of Applied Polymer Science* **2008**, *109* (2), 968–975. https://doi.org/10.1002/app.28107.

(302) Akbari, A.; Rabbani, S.; Irani, S.; Zandi, M.; Sharifi, F.; Ameli, F.; Mohamadali, M. In Vitro and in Vivo Study of Carboxymethyl Chitosan/Polyvinyl Alcohol for Wound Dressing Application. *Journal of Applied Polymer Science* **2022**, *139* (10), 51764. https://doi.org/10.1002/app.51764.

(303) Qian, Y.-F.; Zhang, K.-H.; Chen, F.; Ke, Q.-F.; Mo, X.-M. Cross-Linking of Gelatin and Chitosan Complex Nanofibers for Tissue-Engineering Scaffolds. *Journal of Biomaterials*

Science. Polymer Edition **2011**, *22* (8), 1099–1113. https://doi.org/10.1163/092050610X499447.

(304) Ahmadi, S.; Hivechi, A.; Bahrami, S. H.; Milan, P. B.; Ashraf, S. S. Cinnamon Extract Loaded Electrospun Chitosan/Gelatin Membrane with Antibacterial Activity. *International Journal of Biological Macromolecules* **2021**, *173*, 580–590. https://doi.org/10.1016/j.ijbiomac.2021.01.156.

(305) Lai, J.-Y. Biocompatibility of Genipin and Glutaraldehyde Cross-Linked Chitosan Materials in the Anterior Chamber of the Eye. *International Journal of Molecular Sciences* **2012**, *13* (9), 10970–10985. https://doi.org/10.3390/ijms130910970.

(306) Aubert-Viard, F.; Mogrovejo-Valdivia, A.; Tabary, N.; Maton, M.; Chai, F.; Neut, C.; Martel, B.; Blanchemain, N. Evaluation of Antibacterial Textile Covered by Layer-by-Layer Coating and Loaded with Chlorhexidine for Wound Dressing Application. *Materials Science and Engineering: C* **2019**, *100*, 554–563. https://doi.org/10.1016/j.msec.2019.03.044.

(307) Sergi, R.; Cannillo, V.; Boccaccini, A. R.; Liverani, L. A New Generation of Electrospun Fibers Containing Bioactive Glass Particles for Wound Healing. *Materials* **2020**, *13* (24), 5651. https://doi.org/10.3390/ma13245651.

(308) Panzavolta, S.; Gioffrè, M.; Focarete, M. L.; Gualandi, C.; Foroni, L.; Bigi, A. Electrospun Gelatin Nanofibers: Optimization of Genipin Cross-Linking to Preserve Fiber Morphology after Exposure to Water. *Acta Biomaterialia* **2011**, *7* (4), 1702–1709. https://doi.org/10.1016/j.actbio.2010.11.021.

(309) Esparza, Y.; Ullah, A.; Boluk, Y.; Wu, J. Preparation and Characterization of Thermally Crosslinked Poly(Vinyl Alcohol)/Feather Keratin Nanofiber Scaffolds. *Materials & Design* **2017**, *133*, 1–9. https://doi.org/10.1016/j.matdes.2017.07.052.

(310) Sandri, G.; Rossi, S.; Bonferoni, M. C.; Miele, D.; Faccendini, A.; Del Favero, E.; Di Cola, E.; Icaro Cornaglia, A.; Boselli, C.; Luxbacher, T.; Malavasi, L.; Cantu', L.; Ferrari, F. Chitosan/Glycosaminoglycan Scaffolds for Skin Reparation. *Carbohydrate Polymers* **2019**, *220*, 219–227. https://doi.org/10.1016/j.carbpol.2019.05.069.

(311) Peng, H.-H.; Chen, J.-W.; Yang, T.-P.; Kuo, C.-F.; Wang, Y.-J.; Lee, M.-W. Polygalacturonic Acid Hydrogel with Short-Chain Hyaluronate Cross-Linker to Prevent Postoperative Adhesion. *Journal of Bioactive and Compatible Polymers* **2011**, *26* (6), 552–564. https://doi.org/10.1177/0883911511423562.

(312) Cavalli, R.; Akhter, A. K.; Bisazza, A.; Giustetto, P.; Trotta, F.; Vavia, P. Nanosponge Formulations as Oxygen Delivery Systems. *International Journal of Pharmaceutics* **2010**, *402* (1), 254–257. https://doi.org/10.1016/j.ijpharm.2010.09.025.

(313) Karaky, K.; Brochon, C.; Schlatter, G.; Hadziioannou, G. PH-Switchable Supramolecular "Sliding" Gels Based on Polyrotaxanes of Polyethyleneimine-Block-Poly(Ethylene Oxide)-Block-Polyethyleneimine Block Copolymer and α-Cyclodextrin: Synthesis and Swelling Behaviour. *Soft Matter* **2008**, *4* (6), 1165–1168. https://doi.org/10.1039/B803670E.

(314) Tamer, T. M.; Sabet, M. M.; Omer, A. M.; Abbas, E.; Eid, A. I.; Mohy-Eldin, M. S.; Hassan, M. A. Hemostatic and Antibacterial PVA/Kaolin Composite Sponges Loaded with Penicillin–

Streptomycin for Wound Dressing Applications. *Scientific Reports* **2021**, *11* (1), 3428. https://doi.org/10.1038/s41598-021-82963-1.

(315) Wang, Z.; Song, X.; Cui, Y.; Cheng, K.; Tian, X.; Dong, M.; Liu, L. Silk Fibroin H-Fibroin/Poly(ε-Caprolactone) Core-Shell Nanofibers with Enhanced Mechanical Property and Long-Term Drug Release. *Journal of Colloid and Interface Science* **2021**, *593*, 142–151. https://doi.org/10.1016/j.jcis.2021.02.099.

(316) Thomas, R.; Soumya, K. R.; Mathew, J.; Radhakrishnan, E. K. Electrospun Polycaprolactone Membrane Incorporated with Biosynthesized Silver Nanoparticles as Effective Wound Dressing Material. *Applied Biochemistry and Biotechnology* **2015**, *176* (8), 2213–2224. https://doi.org/10.1007/s12010-015-1709-9.

(317) Zhou, F.; Cui, C.; Sun, S.; Wu, S.; Chen, S.; Ma, J.; Li, C. M. Electrospun ZnO-Loaded Chitosan/PCL Bilayer Membranes with Spatially Designed Structure for Accelerated Wound Healing. *Carbohydrate Polymers* **2022**, *282*, 119131. https://doi.org/10.1016/j.carbpol.2022.119131.

(318) Chaiarwut, S.; Ekabutr, P.; Chuysinuan, P.; Chanamuangkon, T.; Supaphol, P. Surface Immobilization of PCL Electrospun Nanofibers with Pexiganan for Wound Dressing. *Journal of Polymer Research* **2021**, *28* (9), 344. https://doi.org/10.1007/s10965-021-02669-w.

(319) Augustine, R.; Kalarikkal, N.; Thomas, S. Electrospun PCL Membranes Incorporated with Biosynthesized Silver Nanoparticles as Antibacterial Wound Dressings. *Applied Nanoscience* **2016**, *6* (3), 337–344. https://doi.org/10.1007/s13204-015-0439-1.

(320) Asghari, F.; Rabiei Faradonbeh, D.; Malekshahi, Z. V.; Nekounam, H.; Ghaemi, B.; Yousefpoor, Y.; Ghanbari, H.; Faridi-Majidi, R. Hybrid PCL/Chitosan-PEO Nanofibrous Scaffolds Incorporated with A. Euchroma Extract for Skin Tissue Engineering Application. *Carbohydrate Polymers* **2022**, *278*, 118926. https://doi.org/10.1016/j.carbpol.2021.118926.

(321) Jacobs, T.; Declercq, H.; De Geyter, N.; Cornelissen, R.; Dubruel, P.; Leys, C.; Morent, R. Improved Cell Adhesion to Flat and Porous Plasma-Treated Poly-ε-Caprolactone Samples. *Surface and Coatings Technology* **2013**, *232*, 447–455. https://doi.org/10.1016/j.surfcoat.2013.06.001.

(322) Patel, P. R.; Pandey, K.; Killi, N.; Gundloori, R. V. N. Manipulating Hydrophobicity of Polyester Nanofiber Mats with Egg Albumin to Enhance Cell Interactions. *Polymer Engineering & Science* **2021**, *61* (10), 2496–2510. https://doi.org/10.1002/pen.25776.

(323) Ferfera-Harrar, H.; Aouaz, N.; Dairi, N. Environmental-Sensitive Chitosan-g-Polyacrylamide/Carboxymethylcellulose Superabsorbent Composites for Wastewater Purification I: Synthesis and Properties. *Polymer Bulletin* **2016**, *73* (3), 815–840. https://doi.org/10.1007/s00289-015-1521-2.

(324) Ricka, J.; Tanaka, T. Swelling of Ionic Gels: Quantitative Performance of the Donnan Theory. *Macromolecules* **1984**, *17* (12), 2916–2921. https://doi.org/10.1021/ma00142a081.

(325) Zhu, L.; Bratlie, K. M. PH Sensitive Methacrylated Chitosan Hydrogels with Tunable Physical and Chemical Properties. *Biochemical Engineering Journal* **2018**, *132*, 38–46. https://doi.org/10.1016/j.bej.2017.12.012.

(326) Akita, S.; Akino, K.; Imaizumi, T.; Tanaka, K.; Anraku, K.; Yano, H.; Hirano, A. A Polyurethane Dressing Is Beneficial for Split-Thickness Skin-Graft Donor Wound Healing. *Burns* **2006**, *32* (4), 447–451. https://doi.org/10.1016/j.burns.2005.11.015.

(327) Lindholm, C.; Searle, R. Wound Management for the 21st Century: Combining Effectiveness and Efficiency: Wound Management for the 21st Century. *International Wound Journal* **2016**, *13*, 5–15. https://doi.org/10.1111/iwj.12623.

(328) Resch, A.; Staud, C.; Radtke, C. Nanocellulose-based Wound Dressing for Conservative Wound Management in Children with Second-degree Burns. *International Wound Journal* **2021**, *18* (4), 478–486. https://doi.org/10.1111/iwj.13548.

(329) Hauck, S.; Zager, P.; Halfter, N.; Wandel, E.; Torregrossa, M.; Kakpenova, A.; Rother, S.; Ordieres, M.; Räthel, S.; Berg, A.; Möller, S.; Schnabelrauch, M.; Simon, J. C.; Hintze, V.; Franz, S. Collagen/Hyaluronan Based Hydrogels Releasing Sulfated Hyaluronan Improve Dermal Wound Healing in Diabetic Mice via Reducing Inflammatory Macrophage Activity. *Bioactive Materials* **2021**, *6* (12), 4342–4359. https://doi.org/10.1016/j.bioactmat.2021.04.026.

(330) Li, M.; Liang, Y.; Liang, Y.; Pan, G.; Guo, B. Injectable Stretchable Self-Healing Dual Dynamic Network Hydrogel as Adhesive Anti-Oxidant Wound Dressing for Photothermal Clearance of Bacteria and Promoting Wound Healing of MRSA Infected Motion Wounds. *Chemical Engineering Journal* **2022**, *427*, 132039. https://doi.org/10.1016/j.cej.2021.132039.

(331) Liang, Y.; Chen, B.; Li, M.; He, J.; Yin, Z.; Guo, B. Injectable Antimicrobial Conductive Hydrogels for Wound Disinfection and Infectious Wound Healing. *Biomacromolecules* **2020**, *21* (5), 1841–1852. https://doi.org/10.1021/acs.biomac.9b01732.

(332) Wang, J.; Feng, L.; Yu, Q.; Chen, Y.; Liu, Y. Polysaccharide-Based Supramolecular Hydrogel for Efficiently Treating Bacterial Infection and Enhancing Wound Healing. *Biomacromolecules* **2021**, *22* (2), 534–539. https://doi.org/10.1021/acs.biomac.0c01401.

(333) Yao, Z.; Qian, Y.; Jin, Y.; Wang, S.; Li, J.; Yuan, W.-E.; Fan, C. Biomimetic Multilayer Polycaprolactone/Sodium Alginate Hydrogel Scaffolds Loaded with Melatonin Facilitate Tendon Regeneration. *Carbohydrate Polymers* **2022**, *277*, 118865. https://doi.org/10.1016/j.carbpol.2021.118865.

(334) Catanzano, O.; Gomez d'Ayala, G.; D'Agostino, A.; Di Lorenzo, F.; Schiraldi, C.; Malinconico, M.; Lanzetta, R.; Bonina, F.; Laurienzo, P. PEG-Crosslinked-Chitosan Hydrogel Films for in Situ Delivery of Opuntia Ficus-Indica Extract. *Carbohydrate Polymers* **2021**, *264*, 117987. https://doi.org/10.1016/j.carbpol.2021.117987.

(335) Chen, K.; Pan, H.; Ji, D.; Li, Y.; Duan, H.; Pan, W. Curcumin-Loaded Sandwich-like Nanofibrous Membrane Prepared by Electrospinning Technology as Wound Dressing for Accelerate Wound Healing. *Materials Science and Engineering: C* **2021**, *127*, 112245. https://doi.org/10.1016/j.msec.2021.112245.

(336) Salami, M. S.; Bahrami, G.; Arkan, E.; Izadi, Z.; Miraghaee, S.; Samadian, H. Co-Electrospun Nanofibrous Mats Loaded with Bitter Gourd (Momordica Charantia) Extract as the Wound

Dressing Materials: In Vitro and in Vivo Study. *BMC Complementary Medicine and Therapies* **2021**, *21* (1), 111. https://doi.org/10.1186/s12906-021-03284-4.

(337) Du, S.; Liu, B.; Li, Z.; Tan, H.; Qi, W.; Liu, T.; Qiang, S.; Zhang, T.; Song, F.; Chen, X.; Chen, J.; Qiu, H.; Wu, W. A Nanoporous Graphene/Nitrocellulose Membrane Beneficial to Wound Healing. *ACS Applied Bio Materials* **2021**, *4* (5), 4522–4531. https://doi.org/10.1021/acsabm.1c00261.

(338) Zoghi, N.; Fouani, M. H.; Bagheri, H.; Nikkhah, M.; Asadi, N. Characterization of Minocycline Loaded Chitosan/Polyethylene Glycol/Glycerol Blend Films as Antibacterial Wound Dressings. *Journal of Applied Polymer Science* **2021**, *138* (32), 50781. https://doi.org/10.1002/app.50781.

(339) Li, Y.; Ma, Z.; Yang, X.; Gao, Y.; Ren, Y.; Li, Q.; Qu, Y.; Chen, G.; Zeng, R. Investigation into the Physical Properties, Antioxidant and Antibacterial Activity of Bletilla Striata Polysaccharide/Chitosan Membranes. *International Journal of Biological Macromolecules* **2021**, *182*, 311–320. https://doi.org/10.1016/j.ijbiomac.2021.04.037.

(340) Jeckson, T. A.; Neo, Y. P.; Sisinthy, S. P.; Gorain, B. Delivery of Therapeutics from Layer-by-Layer Electrospun Nanofiber Matrix for Wound Healing: An Update. *Journal of Pharmaceutical Sciences* **2021**, *110* (2), 635–653. https://doi.org/10.1016/j.xphs.2020.10.003.

(341) Sirc, J.; Kubinova, S.; Hobzova, R.; Stranska, D.; Kozlik, P.; Bosakova, Z.; Marekova, D.; Holan, V.; Sykova, E.; Michalek, J. Controlled Gentamicin Release from Multi-Layered Electrospun Nanofibrous Structures of Various Thicknesses. *International Journal of Nanomedicine* **2012**, *7*, 5315–5325. https://doi.org/10.2147/IJN.S35781.

(342) Talukder, M. E.; Hasan, K. M. F.; Wang, J.; Yao, J.; Li, C.; Song, H. Novel Fibrin Functionalized Multilayered Electrospun Nanofiber Membrane for Burn Wound Treatment. *J Mater Sci* **2021**, *56* (22), 12814–12834. https://doi.org/10.1007/s10853-021-06123-6.

(343) Yang, Y.; Du, Y.; Zhang, J.; Zhang, H.; Guo, B. Structural and Functional Design of Electrospun Nanofibers for Hemostasis and Wound Healing. *Advanced Fiber Materials* **2022**, *4* (5), 1027–1057. https://doi.org/10.1007/s42765-022-00178-z.

(344) Wang, X.; Sun, X.; Bu, T.; Xu, K.; Li, L.; Li, M.; Li, R.; Wang, L. Germanene-Modified Chitosan Hydrogel for Treating Bacterial Wound Infection: An Ingenious Hydrogel-Assisted Photothermal Therapy Strategy. *International Journal of Biological Macromolecules* **2022**. https://doi.org/10.1016/j.ijbiomac.2022.09.128.

(345) Shan, J.; Zhang, X.; Kong, B.; Zhu, Y.; Gu, Z.; Ren, L.; Zhao, Y. Coordination Polymer Nanozymes-Integrated Colorimetric Microneedle Patches for Intelligent Wound Infection Management. *Chemical Engineering Journal* **2022**, *444*, 136640. https://doi.org/10.1016/j.cej.2022.136640.

(346) Yusufu, D.; Magee, E.; Gilmore, B.; Mills, A. Non-Invasive, 3D Printed, Colourimetric, Early Wound-Infection Indicator. *Chemical Communications* **2022**, *58* (3), 439–442. https://doi.org/10.1039/D1CC06147J.

(347) Join-Lambert, O.; Coignard, H.; Jais, J.-P.; Guet-Revillet, H.; Poirée, S.; Fraitag, S.; Jullien, V.; Ribadeau-Dumas, F.; Thèze, J.; Guern, A.-S. L.; Behillil, S.; Leflèche, A.; Berche, P.; Consigny, P. H.; Lortholary, O.; Nassif, X.; Nassif, A. Efficacy of Rifampin-Moxifloxacin-Metronidazole Combination Therapy in Hidradenitis Suppurativa. *Dermatology* **2011**, *222* (1), 49–58. https://doi.org/10.1159/000321716.

(348) Tsankov, N.; Angelova, I. Rifampin in Dermatology. *Clinics in Dermatology* **2003**, *21* (1), 50–55. https://doi.org/10.1016/S0738-081X(02)00328-0.

(349) Delage, M.; Jais, J.-P.; Lam, T.; Guet-Revillet, H.; Ungeheuer, M.-N.; Consigny, P.-H.; Nassif, A.; Join-Lambert, O. Rifampin-Moxifloxacin-Metronidazole Combination Therapy for Severe Hurley Stage 1 Hidradenitis Suppurativa: Prospective Short-Term Trial and One-Year Follow-up in 28 Consecutive Patients. *Journal of the American Academy of Dermatology* **2020**, *10*, S0190-9622(20)30049-9. https://doi.org/10.1016/j.jaad.2020.01.007.

(350) Ndlovu, S. P.; Fonkui, T. Y.; Kumar, P.; Choonara, Y. E.; Ndinteh, D. T.; Aderibigbe, B. A. Dissolvable Zinc Oxide Nanoparticle-Loaded Wound Dressing with Preferential Exudate Absorption and Hemostatic Features. *Polymer Bulletin* **2022**. https://doi.org/10.1007/s00289-022-04358-0.

(351) Gao, Y.; Qiu, Z.; Liu, L.; Li, M.; Xu, B.; Yu, D.; Qi, D.; Wu, J. Multifunctional Fibrous Wound Dressings for Refractory Wound Healing. *Journal of Polymer Science* **2022**, *60* (15), 2191–2212. https://doi.org/10.1002/pol.20220008.

(352) Li, Y.; Zhang, Y.; Wang, Y.; Yu, K.; Hu, E.; Lu, F.; Shang, S.; Xie, R.; Lan, G. Regulating Wound Moisture for Accelerated Healing: A Strategy for the Continuous Drainage of Wound Exudates by Mimicking Plant Transpiration. *Chemical Engineering Journal* **2022**, *429*, 131964. https://doi.org/10.1016/j.cej.2021.131964.

(353) Boman, G.; Ringberger, V. A. Binding of Rifampicin by Human Plasma Proteins. *European Journal of Clinical Pharmacology* **1974**, *7* (5), 369–373. https://doi.org/10.1007/BF00558209.

(354) Song, X.; Lin, Q.; Guo, L.; Fu, Y.; Han, J.; Ke, H.; Sun, X.; Gong, T.; Zhang, Z. Rifampicin Loaded Mannosylated Cationic Nanostructured Lipid Carriers for Alveolar Macrophage-Specific Delivery. *Pharmaceutical Research* **2015**, *32* (5), 1741–1751. https://doi.org/10.1007/s11095-014-1572-3.

(355) Banères-Roquet, F.; Gualtieri, M.; Villain-Guillot, P.; Pugnière, M.; Leonetti, J.-P. Use of a Surface Plasmon Resonance Method To Investigate Antibiotic and Plasma Protein Interactions. *Antimicrobial Agents and Chemotherapy* **2009**, *53* (4), 1528–1531. https://doi.org/10.1128/AAC.00971-08.

(356) Kamat, B. P.; Seetharamappa, J. Mechanism of Interaction of Vincristine Sulphate and Rifampicin with Bovine Serum Albumin: A Spectroscopic Study. *Journal of Chemical Sciences* **2005**, *117* (6), 649–655. https://doi.org/10.1007/BF02708294.

(357) Wei, Q.; Becherer, T.; Angioletti-Uberti, S.; Dzubiella, J.; Wischke, C.; Neffe, A. T.; Lendlein, A.; Ballauff, M.; Haag, R. Protein Interactions with Polymer Coatings and Biomaterials. *Angewandte Chemie International Edition* **2014**, *53* (31), 8004–8031. https://doi.org/10.1002/anie.201400546.

(358) Berg, J. M.; Eriksson, L. G. T.; Claesson, P. M.; Borve, K. G. N. Three-Component Langmuir-Blodgett Films with a Controllable Degree of Polarity. *Langmuir* **1994**, *10* (4), 1225–1234. https://doi.org/10.1021/la00016a041.

(359) Vogler, E. A. Structure and Reactivity of Water at Biomaterial Surfaces. *Advances in Colloid and Interface Science* **1998**, *74* (1), 69–117. https://doi.org/10.1016/S0001-8686(97)00040-7.

(360) Yu, L.; Schlaich, C.; Hou, Y.; Zhang, J.; Noeske, P.-L. M.; Haag, R. Photoregulating Antifouling and Bioadhesion Functional Coating Surface Based on Spiropyran. *Chemistry – A European Journal* **2018**, *24* (30), 7742–7748. https://doi.org/10.1002/chem.201801051.

(361) Le, T. C.; Penna, M.; Winkler, D. A.; Yarovsky, I. Quantitative Design Rules for Protein-Resistant Surface Coatings Using Machine Learning. *Scientific Reports* **2019**, *9* (1), 265. https://doi.org/10.1038/s41598-018-36597-5.

(362) Ostuni, E.; Chapman, R. G.; Holmlin, R. E.; Takayama, S.; Whitesides, G. M. A Survey of Structure−Property Relationships of Surfaces That Resist the Adsorption of Protein. *Langmuir* **2001**, *17* (18), 5605–5620. https://doi.org/10.1021/la010384m.

(363) Rudawska, A.; Jacniacka, E. Analysis for Determining Surface Free Energy Uncertainty by the Owen–Wendt Method. *International Journal of Adhesion and Adhesives* **2009**, *29* (4), 451–457. https://doi.org/10.1016/j.ijadhadh.2008.09.008.

(364) Milne, S. D.; Seoudi, I.; Al Hamad, H.; Talal, T. K.; Anoop, A. A.; Allahverdi, N.; Zakaria, Z.; Menzies, R.; Connolly, P. A Wearable Wound Moisture Sensor as an Indicator for Wound Dressing Change: An Observational Study of Wound Moisture and Status. *International Wound Journal* **2016**, *13* (6), 1309–1314. https://doi.org/10.1111/iwj.12521.

(365) Jørgensen, B.; Friis, G. J.; Gottrup, F. Pain and Quality of Life for Patients with Venous Leg Ulcers: Proof of Concept of the Efficacy of Biatain®-Ibu, a New Pain Reducing Wound Dressing. *Wound Repair and Regeneration* **2006**, *14* (3), 233–239. https://doi.org/10.1111/j.1743-6109.2006.00116.x.

(366) Ding, Y.-W.; Wang, Z.-Y.; Ren, Z.-W.; Zhang, X.-W.; Wei, D.-X. Advances in Modified Hyaluronic Acid-Based Hydrogels for Skin Wound Healing. *Biomaterials Science* **2022**, *10* (13), 3393–3409. https://doi.org/10.1039/D2BM00397J.

(367) Weng, H.; Jia, W.; Li, M.; Chen, Z. New Injectable Chitosan-Hyaluronic Acid Based Hydrogels for Hemostasis and Wound Healing. *Carbohydrate Polymers* **2022**, *294*, 119767. https://doi.org/10.1016/j.carbpol.2022.119767.

(368) Zou, F.; Wang, Y.; Zheng, Y.; Xie, Y.; Zhang, H.; Chen, J.; Hussain, M. I.; Meng, H.; Peng, J. A Novel Bioactive Polyurethane with Controlled Degradation and L-Arg Release Used as Strong Adhesive Tissue Patch for Hemostasis and Promoting Wound Healing. *Bioactive Materials* **2022**, *17*, 471–487. https://doi.org/10.1016/j.bioactmat.2022.01.009.

(369) Gao, X.; Huang, R.; Jiao, Y.; Groth, T.; Yang, W.; Tu, C.; Li, H.; Gong, F.; Chu, J.; Zhao, M. Enhanced Wound Healing in Diabetic Mice by Hyaluronan/Chitosan Multilayer-Coated PLLA Nanofibrous Mats with Sustained Release of Insulin. *Applied Surface Science* **2022**, *576*, 151825. https://doi.org/10.1016/j.apsusc.2021.151825.

(370) Serag, E.; El-Aziz, A. M. A.; El-Maghraby, A.; Taha, N. A. Electrospun Non-Wovens Potential Wound Dressing Material Based on Polyacrylonitrile/Chicken Feathers Keratin Nanofiber. *Scientific Reports* **2022**, *12* (1), 15460. https://doi.org/10.1038/s41598-022-19390-3.

(371) Zeng, W.; Cheng, N.; Liang, X.; Hu, H.; Luo, F.; Jin, J.; Li, Y. Electrospun Polycaprolactone Nanofibrous Membranes Loaded with Baicalin for Antibacterial Wound Dressing. *Scientific Reports* **2022**, *12* (1), 10900. https://doi.org/10.1038/s41598-022-13141-0.

(372) Götting, M.; Zibell, R.; Jungehülsing, M. Individually Moulded Silicone Dressing in Full Thickness Skin Grafts. *Journal of Otolaryngology - Head & Neck Surgery* **2022**, *51* (1), 33. https://doi.org/10.1186/s40463-022-00577-7.

(373) Chouhan, D.; Thatikonda, N.; Nilebäck, L.; Widhe, M.; Hedhammar, M.; Mandal, B. B. Recombinant Spider Silk Functionalized Silkworm Silk Matrices as Potential Bioactive Wound Dressings and Skin Grafts. *ACS Applied Materials & Interfaces* **2018**, *10* (28), 23560–23572. https://doi.org/10.1021/acsami.8b05853.

(374) Sharifi, E.; Sadati, S. A.; Yousefiasl, S.; Sartorius, R.; Zafari, M.; Rezakhani, L.; Alizadeh, M.; Nazarzadeh Zare, E.; Omidghaemi, S.; Ghanavatinejad, F.; Jami, M.-S.; Salahinejad, E.; Samadian, H.; Paiva-Santos, A. C.; De Berardinis, P.; Shafiee, A.; Tay, F. R.; Pourmotabed, S.; Makvandi, P. Cell Loaded Hydrogel Containing Ag-Doped Bioactive Glass–Ceramic Nanoparticles as Skin Substitute: Antibacterial Properties, Immune Response, and Scarless Cutaneous Wound Regeneration. *Bioengineering & Translational Medicine* **2022**, *7* (3), e10386. https://doi.org/10.1002/btm2.10386.

(375) Kruk, J.; Pancerz, M.; Ptaszek, A. Osmotic Properties of Polysaccharides Solutions, in *Solubility of Polysaccharides, IntechOpen* **2017**, edited by Zhenbo Xu. https://doi.org/10.5772/intechopen.69864.

(376) Wilhelm, K.-P.; Böttjer, B.; Siegers, C.-P. Quantitative Assessment of Primary Skin Irritants in Vitro in a Cytotoxicity Model: Comparison with in Vivo Human Irritation Tests. *British Journal of Dermatology* **2001**, *145* (5), 709–715. https://doi.org/10.1046/j.1365-2133.2001.04497.x.

(377) Rinaldi, F.; Del Favero, E.; Rondelli, V.; Pieretti, S.; Bogni, A.; Ponti, J.; Rossi, F.; Di Marzio, L.; Paolino, D.; Marianecci, C.; Carafa, M. PH-Sensitive Niosomes: Effects on Cytotoxicity and on Inflammation and Pain in Murine Models. *Journal of Enzyme Inhibition and Medicinal Chemistry* **2017**, *32* (1), 538–546. https://doi.org/10.1080/14756366.2016.1268607.

(378) Wilde, P. J.; Rodríguez Niño, Ma. R.; Clark, D. C.; Rodríguez Patino, J. M. Molecular Diffusion and Drainage of Thin Liquid Films Stabilized by Bovine Serum Albumin−Tween 20 Mixtures in Aqueous Solutions of Ethanol and Sucrose. *Langmuir* **1997**, *13* (26), 7151–7157. https://doi.org/10.1021/la970664v.

(379) Ferreira, A. C.; Sullo, A.; Winston, S.; Norton, I. T.; Norton-Welch, A. B. Influence of Ethanol on Emulsions Stabilized by Low Molecular Weight Surfactants. *Journal of Food Science* **2020**, *85* (1), 28–35. https://doi.org/10.1111/1750-3841.14947.

(380) Yan, X. Short-Chain Polysaccharide Analysis in Ethanol–Water Solutions. *Journal of AOAC INTERNATIONAL* **2017**, *100* (4), 1134–1136. https://doi.org/10.5740/jaoacint.16-0426.

(381) Hu, X.; Goff, H. D. Fractionation of Polysaccharides by Gradient Non-Solvent Precipitation: A Review. *Trends in Food Science & Technology* **2018**, *81*, 108–115. https://doi.org/10.1016/j.tifs.2018.09.011.

(382) Harding, K. G.; Moore, K.; Phillips, T. J. Wound Chronicity and Fibroblast Senescence – Implications for Treatment. *International Wound Journal* **2005**, *2* (4), 364–368. https://doi.org/10.1111/j.1742-4801.2005.00149.x.

(383) Levinson, H. A Paradigm of Fibroblast Activation and Dermal Wound Contraction to Guide the Development of Therapies for Chronic Wounds and Pathologic Scars. *Advances in Wound Care* **2013**, *2* (4), 149–159. https://doi.org/10.1089/wound.2012.0389.

(384) Al-Rikabi, A. H. A.; Tobin, D. J.; Riches-Suman, K.; Thornton, M. J. Dermal Fibroblasts Cultured from Donors with Type 2 Diabetes Mellitus Retain an Epigenetic Memory Associated with Poor Wound Healing Responses. *Scientific Reports* **2021**, *11* (1), 1474. https://doi.org/10.1038/s41598-020-80072-z.

(385) Belvedere, R.; Novizio, N.; Morello, S.; Petrella, A. The Combination of Mesoglycan and VEGF Promotes Skin Wound Repair by Enhancing the Activation of Endothelial Cells and Fibroblasts and Their Cross-Talk. *Scientific Reports* **2022**, *12* (1), 11041. https://doi.org/10.1038/s41598-022-15227-1.

(386) Yokota, M.; Häffner, N.; Kassier, M.; Brunner, M.; Shambat, S. M.; Brennecke, F.; Schniering, J.; Marques Maggio, E.; Distler, O.; Zinkernagel, A. S.; Maurer, B. Staphylococcus Aureus Impairs Dermal Fibroblast Functions with Deleterious Effects on Wound Healing. *The FASEB Journal* **2021**, *35* (7), e21695. https://doi.org/10.1096/fj.201902836R.

(387) Severn, M. M.; Horswill, A. R. Staphylococcus Epidermidis and Its Dual Lifestyle in Skin Health and Infection. *Nature Reviews Microbiology* **2022**, 1–15. https://doi.org/10.1038/s41579-022-00780-3.

(388) Oliveira, A.; Sousa, J. C.; Silva, A. C.; Melo, L. D. R.; Sillankorva, S. Chestnut Honey and Bacteriophage Application to Control Pseudomonas Aeruginosa and Escherichia Coli Biofilms: Evaluation in an Ex Vivo Wound Model. *Frontiers in Microbiology* **2018**, *9*, 1–13. https://doi.org/10.3389/fmicb.2018.01725.

(389) DeLeon, S.; Clinton, A.; Fowler, H.; Everett, J.; Horswill, A. R.; Rumbaugh, K. P. Synergistic Interactions of Pseudomonas Aeruginosa and Staphylococcus Aureus in an In Vitro Wound Model. *Infection and Immunity* **2014**, *82* (11), 4718–4728. https://doi.org/10.1128/IAI.02198-14.

(390) Goldstein, B. P. Resistance to Rifampicin: A Review. *The Journal of Antibiotics* **2014**, *67* (9), 625–630. https://doi.org/10.1038/ja.2014.107.

(391) Klibanov, O. M.; Raasch, R. H.; Rublein, J. C. Single Versus Combined Antibiotic Therapy for Gram-Negative Infections. *Annals of Pharmacotherapy* **2004**, *38* (2), 332–337. https://doi.org/10.1345/aph.1D132.

(392) Song, J. Y.; Cheong, H. J.; Lee, J.; Sung, A. K.; Kim, W. J. Efficacy of Monotherapy and Combined Antibiotic Therapy for Carbapenem-Resistant Acinetobacter Baumannii

Pneumonia in an Immunosuppressed Mouse Model. *International Journal of Antimicrobial Agents* **2009**, *33* (1), 33–39. https://doi.org/10.1016/j.ijantimicag.2008.07.008.

(393) Siddiqui, A. R.; Bernstein, J. M. Chronic Wound Infection: Facts and Controversies. *Clinics in Dermatology* **2010**, *28* (5), 519–526. https://doi.org/10.1016/j.clindermatol.2010.03.009.